

Cover Page



Universiteit Leiden



The handle <http://hdl.handle.net/1887/20094> holds various files of this Leiden University dissertation.

**Author:** Melis, Joost

**Title:** Nucleotide excision repair in aging and cancer

Date: 2012-11-06

**NUCLEOTIDE EXCISION REPAIR**

**IN**

**AGING AND CANCER**

Joost Melis

© Copyright 2012 by Joost Melis.

ISBN: 978-90-819434-1-3

Layout & Cover Design: Joost Melis

Production: CPI / Wöhrmann Print Service, Zutphen

Publication of this book was supported by RIVM, LUMC, Merck and VitroMics B.V.

*Voor Kris en mijn ouders*





# **NUCLEOTIDE EXCISION REPAIR IN AGING AND CANCER**

**Proefschrift**

ter verkrijging van de graad van Doctor aan de Universiteit Leiden,

op gezag van Rector Magnificus prof.mr. P.F. van der Heijden

volgens besluit van het College voor Promoties

ter verdediging op dinsdag 6 november 2012

klokke 13.45 uur

door

**Joost Melis**

geboren te Eindhoven

in 1978

## PROMOTIECOMMISSIE

Promotores: Prof. Dr. Harry van Steeg

Prof. Dr. Leon Mullenders

Co-promotor: Dr. Mirjam Luijten

Overige leden: Prof. Dr. Jan Hoeijmakers

Erasmus Medical Center

Prof. Dr. Jan Vijg

Albert Einstein College of Medicine,  
Yeshiva University, New York

Prof. Dr. Frederik-Jan van Schooten University of Maastricht

Prof. Dr. Bob van de Water

Prof. Dr. Eline Slagboom

## Contents

<b>Chapter 1</b>	Introduction	8
<b>Chapter 2</b>	Life-spanning murine gene expression profiles in relation to chronological and pathological aging in multiple organs	34
<b>Chapter 3</b>	Mouse models for xeroderma pigmentosum group A and group C show divergent cancer phenotypes	64
<b>Chapter 4</b>	Mutational and transcriptional responses upon oxidative damage exposure in <i>Xpc</i> <sup>-/-</sup> mice	82
<b>Chapter 5</b>	Detection of genotoxic and non-genotoxic carcinogens in <i>Xpc</i> <sup>-/-</sup> <i>p53</i> <sup>+/-</sup> mice	106
<b>Chapter 6</b>	Genotoxic exposure: novel cause of selection for a functional $\Delta$ N-p53 isoform	126
<b>Chapter 7</b>	Discussion	144
<b>Samenvatting</b>		150
<b>Curriculum vitae</b>		155
<b>Publications</b>		156



# Chapter 1

# Chapter 1

## Introduction

### **Adapted from:**

**Melis JPM**, Luijten M, Mullenders LHF, van Steeg H.

The role of XPC: Implications in cancer and oxidative DNA damage.

**Mutation Research – Reviews in Mutation Research 2011** Nov; 728(3):107-17

**Melis JPM**, Luijten M, Mullenders LHF, van Steeg H.

Nucleotide Excision Repair and Cancer.

**DNA Repair and Human Health 2011** Oct (ISBN 978-953-307-612-6), InTech

**Melis JPM**, van Steeg H, Luijten M.

Oxidative DNA damage and Nucleotide Excision Repair

**Antioxidants & Redox Signaling [accepted], 2012** Dec, epub ahead of print

*“Some things should be simple. Even an end has a start”*

An End Has A Start – Editors, 2007

## **DNA repair and p53 in aging and cancer – Guardians of genomic stability**

### **1. Introduction**

Cancer ranks as one of the most frequent causes of death worldwide and in Western society it is competing with cardiovascular disease as the number one killer. Reason for this high frequency in Western countries can be attributed to lifestyle and environmental factors, only 5-10% of all cancers are directly due to heredity. Common environmental factors leading to cancer include: diet and obesity (30-35%), tobacco (25-30%), infections (15-20%), radiation, lack of physical activity and environmental pollutants or chemicals [1]. Exposure to these endogenous and exogenous factors causes or enhances abnormalities in the genetic material of cells [2]. These changes in the DNA or hereditary predisposition can result into respectively uncontrolled cell growth, invasion and metastasis. Cancer cells can damage tissue and disturb homeostasis leading to dysfunctions in the body that can eventually lead to death.

Under normal conditions cell growth is under strict conditions and control. Hereditary dysfunctions or introduced DNA damage in tumor suppressor genes, oncogenes or DNA repair genes can create an imbalance that may lead to cancer development. DNA repair and cell cycle arrest pathways are essential cellular mechanisms to prevent or repair substantial DNA damage, which subsequently can cause diseases.

Biologically, DNA is considered to be the key to life, since it determines the whole genetic make up and many predispositions and appearances. DNA is well protected for this matter. For one, DNA is packaged in an ingenious manner so its vulnerability is diminished. Additionally, surveying scavengers try to eliminate harmful molecules in cells to prevent DNA damage. However, cells endure a massive attack daily, which makes it impossible to counteract all insults. This is the paradoxical nature of DNA; it is the key to life, but at the same time in the end, it is also the key to death since DNA damage will eventually lead to mutations and an imbalance in homeostasis, resulting in cancer or other age-related diseases. When inescapable DNA damage does occur, organisms rely on DNA repair pathways to prevent and postpone damage in a way it will give nature time to mend and to live a longer and healthier life.

In this thesis one of the most important and versatile DNA repair pathways, the Nucleotide Excision Repair (NER) pathway, is investigated in relation to carcinogenesis and mechanistic modes of action. Additionally, the role in carcinogenesis of the most frequently mutated gene in (human) cancer, the tumor suppressor p53, has been investigated. Several mouse models that have impaired DNA repair capacity and/or impaired p53 functionality were used to clarify the different roles of involved proteins in DNA repair, cancer predisposition and carcinogenesis. Additionally, these models can be used as an alternative improved model for carcinogenicity testing of compounds.

## 2. DNA damage

Genomic assaults are abundant due to environmental factors and continuously ongoing metabolic processes inside the cell [3]. Endogenous DNA damage occurs at an estimated frequency of approximately 20,000 – 50,000 lesions per cell per day in humans [4,5], which roughly adds up to 10 - 40 trillion lesions per second in the human body. Endogenously generated lesions can result in hydrolysis (e.g. depurination, depyrimidination and deamination), oxidation (8-oxoG, thymine glycol, cytosine hydrates and lipid peroxidation products) and non-enzymatic methylation of the DNA components [6,7]. Besides these endogenous insults to the DNA, exogenous factors can play a significant role in damaging the DNA. Examples of exogenous insults are ionizing radiation (IR), ultraviolet (UV) radiation and exposure to chemical agents. One hour of sunbathing for example generates around 80,000 lesions per cell in the human skin [8]. The endogenous and exogenous primary lesions can result in persistent DNA damage if left unattended. Therefore, repair pathways and cellular responses are of vital importance in the prevention of cancer and age-related diseases. DNA repair pathways come in many varieties, Figure 1 shows a schematic overview of DNA repair responses to several types of DNA damage.

Excision repair pathways and reversal of DNA damage are responsible for the fundamental repair of damaged nucleotides, resulting into the correct nucleotide sequence and DNA structure. Besides damaged nucleotides, cells often sustain fracture of the sugar-phosphate backbone, resulting in single- or double-strand breaks [7]. Repairing the DNA damage can occur in an error-free (e.g. Nucleotide Excision Repair (NER), Base Excision Repair (BER), Homologous Recombination (HR)) or by an error-prone pathway like Non-Homologous End-Joining (NHEJ). Besides DNA repair pathways, DNA damage tolerance mechanisms are active to bypass lesions that normally block replication like Translesion Synthesis (TLS) or template switching. Template switching occurs in an error-free way, while TLS acts in an often error-prone manner (although a few polymerases of this kind are able to handle the lesions in an error-free way). Even though error-prone mechanisms do not result in restoration of the original coding information they do enhance the chances of cell survival, which is preferred over correct genomic maintenance in these cases. In this light, cell cycle checkpoint activation and scheduled cell death (apoptosis) also enhance chances of genomic stability and in some cases cell survival [9]. These responses greatly facilitate the efficiency of repair and damage tolerance. Arrested cell cycle progression will result in an increased time window for DNA repair or damage tolerance to occur. In addition, apoptosis will attenuate the risk of genomic instability by programming the cells with extensive DNA damage for cell death. Hereby, annulling the possible negative effect of the DNA damage in those cells and hence maintaining homeostasis [9].

In human, patients that are affected in these DNA repair or tumor suppressive pathways often suffer from increased or cancer susceptibility or other accelerated age-related phenotypes. Patients affected in the NER pathway for example suffer from severe cancer prone or premature aging syndromes depending on which protein is deficient in the pathway. DNA damage induced by sunlight (UV) or chemical exposure or the body's metabolism can't be repaired sufficiently and thereby causes tumor initiation and/or imbalanced cellular homeostasis. This thesis will focus on the functionality of the NER pathway and the additional role of impaired tumor suppression by loss of functionality of p53.



2.1 Nucleotide excision repair

The abundant targeting of bases and nucleotides in the genome makes the Nucleotide Excision Repair (NER) one of the most essential repair pathways. NER is able to repair a wide range of DNA lesions and can restore the correct genomic information. Additionally, replication and transcription can be continued. This pathway can deal with a broad spectrum of (mostly) structurally unrelated bulky DNA lesions, arisen from either endogenous or exogenous sources. Nucleotide excision repair comprises over 30 proteins that eliminate the helix-distorting lesions. As mentioned, lesions of this matter can originate upon exposures to several damaging agents. For instance, UV radiation (sunshine) is a physical DNA-damaging agent that mainly produces cyclobutane pyrimidine dimers (CPDs) and pyrimidine-(6,4)-pyrimidone products (6-4PP) but is also believed to induce oxidative DNA damage [10]. Exposure to numerous chemicals can result into helix-distorting bulky adducts, for example polycyclic aromatic hydrocarbons (present in cigarette smoke or charcoaled meat) [11] (Figure 1).

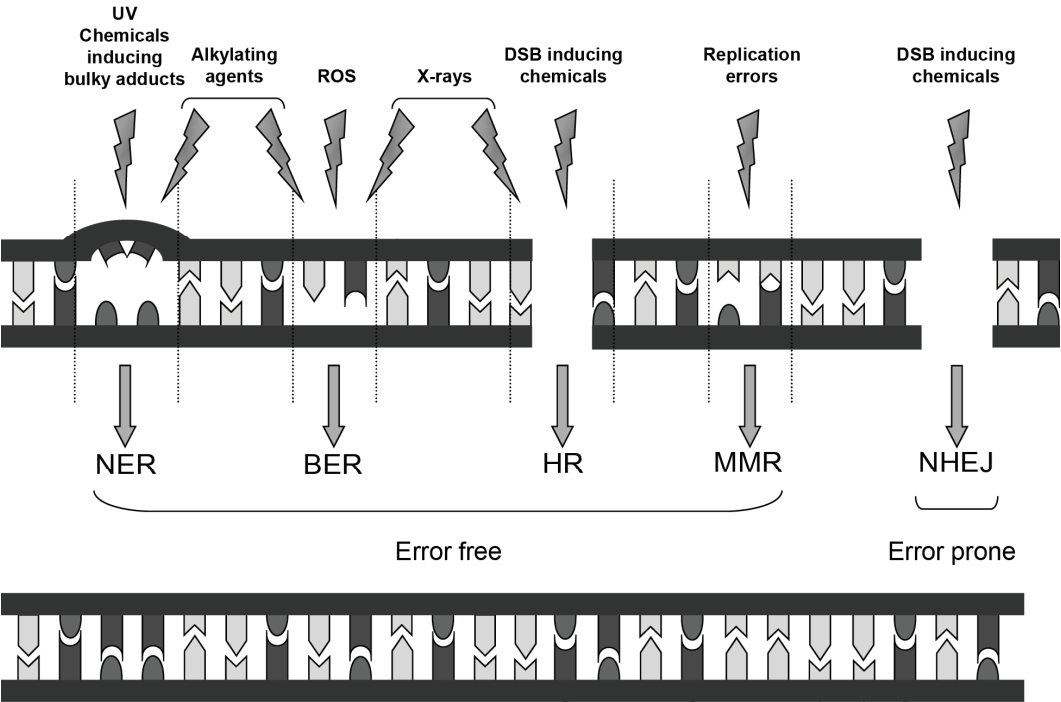


**Figure 1.** DNA repair pathways. Schematic overview of DNA repair pathways. Several types of induced DNA damage can trigger different repair pathways, which can repair the DNA in an error-free or an error-prone manner. NER (nucleotide excision repair), BER (base excision repair), HR (homologous recombination), MMR (mismatch repair), NHEJ (non-homologous end-joining)

### 2.1.1 Global Genome-NER and Transcription Coupled-NER

NER is divided into two subpathways which mechanistically initiate in a divergent manner, but after damage recognition both pathways proceed along the same processes (see Figure 2). The subpathways are designated Global Genome NER (GG-NER) and Transcription Coupled NER (TC-NER). GG-NER recognizes and removes lesions throughout the entire genome, and is considered to be a relatively slow and less efficient process, since it scans the whole genome for DNA damage [12]. However, UV induced helix-distorting lesions like 6-4PPs, are rapidly cleared by GG-NER [13]. TC-NER is responsible for eliminating lesions in the transcribed strand of active genes. This repair process takes care of lesions blocking the transcription machinery and potential subsequent dysfunctions. Since TC-NER is directly coupled to the transcription machinery it is considered to be faster acting and more efficient than GG-NER, but is only initiated when transcription of a gene is blocked.

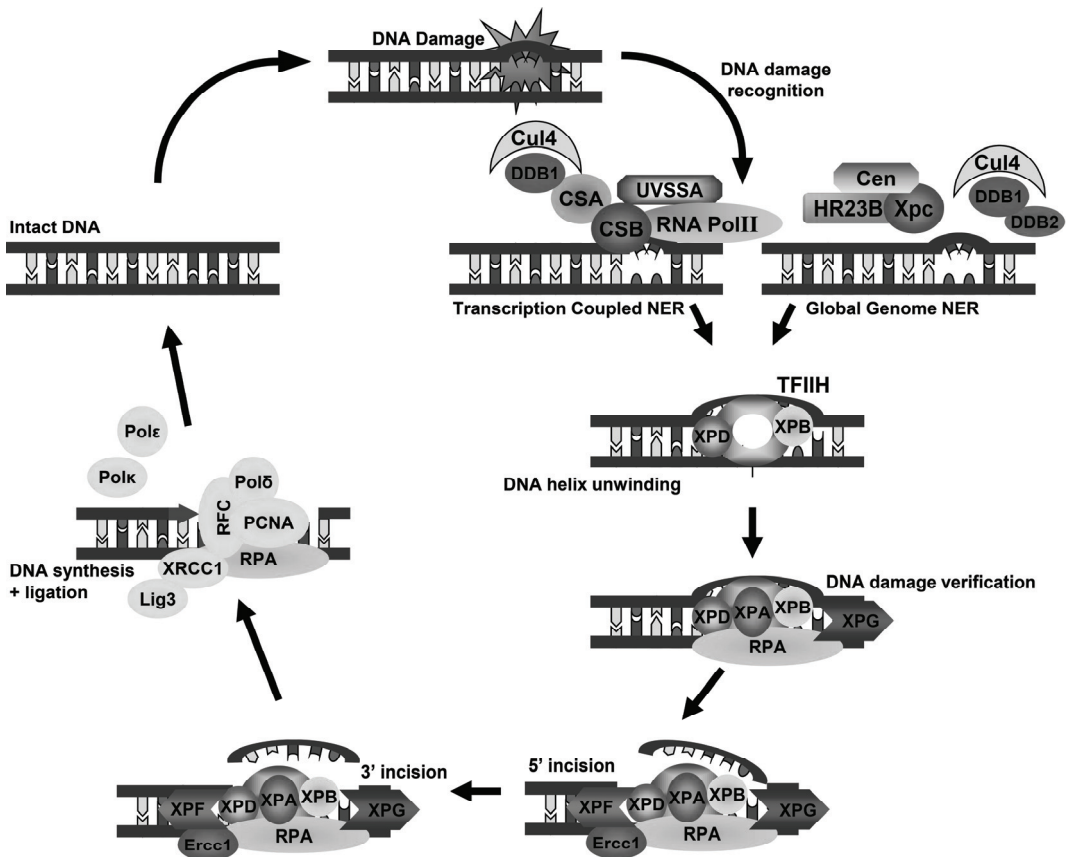


**Figure 2.** Schematic overview of the nucleotide excision repair (NER) pathway. Damaged DNA is recognized by either initial factors of the global genome repair (a.o. XPC) or transcription coupled repair (CSA and CSB), which constitute the two different repair pathways in NER. After DNA damage recognition the repair route progresses along the same way. After helix unwinding and verification the damage incisions are made to remove the faulty stretch of DNA. Finally, DNA synthesis and subsequent ligation reproduce the correct DNA sequence.

### 2.1.2 DNA damage recognition

The difference between the two subpathways is the initial damage recognition step (Figure 2). As mentioned previously, a helical distortion and alteration of DNA chemistry appears to be the first structural element that is recognized. For GG-NER, the XPC/hHR23B complex (including centrin2), together with the UV-Damaged DNA Binding (UV-DDB) protein (assembled by the DDB1 (p127) and DDB2/XPE (p48) subunits), are involved in lesion recognition [14]. The XPC/hHR23B complex is also essential for recruitment of the consecutive components of the NER machinery to the damaged site, also known as the preincision complex [15;16].

It has been shown that XPC itself has affinity for DNA and can initiate GG-NER *in vitro*, but its functionality is enhanced when hHR23b and centrin2 are added [17;18]. Centrin2 as well as hHR23B stabilize the heterotrimer complex, putatively by inhibiting polyubiquitination of XPC and hence preventing subsequent degradation by the 26S proteasome [17]. XPC recognizes various helix-distorting base lesions that do not share a common chemical structure. Biochemical studies have revealed that XPC recognizes a specific secondary DNA structure rather than the lesions themselves [19-21]. XPC (together with DDB1 and DDB2) appears to scan the DNA for distortions by migrating over the DNA, repeatedly binding and dissociating from the double helix [22]. When XPC encounters a lesion the protein changes its conformation and aromatic amino acid residues of XPC stack with unpaired nucleotides opposite the lesion, thereby increasing its affinity and creating a conformation which makes it possible to interact with other NER factors [22].

The binding affinity of XPC to the DNA seems to correlate with the extent of helical distortion. 6-4PP products substantially distort the DNA structure and are more easily recognized by XPC than CPDs, which only induce a minimal helical distortion [23]. More recent studies have indicated that the UV-DDB protein complex facilitates recognition of lesions that are less well-recognized by the XPC-hHR23B complex, like CPDs [24]. The UV-DDB is able to recognize UV-induced photoproducts in the DNA and is now believed to precede binding of XPC-hHR23B to the damaged site. CPD repair is UV-DDB dependent [24;25]. Since affinity of the XPC-hHR23B to CPD sites is low, DDB2 is needed for efficient binding [25]. Upon ubiquitylation DDB2 is degraded by the 26S proteasome [24;26], hereby increasing binding affinity of XPC to the DNA as well as stimulating the interaction of XPC with hHR23B [18;27;28]. Degradation of UV-DDB enhances the binding of XPC-hHR23B to the DNA *in vitro* [23]. Timing of the programmed degradation of DDB2 determines the recruitment of XPC-hHR23B to the UV-damaged site [29].

The XPC protein contains several binding domains: a DNA binding domain, a hHR23B binding domain, centrin2 binding domain and a TFIIH binding domain [30]. TFIIH is a multifunctional transcription initiation factor but is also a core NER component comprising amongst others the helicases XPB and XPD (Figure 2). The complex is essential for the continuation of the NER pathway and is responsible for unwinding the DNA helix after damage recognition by XPC/hHR23B. XPC has been shown to physically interact with TFIIH and *in vivo* and *in vitro* studies show that recruitment of the NER complex to unwind the DNA is executed in a XPC-dependent manner [7;30].

The XPC protein is redundant in TC-NER. Here a stalled RNA polymerase II (RNA polII) is the onset of the NER machinery. CSA and CSB play a crucial role in setting the transcription coupled repair in motion but are also implicated in RNA polII transcription functions. The CSB protein interacts with RNA

polII [31], while CSA does not [32]. CSA mainly interacts with CSB, XAB2 (XPA binding protein 2) and the p44 subunit of the TFIIH complex [33;34]. The function of CSA remains to be elucidated but seems to be implicated in TC-NER during elongation of the transcription process [35;36]. Both CSA and CSB are part of RNA PolII associated complexes, but for CSB additional functions are assigned outside NER [37].

In TC-NER, CSB is thought to be responsible for displacement of the stalled RNA polymerase. Additionally, as with XPC in GG-NER, the preincision complex of NER is recruited in a CSB-dependent manner [38;39]. But first, as in GG-NER, the TFIIH complex is recruited after damage recognition.

### 2.1.3 DNA helix unwinding

After DNA damage recognition and subsequent recruitment of TFIIH, GG-NER and TC-NER converge into the same pathway. The TFIIH complex consists of 10 proteins: XPB, XPD, p62, p52, p44, p34, p8 and the CDK-activating kinase (CAK) complex: MAT1, CDK7 and Cyclin H. TFIIH forms an open bubble structure in the DNA helix [40;41]. The DNA helicases XPB and XPD facilitate the partial unwinding of the DNA duplex in an ATP-dependent manner, allowing the preincision complex to enter the site of the lesion [42] (Figure 2). The preincision complex further consists of the XPA, RPA and XPG proteins and is assembled around the damage site [43] (Figure 2). The function of XPA is verification of the lesion and additionally acts, together with the single strand DNA binding complex RPA, as an organizational factor, so that the repair machinery is positioned around the lesion. Both XPA and RPA are believed to protect the undamaged strand [44;45] and leads to complete opening of the damaged DNA. Some studies suggested this step is essential for the initiation of incision/excision of the damaged DNA [46;47]. Furthermore RPA interacts with several other factors of the nucleotide excision repair pathway, like the endonucleases XPG and the ERCC1-XPF dimer, which are required for the dual incision of the damaged strand (Figure 2). RPA hereby facilitates the correct positioning of the endonucleases and regulates the open complex formation [48;49].

### 2.1.4 Incision, DNA repair synthesis and ligation

When the preincision complex is accurately positioned in relation to the damaged site by the XPA-RPA complex, single strand breaks are introduced by XPG and ERCC1-XPF (Figure 2). Several mechanistic theories were postulated over the years. A general consensus is that the combined actions of XPG and ERCC1-XPF result in excision of a 24-32 nucleotide long single strand fragment including the damaged site [50]. XPG is responsible for the 3' incision and is putatively recruited by the TFIIH complex [43]. According to some studies presence of XPG appears to be necessary for ERCC1-XPF activity, which is responsible for carrying out the 5' incision [7;51]. Others propose a 'cut-patch-cut-patch' mechanism for the incision and resynthesis process within NER, where the 5' incision possibly precedes the 3' incision [52].

XPG is expected to have additional stabilization features, it is able to interact with XPB, XPD and several other subunits of the TFIIH complex [7]. Since loss of XPG results in lethality a few weeks after birth [53] the protein might be involved in systemic and important additional mechanisms, like transcription [54;55]. Furthermore, XPG is believed to play a role in oxidative damage removal [56]. The ERCC1-XPF seems to be a multifunctional complex as well, since it is also involved in interstrand crosslink repair and homologous recombination [57;58].

The excision of the damaged fragment is restored in original (undamaged) state by DNA synthesis and ligation steps (either by cut-patch-cut-patch mechanism or full excision followed by resynthesis and ligation). Both XPG and RPA are thought to be required for the transition between (pre)incision and post-incision events [59]. XPG is thought to be involved in the recruitment of PCNA [52;59]. Resynthesis of DNA requires PCNA because of its ability to interact with DNA polymerases [59]. The way which and how these polymerases are involved in DNA resynthesis is not fully elucidated yet. Recent studies show at least three DNA polymerases are involved. Pol  $\delta$ , Pol  $\kappa$  and Pol  $\epsilon$  are recruited to damage sites (Figure 2). Recent *in vivo* studies show Pol  $\beta$  most likely plays no major role in NER [60;61]. To complete the repair of the damaged DNA site the resynthesized strand needs to be ligated. The primary participant in the subsequent ligation process of NER appears to be the XRCC1-Ligase 3 complex, which is shown to accumulate in both quiescent as well as proliferating cells [61]. Ligase 1 appears to be involved in the ligation step in proliferating cells only [61]. To date, the cross play of over 40 proteins in total is involved in NER to counteract DNA damage in the error free manner described above.

### 3. NER in cancer and aging

DNA repair is vital to all organisms and a defect in one of the genes involved can result in severe syndromes or diseases by loss of genomic stability. Essential consequences of genomic instability can be cancer and other age-related diseases, such as neurological disorders like Huntington's disease and ataxias [7]. DNA damage for example can cause mutations that trigger (pre-)oncogenes, inactivate tumor suppressor genes or other indispensable genes which cause loss of homeostasis. Therefore, organisms that harbor defective DNA repair are often more prone to develop cancer or (segmental) age-related diseases.

In humans, several syndromes have been identified which are the result of an impaired nucleotide excision repair pathway, of which Xeroderma pigmentosum (XP), Cockayne syndrome (CS) and Trichothiodystrophy (TTD) are the most well-known. Since NER is the major defense against UV-induced DNA damage, all three syndromes are hallmarked by an extreme UV-sensitivity, of which XP ensues a highly elevated risk of developing skin cancer [7;62].

The involvement of NER genes in rare and severe syndromes underscores the vital importance of this repair pathway. It is known that accumulative DNA damage is one of the most important causes in cancer development and loss of homeostasis in organisms [4;7;8;11;62]. Defects in DNA repair pathways are therefore also considered to accelerate aging and tumorigenesis. In defective NER both types of endpoints occur, XP patients are predisposed to cancer development while CS and TTD patients are not. The latter exhibit premature aging features which XP patients lack [7;11;62]. Reason for this might be the involvement of several NER proteins in other cellular mechanisms. CSB is believed to be involved in (TC-)BER, while XPD (of which deficiency causes TTD) is assigned to be involved in replication and transcription. Some of these affected mechanisms could overshadow the cancer prone phenotype of a NER deficiency. Severely affected developmental and neurological processes could be more life threatening on the shorter term than tumor development is. This could be the rationale behind the fact that CS and TTD patients are extremely short-lived and not cancer prone. Since the focus of this thesis is the impact of deficiencies in NER on carcinogenesis, the XP syndrome will be discussed in more detail. The CS and TTD syndromes will not be discussed in detail in this thesis, but

more information and details can be obtained in the comprehensive review of NER by Cleaver et al [62].

### 3.1 Xeroderma pigmentosum

Xeroderma pigmentosum (XP), meaning parchment pigmented skin, was the first human causal NER-deficient disease identified [62]. It is a rare, autosomal inherited neurodegenerative and skin disease in which exposure to sunlight (UV) leads to skin cancer. In Western Europe and the USA the incidence frequency is approximately 1:250.000, rates are higher in Japan (1:40.000). XP-C and XP-A are the most common complementation groups of XP [63].

Early malignancies in the skin, eyes and the tip of the tongue develop due to sun-exposure (Table 1). Additionally, benign lesions like blistering, hyperpigmented spots and freckles are abundant. XP is associated with a more than 1000-fold increase in risk of developing skin cancer, comprising basal and squamous cell carcinomas (45% of the XP patients) and to a lesser extent melanomas [7]. Besides skin cancers, XP patients have a 10-20 fold increased risk of developing internal cancers [64]. The median latency time for cutaneous neoplasms is 8 years, which is much shorter as compared to the general population in which the mean latency time is 50 years longer [65]. Progressive neurological degeneration occurs in approximately 20% of the XP patients and can be correlated to deficiencies in specific XP genes (XPA, XPB, XPD and XPG) [62]. XP-C and XP-F patients rarely develop neurological disorders [7,65]. The heterogeneity in symptoms is correlated to the genetic heterogeneity in XP patients. XP-A, XP-B, XP-D and XP-G patients are in general severely affected, possibly because these patients are defective in both the GG-NER and TC-NER subpathways. Solely GG-NER is defective in XP-C and XP-E patients. This could be the reason that XP-C patients suffer less from sunburn. XP-C and XP-E cells have shown higher survival rates after UV exposure than XP-A and XP-D cells for example [7].

Most abundant XP variants in human are XP-A and XP-C (~50% of all XP cases) [66]. To investigate the involvement of these proteins on survival, aging and cancer development mouse models were created, mimicking existing NER mutations or deletions in humans. These mouse models are also crossed with the cancer prone p53 mouse model to investigate the role of NER and p53 in carcinogenesis.

Feature	%/age	Feature	%/age
<i>Cutaneous abnormalities</i>		<i>Neurological abnormalities</i>	
Median age of onset of symptoms	1.5 yr	Median age of onset	6 mo
Median age of onset of freckling	1.5 yr	Association with skin problems	33%
Photosensitivity	19%	Association with ocular abnormalities	36%
Cutaneous atrophy	23%	Low intelligence	80%
Cutaneous telangiectasia	17%	Abnormal motor activity	30%
Actinic keratoses	19%	Areflexia	20%
Malignant skin neoplasms	45%	Impaired hearing	18%
Median age of first cutaneous neoplasm	8 yr	Abnormal speech	13%
<i>Ocular abnormalities</i>		Abnormal EEG	11%
Frequency	40%	Microcephaly	24%
Median age of onset	4 yr	<i>Abnormalities associated with neurological defects</i>	
Conjunctival injection	18%	Slow growth	23%
Corneal abnormalities	17%	Delayed secondary sexual development	12%
Impaired vision	12%		
Photophobia	2%		
Ocular neoplasms	11%		
Median age of first ocular neoplasm	11 yr		

**Table 1.** Overview of most abundant XP features, including average age of onset or frequency of the specific feature in patients overall (indicated by %)

## 3.2 p53 in DNA repair and cell cycle arrest

p53 is the most mutated gene found in (human) cancers. Previous reports estimated that over 50% of the cancers have a mutation in the p53 gene; however, a more recent update even mentions p53 is mutated in 70% of the human cancers (15<sup>th</sup> p53 workshop 2010). In addition, p53 appears to be one of the key regulatory proteins in the cell and is connected to a broad variety of molecular mechanisms. The p53 was first identified as a cellular partner of an oncoprotein in the tumor Simian Virus, but was later dubbed as a tumor suppressor and designated as a transcription factor induced by stress, which can promote cell cycle arrest, apoptosis and senescence [67]. More recently, additional functions were added to the functional spectrum of p53, e.g. the regulation of metabolic pathways and cytokines that are required for embryo implantation [67]. One of the most pivotal roles of p53 is guarding the genome and tissue homeostasis.

The crucial event in the induction of the p53 pathway is the uncoupling of p53 from its key negative regulators, principally MDM2 and MDM4, which leads to the accumulation of stable active p53 (Figure 3). P53 induction in response to DNA damage is coordinated by the ataxia–telangiectasia mutated

(ATM) and ataxia–telangiectasia and Rad3-related (ATR) protein kinases, which mediate the rapid destruction of MDM2 and MDM4 [68;69].

ATM plays a crucial part in the immediate response to double-strand breaks, while replication stress and DNA crosslinking [70] is coordinated mainly through ATR, although interplay does exist. P53 also plays a role in regulating NER ([71;72]).

P53 is stabilized and activated in response to a wide range of cellular stresses, including DNA damage and hyperproliferation [70;73]. Downstream p53 effects are possible by altering gene expression in several processes. Antiproliferative functions of p53 include cell cycle checkpoints, cellular senescence and apoptosis [7;70;74].

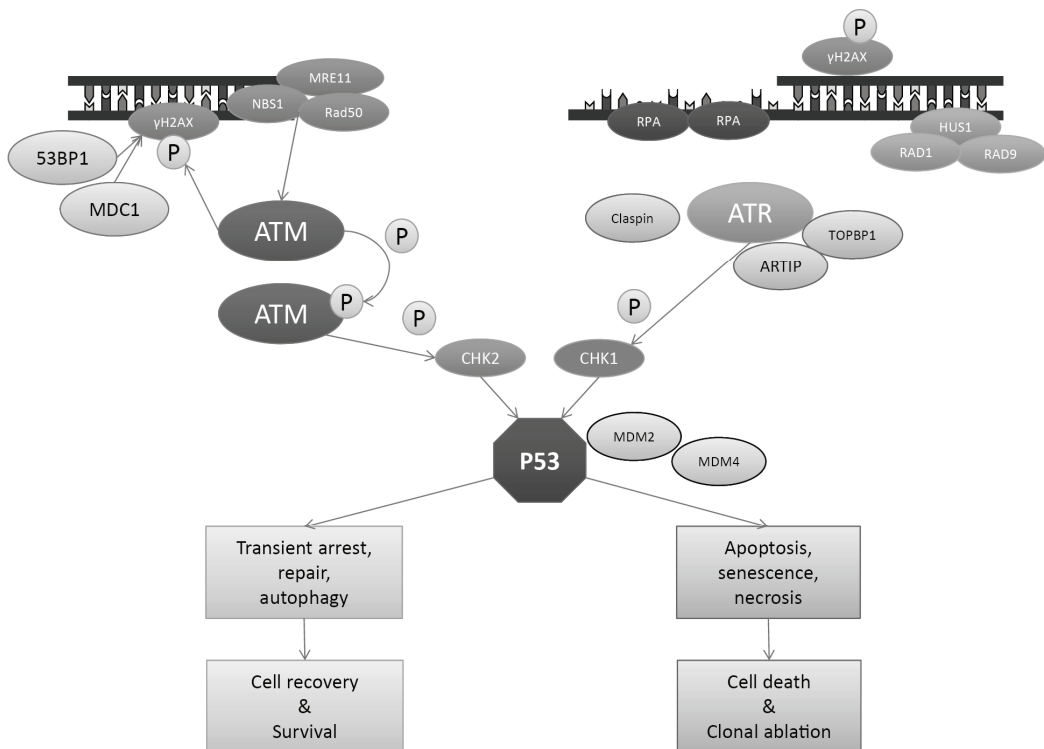


**Figure 3.** Schematic overview of DNA damage response and p53-signaling

Cell cycle checkpoints ensure the fidelity of cell division, verifying whether the processes at each phase of the cell cycle are accurately completed before progression into the following phase. Upon cellular stress cells can undergo growth arrest at these checkpoints, in which p53 regulation plays a key role. Cells can also enter a state of permanent cell cycle arrest, called senescence. Dysfunctional telomeres, DNA damage and excessive mitochondrial signaling are some of the causes that can induce senescence via p53 [74]. Apoptosis is another important effector function of downstream p53



regulation where cells are forced into cell death. In contrast to traumatic cell death (necrosis) apoptosis is a functional, programmed and overall beneficial process. Defective apoptotic routes can lead to a variety of diseases and complications, one of them being cancer development.

The protein's key role in tumor suppression and the fact that p53 has been implied in interacting with and regulation of NER made it very interesting to create mouse models that lack either functional NER and/or have diminished p53 functionality.

## 4. Cancer research - XP and p53 mouse models

### 4.1 NER mouse models in cancer research

To investigate the role of the proteins involved in NER on survival and cancer development several transgenic mouse models were created, mimicking the existing NER mutations or deletions in humans.

Mouse model	Affected repair pathway	Enhanced spontaneous tumor response	Reference	Accelerated aging/developmental problems	Reference
<i>Xpa</i> <sup>-/-</sup>	GG-NER/TC-NER	Yes, liver	[ <sup>81-83</sup> ], this thesis	Shorter median life span, no pathology	This thesis, [ <sup>82</sup> ]
<i>Xpb</i> <sup>-/-</sup>	NER/transcription	n.a.		Very early lethality (2-cell stage)	[ <sup>120</sup> ]
<i>Xpc</i> <sup>-/-</sup>	GG-NER	Yes, lung	[ <sup>82;102</sup> ], this thesis	Shorter life span	This thesis, [ <sup>82</sup> ]
<i>Xpd</i> <sup>TD</sup>	NER/transcription	No	[ <sup>121;122</sup> ]	Shorter life span, aging and CR pathology	[ <sup>121;122</sup> ]
<i>Xpd</i> <sup>XPCS</sup>	NER/transcription	n.d.			
<i>Xpe (DDB2)</i> <sup>-/-</sup>	GG-NER	Yes, various	[ <sup>28;123</sup> ]		
<i>Xpf</i> <sup>m/m</sup>	NER/ICL	n.a.		Very short life span, maximum 3 weeks	[ <sup>124</sup> ]
<i>Xpg</i> <sup>-/-</sup>	TCR/transcription	n.a.		Very short life span, maximum 3 weeks	[ <sup>125</sup> ]
<i>mHR23B</i> <sup>-/-</sup>	GG-NER	n.a.		Very short life span/embryonic lethality	[ <sup>126</sup> ]
<i>Csa</i> <sup>-/-</sup>	TC-NER	No	[ <sup>127</sup> ]		
<i>Csb</i> <sup>-/-</sup>	TCR/transcription	No	[ <sup>128</sup> ]	Normal life span, mild pathology	[ <sup>128</sup> ], unpublished results
<i>Ercc1</i> <sup>-/-</sup>	NER/ICL	n.a.		Very short life span, maximum 4 weeks	[ <sup>129;130</sup> ]
<i>Ercc1</i> <sup>Δ7/-</sup>	NER/ICL	No	van Steeg / Dollé	Short life span of 4–6 months	[ <sup>130</sup> ]

**Table 2.** Overview of spontaneous phenotypes of a selection of NER-deficient mouse models.

n.a.: not applicable, mouse models are too short lived to develop tumors, n.d.: not determined

Table 2 shows an overview of a selection of NER mouse models and their accompanying spontaneous phenotypes. Selected knockout mouse models (*Xpa* and *Xpc*) are described in more detail further below. These two models show a decreased lifespan in comparison to their concurrent wild type controls, but not as extreme as some other NER-deficient mouse models described in Table 2. Therefore the *Xpa* and *Xpc* mouse models survive long enough to study the effect of impaired NER on cancer development. Others, like *Xpb*, *Xpf*, *Xpg* and *Ercc1*-deficient models for example are too short lived to study carcinogenesis, but show signs of accelerated aging and are used to study this process.

#### 4.1.1 *Xpa*-deficient mouse model

The first DNA repair defective models were the *Xpa*-deficient mouse models, generated by de Vries et al. [75] and independently by Nakane et al [76]. *Xpa*-deficient mice appeared more cancer prone compared to their heterozygote and wild type littermates when exposed to carcinogenic and genotoxic compounds [77-81]. As in humans, the mouse model exhibited a marked predisposition to skin cancer upon UV treatment of shaved dorsal skin [75].

Survival studies without directed exposure were performed initially in a mixed genetic background, *i.e.* C57BL/6J/Ola129<sup>[81]</sup> and C3H/heN strains<sup>[77]</sup> and in fairly small numbers. However, both studies indicated that *Xpa*<sup>-/-</sup> mice (from here mentioned as *Xpa* mice) developed a significant number of spontaneous liver tumors. The C3H/heN strain wild type mice already showed 47% liver tumor incidence in the male mice within 16 months. The C57BL/6J/Ola129 mice were more resilient, but no enhanced mortality was observed until the age of 1.5 years. The *Xpa* mice showed a 15% hepatocellular adenoma tumor incidence after 20 months, while there were no tumors in the wild type and heterozygote littermates of the same age. The lack of a congenic background for this and other mouse models made it harder to investigate the phenotype in these mice. Therefore, an *Xpa* mouse model in a congenic C57BL/6J background was investigated (this thesis) [82]. C57BL/6J mice showed a low baseline tumor response and appear therefore suitable for studying mutagenesis and tumorigenesis. In a congenic background a significant increase in liver tumors was also observed (10%). A small (but not significant) increase in lung tumors was also observed (6.6% of the *Xpa* mice) (this thesis) [82]. Correspondingly, mutation accumulation in the C57BL/6J *Xpa* mice was significantly increased during survival compared to wild type mice in liver, implicating an *Xpa* repair defect and subsequent mutation induction in carcinogenesis (this thesis) [82].

Like human XP-A patients, *Xpa* mice appeared predisposed to skin cancer after UV light exposure to shaved dorsal skin of the mice [75;83]. Heterozygous *Xpa* mice did not show this cancer prone phenotype after UV exposure, not even when the *Xpa* mutation was crossed in in hairless mice [84]. Skin cancer predisposition in XP mice might not only involve NER deficiency, but several reports indicate enhanced immunosuppression and impaired natural killer cell function are involved [85-87]. *Xpa* mice were also predisposed to tumors of the cornea when exposed to UV radiation, see Table 3 [88].

Chemical exposure of *Xpa*<sup>-/-</sup> mice to 7,12-dimethyl-1,2-benz[a]anthracene (DMBA) also resulted in skin cancer [75]. Several chemical exposures in *Xpa* mice however shed some more light on the cancer development other than skin cancer, which in humans is the predominant tumor phenotype (Table 3). For example, oral treatment of *Xpa*-deficient mice with genotoxic carcinogens like benzo[a]pyrene (B[a]P), 2-acetylaminofluorene (2-AAF), and 2-amino-1-methyl-6-phenylimidazo [4,5-b]-pyridine (PhIP)

resulted in lung tumors and lymphomas (B[a]P), liver and bladder tumors (2-AAF) and intestinal adenomas plus lymphomas (PhIP) [81;89-91]. Other human carcinogens like Cyclosporin A and DES, although not directly mutagenic, showed to be carcinogenic in *Xpa* mice after 39 week exposure, but in contrast the low potent human carcinogen phenacetin did not result in a significant increase in tumors.

Mouse model	Treatment	Target	Enhanced tumor response*	References
<i>Xpa</i>	UV-B radiation	Skin, eye	Yes	[75;76]
	DMBA paint + TPA	Skin	Yes	[75;76]
	B[a]P gavage	Multiple, lymphomas	Yes	[92;94]
	B[a]P diet	Stomach, esophagus	Yes	[131]
	B[a]P intratracheal instillation	Lung	Yes	[91]
	AFB1 i.p. injection	Liver	Yes	[77]
	PhIP diet	Lung, lymphoma, small intestine	Yes	[132]
	4NQO drinking water	Tongue	Yes	[78]
	2-AAF diet	Liver, bladder, gall bladder	Yes	[79;133]
	CsA	Lymphoma	Yes	[134]
	DES	Osteosarcoma, lymphoma	Yes	[135]
	Wyeth 14.643	Liver	Yes	[133]
	DEHP	Liver	No	This thesis
	p-cres	Liver	Yes	Unpublished results
	Phenacetin	Kidney	No	[136]
<i>Xpc</i>	UV-B radiation	Skin	Yes	[95;97]
	2-AAF diet	Liver, bladder	Yes	[79]
	AAF i.p. injection	Liver, lung	Yes	[101]
	NOH-AAF i.p. injection	Liver, lung	Yes	[101]
	DEHP	Liver	No	This thesis
	p-cres	Liver	Yes	Unpublished results

**Table 3.** Overview of carcinogen exposure in the *Xpa* and *Xpc* mouse models.

\* in comparison to the untreated controls

*LacZ* and *Hprt* mutation measurements in *Xpa* mice after B[a]P and 2-AAF treatment showed a 2-3 fold increase in mutations compared to wild type mice only after 12-13 weeks of exposure [79;92-94]. This increase in mutational load in comparison to wild type indicates *Xpa* mice are more sensitive to mutation accumulation, which consequently corresponds to the increased cancer susceptibility of *Xpa* mice.

The increased sensitivity towards cancer development of *Xpa* mice made it possible to identify genotoxic carcinogens even more accurate and faster when combined with heterozygosity for p53.

This latter mouse model could be beneficial in reducing and refining *in vivo* carcinogenicity testing of compounds.

#### 4.1.2 *Xpc*-deficient mouse model

Two independent *Xpc*-deficient mouse models were also created in the mid-nineties [95,96]. As the *Xpa* mouse model, this model is also informative for human XP and cancer development in general. The model is especially interesting since it is only defective for GG-NER and not for TC-NER. Hereby, differences between pathways can be investigated in *Xpc* and *Xpa*-deficient mouse models.

As in human XP-C patients, *Xpc* mice are highly predisposed to UV radiation-induced skin cancer (Table 3) [95,97-100]. Contrasting to *Xpa*<sup>+/-</sup> mice the heterozygous *Xpc* mice are more susceptible to UV-induced skin cancer when compared to their wild type littermates [99]. The haploinsufficient sensitivity could mean that XPC is a rate limiting factor in NER. Exposure studies with 2-AAF using *Xpc* mice showed a significant predisposition to liver and lung tumors compared to the heterozygous *Xpc* mice and wild types (Table 3) [7,101]. NER is believed to be the sole pathway to remove CPD and 6-4PP lesions, while for several other lesions different repair mechanisms are also present in the cell. In human, other types of cancer generally do not develop fast enough and are possibly overshadowed by skin cancers in XP. Internal tumor incidence is therefore higher in XP mice than in human XP, since mice are not normally exposed to UV.

In a mixed genetic background (C57BL/6J/129) no decrease in survival was found in relation to wild type mice, even though *Xpc* mice showed an extremely high and significantly increased lung tumor incidence (100%). However, the wild type mice were not genetically related to the *Xpc* mice in this study [102]. The spontaneous survival characteristics of *Xpc*-deficient mouse model in a congenic C57BL/6J background together with their related wild type littermates were also investigated (this thesis). *Xpc* mice exhibited a significant decrease in survival, again showed a significant increase in lung and liver tumors and an increased mutation accumulation in these tissues compared to wild type mice (this thesis) [82]. Here, *Xpc* mice showed a divergent tumor spectrum from *Xpa* mice in the same genetic C57BL/6J background. The additional increase in lung tumor development in two independent spontaneous survival studies indicated that XPC is involved in other pathways besides NER. A corresponding strong increase in mutational load during aging was found in lungs of the C57BL/6J *Xpc* mice, which was not the case in *Xpa* mice (this thesis) [82]. Uehara *et al.* [103] have shown that enhanced spontaneous age-related mutation accumulation in *Xpc* mice is tissue dependent. Liver, lung, heart and spleen exhibited an increase in mutant frequency compared to wild type, while this difference was not visible in brain and small intestine. Compared to *Xpa* mice mutant frequency is higher in *Xpc* in liver, lung and spleen, just as the tumor incidence (this thesis) [82]. The additional mutation increase in *Xpc* mice might be caused by increased sensitivity towards oxidative DNA damage. XPC functioning has been implied in other DNA repair pathways like base excision repair and non-homologous end joining or might be involved in redox homeostasis [103-109]. Exposures to B[a]P [110], 3,4-epoxy-1-butene (EB) [110], DMBA [111] and UV-B [112] also showed significantly enhanced mutant frequencies compared to wild type mice in several tissues. Direct comparisons to *Xpa* mice in these studies have not been made, however when *Xpa* and *Xpc* mice were exposed to pro-oxidants (DEHP and paraquat) for 39 weeks, *Xpc* again exhibited a higher mutant frequency than *Xpa* (this thesis).

### 4.1.3 *Xpa*\**p53* and *Xpc*\**p53*-deficient mouse models

Several p53 mouse models have been created over the last decades, many of which are accompanied by an increased response in tumor incidence and tumor onset. The *Trp53* knockout mouse develops normally but has an early spontaneous tumor response, on average 4-5 months of age [<sup>113;114</sup>]. The heterozygous knockout *Trp53* mouse, is also prone to low spontaneous (~50% of the animals after 18 months) and induced tumor formation [<sup>115</sup>]. Spontaneous tumor formation after 26 weeks in p53 heterozygote mice however is low (2.8% in males, 6% in females [<sup>115</sup>]). The heterozygote p53 model is, because of the relatively low spontaneous tumor incidence, suitable for detecting possible carcinogenic potency of compounds (up to 9 months of exposure). However, this model appeared to produce a high rate of false negative and false positive compounds in carcinogenicity testing [<sup>116</sup>].

A deficiency in either the *Xpa* or *Xpc* gene with the heterozygote state of *Trp53* in mice was combined to investigate carcinogenesis and additionally the potential use of these double mutants in carcinogenicity testing ([<sup>117</sup>], this thesis). DNA damage accumulation normally induces a p53 driven anti-proliferative response. The *XP*\**p53* double mutant mouse models would theoretically be able to accumulate more DNA damage, especially upon genotoxic exposure. We have shown that an increase in incidence and a shorter latency period for developing cancer is the result of genotoxic exposure, due to the diminished tumor suppressive capacity of p53. Therefore, the deficient *XP*\**p53* mouse models appear to be suitable for identifying carcinogens.

Previously, we have been able to demonstrate that *Xpa*\**p53* is a promising mouse model to test carcinogenic potency of compounds for humans [<sup>117;118</sup>]. Very high accuracy for predicting genotoxic carcinogenic compounds was established in a relatively short-term bioassay. However, exposure doses have to be adapted compared to the wild type situation to test compound carcinogenicity since *Xpa* deficiency leads to an increased sensitivity towards toxicity (this thesis). The *Xpc*\**p53* mouse model appears to be even more promising for predicting carcinogenicity of compounds ([<sup>119</sup>], this thesis). Since the XPC protein is dispensable for transcription coupled repair, the toxicity sensitivity is comparable to wild type, while the increased sensitivity towards genotoxic carcinogenic compounds remains. Additionally, several non-genotoxic carcinogens which are normally hard to distinguish from non-carcinogens other than in a two-year bioassay can be correctly assessed by the *Xpc*\**p53* model (this thesis).

## 5. Aim and Outline of this thesis

As mentioned in the introduction (**Chapter 1**), the role of DNA repair and tumor suppressor p53 in maintaining genomic stability is vital. Loss of function of DNA repair genes or the p53 gene has a substantial effect on cancer susceptibility. In this thesis the role of the highly versatile and essential DNA repair pathway, the Nucleotide Excision Repair (NER), has been investigated in regards to cancer development. NER-deficient mouse models have been created to mimic the human NER-deficiency, resulting in the highly cancer prone syndrome Xeroderma pigmentosum. Mouse models deficient for two key proteins in NER, XPA or XPC, have been investigated in this thesis. Extensive phenotyping studies have been performed in wild type mice, *Xpa* and *Xpc* mouse models. **Chapter 2** elaborates on the normal (wild type) survival and aging study. Here we investigated which parameters and processes are changed and regulated on pathological and transcriptional level during lifetime and could be

indicative for and contribute to age-related diseases like cancer, inflammation and cardiovascular disease.

The survival studies of both NER-deficient mouse models used for phenotyping these models, demonstrated that these mice are more cancer prone than the wild type mice, even without additional (carcinogenic) exposure (**Chapter 3**). Although being functional in the same DNA repair pathway, the two models exhibited a divergency in mutation induction and consequential tumor spectrum (**Chapter 3**). We accredited the XPC protein having an additional function outside NER, involved in oxidative damage prevention or repair. Therefore, we exposed both NER-deficient mouse models and wild type controls to pro-oxidants. This study indicated that *Xpc*-deficient mice are more sensitive to oxidative DNA damage, resulting in an increased mutational load and subsequent cancer risk (**Chapter 4**). Gene expression profiling revealed that *Xpc*<sup>-/-</sup> mice have a lower anti-oxidant response than *Xpa*<sup>-/-</sup> and wild type mice, supporting recent *in vitro* results by others and possibly explaining the sensitive response towards oxidative DNA damage and the increase in lung tumor response (**Chapter 3 + 4**).

**Chapter 5** describes the effect on cancer susceptibility when NER-deficiency is combined with *p53* heterozygosity. The effect of increased DNA damage accumulation and deregulation in tumor suppressor response results in an increased cancer proneness, which could be applicable as a suitable alternative method for short-term carcinogenicity testing. The *Xpa*\**p53* and *Xpc*\**p53* mouse models were compared to each other in regards to their cancer susceptibility, testing genotoxic as well as non-genotoxic carcinogens. Exposure to one of the genotoxic compounds, 2-AAF, resulted in a substantial increase in bladder tumors, which was also shown in heterozygous *p53* mice. We discovered that this exposure resulted in a novel route of expression of a functional *p53* isoform, namely through the introduction of selective nonsense mutations in the 5' part of the murine *p53* gene (**Chapter 6**). All findings and general conclusions are described in **Chapter 7**.

## Reference List

- [1] P.Anand, A.B.Kunnumakkara, C.Sundaram, K.B.Harikumar, S.T.Tharakan, O.S.Lai, B.Sung, B.B.Aggarwal. Cancer is a preventable disease that requires major lifestyle changes, *Pharm.Res.*, 25, (2008) 2097-2116.
- [2] Kinzler KW, Vogelstein B. The genetic basis of human cancer, McGraw-Hill, New York, 2002.
- [3] H.Lodish, A.Berk, P.Matsudaira, C.A.Kaiser, M.Krieger, M.P.Scott, S.L.Zipurksy, J.Darnell. *Molecular Biology of the Cell*, WH Freeman, 2004.
- [4] T.Lindahl. Instability and decay of the primary structure of DNA, *Nature*, 362, (1993) 709-715.
- [5] E.C.Friedberg. Out of the shadows and into the light: the emergence of DNA repair, *Trends Biochem.Sci.*, 20, (1995) 381.
- [6] J.Cadet, T.Douki, D.Gasparutto, J.L.Ravanat. Oxidative damage to DNA: formation, measurement and biochemical features, *Mutat.Res.*, 531, (2003) 5-23.
- [7] E.C.Friedberg, G.C.Walker, W.Siede, R.D.Wood, R.A.Schultz, T.Ellenberger. *DNA Repair and Mutagenesis*, ASM Press, 2006.
- [8] E.Mullaart, P.H.Lohman, F.Berends, J.Vijg. DNA damage metabolism and aging, *Mutat.Res.*, 237, (1990) 189-210.
- [9] J.Bartek, J.Lukas. DNA damage checkpoints: from initiation to recovery or adaptation, *Curr.Opin.Cell Biol.*, 19, (2007) 238-245.
- [10] H.L.Lo, S.Nakajima, L.Ma, B.Walter, A.Yasui, D.W.Ethell, L.B.Owen. Differential biologic effects of CPD and 6-4PP UV-induced DNA damage on the induction of apoptosis and cell-cycle arrest, *BMC.Cancer*, 5, (2005) 135.
- [11] J.de Boer, J.H.Hoeijmakers. Nucleotide excision repair and human syndromes, *Carcinogenesis*, 21, (2000) 453-460.
- [12] L.P.Guarente, L.Partridge, D.C.Wallace. *Molecular Biology of Aging*, Cold Spring Harbor Laboratory Press, 2008.
- [13] G.A.Garinis, J.Jans, G.T.van der Horst. Photolyases: capturing the light to battle skin cancer, *Future.Oncol.*, 2, (2006) 191-199.
- [14] R.Dip, U.Camenisch, H.Naegeli. Mechanisms of DNA damage recognition and strand discrimination in human nucleotide excision repair, *DNA Repair (Amst)*, 3, (2004) 1409-1423.
- [15] M.Yokoi, C.Masutani, T.Maekawa, K.Sugasawa, Y.Ohkuma, F.Hanaoka. The xeroderma pigmentosum group C protein complex XPC-HR23B plays an important role in the recruitment of transcription factor IIH to damaged DNA, *J.Biol.Chem.*, 275, (2000) 9870-9875.
- [16] S.J.Araujo, E.A.Nigg, R.D.Wood. Strong functional interactions of TFIIH with XPC and XPG in human DNA nucleotide excision repair, without a preassembled repairosome, *Mol.Cell Biol.*, 21, (2001) 2281-2291.
- [17] R.Nishi, Y.Okuda, E.Watanabe, T.Mori, S.Iwai, C.Masutani, K.Sugasawa, F.Hanaoka. Centrin 2 stimulates nucleotide excision repair by interacting with xeroderma pigmentosum group C protein, *Mol.Cell Biol.*, 25, (2005) 5664-5674.
- [18] M.Araki, C.Masutani, M.Takemura, A.Uchida, K.Sugasawa, J.Kondoh, Y.Ohkuma, F.Hanaoka. Centrosome protein centrin 2/caltractin 1 is part of the xeroderma pigmentosum group C complex that initiates global genome nucleotide excision repair, *J.Biol.Chem.*, 276, (2001) 18665-18672.
- [19] K.Sugasawa, T.Okamoto, Y.Shimizu, C.Masutani, S.Iwai, F.Hanaoka. A multistep damage recognition mechanism for global genomic nucleotide excision repair, *Genes Dev.*, 15, (2001) 507-521.
- [20] K.Sugasawa, Y.Shimizu, S.Iwai, F.Hanaoka. A molecular mechanism for DNA damage recognition by the xeroderma pigmentosum group C protein complex, *DNA Repair (Amst)*, 1, (2002) 95-107.
- [21] J.H.Min, N.P.Pavletich. Recognition of DNA damage by the Rad4 nucleotide excision repair protein, *Nature*, 449, (2007) 570-575.
- [22] D.Hoogstraten, S.Bergink, J.M.Ng, V.H.Verbiest, M.S.Luijsterburg, B.Geverts, A.Raams, C.Dinant, J.H.Hoeijmakers, W.Vermeulen, A.B.Houtsmuller. Versatile DNA damage detection by the global genome nucleotide excision repair protein XPC, *J.Cell Sci.*, 121, (2008) 2850-2859.
- [23] K.Sugasawa, Y.Okuda, M.Saijo, R.Nishi, N.Matsuda, G.Chu, T.Mori, S.Iwai, K.Tanaka, K.Tanaka, F.Hanaoka. UV-induced ubiquitylation of XPC protein mediated by UV-DDB-ubiquitin ligase complex, *Cell*, 121, (2005) 387-400.
- [24] M.E.Fitch, S.Nakajima, A.Yasui, J.M.Ford. In vivo recruitment of XPC to UV-induced cyclobutane pyrimidine dimers by the DDB2 gene product, *J.Biol.Chem.*, 278, (2003) 46906-46910.
- [25] J.Y.Tang, B.J.Hwang, J.M.Ford, P.C.Hanawalt, G.Chu. Xeroderma pigmentosum p48 gene enhances global genomic repair and suppresses UV-induced mutagenesis, *Mol.Cell*, 5, (2000) 737-744.

- [26] V.Rapic-Otrin, M.P.McLenigan, D.C.Bisi, M.Gonzalez, A.S.Levine. Sequential binding of UV DNA damage binding factor and degradation of the p48 subunit as early events after UV irradiation, *Nucleic Acids Res.*, 30, (2002) 2588-2598.
- [27] T.G.Ortolan, L.Chen, P.Tongaonkar, K.Madura. Rad23 stabilizes Rad4 from degradation by the Ub/proteasome pathway, *Nucleic Acids Res.*, 32, (2004) 6490-6500.
- [28] J.M.Ng, W.Vermeulen, G.T.van der Horst, S.Bergink, K.Sugasawa, H.Vrieling, J.H.Hoeijmakers. A novel regulation mechanism of DNA repair by damage-induced and RAD23-dependent stabilization of xeroderma pigmentosum group C protein, *Genes Dev.*, 17, (2003) 1630-1645.
- [29] M.A.El Mahdy, Q.Zhu, Q.E.Wang, G.Wani, M.Praetorius-Ibba, A.A.Wani. Cullin 4A-mediated proteolysis of DDB2 protein at DNA damage sites regulates in vivo lesion recognition by XPC, *J.Biol.Chem.*, 281, (2006) 13404-13411.
- [30] K.Sugasawa. XPC: its product and biological roles, *Adv.Exp.Med.Biol.*, 637, (2008) 47-56.
- [31] D.Tantin, A.Kansal, M.Carey. Recruitment of the putative transcription-repair coupling factor CSB/ERCC6 to RNA polymerase II elongation complexes, *Mol.Cell Biol.*, 17, (1997) 6803-6814.
- [32] D.Tantin. RNA polymerase II elongation complexes containing the Cockayne syndrome group B protein interact with a molecular complex containing the transcription factor IIH components xeroderma pigmentosum B and p62, *J.Biol.Chem.*, 273, (1998) 27794-27799.
- [33] K.A.Henning, L.Li, N.Iyer, L.D.McDaniel, M.S.Reagan, R.Legerski, R.A.Schultz, M.Stefanini, A.R.Lehmann, L.V.Mayne, E.C.Friedberg. The Cockayne syndrome group A gene encodes a WD repeat protein that interacts with CSB protein and a subunit of RNA polymerase II TFIIH, *Cell*, 82, (1995) 555-564.
- [34] Y.Nakatsu, H.Asahina, E.Citterio, S.Rademakers, W.Vermeulen, S.Kamiuchi, J.P.Yeo, M.C.Khaw, M.Saijo, N.Kodo, T.Matsuda, J.H.Hoeijmakers, K.Tanaka. XAB2, a novel tetratricopeptide repeat protein involved in transcription-coupled DNA repair and transcription, *J.Biol.Chem.*, 275, (2000) 34931-34937.
- [35] R.Groisman, J.Polanowska, I.Kuraoka, J.Sawada, M.Saijo, R.Drapkin, A.F.Kisselev, K.Tanaka, Y.Nakatani. The ubiquitin ligase activity in the DDB2 and CSA complexes is differentially regulated by the COP9 signalosome in response to DNA damage, *Cell*, 113, (2003) 357-367.
- [36] S.Kamiuchi, M.Saijo, E.Citterio, M.de Jager, J.H.Hoeijmakers, K.Tanaka. Translocation of Cockayne syndrome group A protein to the nuclear matrix: possible relevance to transcription-coupled DNA repair, *Proc.Natl.Acad.Sci.U.S.A*, 99, (2002) 201-206.
- [37] M.Sunesen, T.Stevnsner, R.M.Brosh, Jr., G.L.Dianov, V.A.Bohr. Global genome repair of 8-oxoG in hamster cells requires a functional CSB gene product, *Oncogene*, 21, (2002) 3571-3578.
- [38] M.Fousteri, L.H.Mullenders. Transcription-coupled nucleotide excision repair in mammalian cells: molecular mechanisms and biological effects, *Cell Res.*, 18, (2008) 73-84.
- [39] M.Fousteri, W.Vermeulen, A.A.van Zeeland, L.H.Mullenders. Cockayne syndrome A and B proteins differentially regulate recruitment of chromatin remodeling and repair factors to stalled RNA polymerase II in vivo, *Mol.Cell*, 23, (2006) 471-482.
- [40] G.Giglia-Mari, F.Coin, J.A.Ranish, D.Hoogstraten, A.Theil, N.Wijgers, N.G.Jaspers, A.Raams, M.Argentini, P.J.van der Spek, E.Botta, M.Stefanini, J.M.Egly, R.Aebersold, J.H.Hoeijmakers, W.Vermeulen. A new, tenth subunit of TFIIH is responsible for the DNA repair syndrome trichothiodystrophy group A, *Nat.Genet.*, 36, (2004) 714-719.
- [41] N.Goosen. Scanning the DNA for damage by the nucleotide excision repair machinery, *DNA Repair (Amst)*, 9, (2010) 593-596.
- [42] V.Oksenych, F.Coin. The long unwinding road: XPB and XPD helicases in damaged DNA opening, *Cell Cycle*, 9, (2010) 90-96.
- [43] A.Zotter, M.S.Luijsterburg, D.O.Warmerdam, S.Ibrahim, A.Nigg, W.A.van Cappellen, J.H.Hoeijmakers, R.van Driel, W.Vermeulen, A.B.Houtsmuller. Recruitment of the nucleotide excision repair endonuclease XPG to sites of UV-induced dna damage depends on functional TFIIH, *Mol.Cell Biol.*, 26, (2006) 8868-8879.
- [44] W.L.de Laat, E.Appeldoorn, N.G.Jaspers, J.H.Hoeijmakers. DNA structural elements required for ERCC1-XPF endonuclease activity, *J.Biol.Chem.*, 273, (1998) 7835-7842.
- [45] I.L.Hermanson-Miller, J.J.Turchi. Strand-specific binding of RPA and XPA to damaged duplex DNA, *Biochemistry*, 41, (2002) 2402-2408.
- [46] J.O.Andressoo, J.H.Hoeijmakers, J.R.Mitchell. Nucleotide excision repair disorders and the balance between cancer and aging, *Cell Cycle*, 5, (2006) 2886-2888.
- [47] F.Coin, V.Oksenych, V.Mocquet, S.Groh, C.Blattner, J.M.Egly. Nucleotide excision repair driven by the dissociation of CAK from TFIIH, *Mol.Cell*, 31, (2008) 9-20.



- [48] Y.S.Krasikova, N.I.Rechkunova, E.A.Maltseva, I.O.Petruseva, O.I.Lavrik. Localization of xeroderma pigmentosum group A protein and replication protein A on damaged DNA in nucleotide excision repair, *Nucleic Acids Res.*, (2010).
- [49] C.J.Park, B.S.Choi. The protein shuffle. Sequential interactions among components of the human nucleotide excision repair pathway, *FEBS J.*, 273, (2006) 1600-1608.
- [50] M.T.Hess, U.Schwittler, M.Petretta, B.Giese, H.Naegeli. Bipartite substrate discrimination by human nucleotide excision repair, *Proc.Natl.Acad.Sci.U.S.A.*, 94, (1997) 6664-6669.
- [51] M.Wakasugi, J.T.Reardon, A.Sancar. The non-catalytic function of XPG protein during dual incision in human nucleotide excision repair, *J.Biol.Chem.*, 272, (1997) 16030-16034.
- [52] L.Staresinic, A.F.Fagbemi, J.H.Enzlin, A.M.Gourdin, N.Wijgers, I.Dunand-Sauthier, G.Giglia-Mari, S.G.Clarkson, W.Vermeulen, O.D.Scharer. Coordination of dual incision and repair synthesis in human nucleotide excision repair, *EMBO J.*, 28, (2009) 1111-1120.
- [53] S.W.Wijnhoven, E.M.Hoogervorst, H.de Waard, G.T.van der Horst, H.van Steeg. Tissue specific mutagenic and carcinogenic responses in NER defective mouse models, *Mutat.Res.*, 614, (2007) 77-94.
- [54] T.Bessho. Nucleotide excision repair 3' endonuclease XPG stimulates the activity of base excision repair enzyme thymine glycol DNA glycosylase, *Nucleic Acids Res.*, 27, (1999) 979-983.
- [55] S.K.Lee, S.L.Yu, L.Prakash, S.Prakash. Requirement of yeast RAD2, a homolog of human XPG gene, for efficient RNA polymerase II transcription. implications for Cockayne syndrome, *Cell*, 109, (2002) 823-834.
- [56] G.L.Dianov, T.Thybo, I.I.Dianova, L.J.Lipinski, V.A.Bohr. Single nucleotide patch base excision repair is the major pathway for removal of thymine glycol from DNA in human cell extracts, *J.Biol.Chem.*, 275, (2000) 11809-11813.
- [57] L.J.Niedernhofer, J.Essers, G.Weeda, B.Beverloo, J.de Wit, M.Muijtjens, H.Odijk, J.H.Hoeijmakers, R.Kanaar. The structure-specific endonuclease Ercc1-Xpf is required for targeted gene replacement in embryonic stem cells, *EMBO J.*, 20, (2001) 6540-6549.
- [58] A.Z.Al Minawi, Y.F.Lee, D.Hakansson, F.Johansson, C.Lundin, N.Saleh-Gohari, N.Schultz, D.Jenssen, H.E.Bryant, M.Meuth, J.M.Hinz, T.Helleday. The ERCC1/XPF endonuclease is required for completion of homologous recombination at DNA replication forks stalled by inter-strand cross-links, *Nucleic Acids Res.*, 37, (2009) 6400-6413.
- [59] V.Mocquet, J.P.Laine, T.Riedl, Z.Yajin, M.Y.Lee, J.M.Egly. Sequential recruitment of the repair factors during NER: the role of XPG in initiating the resynthesis step, *EMBO J.*, 27, (2008) 155-167.
- [60] T.Ogi, S.Limsirichaikul, R.M.Overmeer, M.Volker, K.Takenaka, R.Cloney, Y.Nakazawa, A.Niimi, Y.Miki, N.G.Jaspers, L.H.Mullenders, S.Yamashita, M.I.Fousteri, A.R.Lehmann. Three DNA polymerases, recruited by different mechanisms, carry out NER repair synthesis in human cells, *Mol.Cell*, 37, (2010) 714-727.
- [61] J.Moser, H.Kool, I.Giakzidis, K.Caldecott, L.H.Mullenders, M.I.Fousteri. Sealing of chromosomal DNA nicks during nucleotide excision repair requires XRCC1 and DNA ligase III alpha in a cell-cycle-specific manner, *Mol.Cell*, 27, (2007) 311-323.
- [62] J.E.Cleaver, E.T.Lam, I.Revet. Disorders of nucleotide excision repair: the genetic and molecular basis of heterogeneity, *Nat.Rev.Genet.*, 10, (2009) 756-768.
- [63] A.M.Bhutto, S.H.Kirk. Population distribution of xeroderma pigmentosum, *Adv.Exp.Med.Biol.*, 637, (2008) 138-143.
- [64] K.H.Kraemer, M.M.Lee, J.Scotto. DNA repair protects against cutaneous and internal neoplasia: evidence from xeroderma pigmentosum, *Carcinogenesis*, 5, (1984) 511-514.
- [65] K.H.Kraemer. Sunlight and skin cancer: another link revealed, *Proc.Natl.Acad.Sci.U.S.A.*, 94, (1997) 11-14.
- [66] L.Zeng, X.Quilliet, O.Chevallier-Lagente, E.Eveno, A.Sarasin, M.Mezzina. Retrovirus-mediated gene transfer corrects DNA repair defect of xeroderma pigmentosum cells of complementation groups A, B and C, *Gene Ther.*, 4, (1997) 1077-1084.
- [67] A.J.Levine, M.Oren. The first 30 years of p53: growing ever more complex, *Nat.Rev.Cancer*, 9, (2009) 749-758.
- [68] E.Meulmeester, Y.Pereg, Y.Shiloh, A.G.Jochimsen. ATM-mediated phosphorylations inhibit Mdmx/Mdm2 stabilization by HAUSP in favor of p53 activation, *Cell Cycle*, 4, (2005) 1166-1170.
- [69] J.M.Stommel, G.M.Wahl. Accelerated MDM2 auto-degradation induced by DNA-damage kinases is required for p53 activation, *EMBO J.*, 23, (2004) 1547-1556.
- [70] D.W.Meek. Tumour suppression by p53: a role for the DNA damage response?, *Nat.Rev.Cancer*, 9, (2009) 714-723.
- [71] C.P.Rubbi, J.Milner. p53 is a chromatin accessibility factor for nucleotide excision repair of DNA damage, *EMBO J.*, 22, (2003) 975-986.

- [72] S.Adimoolam, J.M.Ford. p53 and regulation of DNA damage recognition during nucleotide excision repair, *DNA Repair (Amst)*, 2, (2003) 947-954.
- [73] A.J.Levine, D.P.Lane. *The p53 Family*, Cold Spring Harbor Laboratory Press, 2010.
- [74] J.T.Zilfou, S.W.Lowe. Tumor suppressive functions of p53, *Cold Spring Harb.Perspect.Biol.*, 1, (2009) a001883.
- [75] A.de Vries, C.T.van Oostrom, F.M.Hofhuis, P.M.Dortant, R.J.Berg, F.R.de Gruijl, P.W.Wester, C.F.van Kreijl, P.J.Capel, H.van Steeg, . Increased susceptibility to ultraviolet-B and carcinogens of mice lacking the DNA excision repair gene XPA, *Nature*, 377, (1995) 169-173.
- [76] H.Nakane, S.Takeuchi, S.Yuba, M.Saijo, Y.Nakatsu, H.Murai, Y.Nakatsuru, T.Ishikawa, S.Hirota, Y.Kitamura, . High incidence of ultraviolet-B-or chemical-carcinogen-induced skin tumours in mice lacking the xeroderma pigmentosum group A gene, *Nature*, 377, (1995) 165-168.
- [77] Y.Takahashi, Y.Nakatsuru, S.Zhang, Y.Shimizu, H.Kume, K.Tanaka, F.Ide, T.Ishikawa. Enhanced spontaneous and aflatoxin-induced liver tumorigenesis in xeroderma pigmentosum group A gene-deficient mice, *Carcinogenesis*, 23, (2002) 627-633.
- [78] F.Ide, H.Oda, Y.Nakatsuru, K.Kusama, H.Sakashita, K.Tanaka, T.Ishikawa. Xeroderma pigmentosum group A gene action as a protection factor against 4-nitroquinoline 1-oxide-induced tongue carcinogenesis, *Carcinogenesis*, 22, (2001) 567-572.
- [79] E.M.Hoogervorst, C.T.van Oostrom, R.B.Beems, J.van Benthem, B.J.van den, C.F.van Kreijl, J.G.Vos, A.de Vries, H.van Steeg. 2-AAF-induced tumor development in nucleotide excision repair-deficient mice is associated with a defect in global genome repair but not with transcription coupled repair, *DNA Repair (Amst)*, 4, (2005) 3-9.
- [80] E.M.Hoogervorst, C.T.van Oostrom, R.B.Beems, J.van Benthem, S.Gielis, J.P.Vermeulen, P.W.Wester, J.G.Vos, A.de Vries, H.van Steeg. p53 heterozygosity results in an increased 2-acetylaminofluorene-induced urinary bladder but not liver tumor response in DNA repair-deficient Xpa mice, *Cancer Res.*, 64, (2004) 5118-5126.
- [81] A.de Vries, C.T.van Oostrom, P.M.Dortant, R.B.Beems, C.F.van Kreijl, P.J.Capel, H.van Steeg. Spontaneous liver tumors and benzo[a]pyrene-induced lymphomas in XPA-deficient mice, *Mol.Carcinog.*, 19, (1997) 46-53.
- [82] J.P.Melis, S.W.Wijnhoven, R.B.Beems, M.Roodbergen, B.J.van den, H.Moon, E.Friedberg, G.T.van der Horst, J.H.Hoeijmakers, J.Vijg, H.van Steeg. Mouse models for xeroderma pigmentosum group A and group C show divergent cancer phenotypes, *Cancer Res.*, 68, (2008) 1347-1353.
- [83] K.Tanaka, S.Kamiuchi, Y.Ren, R.Yonemasu, M.Ichikawa, H.Murai, M.Yoshino, S.Takeuchi, M.Saijo, Y.Nakatsu, H.Miyauchi-Hashimoto, T.Horio. UV-induced skin carcinogenesis in xeroderma pigmentosum group A (XPA) gene-knockout mice with nucleotide excision repair-deficiency, *Mutat.Res.*, 477, (2001) 31-40.
- [84] R.J.Berg, A.de Vries, H.van Steeg, F.R.de Gruijl. Relative susceptibilities of XPA knockout mice and their heterozygous and wild-type littermates to UVB-induced skin cancer, *Cancer Res.*, 57, (1997) 581-584.
- [85] A.A.Gaspari, T.A.Fleisher, K.H.Kraemer. Impaired interferon production and natural killer cell activation in patients with the skin cancer-prone disorder, xeroderma pigmentosum, *J.Clin.Invest*, 92, (1993) 1135-1142.
- [86] T.Horio, H.Miyauchi-Hashimoto, K.Kuwamoto, S.Horiki, H.Okamoto, K.Tanaka. Photobiologic and photoimmunologic characteristics of XPA gene-deficient mice, *J.Investig.Dermatol.Symp.Proc.*, 6, (2001) 58-63.
- [87] H.Miyauchi-Hashimoto, K.Kuwamoto, Y.Urade, K.Tanaka, T.Horio. Carcinogen-induced inflammation and immunosuppression are enhanced in xeroderma pigmentosum group A model mice associated with hyperproduction of prostaglandin E2, *J.Immunol.*, 166, (2001) 5782-5791.
- [88] A.de Vries, T.G.Gorgels, R.J.Berg, G.H.Jansen, H.van Steeg. Ultraviolet-B induced hyperplasia and squamous cell carcinomas in the cornea of XPA-deficient mice, *Exp.Eye Res.*, 67, (1998) 53-59.
- [89] H.van Steeg, H.Klein, R.B.Beems, C.F.van Kreijl. Use of DNA repair-deficient XPA transgenic mice in short-term carcinogenicity testing, *Toxicol.Pathol.*, 26, (1998) 742-749.
- [90] H.van Steeg, L.H.Mullenders, J.Vijg. Mutagenesis and carcinogenesis in nucleotide excision repair-deficient XPA knock out mice, *Mutat.Res.*, 450, (2000) 167-180.
- [91] F.Ide, N.Iida, Y.Nakatsuru, H.Oda, K.Tanaka, T.Ishikawa. Mice deficient in the nucleotide excision repair gene XPA have elevated sensitivity to benzo[a]pyrene induction of lung tumors, *Carcinogenesis*, 21, (2000) 1263-1265.
- [92] C.T.van Oostrom, M.Boeve, B.J.van den, A.de Vries, M.E.Dolle, R.B.Beems, C.F.van Kreijl, J.Vijg, H.van Steeg. Effect of heterozygous loss of p53 on benzo[a]pyrene-induced mutations and tumors in DNA repair-deficient XPA mice, *Environ.Mol.Mutagen.*, 34, (1999) 124-130.
- [93] S.A.Bol, H.van Steeg, J.G.Jansen, C.Van Oostrom, A.de Vries, A.J.de Groot, A.D.Tates, H.Vrieling, A.A.van Zeeland, L.H.Mullenders. Elevated frequencies of benzo(a)pyrene-induced Hprt mutations in internal tissue of XPA-deficient mice, *Cancer Res.*, 58, (1998) 2850-2856.

- [94] A.de Vries, M.E.Dolle, J.L.Broekhof, J.J.Muller, E.D.Kroese, C.F.van Kreijl, P.J.Capel, J.Vijg, H.van Steeg. Induction of DNA adducts and mutations in spleen, liver and lung of XPA-deficient/lacZ transgenic mice after oral treatment with benzo[a]pyrene: correlation with tumour development, *Carcinogenesis*, 18, (1997) 2327-2332.
- [95] A.T.Sands, A.Abuin, A.Sanchez, C.J.Conti, A.Bradley. High susceptibility to ultraviolet-induced carcinogenesis in mice lacking XPC, *Nature*, 377, (1995) 162-165.
- [96] D.L.Cheo, H.J.Ruven, L.B.Meira, R.E.Hammer, D.K.Burns, N.J.Tappe, A.A.van Zeeland, L.H.Mullenders, E.C.Friedberg. Characterization of defective nucleotide excision repair in XPC mutant mice. *Mutat.Res.* 374(1), 1-9. 3-4-1997.
- [97] R.J.Berg, H.J.Ruven, A.T.Sands, F.R.de Gruijl, L.H.Mullenders. Defective global genome repair in XPC mice is associated with skin cancer susceptibility but not with sensitivity to UVB induced erythema and edema, *J.Invest Dermatol.*, 110, (1998) 405-409.
- [98] D.L.Cheo, L.B.Meira, R.E.Hammer, D.K.Burns, A.T.Doughty, E.C.Friedberg. Synergistic interactions between XPC and p53 mutations in double-mutant mice: neural tube abnormalities and accelerated UV radiation-induced skin cancer, *Curr.Biol.*, 6, (1996) 1691-1694.
- [99] D.L.Cheo, L.B.Meira, D.K.Burns, A.M.Reis, T.Issac, E.C.Friedberg. Ultraviolet B radiation-induced skin cancer in mice defective in the Xpc, Trp53, and Apex (HAP1) genes: genotype-specific effects on cancer predisposition and pathology of tumors, *Cancer Res.*, 60, (2000) 1580-1584.
- [100] E.C.Friedberg, D.L.Cheo, L.B.Meira, A.M.Reis. Cancer predisposition in mutant mice defective in the XPC DNA repair gene, *Prog.Exp.Tumor Res.*, 35, (1999) 37-52.
- [101] D.L.Cheo, D.K.Burns, L.B.Meira, J.F.Houle, E.C.Friedberg. Mutational inactivation of the xeroderma pigmentosum group C gene confers predisposition to 2-acetylaminofluorene-induced liver and lung cancer and to spontaneous testicular cancer in Trp53-/- mice, *Cancer Res.*, 59, (1999) 771-775.
- [102] M.C.Hollander, R.T.Philburn, A.D.Patterson, S.Velasco-Miguel, E.C.Friedberg, R.I.Linnoila, A.J.Fornace, Jr. Deletion of XPC leads to lung tumors in mice and is associated with early events in human lung carcinogenesis, *Proc.Natl.Acad.Sci.U.S.A*, 102, (2005) 13200-13205.
- [103] Y.Uehara, H.Ikehata, M.Furuya, S.Kobayashi, D.He, Y.Chen, J.Komura, H.Ohtani, I.Shimokawa, T.Ono. XPC is involved in genome maintenance through multiple pathways in different tissues, *Mutat.Res.*, 670, (2009) 24-31.
- [104] M.D'Errico, E.Parlanti, M.Teson, B.M.de Jesus, P.Degan, A.Calcagnile, P.Jaruga, M.Bjoras, M.Crescenzi, A.M.Pedrin, J.M.Egly, G.Zambruno, M.Stefanini, M.Dizdareglu, E.Dogliotti. New functions of XPC in the protection of human skin cells from oxidative damage, *EMBO J.*, 25, (2006) 4305-4315.
- [105] E.Despras, P.Pfeiffer, B.Salles, P.Calsou, S.Kuhfittig-Kulle, J.F.Angulo, D.S.Biard. Long-term XPC silencing reduces DNA double-strand break repair, *Cancer Res.*, 67, (2007) 2526-2534.
- [106] S.Y.Liu, C.Y.Wen, Y.J.Lee, T.C.Lee. XPC silencing sensitizes glioma cells to arsenic trioxide via increased oxidative damage, *Toxicol.Sci.*, 116, (2010) 183-193.
- [107] Y.Okamoto, P.H.Chou, S.Y.Kim, N.Suzuki, Y.R.Laxmi, K.Okamoto, X.Liu, T.Matsuda, S.Shibutani. Oxidative DNA damage in XPC-knockout and its wild mice treated with equine estrogen, *Chem.Res.Toxicol.*, 21, (2008) 1120-1124.
- [108] H.R.Rezvani, A.L.Kim, R.Rossignol, N.Ali, M.Daly, W.Mahfouf, N.Bellance, A.Taieb, H.de Verneuil, F.Mazurier, D.R.Bickers. XPC silencing in normal human keratinocytes triggers metabolic alterations that drive the formation of squamous cell carcinomas, *J.Clin.Invest.* (2010).
- [109] Y.Shimizu, S.Iwai, F.Hanaoka, K.Sugasawa. Xeroderma pigmentosum group C protein interacts physically and functionally with thymine DNA glycosylase, *EMBO J.*, 22, (2003) 164-173.
- [110] J.K.Wickliffe, L.A.Galbert, M.M.Ammenheuser, S.M.Herring, J.Xie, O.E.Masters, III, E.C.Friedberg, R.S.Lloyd, J.B.Ward, Jr. 3,4-Epoxy-1-butene, a reactive metabolite of 1,3-butadiene, induces somatic mutations in Xpc-null mice, *Environ.Mol.Mutagen.*, 47, (2006) 67-70.
- [111] S.W.Wijnhoven, H.J.Kool, L.H.Mullenders, R.Slater, A.A.van Zeeland, H.Vrieling. DMBA-induced toxic and mutagenic responses vary dramatically between NER-deficient Xpa, Xpc and Csb mice, *Carcinogenesis*, 22, (2001) 1099-1106.
- [112] H.Ikehata, Y.Saito, F.Yanase, T.Mori, O.Nikaido, T.Ono. Frequent recovery of triplet mutations in UVB-exposed skin epidermis of Xpc-knockout mice, *DNA Repair (Amst)*, 6, (2007) 82-93.
- [113] L.A.Donehower, G.Lozano. 20 years studying p53 functions in genetically engineered mice, *Nat.Rev.Cancer*, 9, (2009) 831-841.

- [114] L.A.Donehower. The p53-deficient mouse: a model for basic and applied cancer studies, *Semin.Cancer Biol.*, 7, (1996) 269-278.
- [115] R.D.Storer, J.E.French, J.Haseman, G.Hajian, E.K.LeGrand, G.G.Long, L.A.Mixson, R.Ochoa, J.E.Sagartz, K.A.Soper. P53+/- hemizygous knockout mouse: overview of available data, *Toxicol.Pathol.*, 29 Suppl, (2001) 30-50.
- [116] J.B.Pritchard, J.E.French, B.J.Davis, J.K.Haseman. The role of transgenic mouse models in carcinogen identification, *Environ.Health Perspect.*, 111, (2003) 444-454.
- [117] C.F.van Kreijl, P.A.McAnulty, R.B.Beems, A.Vynckier, H.van Steeg, R.Fransson-Steen, C.L.Alden, R.Forster, J.W.van der Laan, J.Vandenberghe. Xpa and Xpa/p53+/- knockout mice: overview of available data. *Toxicol.Pathol.* 29 Suppl, 117-127. 2001.
- [118] R.B.Beems, C.F.van Kreijl, H.van Steeg. 39-week carcinogenicity study with cyclosporin A in XPA-/- mice, wild type mice and XPA-/-P53+/- double transgenic mice. 650080001. 2001. RIVM.
- [119] S.W.Wijnhoven, H.J.Kool, L.H.Mullenders, R.Slater, A.A.van Zeeland, H.Vrieling. DMBA-induced toxic and mutagenic responses vary dramatically between NER-deficient Xpa, Xpc and Csb mice. *Carcinogenesis* 22(7), 1099-1106. 2001.
- [120] E.C.Friedberg, L.B.Meira. Database of mouse strains carrying targeted mutations in genes affecting biological responses to DNA damage Version 7, *DNA Repair (Amst)*, 5, (2006) 189-209.
- [121] S.W.Wijnhoven, R.B.Beems, M.Roodbergen, B.J.van den, P.H.Lohman, K.Diderich, G.T.van der Horst, J.Vijg, J.H.Hoeijmakers, H.van Steeg. Accelerated aging pathology in ad libitum fed Xpd(TTD) mice is accompanied by features suggestive of caloric restriction, *DNA Repair (Amst)*, 4, (2005) 1314-1324.
- [122] J.de Boer, J.O.Andressoo, J.de Wit, J.Huijman, R.B.Beems, H.van Steeg, G.Weeda, G.T.van der Horst, W.van Leeuwen, A.P.Themmen, M.Meradji, J.H.Hoeijmakers. Premature aging in mice deficient in DNA repair and transcription, *Science*, 296, (2002) 1276-1279.
- [123] T.Yoon, A.Chakraborty, R.Franks, T.Valli, H.Kiyokawa, P.Raychaudhuri. Tumor-prone phenotype of the DDB2-deficient mice, *Oncogene*, 24, (2005) 469-478.
- [124] M.Tian, R.Shinkura, N.Shinkura, F.W.Alt. Growth retardation, early death, and DNA repair defects in mice deficient for the nucleotide excision repair enzyme XPF, *Mol.Cell Biol.*, 24, (2004) 1200-1205.
- [125] Y.N.Harada, N.Shiomi, M.Koike, M.Ikawa, M.Okabe, S.Hirota, Y.Kitamura, M.Kitagawa, T.Matsunaga, O.Nikaido, T.Shiomi. Postnatal growth failure, short life span, and early onset of cellular senescence and subsequent immortalization in mice lacking the xeroderma pigmentosum group G gene, *Mol.Cell Biol.*, 19, (1999) 2366-2372.
- [126] J.M.Ng, H.Vrieling, K.Sugasawa, M.P.Ooms, J.A.Grootegoed, J.T.Vreeburg, P.Visser, R.B.Beems, T.G.Gorgels, F.Hanaoka, J.H.Hoeijmakers, G.T.van der Horst. Developmental defects and male sterility in mice lacking the ubiquitin-like DNA repair gene mHR23B, *Mol.Cell Biol.*, 22, (2002) 1233-1245.
- [127] G.T.van der Horst, L.Meira, T.G.Gorgels, J.de Wit, S.Velasco-Miguel, J.A.Richardson, Y.Kamp, M.P.Vreeswijk, B.Smit, D.Bootsma, J.H.Hoeijmakers, E.C.Friedberg. UVB radiation-induced cancer predisposition in Cockayne syndrome group A (Csa) mutant mice, *DNA Repair (Amst)*, 1, (2002) 143-157.
- [128] G.T.van der Horst, H.van Steeg, R.J.Berg, A.J.van Gool, J.de Wit, G.Weeda, H.Morreau, R.B.Beems, C.F.van Kreijl, F.R.de Gruij, D.Bootsma, J.H.Hoeijmakers. Defective transcription-coupled repair in Cockayne syndrome B mice is associated with skin cancer predisposition, *Cell*, 89, (1997) 425-435.
- [129] J.McWhir, J.Selfridge, D.J.Harrison, S.Squires, D.W.Melton. Mice with DNA repair gene (ERCC-1) deficiency have elevated levels of p53, liver nuclear abnormalities and die before weaning, *Nat.Genet.*, 5, (1993) 217-224.
- [130] G.Weeda, I.Donker, J.de Wit, H.Morreau, R.Janssens, C.J.Vissers, A.Nigg, H.van Steeg, D.Bootsma, J.H.Hoeijmakers. Disruption of mouse ERCC1 results in a novel repair syndrome with growth failure, nuclear abnormalities and senescence, *Curr.Biol.*, 7, (1997) 427-439.
- [131] E.M.Hoogervorst, A.de Vries, R.B.Beems, C.T.van Oostrom, P.W.Wester, J.G.Vos, W.Bruins, M.Roodbergen, F.R.Cassee, J.Vijg, F.J.van Schooten, H.van Steeg. Combined oral benzo[a]pyrene and inhalatory ozone exposure have no effect on lung tumor development in DNA repair-deficient Xpa mice, *Carcinogenesis*, 24, (2003) 613-619.
- [132] J.C.Klein, R.B.Beems, P.E.Zwart, M.Hamzink, G.Zomer, H.van Steeg, C.F.van Kreijl. Intestinal toxicity and carcinogenic potential of the food mutagen 2-amino-1-methyl-6-phenylimidazo[4,5-b]pyridine (PhIP) in DNA repair deficient XPA-/- mice, *Carcinogenesis*, 22, (2001) 619-626.
- [133] C.F.van Kreijl, P.A.McAnulty, R.B.Beems, A.Vynckier, H.van Steeg, R.Fransson-Steen, C.L.Alden, R.Forster, J.W.van der Laan, J.Vandenberghe. Xpa and Xpa/p53+/- knockout mice: overview of available data, *Toxicol.Pathol.*, 29 Suppl, (2001) 117-127.

- [134] P.C.van Kesteren, R.B.Beems, M.Luijten, J.Robinson, A.de Vries, H.van Steeg. DNA repair-deficient Xpa/p53 knockout mice are sensitive to the non-genotoxic carcinogen cyclosporine A: escape of initiated cells from immunosurveillance?, *Carcinogenesis*, 30, (2009) 538-543.
- [135] P.A.McAnulty, M.Skydsgaard. Diethylstilbestrol (DES): carcinogenic potential in Xpa-/-, Xpa-/- / p53+/-, and wild-type mice during 9 months' dietary exposure, *Toxicol.Pathol.*, 33, (2005) 609-620.
- [136] B.A.Lina, R.A.Woutersen, J.P.Bruijntjes, J.van Benthem, J.A.van den Berg, J.Monbaliu, B.J.Thoolen, R.B.Beems, C.F.van Kreijl. Evaluation of the Xpa-deficient transgenic mouse model for short-term carcinogenicity testing: 9-month studies with haloperidol, reserpine, phenacetin, and D-mannitol, *Toxicol.Pathol.*, 32, (2004) 192-201.





# Chapter 2

# Chapter 2

## Life-spanning murine gene expression profiles in relation to chronological and pathological aging in multiple organs

**Melis JPM**, Jonker MJ, Kuiper RV, van der Hoeven TV, Robinson J, van der Horst GTJ, Breit TM, Vijg J, Dollé MET, Hoeijmakers JHJ, van Steeg H.

Life-spanning murine gene expression profiles in relation to chronological and pathological aging in multiple organs

**Aging Cell, Revisions, 2012**

*“Live, in the moment, never count on longevity”*

Longevity – Yeasayer, 2012



## Abstract

Aging is a complex biological process without satisfactory mechanistic explanations that accounts for a majority of observed aging effects, ranging from molecular cellular responses to organismal health deterioration and loss of homeostasis. We present a systematic *in vivo* aging study of C57BL/6J female mice, with regular sampling spanning the entire murine lifespan (13, 26, 52, 78, 104 and 130 weeks of age) from five organs for pathology and gene expression analyses. We set out to characterize aging responses in and/or between different tissues and additionally follow age-related pathways and genes in a temporal fashion throughout the lifespan. Pathological hallmarks that changed consistently during chronological aging were identified and further used to interpret biological aging, since the pathology data also revealed inter- and intra-individual variation. Aging was therefore assessed per tissue along a chronological and pathology-driven (biological) axis, correlating age-related pathological findings to gene expression profiles. Pathway analyses revealed immune responses to be commonly changed in most tissues, albeit in a tissue-specific manner. Our results furthermore indicate changes in processes that are related to imbalanced energy homeostasis, increased levels of ROS, cell cycle, cell motility and DNA damage responses. Our study enables studying temporal dynamics of genes and processes during the entire lifespan over multiple tissues, providing more insight in the temporal functional shifts that occur during aging.

## Introduction

Aging is a complex process comprising a wide variety of related features and outcomes, which contribute to health deterioration with time, and eventually lead to death. Progressive functional decline, gradual deterioration of physiological function, decrease in fertility and viability and increase in vulnerability have all been related to the term aging [1].

Time and decline of physical health are the most correlated aging factors, however pinpointing specific underlying mechanisms and finding consistent aging markers is troublesome. We measured genome-wide gene expression in female C57BL/6J mice in a stringently controlled *in vivo* aging study, and incorporated time and physical health aspects in our analysis. To address the factor time, biological samples to monitor the aging process were taken systematically at regular time intervals, spanning the entire C57BL/6J lifespan. To address health and physiological deterioration, pathological and full genome expression analyses on five different organs were performed of every time point. This approach therefore permits temporal monitoring of aging during the entire lifespan ('chronological aging') and additionally can link gene expression to age-related pathology providing novel insight on 'biological aging'. Previously, numerous aging studies have provided great insight into the mechanisms that vary and play a role during aging [2-7]. However, following the temporal dynamics of proposed age-related mechanisms in a controlled setting and in multiple tissues is still troublesome. For example, the majority of microarray-based aging studies compared only two age groups (young versus old) with each other [3,8,9], or investigated model organisms with prolonged or reduced longevity [4,10]. Alternatively, *in vivo* gene expression in relation to aging has been studied using samples from a (human) population [11,12], allowing for more genetic and environmental variation. Others sampled more than three time points but have not used a full genome platform [7]. These and other large-scale meta-analyses studies [5,6] proved to be very valuable in uncovering several aging-related processes among multiple species, genotypes and tissues, but were not fit to temporally track and investigate age-related processes over the entire lifespan in multiple organs.

Previously mentioned gene expression studies revealed fairly consistent changes in the immune system and in metabolic rate during aging [3,5]. Also, several mechanisms have been postulated from previous research to at least partly explain or influence aging at the cellular level. One prevailing theory, the free radical or oxidative damage theory of aging, proposes that macromolecular damage, either due to normal toxic by-products of metabolism or inefficient repair/defensive systems, accumulates during lifespan and causes aging [13-15]. In addition, molecular pathways involving the IGF-1/GH axis [16,17] and mTOR [18,19] have also been implicated in the aging process. Nevertheless, it is still challenging to specifically indicate when, how and to what extent these molecular mechanisms affect general health deterioration and loss of homeostasis. Our study allows monitoring of these and other age-related pathways on a chronological and pathologically driven (biological) axis in multiple tissues. The latter approach additionally reveals processes that follow cellular health decline in multiple tissues.

## Experimental procedures

### *Experimental Design*

Female C57BL6/J mice were marked and randomized at the day of birth in different groups; i.e. longevity cohorts (previously described in Wijnhoven *et al.* [20]), or cross-sectional cohorts in which the mice were sacrificed at fixed time points. Cross-sectional cohorts C57BL6/J mice were sacrificed at a fixed age of 13, 26, 52, 78, 104 and 130 weeks. During the entire experiment, animals were kept in the same stringently controlled pathogen-free (spf) environment. The microbiological status of the cohorts was monitored every 3 months during the entire study. Mice were bred in-house and accommodated under pathogen-free conditions and strictly standardized day/night (12:12hr) regime at consistent temperature (20°C) and controlled air pressure. Moreover, to minimize confounding effects on health status mice were housed in small groups of 4-5 in Macrolon II type cages with sufficient cage-enrichment. Standard lab chow (Hope Farms, The Netherlands) and water were supplied ad libitum. Complete autopsy was performed on the mice; tissues were isolated from each animal and stored for further histopathological analysis (see below). Tissues were snap frozen in liquid nitrogen for gene expression profiling.

### *Histopathology*

Organ samples of each animal were preserved in a neutral aqueous phosphate-buffered 4% solution of formaldehyde. Tissues required for microscopic examination were processed, embedded in paraffin wax, sectioned at 4 µm and stained with haematoxylin and eosin. Detailed microscopic examination was performed on 5 major organs of the mice from the interim cohort and on all gross lesions suspected of being tumors or representing major pathological conditions. For each animal, histopathological abnormalities, tumors as well as non-neoplastic lesions, were recorded and if applicable, establishing a cause of death was attempted.

The difference between the age groups of binomial data was tested using a chi-squared contingency table test. The difference between the age groups of ordinal data was tested using Kruskal-Wallis rank sum test. To determine to which extent the pathology was indicative for aging the following analysis was performed. For each pathological variable the samples were clustered on severity, using hierarchical clustering and the complete agglomeration method (with binary distance if required). The average age of the two main clusters was calculated. The allocation of each sample to either a “young” cluster or an “old” age group was afterwards compared to the chronological age of this sample to check for consistency.

### *Microarray analysis*

Total RNA was isolated from liver, kidney, spleen, lung and brain, using the RNeasy Midi Kit (Qiagen, Valencia, CA, USA;). RNA quality was tested using automated gel electrophoresis (Bioanalyzer 2100; Agilent technologies, Amstelveen, the Netherlands (RIN > 7)). RNA samples (n = 3 per time point per tissue, 90 samples in total) were labelled and hybridized to Mouse GeneChip 430 2.0 (Affymetrix, Santa Clara, CA, USA) arrays according to the manufacturer's protocol. All raw data passed the quality criteria, but relevant effects of labelling batches were detected. The raw data from each tissue was normalized using the robust multi-array average (RMA) algorithm [21] and annotated according de

Leeuw [22]. The data were corrected for labelling-batch effects using a linear model with group-means-parametrization and coefficients for age (fixed) and labelling-batch (random). The resulting normalized expression values were analyzed for differentially expressed genes (DEGs) as described by Storey *et al.* [23], using a false discovery rate corrected  $p$ -value cut-off of  $< 0.05$  [24]. Linear DEGs were defined based on a fitted linear regression model: each age group should have positive and negative residuals with respect to the model prediction, and average expression levels of each successive age group should change unidirectionally.

In order to discover common functionally related gene-sets in multiple tissues, the top 10% of most significantly differentially expressed genes in each tissue were tested for overrepresentation (ORA) of functionally related genes [25], using the hypergeometric test and gene-sets defined by the Gene Ontology (GO), Metacore (<http://www.genego.com/metacore.php>) and a predefined list of gene-sets (SI12). The intersection between the top 10% genes and a gene-set was called the responsive set of the gene-set. Gene-sets detected with  $p < 10^{-3}$  were considered for interpretation. The profile of a gene-set was determined through the genes in the responsive set ( $y_i$ ) by calculating the eigengene  $x$  [26], and the direction by  $\Sigma_i \text{cor}(x, y_i)$ : a negative score resulted in reversion of the eigengene. Gene-set clustering [27] was used to aid the interpretation gene-sets. ORA results were compared with the Wilcoxon rank test ( $p < 10^{-5}$ , gene-set analysis GSA; [28]) to examine consistency.

Co-expression was quantified using  $\rho_{x,y}$  and  $\rho_{x,y \cdot z}$ , where  $\rho$  indicates Spearman rank correlation,  $x$  indicates a phenotypic variable,  $y$  indicates a gene and  $z$  indicates age.  $P$ -values for  $\rho_{x,y}$  were determined using a permutation-based Spearman rank correlation test (ordinal data), or using a chi-squared contingency test (binomial data) and for  $\rho_{x,y \cdot z}$  a conditional Spearman correlation test (ordinal data) or a Cochran-Mantel-Haenszel test (binomial data). A score for co-expression was calculated as the negative sum of the logs of the  $p$ -values of the correlation and the conditional correlation test. This methodology corrects for correlations with age. Genes in the top 3% (1000) highest co-expression scores were used for functional characterization using ORA as described above. The results were validated using GSA [28]. Gene expression data has been submitted to the public Gene Expression Omnibus, number GSE34378.

## Results

### *Survival and intercurrent experimental setup*

We have investigated six cross-sectional age groups (13, 26, 52, 78, 104 and 130 weeks of age) spanning the adult lifespan of C57BL6/J female mice. Mice were bred in-house and accommodated under specific pathogen-free (spf) conditions and strict standardized conditions. Per age group we investigated five organs (liver, kidney, spleen, lung and brain) for age-related pathology and gene expression changes. Survival and cause of death pathology could not be assessed as we sampled cross-sectional time points, but relevant information can be obtained from the concurrent longevity cohort of female mice ( $n=50$ , [20;29]). The most prevalent causes of death were neoplasms, inflammation and general conditional decline. To emphasize the stringent standardized conditions SI01 depicts the survival curves of the concurrent female C57BL/6J longevity study of this manuscript together with another female C57BL/6J cohort which was executed 5 years later. The comparison showed highly reproducible results, indicating these comprehensive aging studies are performed in a very

standardized and stringent setting. The percentage of animals that died per cross-sectional time point was derived from the concurrent comprehensive survival study for this manuscript: 100% of the mice in this cohort survived past the age of 52 weeks, 96% survived at 78 weeks and at 104 and 130 weeks 48% and 6% survived, respectively. The median lifespan of this cohort was 103 weeks of age and the maximum lifespan was 133 weeks (SI01).

### ***Aging pathology in multiple tissues***

The results of the pathological analyses of the six cross-sectional time points are shown in Table 1. The “Age in weeks” section of the table depicts the severity of the pathological observation represented by average scores per age group, either based on presence-absence, percentage or ordinal scoring. The last column indicates significance of the differences between the age groups. For instance, severity of karyomegaly in liver significantly increases ( $p < 0.002$ ) with age from 3 to 5 (on an ordinal scale from 0-5). A generally accepted marker of aging at the tissue level is accumulation of lipofuscin [30]. We have scored lipofuscin accumulation during aging in a mitotic as well as a post-mitotic organ, respectively liver and brain, and found a high correlation with chronological age in both organs. Several other pathological age-related hallmarks have been scored in five tissues (Table 1). Significant aging effects were found for several parameters, but their dynamics over time vary (SI02). The most significant aging effects were found for lipofuscin accumulation in liver and brain and for glomerular membrane thickening in the kidney. Moreover, these three parameters all consistently increased over time during the entire lifespan (SI02).

Tissue	Pathology	Age in weeks						Age effect p-value
		13	26	52	78	104	130	
Liver	focal lymphoid proliferation (0-1)	33 (9)	33 (9)	17 (6)	100 (7)	80 (10)	100 (2)	0.002
	scattered extramedullary hematopoiesis (0-5)	1 (9)	1 (9)	0 (9)	1 (10)	1 (10)	4 (3)	0.10
	karyomegaly (0-5)	3 (9)	3 (9)	3 (9)	3.5 (10)	4 (9)	5 (3)	0.002
	Intranuclear droplets (%)	0 (9)	0 (9)	0 (9)	30 (10)	89 (9)	33 (3)	0.0005
	hepatocellular vacuolization (0-5)	1 (9)	1 (8)	2 (9)	3 (10)	4 (10)	1 (3)	0.0005
	ito cell vacuolisation (0-5)	0 (9)	0 (9)	3 (8)	2 (8)	3 (7)	3 (3)	0.005
	lipofuscin index	0.63 (9)	5.44 (9)	39.40 (10)	86.63 (10)	112.4 (10)	231.1 (3)	$2 \times 10^{-7}$
kidney	karyomegaly (0-5)	1 (9)	0 (9)	1 (10)	1 (10)	1 (10)	2 (3)	0.3067
	lymphoid proliferation (0-1)	0 (10)	0 (9)	56 (9)	30 (10)	40 (10)	33 (3)	0.02549
	Glomerular membrane thickening (0-5)	0 (10)	0 (8)	0 (9)	2 (10)	2.5 (10)	4 (3)	$3 \times 10^{-6}$
	tubular degeneration (0-5)	0 (10)	0 (9)	0 (8)	1.5 (10)	1.5 (10)	2 (3)	0.0008
spleen	Lymphocytolysis (0-5)	3 (10)	2 (8)	1.5 (8)	1.5 (10)	0 (10)	0 (3)	0.0004
	iron laden macrophages (0-5)	0 (10)	0 (8)	2.5 (8)	3 (10)	2 (10)	1 (3)	0.005
lung	Peribronchiolar lymphoid proliferation (0-1)	10 (10)	0 (8)	50 (10)	89 (9)	89 (9)	50 (2)	0.0005
brain	vacuolisation white matter (0-5)	0 (9)	0 (7)	1 (10)	2 (10)	3 (10)	5 (3)	$1 \times 10^{-5}$
	lipofuscinosis neurons HE (0-5)	0 (9)	0 (7)	0 (8)	2 (10)	2 (10)	2.5 (2)	$7 \times 10^{-6}$
	periventricular GFAP* (0-4)	1 (9)	0 (6)	2 (10)	2 (10)	1 (9)	3 (3)	0.005
	hippocampus GFAP* (0-4)	1 (9)	0 (6)	2 (10)	2 (10)	2 (9)	4 (3)	0.002

\*Glial Fibrillary Acidic Protein IHC staining

**Table 1.** Relationship between chronological aging and pathological characteristics. The pathological markers are either quantified on a continuous scale, an ordinal scale using four or five levels of severity (0-4 or 0-5), or on occurrence (absent - present). The values indicate the mean (continuous), median (ordinal) or percentage (binary) for each age class with the number of observations between brackets. The lipofuscin index in liver was calculated combining the abundance, intensity (ordinal) and size (ordinal) of lipofuscin spots. The last column indicates the significance of a difference between age classes (Age effect).

We wanted to identify the pathological hallmarks that were most likely related to biological aging. As biological and chronological aging are correlated (albeit biological variability), we hypothesized that pathological variables that are indicative for chronological age classes can potentially be related to biological aging. Figure 1A illustrates to what extent the pathology was indicative for age. For each pathological variable the samples were clustered on severity and the average age of the two main clusters was calculated (see SI03). For each individual sample, the heatmap displays whether it was allocated to the “young” group (grey = below average) or the “old” group (black = above average). Many of the variables did not yield a perfect separation between “young” and “old” in this analysis. We hypothesized that pathological variables were only indicative for aging if the two youngest cohorts (13 and 26 weeks) were assigned as “young” and the two oldest cohorts (104 and 130 weeks) were labelled as “old”. SI03 shows the percentage of correctly predicted samples for this hypothesis. Based on the best predictive values (Figure 1A and SI03), the results in Table 1 and the dynamics over time (SI02), the overall best correlating pathological parameters per tissue for chronological aging were: lipofuscin accumulation in the brain and liver, glomerular membrane thickening in the kidney, a decrease in lymphocytolysis in the spleen and increased peribronchiolar lymphoid proliferation in lung.

We also investigated if individuals showed a consistently “young” or “old” phenotype across the multiple tissues and their pathological observations and therefore systemic biological aging. Figure 1A already shows that within one animal the predicted age class can vary between and within tissues. These results indicate that there is inter- and intra-individual variation, despite the fact that some parameters give a general good indication of young and old age. The rate of biological aging was not consistently reflected in multiple pathological observations over multiple tissues, which is illustrated by Figure 1B. Here the best overall pathological parameters per tissue are depicted and four of them are shown at higher resolution than in Figure 1A. For these parameters the greyscale indicates the five levels of an ordinal scale (lymphoid proliferation in the lung was originally quantified on a binary scale). Hardly any of the individuals showed an identical ranking of greyscale for all parameters, especially in older animals.

In conclusion, several pathological hallmarks were highly correlated with chronological aging based on average scores per age group. We therefore assumed that chronological age reflected the “average ageing process” in this population. The pathology data however also indicated that there is inter- and intra-individual variation. Besides inter individual differences, aging also demonstrated to be tissue-specific within one animal. These observations let to the following strategy with respect to the gene expression analysis. We first studied gene expression profiles per tissue based on chronological age (average aging process over time). To address the biological (pathologically driven) aging, gene expression profiles were ranked for each tissue according to their co-expression with the best pathological marker for each tissue identified above.

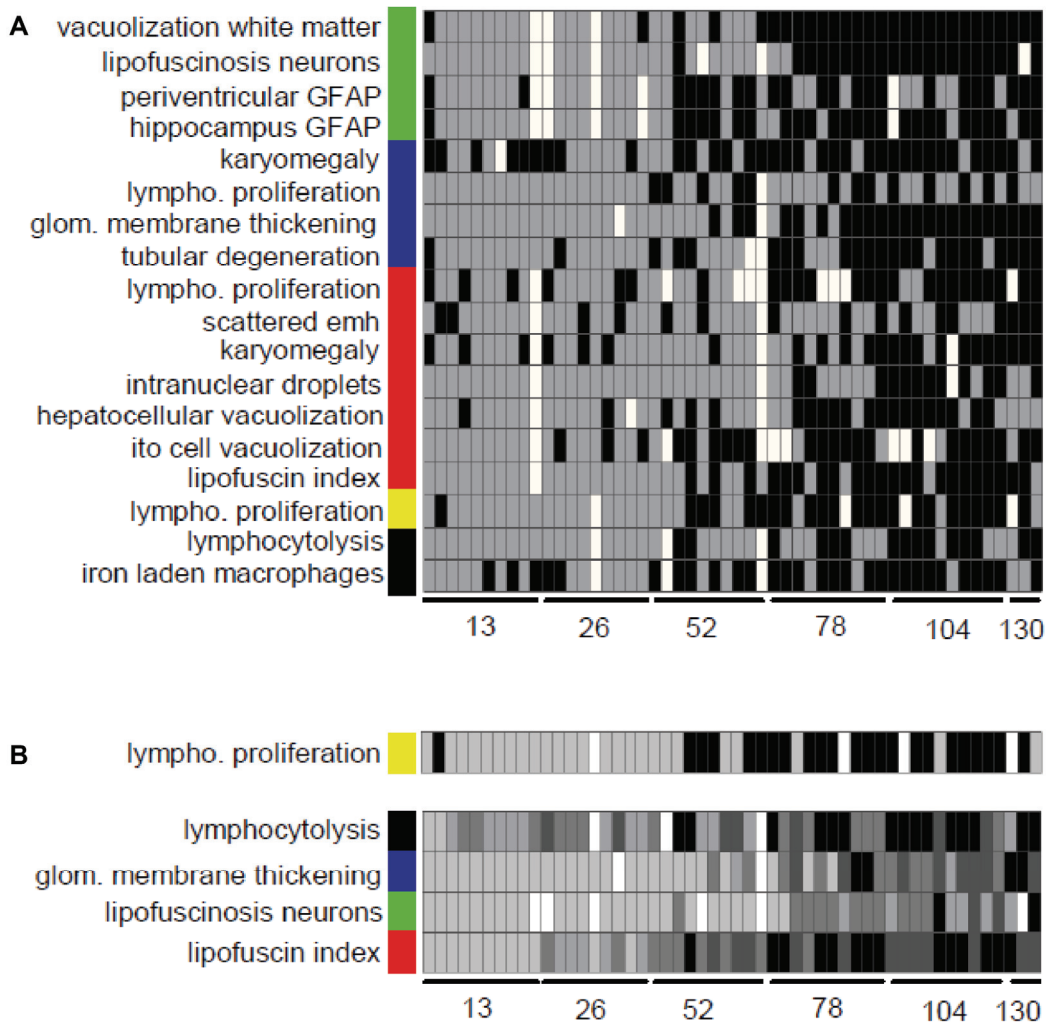


**Figure 1.** Heatmap indicating general age prediction (young or old) of individual samples based on the measured pathological characteristics. **(A)** Each phenotypic observation was used to cluster the samples and the average age age of the two main clusters was calculated. The heatmap indicates whether samples were part of the “young” group (grey) or the “old” group (black). White indicates missing values. The colour bar indicates tissue: brain (green), kidney (blue), liver (red), lung (yellow) and spleen (black). **(B)** The five most indicative pathological markers, of which four are shown at an ordinal scale from one (light gray) to four (black), to enable detailed comparison within individuals. Lymphoid proliferation in lung was originally measured on a binary scale, and could therefore not be transformed to the ordinal scale. White indicates missing values. The colour bar indicates tissue: brain (green), kidney (blue), liver (red), lung (yellow) and spleen (black).

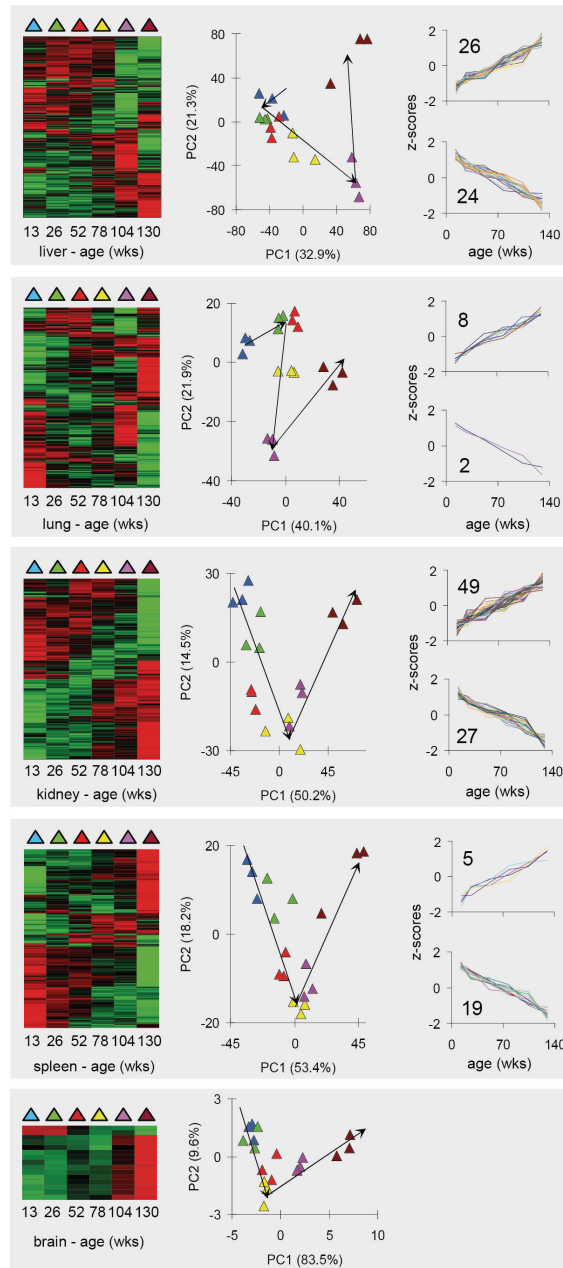


**Figure 2.** Age dependence of differentially expressed gene expression profiles in liver, lung, kidney, spleen and brain. The first column shows heatmaps after clustering the genes (dendrograms not shown). The second column shows scatterplots with samples plotted against the first two principal components calculated from centred and scaled expression values from the differentially expressed genes. The colours indicate age: light-blue: 13 weeks, green: 26 weeks, red: 52 weeks, yellow: 78 weeks, purple: 104 weeks and brown: 130 weeks. The last column shows graphs depicting the genes with linear expression profiles. The numbers indicate the numbers of genes.



### Gene expression dynamics during chronological aging

Parallel to pathological analyses, microarray analyses were performed on all age groups in all five tissues (Figure 2). Plotting the samples against the principal components indicated that the strongest variance was explained by the differences between tissues (SI04, data not shown in this thesis). The numbers of differentially expressed genes (DEGs) based on chronological age were (FDR < 0.05): 6973 in liver tissue, 1025 in lung tissue, 2325 in kidney, 925 in spleen tissue and 15 in brain (Figure 2). All changes in expression levels of 35.283 transcripts during aging per tissue, their corresponding p-values, q-values and aging dynamics are listed in SI05 (data not shown in this thesis). Principal component analysis revealed that in general the age groups clustered, and showed a marked difference in mice of 104 and 130 weeks (Figure 2). We did not observe many transcripts with a strictly increasing or decreasing expression profile (Figure 2 and SI04). We also observed that several established age-related genes based on literature generally showed non-linear and sometimes undulating expression patterns and often revealed a tissue-specific response (SI06 depicts gene expression dynamics for *mTOR*, *p16*, *GH*, *IGF*, *PTEN*, *Sirt1*, *TGFB*, *TERT*). Emphasising the irregularity in dynamics of single genes, only a small percentage of the DEGs followed a linear expression pattern (log2 scale, see M&M, Figure 2). Among the 6973 changing genes in the liver we found 50 DEGs with linear profiles (0.7%). In the lung, kidney and spleen we found 10, 76 and 24 DEGs with linear profiles: 1.0%, 3.3% 2.6% respectively. In summary, these analyses suggest that most age-related changes of the transcriptome are tissue-specific and the dynamics of gene expression can fluctuate greatly during the life span.

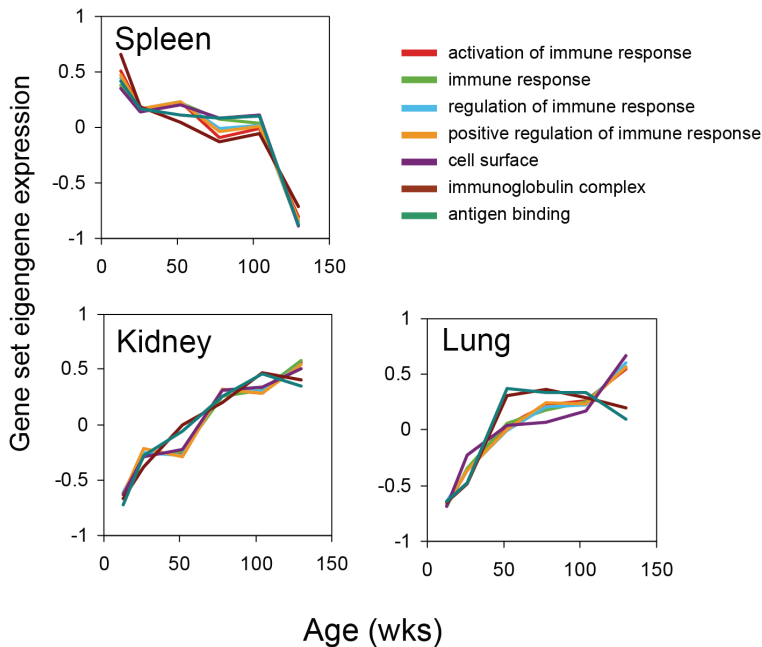


**Figure 3.** Tissue-specific immune-related gene-sets changes in spleen, kidney and lung. Seven gene-sets were found to have commonly changed with age in three tissues but demonstrated a tissue-specific response. The gene-sets were found through 62 responsive genes in spleen, 61 in kidney and 50 in lung. The profiles of the gene-sets, quantified using the first eigengenes of the responsive genes in the gene-sets.

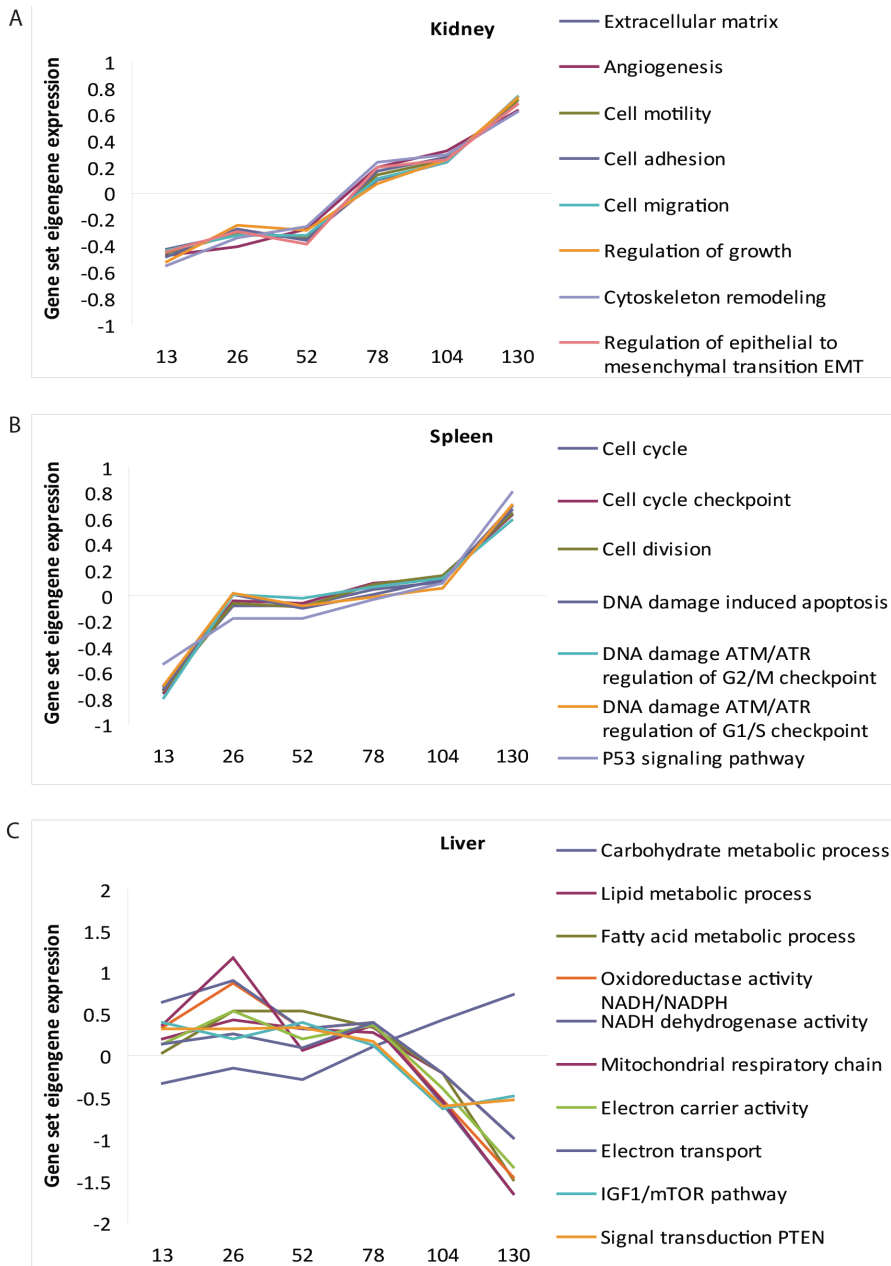


**Figure 4.** Dynamics of tissue-specific age-related changes. **(A)** Profiles of the gene-sets related to cell motility, migration and growth in kidney, quantified using the first eigengenes of the responsive genes in the gene-sets. **(B)** Profiles of the gene-sets related to cell cycle and DNA damage in spleen, quantified using the first eigengenes of the responsive genes in the gene-sets. **(C)** Profiles of the gene-sets related to metabolism and electron transport in liver, quantified using the first eigengenes of the responsive genes in the gene-sets.

### ***Functional characterization of chronological age-related gene expression changes and dynamics***

Next, we aimed to identify functional processes involved in aging in different tissues. We first used the Gene Ontology and overrepresentation analysis (ORA) and gene set analysis (GSA). We followed Tomlins *et al.* [25] and adopted a statistically lenient approach. The top 10% of most significant genes for each tissue were tested for overrepresentation (ORA) of functionally related genes, and the results were compared between tissues (Figure 3, 4 and detailed overview in SI07 (data not shown in this thesis)). The analyses demonstrated that most age-related changes are tissue-specific. The microarray results from brain are prone to false discoveries due to the low amount of DEGs and were therefore discarded in further analysis. Both ORA and GSA in lung, kidney and spleen indicated that the most notable gene-sets that changed during the aging process were immunological responses (Figure 3). Plotting the gene-set profiles revealed opposite directions of expression in the spleen as compared to kidney and lung, stressing a tissue-specific transcriptional response.

Besides immune response other tissue-specific, age-related changes were apparent (Figure 4). In kidney (Figure 4A), gene-sets linked to the extracellular matrix, cell motility, cell migration, angiogenesis and cell adhesion showed an age-related increase. In spleen (Figure 4B), cell cycle, cell division and DNA damage response pathways were differentially up-regulated during the lifespan.

In the liver, the majority of age-related changes in gene expression was not associated with immune response, but with metabolism and electron transport associated processes, which were mostly down-regulated (Figure 4C). Gene-set clustering on all ORA gene sets ( $p \leq 0.001$ ) in SI07 indicated that many genes in these gene-sets were related to the mitochondrial membrane and oxidative phosphorylation (SI08). Also, PTEN and mTOR signalling pathways revealed a similar down-regulation from 78 weeks in liver (Figure 4C).

### ***Functional pathology-related gene expression profiles***

To address biological aging we focussed on the pathological variables with the best predictive values in the previous analysis: lipofuscin levels in liver or brain, thickening of the glomerular membrane in kidney, increase in peribronchiolar lymphoid proliferation in lung and the decrease in lymphocytolysis in spleen. The severity of the pathological observation was assumed to indicate the level of biological aging and all individual samples were ranked along this axis per tissue. For example, we hypothesized that a liver sample isolated from a 130 week old mouse, could biologically speaking be regarded as “younger” when the level of lipofuscin accumulation is low. A tissue sample of a 26 week old mouse with a relatively high lipofuscin level is regarded as “older”. After ranking the samples according to their biological age per tissue, we screened for genes showing co-expression with each pathological parameter. Examples of the top 10 annotated genes which are most strongly co-expressed (either positive or negative) with the biological aging parameters are shown in Figure 5. It can be seen that *Clec7a* and *Clec1b* are co-expressed with lipofuscin in liver. *Trim2* is inversely co-expressed with lymphocytolysis in spleen. Fully listed co-expression data for each tissue are fully listed in SI09 (data not shown in this thesis).

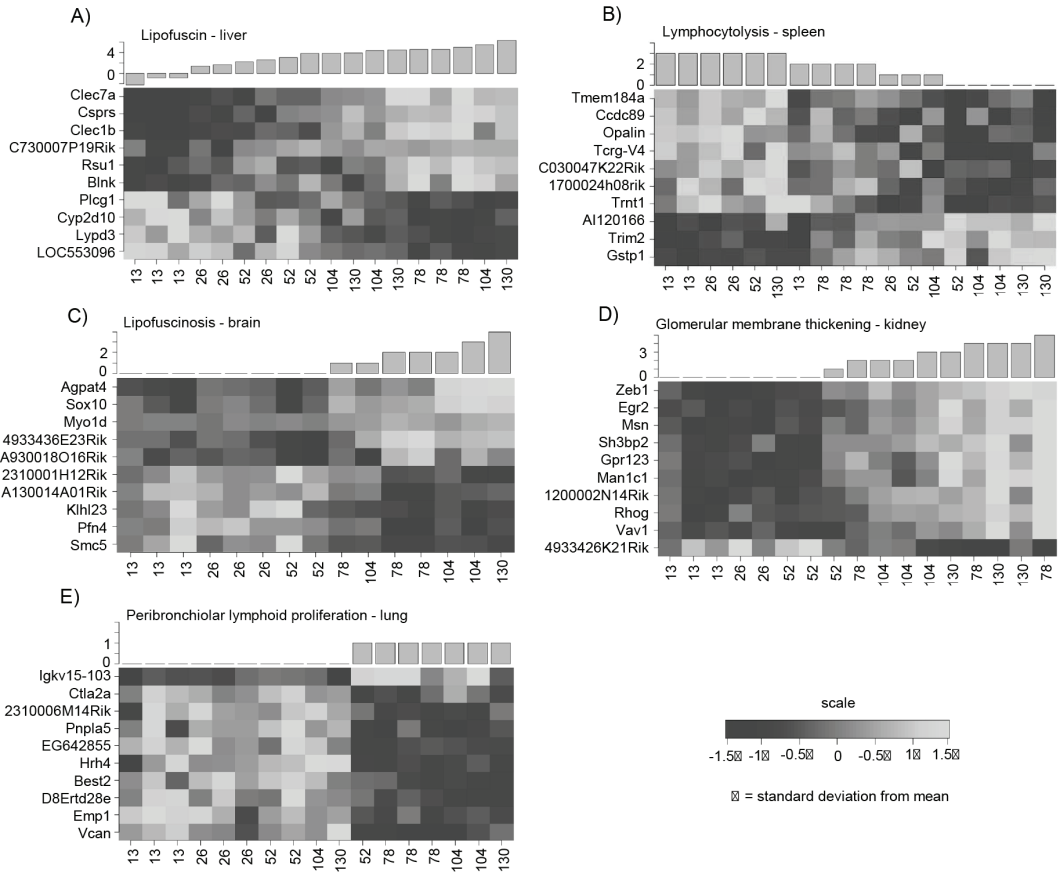


**Figure 5.** Biological aging biomarker per tissue. Heatmaps depicting the top 10 co-expression relationship between annotated genes and pathological aging parameters for (A) lipofuscin accumulation in the liver, (B) decrease in lymphocytolysis in the spleen, (C) lipofuscin accumulation in the brain, (D) glomerular membrane thickening in the kidney, and (E) increased peribronchiolar lymphoid proliferation in lung.

To functionally characterize pathology-driven gene expression profiles we used the same Gene Ontology and overrepresentation analysis (ORA) and gene set analysis (GSA) approaches as previously described, only now with co-expressed genes of the biological marker as input per tissue. Most of the significantly correlated gene-sets ( $p < 0.0001$ ) found through GSA analysis were for liver lipofuscin accumulation (54 gene-sets) and kidney glomerular membrane thickening (90 gene-sets), while hardly any gene-sets were obtained for the other tissues (SI10, data not shown in this thesis). In liver, the most significantly related gene-sets indicated changes in cellular components (mostly mitochondrial (gsea)) and changes in immune response (antigen processing, presentation and binding, phagocytosis, adaptive immune response, B-cell or immunoglobulin mediated responses). In kidney, these processes were also significantly changed in correlation with biological aging. Additionally, cytoskeleton organization seemed affected, as well as cell motility, migration and adhesion (SI10). More in-depth pathway responses were further characterized in more detail per tissue using Metacore GeneGO

Pathway Maps (Table 2 and fully listed in SI11). The analyses using the top 3% of most co-expressed genes per pathological parameter as input yielded a variable number of significantly regulated pathways per tissue ( $p < 0.01$ , FDR < 5%): Corresponding to the general results of the GSA and ORA most pathways were found for lipofuscin accumulation in liver (35) and glomerular membrane thickening in kidney (100). The other tissues showed only a small set of pathways (all results are fully listed in SI11).

Pathways in liver were involved in the immune response, development, TGF-Beta-related epithelial-to-mesenchymal transition (EMT) response and Reactive Oxygen Species (ROS)-related pathways. In kidney, regulation of EMT was the most significant result and several TGF-Beta induced EMT pathways are significant. Further, cell adhesion and migration, cytoskeletal remodelling and several immune responses also appeared correlated to biological aging in the kidney. The few pathways yielded for biological aging in lung described amongst others immune response, cell cycle, cytoskeletal and cell adhesion-related pathways. The POMC processing pathway, involved in protein folding and maturation was the most significantly overrepresented pathway in lung. Lastly, in brain mostly immune-related pathways were significant, but also one DNA damage pathway, mismatch repair, is represented (Table 2 and SI11).

<b>Pathological-related functional gene expression (Metacore GeneGO Pathway Maps <math>p &lt; 0.01</math>)</b>		
<b>Liver</b>	Immune response	46% (16 from 35)
	Development	17% (6 from 35)
	ROS-related	9% (3 from 35)
	EMT-related	6% (2 from 35)
<b>Kidney</b>	Immune response	27% (27 from 100)
	Development	18% (18 from 100)
	Cell adhesion	12% (12 from 100)
	Cytoskeletal remodelling	12% (12 from 100)
	EMT-related	6% (6 from 100)
<b>Lung</b>	Cell adhesion	18% (2 from 11)
	Protein folding and maturation	9% (1 from 11)
<b>Spleen</b>	no significant pathways	-
<b>Brain</b>	Apoptosis	33% (3 from 9)
	Immune response	22% (2 from 9)
	Development	22% (2 from 9)
	DNA damage	11% (1 from 9)

**Table 2.** General overview of functional responses of biological aging. General overview of functional GeneGO Maps of biological (pathology-related) aging. General terms are listed in this table, detailed GeneGO Pathway Maps are fully listed in SI11.

GeneGO pathway analyses revealed aging processes that were only visualized by the biological aging analyses. For example, biological aging analyses in liver (based on the pathological aging marker lipofuscin accumulation) yielded specific pathways that are related to reactive oxygen species and numerous immune-related responses. These responses were not visualized by the chronological aging

analyses. These results suggest a correlation between immune response and the level of oxidative stress during aging in liver. By combining the temporal responses during the entire lifespan and gene expression patterns linked to aging pathology our study can therefore shed some more light on the intricate processes involved in aging.

## Discussion

In this comprehensive study we analysed systematic *in vivo* aging of C57BL6/J mice, based on regular samples taken during their lifespan (13, 26, 52, 78, 104 and 130 weeks of age) from five organs for pathology and gene expression analyses. We identified pathological hallmarks that are correlated with chronological aging and employed these to assess individual pathology-related (biological) aging. Besides the generally accepted aging marker lipofuscin accumulation several, potentially novel, hallmarks of aging were revealed in five different tissues (e.g. glomerular membrane thickening, lymphocytolysis in spleen and lymphoid proliferation in kidney and lung). Chronological and biological aging were functionally characterized by gene expression profiling, with the ultimate aim to confirm or find novel underlying mechanisms for aging and investigate their temporal responses during the lifespan. The combined pathological parameters in our current study demonstrated that signs of aging are predominantly tissue-specific, and the gene expression profiles confirmed this tissue-specific regulation during the course of chronological and biological aging. However, analyses based on individual genes as well as on functionally related genes gave one generally common result: the genes involved in aging commonly changing in multiple tissues were related to the immune response. The pronounced response of the immune system was also found previously in other large-scale age-related gene expression studies [<sup>35,7</sup>]. In the comprehensive meta-analysis study of Swindell, immune responses were also the most commonly regulated processes over all tissues examined, but also biological processes like cellular respiration and other mitochondrial-related processes in liver were significantly regulated. Our study now makes it possible to monitor temporal dynamics of these and other possible age-related processes during the entire murine lifespan, which is an attractive extension for the aging field. In this study we have chosen to assess aging responses in a temporal chronological and pathology-driven (biological) manner, however, this study and accessible data also provides others with novel possibilities to address aging on a different level.

Functional characterization of the gene expression pinpointed immune responses which steadily increase or decrease with age, depending on the tissue type. Figure 3 depicted a decreasing expression of immune-related gene-sets in spleen, but an increasing expression in kidney, lung. The temporal analysis showed that the decreasing expression in spleen occurred quite sudden after 104 weeks, but increasing expression in the other tissues was more gradual. This may indicate increased immune cell infiltration upon cell death or cellular senescence in the tissues with age, but an overall decline in functionality of the immune system in spleen. The intercurrent pathological observation of lymphoid proliferation (in lung, kidney and liver) and the decrease of lymphocytolysis in spleen could partially reflect these transcriptome changes.

Our study also demonstrated that the most apparent gene expression changes observed in the liver were related to electron transport chain, metabolic processes and the mitochondrial membrane, which can reflect increasing mitochondrial and cellular dysfunction over time. The consequences of aging for mitochondria and oxidative phosphorylation have extensively been reviewed [<sup>31</sup>] and

decreased levels in electron transport chain have been shown in aging human tissue and other species [7]. Previous data support the finding that the rate of oxidative phosphorylation decreases during aging [32]. Our results now indicate that mitochondrial processes and oxidative phosphorylation increased moderately from very young adulthood to mature adulthood, remained constant until 78 weeks of age and then decreased considerably during the remainder of the lifespan (104 and 130 weeks). The mTOR and PTEN signaling pathways also followed this dynamic in liver. Dysregulation in both pathways has been associated with metabolic changes during aging and can also affect cancer susceptibility [33,34]. Also in other tissues we found gene expression changes that have been associated with cancer. In kidney the gene expression profiles revealed an up-regulation during aging of processes like cell motility, cell migration and angiogenesis. Several cancer associated pathways were also up-regulated in spleen: increased cell cycle and DNA damage responses were apparent, especially during the final stages of the lifespan.

Our study also showed that the pathological biomarker for ROS, lipofuscin accumulation [35], gradually increased over time, in mitotic as well as post-mitotic tissue. This supports the hypothesis that ROS and free radicals contribute to protein, lipid, RNA and DNA damage accumulation and homeostatic imbalance during aging in our study. Interestingly, the gene most strongly co-expressed with lipofuscin accumulation in liver was *Clec7a*, which is an innate immune receptor and can mediate production of ROS in the cell [36]. Also, *Hmox1* (associated with oxidative stress defense) was found to be highly correlated to lipofuscin accumulation in liver (SI09). Part of the correlated pathways to biological aging in liver revealed additional processes that were linked to ROS: e.g. TGF-beta-induction of EMT by ROS and angiotensin II-induced production of ROS (SI11). The latter pathway was also correlated to biological aging in kidney, and additionally several other EMT-related processes were notable in this tissue. Another interesting result linking lipofuscin accumulation to increased ROS was the fact that biological aging analyses in liver yielded pathways related to reactive oxygen species and numerous immune-related responses, while these responses were not identified by chronological aging analyses. These results suggest a correlation between immune response and the level of oxidative stress during aging in liver and moreover exemplify the added value of pathology-driven aging analyses. Combining temporal responses spanning the murine C57BL/6J lifespan and gene expression patterns linked to aging pathology our study provides more information on the intricate processes involved in aging.

Processes identified to be differentially regulated during aging, like mitochondrial dysfunction and the regulation of immune-related processes, are able to greatly increase ROS in cells [37,38], thereby potentially causing collateral DNA and other macromolecular damage. Since our data did not show a considerable regulation of DNA repair pathways over time or over biological aging, we expect this damage to accumulate slowly over time and influence age-related disease in most tissues, but at different rates. We have previously shown that mutations, caused by intrinsic DNA damage, increased at different rates during aging in several tissues in mice from the same intercurrent aging cohorts that were used in our current study [29]. Reversely, *in vivo* defects in DNA damage repair machinery have demonstrated to promote (segmental) accelerated aging phenotypes [20,39].

In this extensive study we analysed the process of aging on multiple levels: biological and chronological aging were assessed, combining age-related pathology and gene expression profiling. We proposed several distinguishable and potentially novel pathological hallmarks that are highly correlated to chronological aging in different tissues, but because of inter- and intra-individual variation are additionally useful to study pathology-driven, biological aging. In this study it was evident

that the immune responses played the most distinguished role in both chronological and biological aging, but manifested itself with highly tissue-specific dynamics. Our results furthermore support several aging hypotheses at the cellular level, like processes that can cause increased levels of ROS, an imbalanced metabolic or energy homeostasis or increased mutational load. Moreover, our study now enables studying temporal dynamics of genes and processes spanning the entire lifespan over multiple tissues.

## **Acknowledgements**

We thank the Animal Facilities of the Netherlands Vaccine Institute (NVI) for their skilful (bio)technical support. The work presented here was in part financially supported by IOP Genomics IGE03009, NIH/NIA (3PO1 AG017242), STW Grant STW-LGC.6935 and NBIC BioRange II – BR4.1. Support was also obtained from Markage (FP7-Health-2008-200880), LifeSpan (LSHG-CT-2007-036894), European Research Council (ERC advanced scientist grant JHJH).

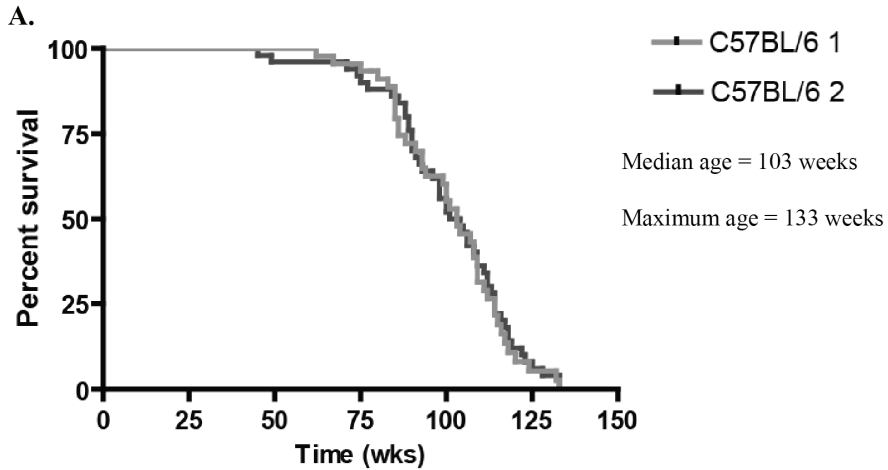


## Reference List

- [1] A.Y.Maslov, J.Vijg. Genome instability, cancer and aging, *Biochim.Biophys.Acta*, 1790, (2009) 963-969.
- [2] J.P.de Magalhaes, J.Curado, G.M.Church. Meta-analysis of age-related gene expression profiles identifies common signatures of aging, *Bioinformatics.*, 25, (2009) 875-881.
- [3] S.K.Park, K.Kim, G.P.Page, D.B.Allison, R.Weindruch, T.A.Prolla. Gene expression profiling of aging in multiple mouse strains: identification of aging biomarkers and impact of dietary antioxidants, *Aging Cell*, 8, (2009) 484-495.
- [4] W.R.Swindell. Gene expression profiling of long-lived dwarf mice: longevity-associated genes and relationships with diet, gender and aging, *BMC.Genomics*, 8, (2007) 353.
- [5] W.R.Swindell. Genes and gene expression modules associated with caloric restriction and aging in the laboratory mouse, *BMC.Genomics*, 10, (2009) 585.
- [6] W.R.Swindell, A.Johnston, L.Sun, X.Xing, G.J.Fisher, M.L.Bulyk, J.T.Elder, J.E.Gudjonsson. Meta-profiles of gene expression during aging: limited similarities between mouse and human and an unexpectedly decreased inflammatory signature, *PLoS One*, 7, (2012) e33204.
- [7] J.M.Zahn, S.Poosala, A.B.Owen, D.K.Ingram, A.Lustig, A.Carter, A.T.Weeraratna, D.D.Taub, M.Gorospe, K.Mazan-Mamczarz, E.G.Lakatta, K.R.Boheler, X.Xu, M.P.Mattson, G.Falco, M.S.Ko, D.Schlessinger, J.Firman, S.K.Kummerfeld, W.H.Wood, III, A.B.Zonderman, S.K.Kim, K.G.Becker. AGEMAP: a gene expression database for aging in mice, *PLoS Genet.*, 3, (2007) e201.
- [8] J.L.Barger, T.Kayo, J.M.Vann, E.B.Arias, J.Wang, T.A.Hacker, Y.Wang, D.Raederstorff, J.D.Morrow, C.Leeuwenburgh, D.B.Allison, K.W.Saupe, G.D.Cartee, R.Weindruch, T.A.Prolla. A low dose of dietary resveratrol partially mimics caloric restriction and retards aging parameters in mice, *PLoS.One.*, 3, (2008) e2264.
- [9] L.K.Southworth, A.B.Owen, S.K.Kim. Aging mice show a decreasing correlation of gene expression within genetic modules, *PLoS.Genet.*, 5, (2009) e1000776.
- [10] B.Schumacher, d.P.van, I, M.J.Moorhouse, T.Kosteas, A.R.Robinson, Y.Suh, T.M.Breit, H.van Steeg, L.J.Niedernhofer, W.van Ijcken, A.Bartke, S.R.Spindler, J.H.Hoeijmakers, G.T.van der Horst, G.A.Garinis. Delayed and accelerated aging share common longevity assurance mechanisms, *PLoS.Genet.*, 4, (2008) e1000161.
- [11] M.L.Gron Dahl, A.C.Yding, J.Bogstad, F.C.Nielsen, H.Meinertz, R.Borup. Gene expression profiles of single human mature oocytes in relation to age, *Hum.Reprod.*, 25, (2010) 957-968.
- [12] J.M.Zahn, R.Sonu, H.Vogel, E.Crane, K.Mazan-Mamczarz, R.Rabkin, R.W.Davis, K.G.Becker, A.B.Owen, S.K.Kim. Transcriptional profiling of aging in human muscle reveals a common aging signature, *PLoS.Genet.*, 2, (2006) e115.
- [13] G.A.Garinis, G.T.van der Horst, J.Vijg, J.H.Hoeijmakers. DNA damage and ageing: new-age ideas for an age-old problem, *Nat.Cell Biol.*, 10, (2008) 1241-1247.
- [14] T.L.Parkes, A.J.Elia, D.Dickinson, A.J.Hilliker, J.P.Phillips, G.L.Boulianne. Extension of *Drosophila* lifespan by overexpression of human SOD1 in motorneurons, *Nat.Genet.*, 19, (1998) 171-174.
- [15] N.Treiber, P.Maity, K.Singh, M.Kohn, A.F.Keist, F.Ferchiu, L.Sante, S.Frese, W.Bloch, F.Kreppel, S.Kochanek, A.Sindrilariu, S.Iben, J.Hogel, M.Ohnmacht, L.E.Claes, A.Ignatius, J.H.Chung, M.J.Lee, Y.Kamenisch, M.Berneburg, T.Nikolaus, K.Braunstein, A.D.Sperfeld, A.C.Ludolph, K.Briviba, M.Wlaschek, L.Florin, P.Angel, K.Scharffetter-Kochanek. Accelerated aging phenotype in mice with conditional deficiency for mitochondrial superoxide dismutase in the connective tissue, *Aging Cell*, 10, (2011) 239-254.
- [16] G.A.Garinis, L.M.Uittenboogaard, H.Stachelscheid, M.Fousteri, W.van Ijcken, T.M.Breit, H.van Steeg, L.H.Mullenders, G.T.van der Horst, J.C.Bruning, C.M.Niessen, J.H.Hoeijmakers, B.Schumacher. Persistent transcription-blocking DNA lesions trigger somatic growth attenuation associated with longevity, *Nat.Cell Biol.*, 11, (2009) 604-615.

- [17] G.Marino, A.P.Ugalde, A.F.Fernandez, F.G.Osorio, A.Fueyo, J.M.Freije, C.Lopez-Otin. Insulin-like growth factor 1 treatment extends longevity in a mouse model of human premature aging by restoring somatotroph axis function, *Proc.Natl.Acad.Sci.U.S.A*, 107, (2010) 16268-16273.
- [18] T.Vellai, K.Takacs-Vellai, Y.Zhang, A.L.Kovacs, L.Orosz, F.Muller. Genetics: influence of TOR kinase on lifespan in *C. elegans*, *Nature*, 426, (2003) 620.
- [19] D.E.Harrison, R.Strong, Z.D.Sharp, J.F.Nelson, C.M.Astle, K.Flurkey, N.L.Nadon, J.E.Wilkinson, K.Frenkel, C.S.Carter, M.Pahor, M.A.Javors, E.Fernandez, R.A.Miller. Rapamycin fed late in life extends lifespan in genetically heterogeneous mice, *Nature*, 460, (2009) 392-395.
- [20] S.W.Wijnhoven, R.B.Beems, M.Roodbergen, B.J.van den, P.H.Lohman, K.Diderich, G.T.van der Horst, J.Vijg, J.H.Hoeijmakers, H.van Steeg. Accelerated aging pathology in ad libitum fed Xpd(ITT) mice is accompanied by features suggestive of caloric restriction, *DNA Repair (Amst)*, 4, (2005) 1314-1324.
- [21] R.A.Irizarry, B.Hobbs, F.Collin, Y.D.Beazer-Barclay, K.J.Antonellis, U.Scherf, T.P.Speed. Exploration, normalization, and summaries of high density oligonucleotide array probe level data, *Biostatistics*, 4, (2003) 249-264.
- [22] W.C.de Leeuw, H.Rauwerda, M.J.Jonker, T.M.Breit. Salvaging Affymetrix probes after probe-level re-annotation, *BMC.Res.Notes*, 1, (2008) 66.
- [23] J.D.Storey, W.Xiao, J.T.Leek, R.G.Tompkins, R.W.Davis. Significance analysis of time course microarray experiments, *Proc.Natl.Acad.Sci.U.S.A*, 102, (2005) 12837-12842.
- [24] J.D.Storey, R.Tibshirani. Statistical significance for genomewide studies, *Proc.Natl.Acad.Sci.U.S.A*, 100, (2003) 9440-9445.
- [25] S.A.Tomlins, R.Mehra, D.R.Rhodes, X.Cao, L.Wang, S.M.Dhanasekaran, S.Kalyana-Sundaram, J.T.Wei, M.A.Rubin, K.J.Pienta, R.B.Shah, A.M.Chinnaiyan. Integrative molecular concept modeling of prostate cancer progression, *Nat.Genet.*, 39, (2007) 41-51.
- [26] O.Alter, P.O.Brown, D.Botstein. Singular value decomposition for genome-wide expression data processing and modeling, *Proc.Natl.Acad.Sci.U.S.A*, 97, (2000) 10101-10106.
- [27] d.W.Huang, B.T.Sherman, Q.Tan, J.R.Collins, W.G.Alvord, J.Roayaei, R.Stephens, M.W.Baseler, H.C.Lane, R.A.Lempicki. The DAVID Gene Functional Classification Tool: a novel biological module-centric algorithm to functionally analyze large gene lists, *Genome Biol.*, 8, (2007) R183.
- [28] J.Michaud, K.M.Simpson, R.Escher, K.Buchet-Poyau, T.Beissbarth, C.Carmichael, M.E.Ritchie, F.Schutz, P.Cannon, M.Liu, X.Shen, Y.Ito, W.H.Raskind, M.S.Horwitz, M.Osato, D.R.Turner, T.P.Speed, M.Kavallaris, G.K.Smyth, H.S.Scott. Integrative analysis of RUNX1 downstream pathways and target genes, *BMC.Genomics*, 9, (2008) 363.
- [29] J.P.Melis, S.W.Wijnhoven, R.B.Beems, M.Roodbergen, B.J.van den, H.Moon, E.Friedberg, G.T.van der Horst, J.H.Hoeijmakers, J.Vijg, H.van Steeg. Mouse models for xeroderma pigmentosum group A and group C show divergent cancer phenotypes, *Cancer Res.*, 68, (2008) 1347-1353.
- [30] D.A.Gray, J.Woulfe. Lipofuscin and aging: a matter of toxic waste, *Sci.Aging Knowledge Environ.*, 2005, (2005) re1.
- [31] E.J.Lesnefsky, C.L.Hoppel. Oxidative phosphorylation and aging, *Ageing Res.Rev.*, 5, (2006) 402-433.
- [32] Y.Okatani, A.Wakatsuki, R.J.Reiter, Y.Miyahara. Hepatic mitochondrial dysfunction in senescence-accelerated mice: correction by long-term, orally administered physiological levels of melatonin, *J.Pineal Res.*, 33, (2002) 127-133.
- [33] R.Zoncu, A.Efeyan, D.M.Sabatini. mTOR: from growth signal integration to cancer, diabetes and ageing, *Nat.Rev.Mol.Cell Biol.*, 12, (2011) 21-35.
- [34] M.Keniry, R.Parsons. The role of PTEN signaling perturbations in cancer and in targeted therapy, *Oncogene*, 27, (2008) 5477-5485.
- [35] T.Jung, N.Bader, T.Grune. Lipofuscin: formation, distribution, and metabolic consequences, *Ann.N.Y.Acad.Sci.*, 1119, (2007) 97-111.

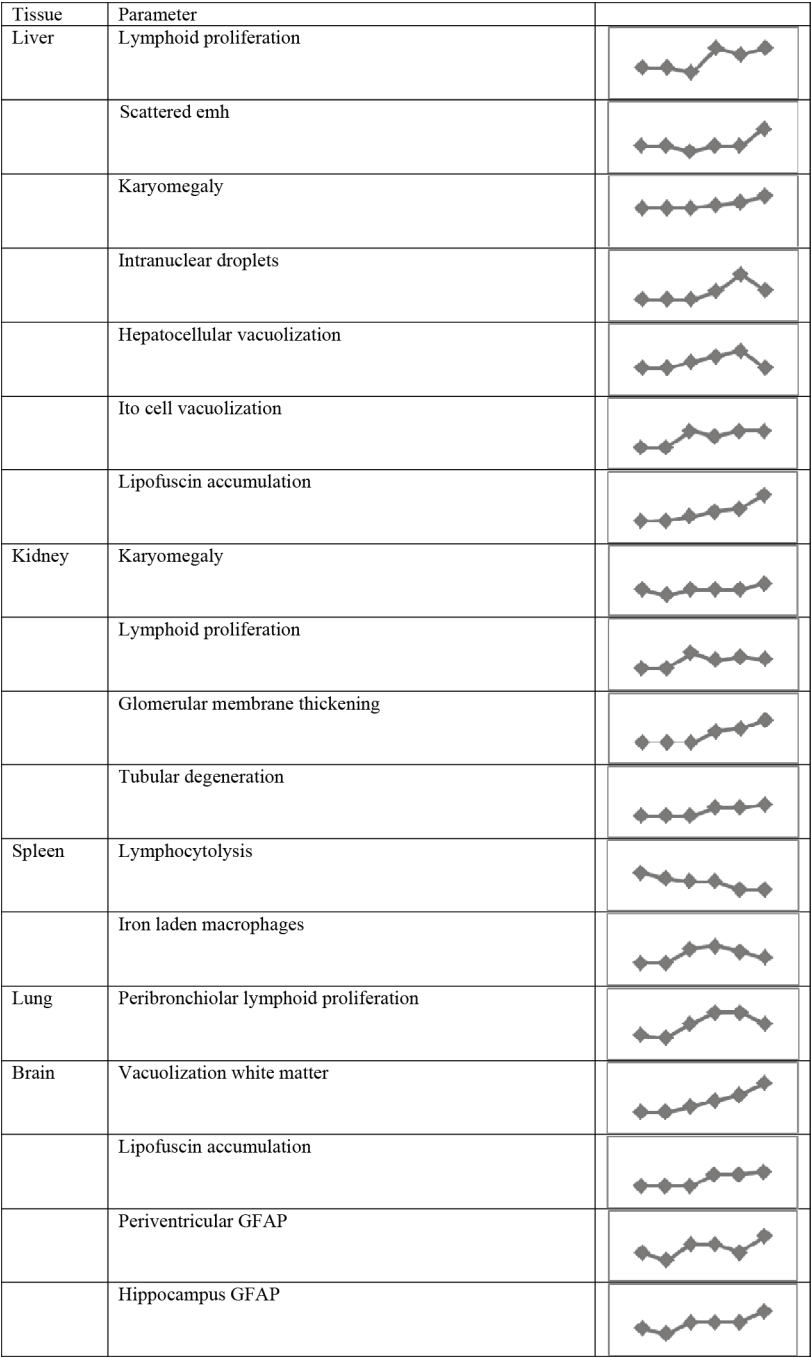
- [36] H.S.Goodridge, C.N.Reyes, C.A.Becker, T.R.Katsumoto, J.Ma, A.J.Wolf, N.Bose, A.S.Chan, A.S.Magee, M.E.Danielson, A.Weiss, J.P.Vasilakos, D.M.Underhill. Activation of the innate immune receptor Dectin-1 upon formation of a 'phagocytic synapse', *Nature*, 472, (2011) 471-475.
- [37] H.Cui, Y.Kong, H.Zhang. Oxidative stress, mitochondrial dysfunction, and aging, *J.Signal.Transduct.*, 2012, (2012) 646354.
- [38] A.P.West, I.E.Brodsky, C.Rahner, D.K.Woo, H.Erdjument-Bromage, P.Tempst, M.C.Walsh, Y.Choi, G.S.Shadel, S.Ghosh. TLR signalling augments macrophage bactericidal activity through mitochondrial ROS, *Nature*, 472, (2011) 476-480.
- [39] S.W.Wijnhoven, E.M.Hoogervorst, H.de Waard, G.T.van der Horst, H.van Steeg. Tissue specific mutagenic and carcinogenic responses in NER defective mouse models, *Mutat.Res.*, 614, (2007) 77-94.



**B.**

Age (weeks) Cohort 1	% survival Cohort 1	Sample size (Intercurrent study)
13	100%	10 mice
26	100%	9 mice
52	100%	10 mice
78	96%	10 mice
104	48%	10 mice
130	6%	3 mice

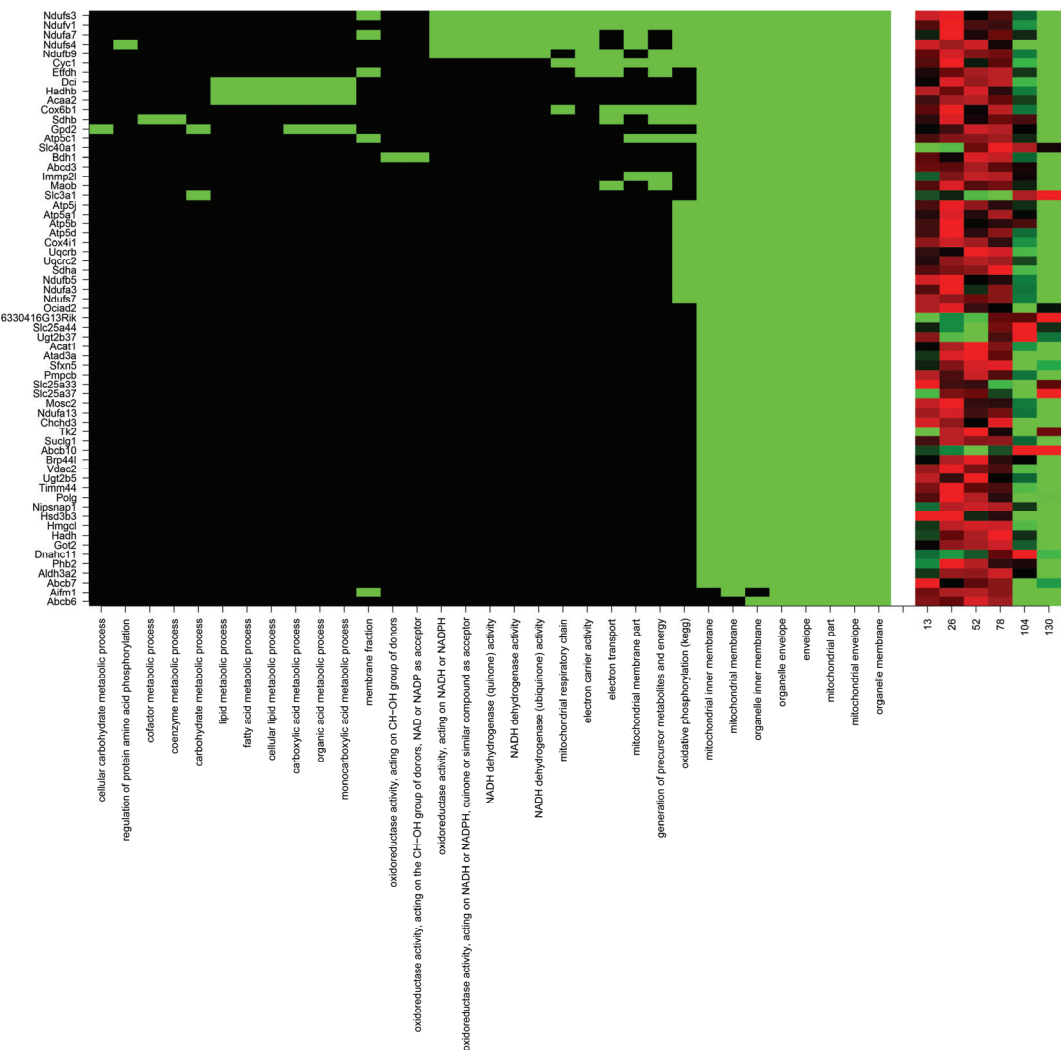
**Supplemental information 1. A.** Survival curves of the concurrent female wild type longevity cohort (C57BL/6J 1,  $n=50$ ) of the study presented in this manuscript. Female cohort (C57BL/6J 2,  $n=50$ ) was executed several years later and shows very high reproducibility. The median and maximum age for both longevity cohorts was 103 weeks and 133 weeks respectively. **B.** Overview of representative survival percentages for the intercurrent age groups used in this manuscript (deducted from cohort C57BL/6J 1). The sample size of the intercurrent age groups are also shown here. Per age group 3 samples were used for gene expression profiling and the highest number possible for pathology analysis shown in Table 1.



**Supplemental information 2.** Dynamics of age-related pathological parameters during lifespan in 5 tissues

		Y	O	correct prediction young	% correct	correct prediction old	% correct
Brain	Vacuolization white matter	29.7	85.9	14/16	87.50	13/13	100.00
	<b>Lipofuscin neurons</b>	32.8	94.1	16/16	100.00	12/12	100.00
	Periventricular GFAP	48.4	76.8	13/15	86.67	7/12	58.33
	Hippocampus GFAP	39.0	81.6	14/15	93.33	10/12	83.33
Kidney	Karyomegaly	46.6	67.3	10/19	52.63	11/13	84.62
	Lymphoid proliferation	52.7	80.0	19/19	100.00	5/13	38.46
	<b>Glomerular membrane thickening</b>	32.7	92.7	18/18	100.00	13/13	100.00
	Tubular degeneration	38.0	85.3	17/19	89.47	11/13	84.62
Liver	Lymphoid proliferation	36.9	75.3	12/18	66.67	10/12	83.33
	Scattered emh	53.1	76.4	14/18	77.78	7/13	53.85
	Karyomegaly	44.0	77.4	12/18	66.67	11/12	91.67
	Intranuclear droplets	46.7	99.7	18/18	100.00	9/12	75.00
	Hepatocellular vacuolization	49.3	78.6	15/17	88.24	8/13	61.54
	Ito cell vacuolization	36.5	75.7	15/18	83.33	8/10	80.00
	<b>Lipofuscin</b>	38.1	89.8	18/18	100.00	11/13	84.62
	<b>Lymphoid proliferation</b>	35.9	80.8	17/18	94.44	9/11	81.82
Lung	<b>Lymphocytolysis</b>	45.9	93.6	18/18	100.00	9/13	69.23
Spleen	Iron laden macrophages	43.6	72.1	13/18	72.22	10/13	76.92

**Supplemental information 3.** Predictive accuracy of each pathological parameter. The allocations of the samples to age groups indicated in Figure 1 were used to test the accuracy of the predictive age for each pathological parameter. Per age group the number of individual correct predictions were assessed where possible (absent predictions (white) were excluded from the analysis). For the young group (13 and 26 weeks) individuals should be predicted as “young” (grey) in Figure 1. For the old group (104 and 130 weeks) individuals should be predicted as “old” (black) in Figure 1. Per tissue, parameters in bold are considered most predictive and most correlated to aging. The first column (Y) indicates the average age of the samples in the young age group in weeks, the second column (O) indicates the average age of the samples in the old age group in weeks, the third column indicates the number of correct allocations to the young age group compared to the number of samples, the fourth column represents this number as a percentage, the fifth column indicates the number of correct allocations to the old age group compared to the number of samples, the sixth column represents this number as a percentage.



**Supplemental information 8.** Left panel: clustering analysis indicating the overlap of genes (rows) between gene-sets (columns) found in the pathways related to metabolism, oxidative phosphorylation and mitochondrial membrane. Right panel: heatmap showing the expression profiles of the genes in the gene-set-cluster across the six time points: 13, 26, 52, 78, 104 and 130 weeks.

**Supplemental information 11.** Complete overview of significantly regulated Metacore GeneGO Pathway Maps related to biological aging for each tissues ( $p < 0.01$ ).

#### Lipofuscin accumulation - Liver

#	Maps	pValue	Ratio
1	Immune response_ Immunological synapse formation	4.608E-08	12 59
2	Immune response_ BCR pathway	1.674E-07	11 54
3	Immune response_ CCR3 signaling in eosinophils	6.724E-06	11 77
4	Immune response_ Fc epsilon RI pathway	1.528E-05	9 55
5	Immune response_ PIP3 signaling in B lymphocytes	1.229E-04	7 42
6	Immune response_ ETV3 affect on CSF1-promoted macrophage differentiation	1.607E-04	6 31
7	Immune response_ IL-5 signalling	1.666E-04	7 44
8	Development_ EPO-induced MAPK pathway	1.928E-04	7 45
9	Immune response_ Antigen presentation by MHC class II	2.251E-04	4 12
10	Oxidative stress_ Angiotensin II-induced production of ROS	3.235E-04	6 35
11	Inhibitory action of Lipoxins on Superoxide production in neutrophils	3.327E-04	7 49
12	G-protein signaling_ Rac2 regulation pathway	3.794E-04	6 36
13	Immune response_ NFAT in immune response	4.281E-04	7 51
14	Immune response_ Inhibitory action of lipoxins on superoxide production induced by IL-8 and Leukotriene B4 in neutrophils	4.281E-04	7 51
15	Immune response_ CD16 signaling in NK cells	5.427E-04	8 69
16	Blood coagulation_ GPVI-dependent platelet activation	6.842E-04	7 55
17	Chemotaxis_ Leukocyte chemotaxis	9.510E-04	8 75
18	Apoptosis and survival_ Inhibition of ROS-induced apoptosis by 17beta-estradiol	1.146E-03	6 44
19	Chemotaxis_ CCR4-induced leukocyte adhesion	1.182E-03	5 30
20	Development_ TGF-beta-induction of EMT via ROS	1.517E-03	4 19
21	Development_ TGF-beta-dependent induction of EMT via MAPK	1.629E-03	6 47
22	Development_ HGF signaling pathway	1.629E-03	6 47
23	Immune response_ IL-2 activation and signaling pathway	2.028E-03	6 49
24	Cell adhesion_ Alpha-4 integrins in cell migration and adhesion	2.113E-03	5 34
25	Chemotaxis_ Inhibitory action of lipoxins on IL-8- and Leukotriene B4-induced neutrophil migration	2.496E-03	6 51
26	Immune response_ Role of DAP12 receptors in NK cells	3.345E-03	6 54
27	Immune response_ Role of integrins in NK cells cytotoxicity	3.489E-03	5 38
28	Inhibitory action of Lipoxins on neutrophil migration	4.393E-03	6 57
29	Neurophysiological process_ Dopamine D2 receptor transactivation of PDGFR in CNS	5.038E-03	4 26
30	Regulation of lipid metabolism_ G-alpha(q) regulation of lipid metabolism	5.214E-03	6 59
31	Development_ EPO-induced PI3K/AKT pathway and Ca(2+) influx	5.993E-03	5 43
32	Development_ Angiotensin signaling via PYK2	5.993E-03	5 43
33	Immune response_ IL-15 signaling	7.754E-03	6 64
34	Immune response_ Fc gamma R-mediated phagocytosis in macrophages	8.747E-03	5 47
35	Cytoskeleton remodeling_ Reverse signaling by ephrin B	9.535E-03	4 31

#### Glomerular membrane thickening - Kidney

#	Maps	pValue	Ratio
1	Development_ Regulation of epithelial-to-mesenchymal transition (EMT)	7.206E-10	15 64
2	Chemotaxis_ Leukocyte chemotaxis	7.565E-09	15 75
3	Development_ Slit-Robo signaling	1.299E-08	10 30
4	Transcription_ NF-kB signaling pathway	1.741E-08	11 39
5	Cytoskeleton remodeling_ Regulation of actin cytoskeleton by Rho GTPases	2.673E-07	8 23
6	Apoptosis and survival_ Anti-apoptotic TNFs/NF-kB/IgI-2 pathway	3.575E-07	10 41
7	Development_ TGF-beta-dependent induction of EMT via RhoA, PI3K and ILK.	1.132E-06	10 46
8	Bacterial infections in CF airways	1.395E-06	11 58
9	Cell adhesion_ Role of tetraspanins in the integrin-mediated cell adhesion	1.434E-06	9 37
10	Immune response_ Immunological synapse formation	1.668E-06	11 59
11	Cell adhesion_ Chemokines and adhesion	2.395E-06	14 100
12	Transport_ Macropinocytosis regulation by growth factors	3.286E-06	11 63
13	Cell adhesion_ ECM remodeling	3.724E-06	10 52
14	Immune response_ CCR3 signaling in eosinophils	4.071E-06	12 77
15	Immune response_ IFN alpha/beta signaling pathway	5.904E-06	7 24
16	Cell adhesion_ Integrin inside-out signaling	7.507E-06	10 56
17	Cytoskeleton remodeling_ Neurofilaments	7.983E-06	7 25
18	Development_ TGF-beta-dependent induction of EMT via SMADs	9.260E-06	8 35
19	Chemotaxis_ Lipoxin inhibitory action on fMLP-induced neutrophil chemotaxis	9.926E-06	9 46
20	Immune response_ Oncostatin M signaling via JAK-Stat in mouse cells	1.192E-05	6 18
21	Immune response_ Fc gamma R-mediated phagocytosis in macrophages	1.195E-05	9 47
22	Immune response_ Bacterial infections in normal airways	2.023E-05	9 50
23	Cytokine production by Th17 cells in CF	2.172E-05	8 39
24	Immune response_ Oncostatin M signaling via JAK-Stat in human cells	2.361E-05	6 20
25	Apoptosis and survival_ Lymphotoxin-beta receptor signaling	3.841E-05	8 42
26	Blood coagulation_ GPVI-dependent platelet activation	4.479E-05	9 55
27	Cytoskeleton remodeling_ Keratin filaments	1.033E-04	7 36
28	Blood coagulation_ GPIIb-IX-V-dependent platelet activation	1.036E-04	10 75
29	Cytokine production by Th17 cells in CF (Mouse model)	1.215E-04	8 49
30	Cell adhesion_ Cell-matrix glycoconjugates	1.480E-04	7 38
31	Apoptosis and survival_ Anti-apoptotic TNFs/NF-kB/IAP pathway	1.500E-04	6 27
32	Chemotaxis_ Inhibitory action of lipoxins on IL-8- and Leukotriene B4-induced neutrophil migration	1.625E-04	8 51
33	Immune response_ Innate immune response to RNA viral infection	1.859E-04	6 28
34	Cytoskeleton remodeling_ Role of PKA in cytoskeleton reorganisation	2.073E-04	7 40



35	Chemotaxis_CCR4-induced leukocyte adhesion	2.780E-04	6	30
36	Immune response_TLR signaling pathways	3.167E-04	8	56
37	Blood coagulation_GPCRs in platelet aggregation	3.392E-04	9	71
38	Inhibitory action of Lipoxins on neutrophil migration	3.586E-04	8	57
39	Development_PDGF signaling via STATs and NF-κB	4.026E-04	6	32
40	Neurophysiological process_Receptor-mediated axon growth repulsion	4.416E-04	7	45
41	Role of alpha-6/beta-4 integrins in carcinoma progression	4.416E-04	7	45
42	Cell adhesion_Histamine H1 receptor signaling in the interruption of cell barrier integrity	4.416E-04	7	45
43	Development_Thrombopoietin signaling via JAK-STAT pathway	4.888E-04	5	22
44	Cell adhesion_Alpha-4 integrins in cell migration and adhesion	5.670E-04	6	34
45	Development_TGF-beta-dependent induction of EMT via MAPK	5.803E-04	7	47
46	Immune response_IL-27 signaling pathway	7.495E-04	5	24
47	Signal transduction_PKA signaling	9.605E-04	7	51
48	Immune response_Role of integrins in NK cells cytotoxicity	1.048E-03	6	38
49	Immune response_Antiviral actions of Interferons	1.081E-03	7	52
50	Cell adhesion_Cadherin-mediated cell adhesion	1.102E-03	5	26
51	Development_Cross-talk between VEGF and Angiopoietin 1 signaling pathways	1.102E-03	5	26
52	Immune response_IL-10 signaling pathway	1.102E-03	5	26
53	Development_S1P2 and S1P3 receptors in cell proliferation and differentiation	1.102E-03	5	26
54	Apoptosis and survival_APRIL and BAFF signaling	1.207E-03	6	39
55	Cytoskeleton remodeling_Cytoskeleton remodeling	1.272E-03	10	102
56	Immune response_CD16 signaling in NK cells	1.314E-03	8	69
57	Immune response_IFN gamma signaling pathway	1.357E-03	7	54
58	Immune response_MIF in innate immunity response	1.384E-03	6	40
59	Development_Delta-type opioid receptor signaling via G-protein alpha-14	1.565E-03	5	28
60	Regulation of lipid metabolism_Stimulation of Arachidonic acid production by ACM receptors	1.736E-03	8	72
61	Immune response_Neurotensin-induced activation of IL-8 in colonocytes	1.795E-03	6	42
62	NGF activation of NF-κB	1.843E-03	5	29
63	Apoptosis and survival_TNFR1 signaling pathway	2.032E-03	6	43
64	Muscle contraction_S1P2 receptor-mediated smooth muscle contraction	2.156E-03	5	30
65	Cytoskeleton remodeling_Ra1A regulation pathway	2.156E-03	5	30
66	Cell adhesion_Gap junctions	2.156E-03	5	30
67	Cytoskeleton remodeling_TGF, WNT and cytoskeletal remodeling	2.408E-03	10	111
68	Cytoskeleton remodeling_Fibronectin-binding integrins in cell motility	2.507E-03	5	31
69	Apoptosis and survival_Role of IAP-proteins in apoptosis	2.507E-03	5	31
70	Cytoskeleton remodeling_Reverse signaling by ephrin B	2.507E-03	5	31
71	Transcription_Androgen Receptor nuclear signaling	2.577E-03	6	45
72	Immune response_ICOS pathway in T-helper cell	2.888E-03	6	46
73	Development_Transcription regulation of granulocyte development	2.896E-03	5	32
74	Development_FGF2-dependent induction of EMT	3.045E-03	4	20
75	Cell adhesion_Integrin-mediated cell adhesion and migration	3.592E-03	6	48
76	Immune response_CD40 signaling	3.988E-03	7	65
77	Cytoskeleton remodeling_Integrin outside-in signaling	3.988E-03	6	49
78	Development_EPO-induced Jak-STAT pathway	4.327E-03	5	35
79	Development_Angiopoietin - Tie2 signaling	4.327E-03	5	35
80	Oxidative stress_Angiotensin II-induced production of ROS	4.327E-03	5	35
81	Cytoskeleton remodeling_ESR1 action on cytoskeleton remodeling and cell migration	4.377E-03	4	22
82	Immune response_MIF-mediated glucocorticoid regulation	4.377E-03	4	22
83	Cytoskeleton remodeling_CDC42 in cellular processes	4.377E-03	4	22
84	Development_GM-CSF signaling	4.416E-03	6	50
85	Immune response_NFAT in immune response	4.877E-03	6	51
86	Some pathways of EMT in cancer cells	4.877E-03	6	51
87	Immune response_IL-9 signaling pathway	4.899E-03	5	36
88	Immune response_T cell receptor signaling pathway	5.372E-03	6	52
89	G-protein signaling_G-Protein alpha-12 signaling pathway	5.522E-03	5	37
90	Development_MAG-dependent inhibition of neurite outgrowth	5.522E-03	5	37
91	Development_WNT signaling pathway_Part 2	5.903E-03	6	53
92	Cell adhesion_Endothelial cell contacts by non-junctional mechanisms	6.054E-03	4	24
93	Immune response_CD28 signaling	6.471E-03	6	54
94	Immune response_Role of DAP12 receptors in NK cells	6.471E-03	6	54
95	Immune response_BCR pathway	6.471E-03	6	54
96	Translation_Regulation of EIF2 activity	6.935E-03	5	39
97	Immune response_Fc epsilon RI pathway	7.078E-03	6	55
98	Muscle contraction_Delta-type opioid receptor in smooth muscle contraction	8.111E-03	4	26
99	Cell adhesion_Endothelial cell contacts by junctional mechanisms	8.111E-03	4	26
100	Development_Role of IL-8 in angiogenesis	9.145E-03	6	58

## Peribronchiolar lymphoid proliferation - Lung

#	Maps	pValue	Ratio
1	Protein folding and maturation_POMC processing	2.924E-24	17
2	Immune response_IL-27 signaling pathway	2.301E-05	5
3	Atherosclerosis_Role of ZNF202 in regulation of expression of genes involved in Atherosclerosis	2.315E-04	4
4	Development_Melanocyte development and pigmentation	7.666E-04	5
5	Beta-alanine metabolism/ Rodent version	1.225E-03	4
6	Development_Angiopoietin - Tie2 signaling	1.724E-03	4
7	Translation_Non-genomic (rapid) action of Androgen Receptor	2.841E-03	4

8	Cell cycle_Chromosome condensation in prometaphase	3,536E-03	3	21
9	Cytoskeleton remodeling_Regulation of actin cytoskeleton by Rho GTPases	4,607E-03	3	23
10	Cell adhesion_ECM remodeling	7,339E-03	4	52
11	Cell adhesion_Gap junctions	9,792E-03	3	30

**Lymphocytolysis - Spleen**

No significant Pathway Maps

**Lipofuscin accumulation - Brain**

#	Maps	pValue	Ratio	
1	Development_Role of IL-8 in angiogenesis	2,591E-04	6	58
2	Regulation of lipid metabolism_Regulation of lipid metabolism via LXR, NF-Y and SREBP	2,765E-04	5	38
3	Apoptosis and survival_APRIL and BAFF signaling	3,133E-04	5	39
4	Immune response_Lectin induced complement pathway	9,168E-04	5	49
5	DNA damage_Mismatch repair	3,426E-03	3	20
6	Apoptosis and survival_Anti-apoptotic TNFs/NF-kB/Bcl-2 pathway	3,589E-03	4	41
7	Development_PEDF signaling	6,827E-03	4	49
8	Immune response_Classical complement pathway	8,419E-03	4	52
9	Apoptosis and survival_Endoplasmic reticulum stress response pathway	8,999E-03	4	53

Source	Gene set	# genes
Gene Ontology	aging_GO:0007568	24
Gene Ontology	cell aging_GO:0007569	10
Gene Ontology	multicellular organismal aging_GO:0010259	7
Gene Ontology	response to reactive oxygen species_GO:0000302	16
Gene Ontology	response to hydrogen peroxide_GO:0042542	10
Gene Ontology	response to oxygen radical_GO:0000305	5
Gene Ontology	DNA repair_GO:0006281	177
Gene Ontology	base-excision repair_GO:0006284	16
Gene Ontology	double-strand break repair_GO:0006302	18
Gene Ontology	mismatch repair_GO:0006298	9
Gene Ontology	non-recombinational repair_GO:0000726	6
Gene Ontology	nucleotide-excision repair_GO:0006289	22
Gene Ontology	recombinational repair_GO:0000725	6
Gene Ontology	telomere maintenance_GO:0000723	17
Gene Ontology	response to oxidative stress_GO:0006979	45
Literature	Energy_restriction_and_the_GH.IGF.1_axis	13
Literature	DNA_metabolism	30
Literature	Oxidant_levels_and_redox_potential	18
Literature	Stress_response	5
BIOCARTA	ARENRF2_PATHWAY	14
BIOCARTA	INFLAM_PATHWAY	26
BIOCARTA	DEATH_PATHWAY	30
BIOCARTA	LONGEVITY_PATHWAY	15
BIOCARTA	STRESS_PATHWAY	25
BIOCARTA	WNT_PATHWAY	25
BIOCARTA	P53_PATHWAY	16
BIOCARTA	NFKB_PATHWAY	22
BIOCARTA	IGF1MTOR_PATHWAY	19
BIOCARTA	IGF1_PATHWAY	22
BIOCARTA	MTOR_PATHWAY	23
KEGG	OXIDATIVE_PHOSPHORYLATION	110
KEGG	MTOR_SIGNALING_PATHWAY	52
KEGG	BASE_EXCISION_REPAIR	30
KEGG	NUCLEOTIDE_EXCISION_REPAIR	43
KEGG	MISMATCH_REPAIR	22
KEGG	WNT_SIGNALING_PATHWAY	148
REACTOME	BASE_EXCISION_REPAIR	16
REACTOME	CELL_DEATH_SIGNALLING_VIA_NRAGE_NRIF_AND_NADE	54
REACTOME	DEATH_RECEPTOR_SIGNALLING	11
REACTOME	DNA_REPAIR	82
REACTOME	DOUBLE_STRAND_BREAK_REPAIR	19
REACTOME	EXTENSION_OF_TELOMERES	23
REACTOME	SIGNALING_BY_WNT	16
REACTOME	SYNTHESIS_OF_DNA	46
REACTOME	TELOMERE_MAINTENANCE_hs	37
REACTOME	APOPTOSIS	82
REACTOME	ENERGY_DEPENDENT_REGULATION_OF_MTOR_BY_LKB1_AMPK	12
REACTOME	MTOR_SIGNALLING	22
REACTOME	MTORC1_MEDIATED_SIGNALLING	10

**Supplemental information 12.** Predefined list of aging-related gene-sets based on literature





# Chapter 3

# Chapter 3

## Mouse models for Xeroderma pigmentosum group A and group C show divergent cancer phenotypes

**Melis JPM**, Wijnhoven SW, Beems RB, Roodbergen M, van den Berg J, Moon H, Friedberg E, van der Horst GTJ, Hoeijmakers JHJ, Vijg J, van Steeg H.

Mouse models for Xeroderma pigmentosum group A and group C show divergent cancer phenotypes

**Cancer Res.** 2008 Mar 1;68(5):1347-53.

*"I'll need some information first, just the basic facts"*

Comfortably Numb – Pink Floyd, 1979

## Abstract

The accumulation of DNA damage is a slow but hazardous phenomenon that may lead to cell death, accelerated aging and cancer. One of the most versatile defense mechanisms against the accumulation of DNA damage is nucleotide excision repair, in which, amongst others, the XPC and XPA protein are involved.

To elucidate differences in the functions of these two proteins comprehensive survival studies with *Xpa*<sup>-/-</sup>, *Xpc*<sup>-/-</sup> and wild type control, female mice in a pure C57BL/6J background were performed. The median survival of *Xpc*<sup>-/-</sup> mice showed a significant decrease in survival, while the median survival of *Xpa*<sup>-/-</sup> mice did not. Strikingly, *Xpa*<sup>-/-</sup> and *Xpc*<sup>-/-</sup> mice also showed a phenotypical difference in terms of tumor spectrum. *Xpc*<sup>-/-</sup> mice displayed a significant increase in lung tumors and a trend towards increased liver tumors compared to *Xpa*-deficient or wild type mice. *Xpa*<sup>-/-</sup> mice showed a significant elevation in liver tumors. Additionally, *Xpc*-deficient mice exhibited a strong increase in mutant frequency in lung compared to *Xpa*<sup>-/-</sup> mice, whereas in both models mutant frequency is increased in liver. Our *in vitro* data displayed an elevated sensitivity to oxygen in *Xpc*<sup>-/-</sup> in mouse embryonic fibroblasts, when compared to *Xpa*<sup>-/-</sup> and wild type fibroblasts.

We believe that XPC plays a role in the removal of oxidative DNA damage and that therefore *Xpc*<sup>-/-</sup> mice display a significant increase in lung tumors, a significant elevation in mutant frequency in lung and *Xpc*-deficient embryonic fibroblasts are more sensitive to oxygen when compared to *Xpa*<sup>-/-</sup> and wild type mice.

## Introduction

Cancer remains one of the main causes of death nowadays in both men and women and is accompanied by a kaleidoscope of unsolved questions about the induction and progress of this disease. An important factor in the development of cancer is the accumulation of somatic DNA damage [1]. Normally, several sophisticated defense mechanisms are active to repair the modified DNA to prevent mutations and damage accumulation. Base excision repair (BER) for example will remove most small base modifications (e.g. oxidative DNA damage). Nucleotide excision repair (NER) has a very broad lesion spectrum and is responsible for the removal of bulky, DNA helix-distorting adducts [2-7].

The autosomal recessive disorder Xeroderma pigmentosum (XP) is an elucidative example of the influence of a DNA repair defect on cancer predisposition. XP patients exhibit extreme UV-sensitivity and are predisposed to skin cancer by a 1000-fold higher risk [8,9]. Until now seven complementation groups (XP-A through XP-G) plus a variant form (XP-V) were identified. XP disorders arise from a deficiency in one or more of these XP proteins, which belong to the NER pathway, with the notable exception of the XPV protein, which is involved in translesion synthesis of UV-damaged DNA [10].

NER can be subdivided in two subpathways: global genome NER (GG-NER), which covers the complete genome, and transcription coupled NER (TC-NER), which focuses on repair of the transcribed strand of active genes [11,12]. XPC is associated with the GG-NER while XPA plays a role in both GG-NER and TC-NER. The XPC protein, in complex with the HR23B protein, is responsible for DNA damage recognition [6,13]. Following detection of distorted helix structures, the XPC/HR23B-complex will initiate the GG-NER process [14]. Subsequently, the XPC/HR23B-complex will dissociate from the damaged DNA strand when the transcription factor TFIIH in combination with the XPA and RPA protein set the verification of the DNA damage in motion [15]. XPC-HR23B is dispensable for TC-NER; the CSA and CSB proteins, together with RNA polymerase II stalled at a lesion, fulfill the role of recognition factor in this pathway. As in GG-NER, DNA damage verification in TC-NER requires presence of the TFIIH-XPA-RPA complex [16].

When TC-NER components or the more common elements in NER (e.g. XPA) are affected, very complex clinical features are observed [17]. Patients with a defect in genes unique to GG-NER (like XPC) exhibit fewer clinical symptoms besides cancer. In general, deficiencies in the TC-NER pathway are related to neurodegenerative disorders, while defects in the GG-NER pathway are designated as more cancer prone [18-21].

The XP-C is the most common type of the XP disease in North-America and Europe [22]. This form is only defective in the GG-NER pathway. XP-A patients are disrupted in both their GG-NER and TC-NER pathways. Mutant frequency analyses at the *Hprt* locus in mouse models of these two forms of XP previously uncovered striking differences. *Hprt* mutant frequencies in the spleen of *Xpc*<sup>-/-</sup> mice in a mixed genetic background were highly elevated in comparison to their wild type controls but also compared to *Xpa*<sup>-/-</sup>, both in a pure C57BL/6J background [23]. This indicates that knockout mouse models of *Xpc* and *Xpa* may also exhibit different spontaneous phenotypes. *Xpc*<sup>-/-</sup> mice of a mixed background (25% 129, 75% C57BL/6J) were shown to exhibit a high prevalence of lung tumors [24], but this has not been studied in a pure C57BL/6J background. Also a clean comparison with *Xpa*<sup>-/-</sup> mice has not yet been made.



To refine and expand our knowledge on human XP-A and XP-C, *Xpa*<sup>-/-</sup> and *Xpc*<sup>-/-</sup> mice were used. To investigate the phenotypic differences between these mice we performed a more comprehensive study with both mouse models in a pure C57BL/6J background. We compared the lifespan of the two models and determined pathology with the focus on tumor development. In addition, to help explain the differences in tumor outcomes we performed mutation analyses in several organs. Our data suggest that *Xpc*-deficient mice are more sensitive to (oxidative) DNA-damaging agents in the lung compared to the *Xpa*-deficient mice and wild type controls. These findings support evidence provided in various studies that XPC, in addition to its function in GG-NER, is also involved in the repair of oxidative DNA damage. Therefore, *Xpc*<sup>-/-</sup> mice seem more sensitive to oxidative stress and lung tumor development than their NER-deficient counterparts, *Xpa*<sup>-/-</sup> mice.

## Materials and Methods

### Mice

The generation and characterization of *Xpa*<sup>-/-</sup> and *Xpc*<sup>-/-</sup> mice and has been described before [<sup>25,26</sup>]. To obtain a genetically homogenous background, *Xpa*- and *Xpc*-deficient mice were back-crossed over 10 times with C57BL/6J animals (Harlan). To offer the future possibility to monitor genomic instability, the heterozygous mutant mice strains as well as C57BL/6J controls were crossed with pUR288-*lacZ* C57BL/6J transgenic mice line 30, homozygous for *lacZ* integration on chromosome 11 [<sup>27</sup>]. In the second round of breeding, double heterozygous mice were intercrossed to obtain homozygous mice carrying one locus of the integrated copies of the *lacZ* marker, used in the third breeding round to generate the experimental animals for the aging and cross-sectional studies as described below. Mice were genotyped by a standard PCR reaction using DNA isolated from tail tips. Primers to amplify the wild type and targeted *Xpa* and *Xpc* allele, as well as primer sequences for *lacZ* determination have been described previously [<sup>27,28</sup>]. The experimental setup of the studies was examined and agreed upon by the institute's Ethical Committee on Experimental Animals, according to national legislation.

### Experimental Design

Female mice were marked and randomized at the day of birth in different groups; i.e. longevity cohorts, or cross-sectional cohorts in which the mice were sacrificed at fixed time points. Cross-sectional cohorts of *Xpa*<sup>-/-</sup>, *Xpc*<sup>-/-</sup> and their C57BL/6J controls were sacrificed at a fixed age of 13, 52, and 78 and 104 weeks. The interim cohorts consisted of at least 15 female mice per time point and genotype. In the longevity cohorts, a total of 45 *Xpa*<sup>-/-</sup> and 50 *Xpc*<sup>-/-</sup> female mice and 45 or 50 of their wild type controls (referred to in the text as C57BL/6J 1 and C57BL/6J 2) were monitored during their entire life span. The health state of the mice was checked daily, beginning at the day of weaning. Individual animals were weighed biweekly to determine live weights. During the entire experiment, animals were kept in the same stringently controlled (spf) environment, fed *ad libitum* and kept under a normal day/night rhythm. The microbiological status of the cohorts was monitored every 3 months. Animals from the longevity cohort were removed from the study when found dead or moribund. Complete autopsy was performed on animals of all cohorts; a total of 45 different tissues was isolated from each animal and stored for further histopathological analysis (see below). In addition, a selective set of 20 different tissues were snap frozen in liquid N<sub>2</sub> for molecular analyses, like *lacZ* mutant

frequency analyses. Total animal weights, as well as various organ weights, were determined at time of death or when killed.

### **Histopathology**

Organ samples (45 organs and tissues) of each animal were preserved in a neutral aqueous phosphate-buffered 4% solution of formaldehyde. Tissues required for microscopic examination were processed, embedded in paraffin wax, sectioned at 5µm and stained with haematoxylin and eosin. Detailed microscopic examination was performed on 9 major organs of all female mice from the longevity cohort and on all gross lesions suspected of being tumors or representing major pathological conditions. For each animal, histopathological abnormalities, tumors as well as non-neoplastic lesions, were recorded using the PATHOS pathology data acquisition software and if possible, a cause of death was established.

### **Hprt mutant frequency analyses**

*Xpc*<sup>-/-</sup>, *Xpc*<sup>+/-</sup> mice and their wild type controls were sacrificed at 13 or 52 weeks and spleens were isolated to determine spontaneous *Hprt* mutant frequencies. All mice were in pure C57BL/6J background. The number of mice within one genotype and age group varied between 4 and 10.

Priming and cloning of T-lymphocytes was done in RPMI culture medium 1640 as described by Tate et al. [29] with some minor modifications [30]. Mouse T-lymphocytes were isolated from the spleen by rubbing the spleen through a sterile 70-µm nylon mesh (Falcon Cell Strainer, 2350). Subsequently cells were frozen in RPMI medium 1640 supplemented with 10% dimethyl sulfoxide and 40% fetal bovine serum by using a Cryomed freezing apparatus (Forma Scientific, Marietta, OH). When required, frozen cells were thawed and immediately stored on ice. Stimulated T-lymphocytes were cultured and selected for *Hprt*-deficiency in the presence of lethally irradiated (30 Gy X-rays) mouse lymphoblastoid Sp2/0 feeder cells [29]. Cloning efficiencies and mutant frequencies were calculated as described [29]. Further details on the procedure were described by Wijnhoven et al. [30].

### **LacZ mutant frequency analyses**

From a selected set of snap frozen tissues DNA was extracted with a phenol/chloroform/iso-amyl alcohol mixture (25:24:1). Complete protocols for plasmid rescue and mutant frequency determinations with the pUR288 model have been described elsewhere [31]. Briefly, between 10 and 20 µg genomic DNA was digested with HindIII for 1 h in the presence of magnetic beads (Dynal), recoated with lacI-lacZ fusion protein. The beads were washed three times to remove the unbound mouse genomic DNA. Plasmid DNA was subsequently eluted from the beads by IPTG and circularized with T4 DNA ligase. Next, ethanol-precipitated plasmids were used to transform *E. coli* C (ΔlacZ, galE-) cells. One thousandth of the transformed cells was plated on the titer plate (with X-gal) and the remainder on the selective plate (with p-gal). The plates were incubated for 15 h at 37 °C. Mutant frequencies were determined as the number of colonies on the selective plates versus the number of colonies on the titer plate (times the dilution factor of 1000). Each mutant frequency is based on at least 300,000 recovered plasmids.

### Statistical evaluation

Incidences of tumors were analyzed with the method of Peto (SAS) [32] and with the poly-3 and poly-k method [33]. These tests for statistical analysis of tumor incidences take differences in survival of the various groups into account. The poly-3 and poly-k test were performed by Dr H. Moon, California State University, Long Beach CA, USA.

### Cell culture

Primary mouse embryonic fibroblasts (MEFs) were isolated from E13.5 day embryos, all in C57BL/6J background, and genotyped as described previously [27;28]. MEFs were cultured as described before [34] in Dulbecco's modified Eagle Medium (DMEM, Gibco) supplemented with 10% fetal bovine serum (FCS Biocell), 1% non essential amino acids (Gibco), penicillin (0,6 µg/ml) and streptomycin (1 µg/ml) at 37°C, 5% CO<sub>2</sub>. MEFs were cultured 3 days per passage at 3% or 20% O<sub>2</sub>. Cell survival was determined by blue/white screening using Trypan Blue Stain 0.4% (Gibco) (1:1), counting a minimum of 200 cells per sample. A minimum of 3 different embryos were used per genotype, plus a technical replica of all samples was used.

### Results

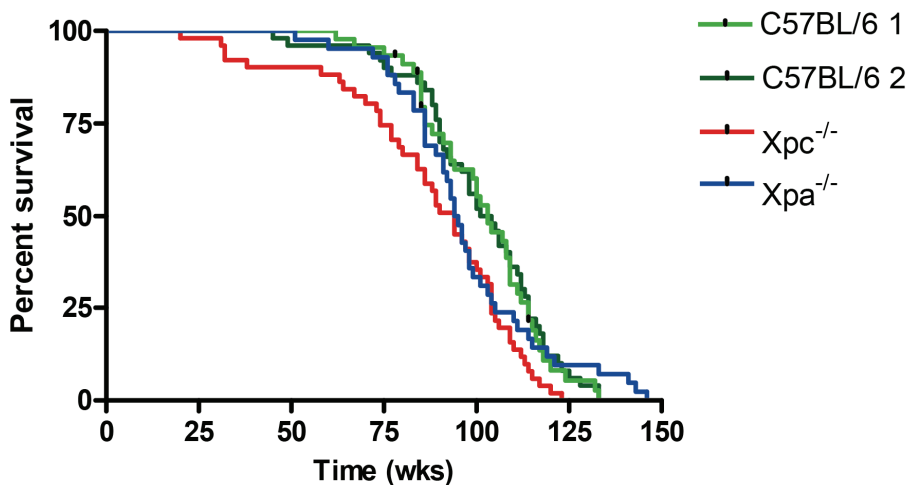


**Figure 1.** Survival curves of female *Xpc*<sup>-/-</sup>, *Xpa*<sup>-/-</sup> and their wild type control cohorts. C57BL/6 1 is the control cohort for *Xpa*<sup>-/-</sup>. C57BL/6 2 is the control cohort for *Xpc*<sup>-/-</sup>. Median survival of the cohorts are: C57BL/6 1 = 103 weeks (light green line), C57BL/6 2 = 102.5 weeks (dark green line), *Xpc*<sup>-/-</sup> = 94 weeks ( $p = 0.0023$ ) (red line), *Xpa*<sup>-/-</sup> = 94.5 weeks ( $p = 0.6023$ ) (blue line). For further details see materials and methods.

To determine the average life span of *Xpc*<sup>-/-</sup> and *Xpa*<sup>-/-</sup> mice, 45-50 mutant females and corresponding C57BL/6J control mice were followed during aging. The survival curves for the longevity cohorts of female *Xpc*<sup>-/-</sup>, *Xpa*<sup>-/-</sup> and both matching wild type control groups are depicted in Figure 1. The median survival of female *Xpc*<sup>-/-</sup> mice (94 weeks) was significantly reduced ( $p=0.0023$ , Kaplan-Meier with Log

rank test) compared to the median survival of their female wild type C57BL/6J controls (C57BL/6J 2, 102.5 weeks). Female *Xpa*<sup>-/-</sup> median survival (94.5 weeks) on the other hand was not significantly reduced ( $p=0.6023$ , Kaplan-Meier with Log rank test) compared to the median survival of its female C57BL/6J controls (C57BL/6J 1, 103 weeks). This difference in significance is mainly caused by the fact that a certain fraction ( $\pm 10\%$ ) of the *Xpa*<sup>-/-</sup> animals survive extremely long (see Figure 1). Survival curves of both wild type control studies show a very similar median survival and shape of the curve.

		WT1	<i>Xpa</i> <sup>-/-</sup>	P-value	WT2	<i>Xpc</i> <sup>-/-</sup>	P-value
	<i>Number of animals (absolute)</i>	40	31		29	38	
All organs	Tumor bearing animals	<b>30</b> (75)	<b>21</b> (68)		<b>24</b> (83)	<b>23</b> (61)	
Liver	Hepatocellular tumor	<b>0</b> (0)	<b>3</b> (10)	0.0002	<b>2</b> (7)	<b>5</b> (13)	*
Lung	Bronchiolo-alveolar tumor	<b>0</b> (0)	<b>2</b> (6)		<b>1</b> (3)	<b>6</b> (16)	0.02
Pituitary	Pars distalis adenoma	<b>20</b> (50)	<b>8</b> (26)	*	<b>20</b> (70)	<b>9</b> (24)	0.01
All organs	Pituitary adenomas excluded	<b>18</b> (45)	<b>19</b> (61)	0.001	<b>21</b> (72)	<b>23</b> (61)	**

**Table 1.** Tumor incidences and  $p$ -values for difference between mutant and their concurrent wild type group. Absolute values are in bold, percentages are between brackets. Statistics: poly-k test (poly-3 test and Peto test generally gave similar significances, though exact  $p$ -value may differ).

\* = approaches significance with poly-3 test only ( $p=0.08$  for *Xpc*<sup>-/-</sup> liver and  $p=0.054$  for *Xpa*<sup>-/-</sup> pituitary).

\*\* = not reaching significance with poly-k test, but  $p$ -value for the Peto test = 0.05 (positive trend) in this case

Of all groups approximately 30 or more animals were histopathologically examined. Neoplasms and inflammation (mainly ulcerative dermatitis) are the most common cause of demise in all groups, ranging from 72% in wild type controls up to 87 % in *Xpc*<sup>-/-</sup> mice (data not shown). Occasionally more than one pathological condition might have contributed to death, in which case the most pronounced condition was taken as cause of demise. Incidences of major tumor types at the time of death are listed in Table 1. *Xpa*<sup>-/-</sup> and *Xpc*<sup>-/-</sup> mice lived shorter than their respective wild type controls. Accordingly, lower tumor incidences were expected in the mutant animals, since they had less time to develop tumors. Statistical methods that take differences in survival into account were therefore used in this case to evaluate the significance of differences in tumor incidences. Nevertheless, some tumor types were increased in either *Xpc*<sup>-/-</sup> or *Xpa*<sup>-/-</sup> mice. *Xpc*<sup>-/-</sup> mice show a significant increase ( $p = 0.02$ ) in bronchio-alveolar lung tumors and near significant elevation ( $p = 0.054$ ) in hepatocellular tumors. *Xpa*<sup>-/-</sup> mice solely show a significant increase ( $p < 0.01$ ) in hepatocellular tumors when compared to their matching wild type control group. Furthermore, female *Xpc*<sup>-/-</sup> mice also show a significant increase in acidophilic macrophage pneumonia ( $p = 0.032$ , data not shown), which is not apparent in *Xpa*<sup>-/-</sup> mice.

The percentage of tumor bearing NER-deficient animals (all types together) is surprisingly lower than the corresponding NER-proficient control groups. In addition to the shorter lifespan, the strong and significant decrease in benign pituitary adenomas in both *Xpc*<sup>-/-</sup> and *Xpa*<sup>-/-</sup> mice is mostly responsible for this lower percentage in tumor bearing animals. The increase in number of tumor bearing animals (excluding the pituitary adenomas and taking into account the survival distribution) reaches

significance for *Xpa*<sup>-/-</sup> mice ( $p < 0.01$ ) and approaches significance for *Xpc*<sup>-/-</sup> animals ( $p = 0.05$ ) using the Peto test.

Although a variety of non-neoplastic changes was observed in the organs of mutant as well as wild type mice, there were no obvious genotype specific pathologies typical for *Xpc*<sup>-/-</sup> or *Xpa*<sup>-/-</sup> mice. The observed changes belonged to the normal background pathology of C57BL/6J mice and generally occurred to about the same degree in all groups. Since mutant animals died slightly earlier than wild type mice it may well be that these spontaneous aging lesions occurred slightly earlier in *Xpc*<sup>-/-</sup> and *Xpa*<sup>-/-</sup> mice than in wild type animals. However, this aspect was not explicitly investigated in this study.

### Mutant frequency analyses

A comprehensive analysis of spontaneous *Hprt* mutant frequency was performed with *Xpc*<sup>-/-</sup>, *Xpc*<sup>+/-</sup> and their wild type control mice in a pure C57BL/6J background (Figure 2). At the age of 52 weeks, *Hprt* mutant frequencies in wild type mice ( $MF = 0.9 \times 10^{-6}$ ) were in the same range as previously reported [23]. At this age, mutant frequencies in *Xpc*<sup>-/-</sup> and *Xpc*<sup>+/-</sup> mice were elevated 15 and 3 fold, respectively, when compared to their age-matched wild type controls. In addition, *Xpc*<sup>-/-</sup> mice of 13 weeks old already exhibited a 5-fold increase in mutant frequency compared to the 52 weeks old wild type control animals.

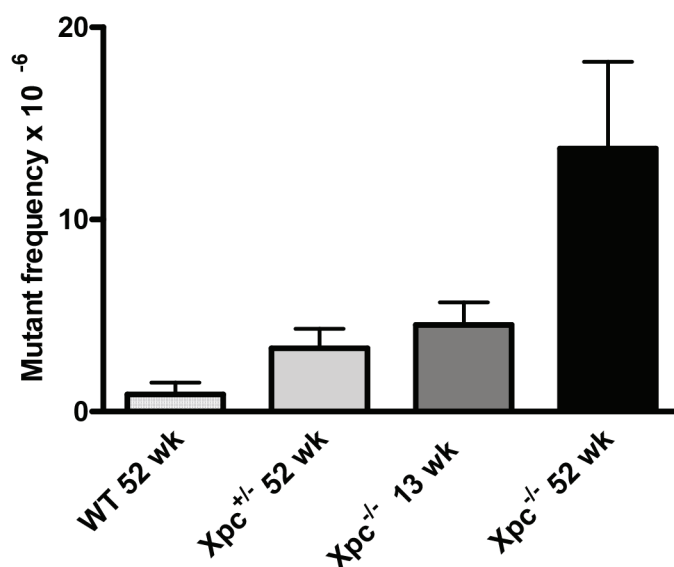


**Figure 2.** *Hprt* mutant frequencies including standard deviations of *Xpc*<sup>-/-</sup>, *Xpc*<sup>+/-</sup> and wild type controls at an age of 13 and 52 weeks in spleen. The numbers of biological replicas are between 4 and 10. For further details see Materials and Methods section.

In addition, we determined mutant frequencies in several tissues of C57BL/6J, *Xpc*<sup>-/-</sup> and *Xpa*<sup>-/-</sup> mice using the *LacZ* recovery system. Samples were taken from spleen, liver and lung of 13, 52 and 78 week old animals which were of age. Results are shown in Figure 3. Table 2 depicts the  $p$ -values of the

compared genotypes in all three tissues at different ages. Mutant frequencies increased over time in spleen, liver and lung of *Xpc*<sup>-/-</sup> mice. In *Xpa*<sup>-/-</sup> and C57BL/6J wild type mice an increase over time was visible in liver and lung, but not in spleen. Mutant frequencies in spleen showed a significant increase in mutants in 52 and 78 week old *Xpc*<sup>-/-</sup> mice compared to their age matched *Xpa*<sup>-/-</sup> and wild type samples (Figure 3A). Samples of *Xpa*<sup>-/-</sup> exhibited a similar *LacZ* mutant frequency pattern in the spleen as the wild type samples over the entire lifespan. The liver of *Xpc*<sup>-/-</sup> and *Xpa*<sup>-/-</sup> mice showed a strong increase in mutant frequency compared to that of wild type at 52 and 78 weeks of age (Figure 3B). *Xpc*<sup>-/-</sup> liver samples exhibited slightly higher values on average than *Xpa*<sup>-/-</sup> samples at those time points.

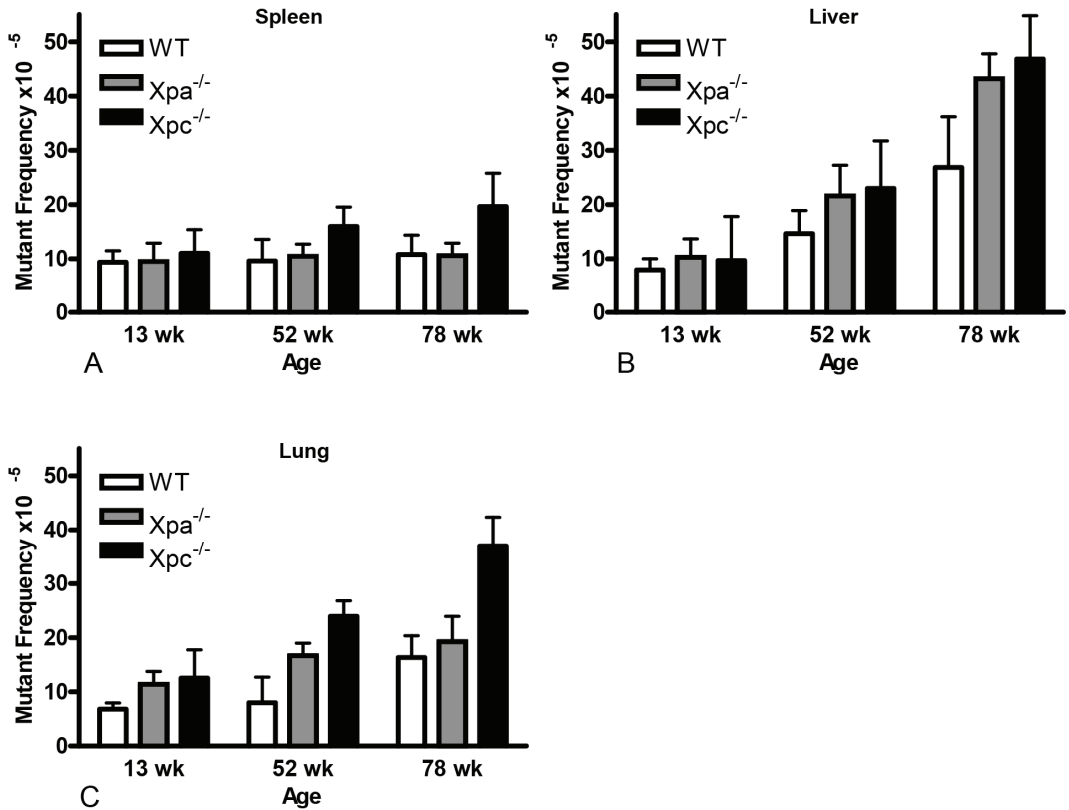


**Figure 3.** *LacZ* mutant frequencies including standard deviations of *Xpc*<sup>-/-</sup>, *Xpa*<sup>-/-</sup> and wild type controls at an age of 13, 52 and 78 weeks in spleen (A), liver (B) and lung (C). The numbers of biological replicas are between 5 and 6. For further details see materials and methods.

The mutant frequency in *Xpc*<sup>-/-</sup> lung samples was significantly elevated in comparison to wild type controls at all time points. *Xpa*<sup>-/-</sup> mice only exhibited this increase at 13 and 52 week of age. At 78 weeks the mutant frequency of *Xpa*<sup>-/-</sup> lungs was comparable to that of wild type controls. Strikingly, *Xpc*<sup>-/-</sup> lungs showed a significant elevation in mutant frequency at an age of 52 and 78 weeks as compared to their NER-deficient counterpart *Xpa*<sup>-/-</sup>. A twofold increase was visible in *Xpc*<sup>-/-</sup> lung samples at 78 weeks in relation to both wild type controls and *Xpa*<sup>-/-</sup> deficient samples (see Figure 3C).

Spleen	13wk	52wk	78wk	Liver	13wk	52wk	78wk	Lung	13wk	52wk	78wk
<i>Xpc</i> vs <i>WT</i>		0.016	0.012	<i>Xpc</i> vs <i>WT</i>			0.002	<i>Xpc</i> vs <i>WT</i>	0.04	0.00003	0.0001
<i>Xpc</i> vs <i>Xpa</i>		0.0098	0.007	<i>Xpc</i> vs <i>Xpa</i>				<i>Xpc</i> vs <i>Xpa</i>		0.02	0.0005
<i>Xpa</i> vs <i>WT</i>				<i>Xpa</i> vs <i>WT</i>		0.04	0.002	<i>Xpa</i> vs <i>WT</i>	0.003	0.003	

**Table 2.** *P*-values of mutant frequency comparisons between genotypes, depicted per age per tissue. Open cells represent non-significant ( $p > 0.05$ ) differences.

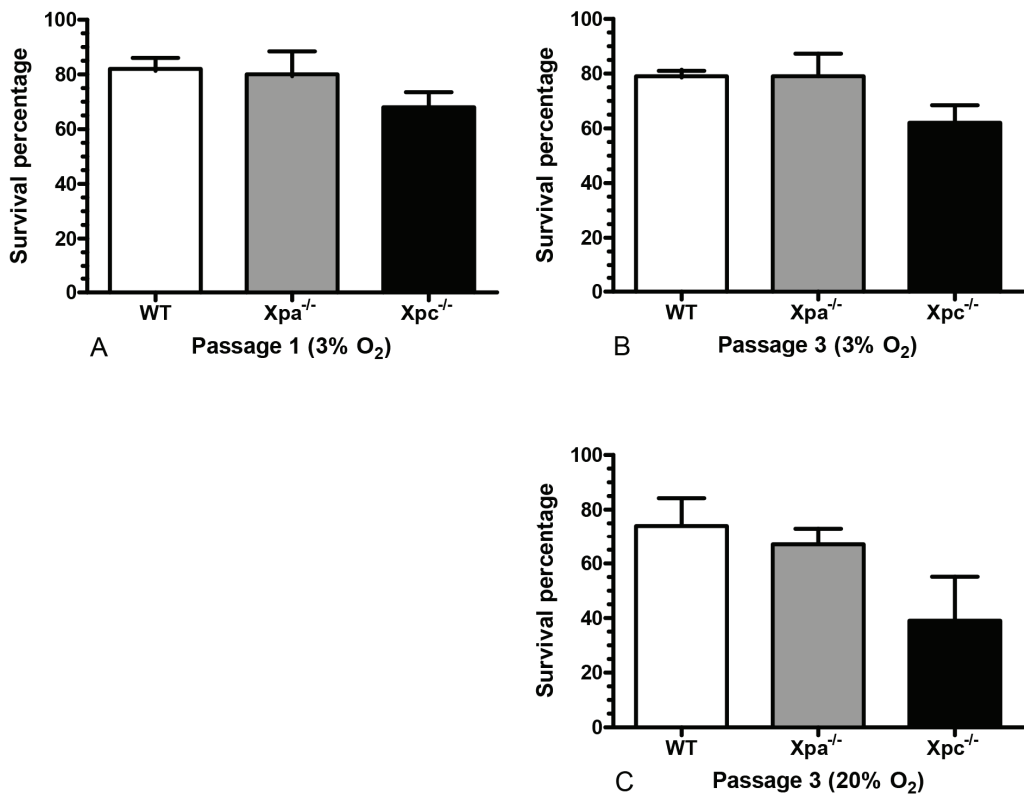


**Figure 4.** Survival of mouse embryonic fibroblasts including standard deviations of *Xpc*<sup>-/-</sup>, *Xpa*<sup>-/-</sup> and their wild type controls under different levels of oxygen pressure. Cells at the first passage were all cultured at 3% oxygen (A); subsequent passages were cultured under 3% (B) or 20% oxygen (C), respectively.

### Cell survival under oxygen exposure

In view of the increased tumor incidence and elevated spontaneous mutant frequency in lung we suspected that the *Xpc*<sup>-/-</sup> animals were more susceptible to oxidative stress. To directly test this hypothesis we investigated the effects of exposure to different levels of oxygen, 3% and 20%, on *Xpa*<sup>-/-</sup>, *Xpc*<sup>-/-</sup> and wild type mouse embryonic fibroblasts (MEFs). Results are shown in Figure 4. *Xpc*<sup>-/-</sup> fibroblasts subjected to 3% oxygen level appeared to be slightly more sensitive than *Xpa*<sup>-/-</sup> and wild type MEFs in the first passage. Survival of *Xpc*<sup>-/-</sup> fibroblasts was 68% after 3 days of culturing (first passage in figure 4), while *Xpa*<sup>-/-</sup> and wild type fibroblasts exhibited 80% and 82% survival respectively. After two more passages, at 3% oxygen pressure, 62% survival was visible in cultured *Xpc*<sup>-/-</sup> fibroblasts that were cultured. The survival of *Xpa*<sup>-/-</sup> and wild type MEFs, at this point and under 3% oxygen pressure, was 79%. When, after the initial passage of 3% oxygen, the fibroblasts were cultured for two more passages at 20% oxygen pressure, a severe decrease in survival was exhibited in *Xpc*<sup>-/-</sup> fibroblasts. The percentage of survival dropped to a mere 39%. This dramatic decrease was not observed for *Xpa*<sup>-/-</sup> and wild type (67% and 74% survival respectively).

### Discussion

Previous results obtained in separate studies in which patterns of survival, tumor formation and mutation accumulation were determined in *Xpc*- and *Xpa*-deficient mice were difficult to interpret because of variation in genetic background and the use of different mutational reporter genes. Here we performed a side-by-side comprehensive study of these endpoints in the same genetic background using both the *Hprt* and *LacZ* mutational target genes.

NER-deficient mouse models lacking a functional XPA or XPC protein show phenotypic differences when compared to their wild type controls. A significant reduction in spontaneous survival was observed in our comprehensive longevity studies for female *Xpc*-deficient mice in a pure C57BL/6J background. *Xpa*-deficient female mice also showed a decrease in survival when compared to their wild type control although not statistically significantly. Previously reported survival studies of *Xpc*<sup>-/-</sup> mice in a mixed background did not exhibit a decrease in survival [24]. Female *Xpa*<sup>-/-</sup> and *Xpc*<sup>-/-</sup> mice in our studies reached an average median age of 94.5 and 94 weeks, respectively, while their matching wild type controls attained a median survival of 103 and 102.5 weeks. Both the wild type control cohorts show a similar survival pattern and a comparable median age of 50% survival. As in humans, a deficiency in one of these NER proteins leads to a reduced lifespan and therefore XPA and XPC prove to be part of delicate and important processes that have a substantial effect on survival.

Additional pathological analyses of female *Xpa*<sup>-/-</sup> and *Xpc*<sup>-/-</sup> mice showed that the cause of death in many of these animals was not accountable to the presence of neoplasms. Another main cause of death of the NER-deficient mice was in fact the occurrence of inflammation, mainly ulcerative dermatitis. For the C57BL/6J 1 group (which was simultaneously executed with the *Xpa*<sup>-/-</sup> study) and *Xpa*<sup>-/-</sup> high incidences of inflammation were apparent (50 and 61% respectively). The C57BL/6J 2 and the *Xpc*<sup>-/-</sup> studies showed a somewhat lower incidence of inflammation (24% and 55% respectively). High incidences of ulcerative dermatitis in control C57BL/6J mice are considered an inevitable byproduct of handling the animals during their entire lifespan and are a result of a *Staphylococcus aureus* infection. Also the type of diet appears to play a role in the severity of this skin phenotype.



These findings are, however, clearly in line with our earlier findings [35] and those of others [36;37] working with particularly female C57BL/6J mice.

To our surprise the percentage of tumor bearing animals (TBA) was higher in NER-proficient mice than in the NER-deficient counterparts. This observation is, next to the longer lifespan observed in wild type mice, mostly attributable to a dramatic decrease in pituitary tumor development in *Xpc*<sup>-/-</sup> mice (from 70% to 24% occurrence) and in *Xpa*<sup>-/-</sup> mice (from 51% to 26% occurrence). A similar strong reduction in pituitary tumor development was observed in another NER-deficient mouse model, namely *Xpd*<sup>TTD</sup> [35]. Here a significant decrease from 50% to 9% occurred. Interestingly, no such a decrease in pituitary tumor development was found in the TC-NER-deficient *Csb* mouse model (data not shown). Apparently, a defect in GG-NER is accompanied by suppression of a specific set of tumor types. Further studies are needed to substantiate this hypothesis.

A distinct difference between the two NER-deficient mouse models is the observed tumor spectrum. Female *Xpa*<sup>-/-</sup> mice exhibit a significant increase in hepatocellular adenomas compared to wild types. Female *Xpc*<sup>-/-</sup> mice also show an elevation in the number of hepatocellular neoplasms which approaches significance. Additionally, female *Xpc*<sup>-/-</sup> mice do show a significant increase in bronchio-alveolar neoplasms compared to their proficient controls. Such an increase is absent in female *Xpa*<sup>-/-</sup> mice.

Our results showed that female *Xpc*<sup>-/-</sup> mice in a pure C57BL/6J background are susceptible to lung cancer and support the previous findings of the lung cancer susceptibility in *Xpc*<sup>-/-</sup> mice in the more sensitive mixed background [24]. However, in this previous study the lung tumors observed and diagnosed as adenomas and adenocarcinomas appeared to be more malignant and were accompanied by a higher incidence of atypical hyperplasia. Possibly, depending on the genetic background and spontaneous (oxidative) DNA damage levels, tumors will progress earlier to a more malignant state. Next, several studies provide information that *Xpc* polymorphisms in humans may also contribute to genetic susceptibility for lung cancer [38-40]. Exposure of *Xpc*-deficient mice (in a mixed genetic background) to the harmful genotoxic carcinogen 2-AAF resulted in a significant elevation in the number of liver and lung tumors compared to wild type animals [18;41]. In contrast, *Xpa*<sup>-/-</sup> mice in a pure C57BL/6J background only show an elevation in liver tumors after exposure to 2-AAF and no increase in lung tumors was apparent in that study (18). The occurrence of lung tumors in *Xpc*<sup>-/-</sup> mice in pure C57BL/6J background after exposure to 2-AAF has not yet been assessed. The difference in tumor spectrum between *Xpc*<sup>-/-</sup> and *Xpa*<sup>-/-</sup> mice in our study indicates that the XPC protein is, besides active in NER, possibly also involved other repair systems, most likely including BER. This idea was recently also put forward by others [42]. The outcome of an increase in lung tumors in *Xpc*<sup>-/-</sup> mice could, therefore, point to an involvement of the XPC protein in the repair of oxidative DNA damage.

To analyze the mutation spectrum in DNA repair-deficient mice in the different organs, we conducted additional mutant frequency analyses on several tissues of wild type, *Xpa*<sup>-/-</sup> and *Xpc*<sup>-/-</sup> female mice. Initial spontaneous *Hprt* mutant analyses in spleen showed a strong increase of mutant frequency in T-lymphocytes of 52 week old *Xpc*<sup>-/-</sup> mice compared to their age-matched *Xpa*<sup>-/-</sup> and C57BL/6J controls. However, in an earlier study, *Xpc*<sup>-/-</sup> mice with a mixed background were used [23]. More comprehensive *Hprt* analyses using *Xpc*-deficient mice in a pure C57BL/6J background were performed here. The strong increase in mutant frequency compared to the wild type control was reproducible in *Xpc*<sup>-/-</sup> in a pure C57BL/6J background, albeit lower than in a mixed background. The results obtained with *LacZ*

mutant analyses show a more moderate response in spleen when *Xpc*<sup>-/-</sup> is compared to wild type. This can be explained by the fact that the background level of the *LacZ* mutant analyses is higher than that of *Hprt*. Although *Hprt* analysis is a more sensitive method than *LacZ* analyses, its drawback is that it is only applicable to the spleen. Other previous studies conducted here showed an elevation of mutant frequencies in *Xpa*<sup>-/-</sup> in liver and kidney using *LacZ* analyses [<sup>43;44</sup>].

Our results of the *LacZ* mutant analyses show a striking increase of mutant frequency in lung tissue of *Xpc*<sup>-/-</sup> mice when compared to wild type and *Xpa*<sup>-/-</sup> mice, especially at an age of 78 weeks. The fact that no severe increase in lung is observed in *Xpa*<sup>-/-</sup> mice but is distinctly present in *Xpc*<sup>-/-</sup> mice supports the hypothesis that the XPC protein might be involved in the removal of oxidative DNA damage since the level of oxidative stress is higher in lungs compared to other tissues due to the constant exposure of this tissue to oxygen [<sup>45</sup>]. In the spleen, *Xpc*<sup>-/-</sup> mice also shows a significant increase in mutant frequency compared to wild type and *Xpa*<sup>-/-</sup> at 52 and 78 weeks. In liver, on the other hand, the mutant frequencies of *Xpa*<sup>-/-</sup> and *Xpc*<sup>-/-</sup> liver are virtually equal over all time points. DNA damage in the liver most likely arises as a result of genotoxic bulky byproducts of metabolism. Compared to wild type, 78 week-old NER-deficient mouse livers do show a significant elevation of mutant frequency. This illustrates the sensitivity of the NER-deficient mouse strains to DNA damage. Over time and in all investigated tissues *Xpc*<sup>-/-</sup> mice show the highest mutant frequency, indicating an even higher sensitivity to DNA damage than *Xpa*<sup>-/-</sup> animals.

The putative role in the removal of oxidative damage is supported by our *in vitro* data, in which *Xpc*<sup>-/-</sup> mouse embryonic fibroblasts exhibit a severe decrease in survival when cultured at 20% oxygen compared to 3% oxygen pressure. We believe that the excess of oxidative damage is most likely the cause of death, since oxygen pressure is the only variable that was changed in culturing. *Xpc*-deficient fibroblasts seem to be impaired in the removal of this damage. Even at a low oxygen level of 3%, growth of *Xpc*-deficient cells seems more sensitive compared to *Xpa*-deficient and wild type fibroblasts.

The high mutant frequencies in oxygen rich surroundings in *Xpc*<sup>-/-</sup> cells and the severe decrease in cell survival under 20% oxygen pressure are concurrent with the present understandings and recent discoveries about the XPC protein. Several recent studies provide information about the involvement of XPC in base excision repair (BER) and the putative role in the repair of oxidative DNA damage. BER is mainly responsible for mending the DNA damage caused by oxidative stress [<sup>46</sup>]. XPC can physically and functionally interact with thymine DNA glycosylase, which plays a role in BER [<sup>47</sup>]. XPC-HR23B also has been assigned as a cofactor for base excision repair of 8-hydroxyguanine, by stimulating the activity of its specific DNA glycosylase OGG1 [<sup>48</sup>]. In addition, a recent study has shown a deficient BER after oxidative DNA damage induced by methylene blue plus visible light in XPC fibroblasts [<sup>49</sup>]. Methylene blue and visible light produce oxidative DNA damage, amongst others 8-OH-Gua.

Our results indicate the importance of the XPC protein *in vivo*, where the absence of the protein is responsible for susceptibility to lung tumors in mice compared to wild type and their NER-deficient counterpart *Xpa*<sup>-/-</sup>. Mutant frequency analyses show an additional sensitivity in spleen compared to *Xpa*-deficient animals. In accordance with *Xpa*-deficiency, *Xpc*<sup>-/-</sup> mice also show a high mutant frequency in liver. Therefore our results, together with the accumulating evidence provided by others, support the theory of XPC involvement in BER or additional pathways and the removal of oxidative

DNA damage. A subsequent consequence of this engagement could explain the difference in tumor spectrum between *Xpa*<sup>-/-</sup> and *Xpc*<sup>-/-</sup> mice.

### **Acknowledgements**

We are very grateful to Piet de With, Gwen Intres, Conny van Oostrom, Coen Moolenbeek, Christine Soputan, Sandra de Waal, Sisca de Vlugt and Ewoud Speksnijder for their skilful technical assistance. This work was financially supported by National Institute of Health (NIH)/National Institute of Aging (NIA), grant number 1 PO1 AG-17242, NIEHS (1UO1 ES011044), Netherlands Organization for Scientific Research (NWO) through the foundation of the Research Institute Diseases of the Elderly, as well as grants from the Dutch Cancer Society, (EUR 99-2004) and EC (QRTL-1999-02002).

## Reference List

- [1] C.Lengauer, K.W.Kinzler, B.Vogelstein. Genetic instabilities in human cancers, *Nature*, 396, (1998) 643-649.
- [2] M.Takata, M.S.Sasaki, E.Sonoda, C.Morrison, M.Hashimoto, H.Utsumi, Y.Yamaguchi-Iwai, A.Shinohara, S.Takeda. Homologous recombination and non-homologous end-joining pathways of DNA double-strand break repair have overlapping roles in the maintenance of chromosomal integrity in vertebrate cells, *EMBO J.*, 17, (1998) 5497-5508.
- [3] E.C.Friedberg. DNA damage and repair, *Nature*, 421, (2003) 436-440.
- [4] E.C.Friedberg. How nucleotide excision repair protects against cancer, *Nat.Rev.Cancer*, 1, (2001) 22-33.
- [5] A.S.Balajee, V.A.Bohr. Genomic heterogeneity of nucleotide excision repair, *Gene*, 250, (2000) 15-30.
- [6] B.S.Thoma, K.M.Vasquez. Critical DNA damage recognition functions of XPC-hHR23B and XPA-RPA in nucleotide excision repair, *Mol.Carcinog.*, 38, (2003) 1-13.
- [7] W.C.van der, J.Jansen, H.Vrieling, L.A.van der, A.Van Zeeland, L.Mullenders. Nucleotide excision repair in differentiated cells, *Mutat.Res.*, 614, (2007) 16-23.
- [8] K.H.Kraemer, N.J.Patronas, R.Schiffmann, B.P.Brooks, D.Tamura, J.J.DiGiovanna. Xeroderma pigmentosum, trichothiodystrophy and Cockayne syndrome: a complex genotype-phenotype relationship, *Neuroscience*, 145, (2007) 1388-1396.
- [9] J.de Boer, J.H.Hoeijmakers. Nucleotide excision repair and human syndromes, *Carcinogenesis*, 21, (2000) 453-460.
- [10] D.Bootsma, G.Weeda, W.Vermeulen, H.van Vuuren, C.Troelstra, S.P.van der, J.Hoeijmakers. Nucleotide excision repair syndromes: molecular basis and clinical symptoms, *Philos.Trans.R.Soc.Lond B Biol.Sci.*, 347, (1995) 75-81.
- [11] T.Yasuda, K.Sugasawa, Y.Shimizu, S.Iwai, T.Shioimi, F.Hanaoka. Nucleosomal structure of undamaged DNA regions suppresses the non-specific DNA binding of the XPC complex, *DNA Repair (Amst)*, 4, (2005) 389-395.
- [12] P.C.Hanawalt, J.M.Ford, D.R.Lloyd. Functional characterization of global genomic DNA repair and its implications for cancer, *Mutat.Res.*, 544, (2003) 107-114.
- [13] M.Yokoi, C.Masutani, T.Maekawa, K.Sugasawa, Y.Ohkuma, F.Hanaoka. The xeroderma pigmentosum group C protein complex XPC-HR23B plays an important role in the recruitment of transcription factor IIH to damaged DNA, *J.Biol.Chem.*, 275, (2000) 9870-9875.
- [14] K.Sugasawa. The xeroderma pigmentosum group C protein complex and ultraviolet-damaged DNA-binding protein: functional assays for damage recognition factors involved in global genome Repair, *Methods Enzymol.*, 408, (2006) 171-188.
- [15] C.J.Park, B.S.Choi. The protein shuffle. Sequential interactions among components of the human nucleotide excision repair pathway, *FEBS J.*, 273, (2006) 1600-1608.
- [16] R.M.Costa, V.Chigancas, R.S.Galhardo, H.Carvalho, C.F.Menck. The eukaryotic nucleotide excision repair pathway, *Biochimie*, 85, (2003) 1083-1099.
- [17] J.E.Cleaver. Cancer in xeroderma pigmentosum and related disorders of DNA repair, *Nat.Rev.Cancer*, 5, (2005) 564-573.
- [18] E.M.Hoogervorst, C.T.van Oostrom, R.B.Beems, J.van Benthem, B.J.van den, C.F.van Kreijl, J.G.Vos, A.de Vries, H.van Steeg. 2-AAF-induced tumor development in nucleotide excision repair-deficient mice is associated with a defect in global genome repair but not with transcription coupled repair, *DNA Repair (Amst)*, 4, (2005) 3-9.
- [19] A.de Vries, C.T.van Oostrom, F.M.Hofhuis, P.M.Dortant, R.J.Berg, F.R.de Gruijl, P.W.Wester, C.F.van Kreijl, P.J.Capel, H.van Steeg. Increased susceptibility to ultraviolet-B and carcinogens of mice lacking the DNA excision repair gene XPA, *Nature*, 377, (1995) 169-173.

- [20] G.T.van der Horst, H.van Steeg, R.J.Berg, A.J.van Gool, J.de Wit, G.Weeda, H.Morreau, R.B.Beems, C.F.van Kreijl, F.R.de Gruijl, D.Bootsma, J.H.Hoeijmakers. Defective transcription-coupled repair in Cockayne syndrome B mice is associated with skin cancer predisposition, *Cell*, 89, (1997) 425-435.
- [21] R.J.Berg, A.de Vries, H.van Steeg, F.R.de Gruijl. Relative susceptibilities of XPA knockout mice and their heterozygous and wild-type littermates to UVB-induced skin cancer, *Cancer Res.*, 57, (1997) 581-584.
- [22] L.B.Meira, A.M.Reis, D.L.Cheo, D.Nahari, D.K.Burns, E.C.Friedberg. Cancer predisposition in mutant mice defective in multiple genetic pathways: uncovering important genetic interactions, *Mutat.Res.*, 477, (2001) 51-58.
- [23] S.W.Wijnhoven, H.J.Kool, L.H.Mullenders, A.A.van Zeeland, E.C.Friedberg, G.T.van der Horst, H.van Steeg, H.Vrieling. Age-dependent spontaneous mutagenesis in *Xpc* mice defective in nucleotide excision repair, *Oncogene*, 19, (2000) 5034-5037.
- [24] M.C.Hollander, R.T.Philburn, A.D.Patterson, S.Velasco-Miguel, E.C.Friedberg, R.I.Linnoila, A.J.Fornace, Jr. Deletion of XPC leads to lung tumors in mice and is associated with early events in human lung carcinogenesis, *Proc.Natl.Acad.Sci.U.S.A.*, 102, (2005) 13200-13205.
- [25] A.de Vries, H.van Steeg. *Xpa* knockout mice, *Semin.Cancer Biol.*, 7, (1996) 229-240.
- [26] D.L.Cheo, H.J.Ruven, L.B.Meira, R.E.Hammer, D.K.Burns, N.J.Tappe, A.A.van Zeeland, L.H.Mullenders, E.C.Friedberg. Characterization of defective nucleotide excision repair in XPC mutant mice, *Mutat.Res.*, 374, (1997) 1-9.
- [27] M.E.Dolle, H.Giese, C.L.Hopkins, H.J.Martus, J.M.Hausdorff, J.Vijg. Rapid accumulation of genome rearrangements in liver but not in brain of old mice, *Nat.Genet.*, 17, (1997) 431-434.
- [28] S.W.Wijnhoven, H.J.Kool, L.H.Mullenders, R.Slater, A.A.van Zeeland, H.Vrieling. DMBA-induced toxic and mutagenic responses vary dramatically between NER-deficient *Xpa*, *Xpc* and *Csb* mice, *Carcinogenesis*, 22, (2001) 1099-1106.
- [29] A.D.Tates, F.J.van Dam, A.T.Natarajan, A.H.Zwinderman, S.Sosanto. Frequencies of HPRT mutants and micronuclei in lymphocytes of cancer patients under chemotherapy: a prospective study, *Mutat.Res.*, 307, (1994) 293-306.
- [30] S.W.Wijnhoven, E.Sonneveld, H.J.Kool, C.M.van Teijlingen, H.Vrieling. Chemical carcinogens induce varying patterns of LOH in mouse T-lymphocytes, *Carcinogenesis*, 24, (2003) 139-144.
- [31] M.E.Dolle, H.J.Martus, J.A.Gossen, M.E.Boerrigter, J.Vijg. Evaluation of a plasmid-based transgenic mouse model for detecting in vivo mutations, *Mutagenesis*, 11, (1996) 111-118.
- [32] R.Peto, M.C.Pike, N.E.Day, R.G.Gray, P.N.Lee, S.Parish, J.Peto, S.Richards, J.Wahrendorf. Guidelines for simple, sensitive significance tests for carcinogenic effects in long-term animal experiments, *IARC Monogr Eval.Carcinog.Risk Chem.Hum.Suppl.*, (1980) 311-426.
- [33] H.Moon, H.Ahn, R.L.Kodell. An age-adjusted bootstrap-based Poly-k test, *Stat.Med.*, 24, (2005) 1233-1244.
- [34] J.Brugarolas, C.Chandrasekaran, J.I.Gordon, D.Beach, T.Jacks, G.J.Hannon. Radiation-induced cell cycle arrest compromised by p21 deficiency, *Nature*, 377, (1995) 552-557.
- [35] S.W.Wijnhoven, R.B.Beems, M.Roodbergen, B.J.van den, P.H.Lohman, K.Diderich, G.T.van der Horst, J.Vijg, J.H.Hoeijmakers, H.van Steeg. Accelerated aging pathology in ad libitum fed *Xpd*(TTD) mice is accompanied by features suggestive of caloric restriction, *DNA Repair (Amst)*, 4, (2005) 1314-1324.
- [36] R.J.Kastenmayer, M.A.Fain, K.A.Perdue. A retrospective study of idiopathic ulcerative dermatitis in mice with a C57BL/6 background, *J.Am.Assoc.Lab Anim Sci.*, 45, (2006) 8-12.
- [37] G.W.Lawson, A.Sato, L.A.Fairbanks, P.T.Lawson. Vitamin E as a treatment for ulcerative dermatitis in C57BL/6 mice and strains with a C57BL/6 background, *Contemp.Top.Lab Anim Sci.*, 44, (2005) 18-21.
- [38] G.Y.Lee, J.S.Jang, S.Y.Lee, H.S.Jeon, K.M.Kim, J.E.Choi, J.M.Park, M.H.Chae, W.K.Lee, S.Kam, I.S.Kim, J.T.Lee, T.H.Jung, J.Y.Park. XPC polymorphisms and lung cancer risk, *Int.J.Cancer*, 115, (2005) 807-813.

- [39] Y.Bai, L.Xu, X.Yang, Z.Hu, J.Yuan, F.Wang, M.Shao, W.Yuan, J.Qian, H.Ma, Y.Wang, H.Liu, W.Chen, L.Yang, G.Jing, X.Huo, F.Chen, Y.Liu, L.Jin, Q.Wei, W.Huang, H.Shen, D.Lu, T.Wu. Sequence variations in DNA repair gene XPC is associated with lung cancer risk in a Chinese population: a case-control study, *BMC.Cancer*, 7, (2007) 81.
- [40] Z.Hu, Y.Wang, X.Wang, G.Liang, X.Miao, Y.Xu, W.Tan, Q.Wei, D.Lin, H.Shen. DNA repair gene XPC genotypes/haplotypes and risk of lung cancer in a Chinese population, *Int.J.Cancer*, 115, (2005) 478-483.
- [41] D.L.Cheo, D.K.Burns, L.B.Meira, J.F.Houle, E.C.Friedberg. Mutational inactivation of the xeroderma pigmentosum group C gene confers predisposition to 2-acetylaminofluorene-induced liver and lung cancer and to spontaneous testicular cancer in Trp53<sup>-/-</sup> mice, *Cancer Res.*, 59, (1999) 771-775.
- [42] D.Nahari, L.D.McDaniel, L.B.Task, R.L.Daniel, S.Velasco-Miguel, E.C.Friedberg. Mutations in the Trp53 gene of UV-irradiated Xpc mutant mice suggest a novel Xpc-dependent DNA repair process, *DNA Repair (Amst)*, 3, (2004) 379-386.
- [43] M.E.Dolle, R.A.Busuttill, A.M.Garcia, S.Wijnhoven, E.van Drunen, L.J.Niedernhofer, H.G.van der, J.H.Hoeijmakers, H.van Steeg, J.Vijg. Increased genomic instability is not a prerequisite for shortened lifespan in DNA repair deficient mice, *Mutat.Res.*, 596, (2006) 22-35.
- [44] H.Giese, M.E.Dolle, A.Hezel, H.van Steeg, J.Vijg. Accelerated accumulation of somatic mutations in mice deficient in the nucleotide excision repair gene XPA, *Oncogene*, 18, (1999) 1257-1260.
- [45] d.van, V, C.E.Cross. Oxidants, nitrosants, and the lung, *Am.J.Med.*, 109, (2000) 398-421.
- [46] T.K.Hazra, A.Das, S.Das, S.Choudhury, Y.W.Kow, R.Roy. Oxidative DNA damage repair in mammalian cells: a new perspective, *DNA Repair (Amst)*, 6, (2007) 470-480.
- [47] Y.Shimizu, S.Iwai, F.Hanaoka, K.Sugasawa. Xeroderma pigmentosum group C protein interacts physically and functionally with thymine DNA glycosylase, *EMBO J.*, 22, (2003) 164-173.
- [48] M.D'Errico, E.Parlanti, M.Teson, B.M.de Jesus, P.Degan, A.Calcagnile, P.Jaruga, M.Bjoras, M.Crescenzi, A.M.Pedrin, J.M.Egly, G.Zambruno, M.Stefanini, M.Dizdaroglu, E.Dogliotti. New functions of XPC in the protection of human skin cells from oxidative damage, *EMBO J.*, (2006).
- [49] S.N.Kassam, A.J.Rainbow. Deficient base excision repair of oxidative DNA damage induced by methylene blue plus visible light in xeroderma pigmentosum group C fibroblasts, *Biochem.Biophys.Res.Comm.*, 359, (2007) 1004-1009.



# Chapter 4

# Chapter 4

## Mutational and transcriptional responses upon oxidative damage exposure in $Xpc^{-/-}$ mice

**Melis JPM**, Kuiper RV, Pennings JLA, Zwart E, Robinson J, van Oostrom CTM, Luijten M, van Steeg H.

Mutational and transcriptional responses upon oxidative damage exposure in  $Xpc^{-/-}$  mice

**Revisions, Antioxidants & Redox Signaling (Special Issue December 2012)**

*"Yes, there are two paths you can go by, but in the long run,  
There's still time to change the road you're on"*

Stairway To Heaven – Led Zeppelin, 1971



## Abstract

The Nucleotide Excision Repair (NER) pathway is one of the main and most versatile mechanisms preventing DNA damage accumulation and subsequent cancer development. Previously we demonstrated that NER-deficient mouse models *Xpa*<sup>-/-</sup> and *Xpc*<sup>-/-</sup> are both cancer prone, but exhibit a divergent tumor spectrum and incidence. Here, we report, *in vitro* and for the first time *in vivo*, that *Xpc*<sup>-/-</sup> mice are more sensitive to exogenously induced oxidative DNA damage.

*Xpc*<sup>-/-</sup> mouse embryonic fibroblasts exposed to normoxic and atmospheric oxygen pressures were more sensitive to atmospheric oxygen levels and showed a significantly increased mutational load, contrary to wild type and *Xpa*<sup>-/-</sup> cells. Additionally, comprehensive *in vivo* studies in wild type, *Xpa*<sup>-/-</sup> and *Xpc*<sup>-/-</sup> mice with the pro-oxidants DEHP and paraquat increased oxidative stress levels in liver of all genotypes, indicated by amongst others the level of lipofuscin accumulation. After long-term pro-oxidant exposures *Xpc*<sup>-/-</sup> mice, but not *Xpa*<sup>-/-</sup> and wild type mice, revealed significantly elevated mutational levels in liver. Transcriptomic analyses provided insight into this divergent response between *Xpa*<sup>-/-</sup> and *Xpc*<sup>-/-</sup> mice. Gene expression profiles overall were similar between all genotypes. However, *Xpc*<sup>-/-</sup> mice, compared to wild type and *Xpa*<sup>-/-</sup>, showed a lower transcriptional glutathione metabolism response, corroborating previous *in vitro* results by others. Our studies reveal that long-term *in vivo* XPC deficiency contributes to an increased oxidative DNA damage accumulation and subsequent mutational load. These findings further support our view that the XPC protein has a cancer prevention function outside of NER, which is involved in the prevention of oxidative DNA damage.

## Introduction

The excessive amount of genomic assaults in cells, either by endogenous or exogenous factors, results into billions of lesions in the human body per day [<sup>1</sup>]. These lesions can result into persistent DNA damage if left unattended, and subsequently can cause cell death, cancer and accelerated aging due to loss of homeostasis [<sup>2,3</sup>].

In the defense against induced DNA damage DNA repair mechanisms are vital. Several DNA repair pathways cooperate to minimize the detrimental impact of the genomic insults. Damaged or incorrect bases can be corrected by amongst others base excision repair (BER) and nucleotide excision repair (NER). BER is mainly responsible for the removal of oxidative DNA damage [<sup>4,5</sup>], while the NER pathway is known to be accountable for removing bulky and helix-distorting lesions in the DNA [<sup>3</sup>]. However, overlap between the latter two pathways has been proposed [<sup>6-11</sup>].

In NER, over 30 proteins are involved in the complete removal and repair of the DNA lesions [<sup>3</sup>]. Two pivotal proteins in this cascade are XPA and XPC, which belong to the family of XP proteins linked to the severe autosomal recessive disorder Xeroderma pigmentosum (XP). XP in humans is marked by a 1,000-fold increased risk for sunlight-induced skin cancer [<sup>1</sup>]. Fewer than 40% of individuals with the disease, of which XP-A and XP-C patients are the most common worldwide, survive beyond age 20 years [<sup>1,12-14</sup>].

The NER pathway can be divided in two sub-pathways: global genome NER (GG-NER), which covers repair genome-wide, and transcription coupled NER (TC-NER), which is responsible for repair of the transcribed strand of active genes [<sup>1,15,16</sup>]. XP-C patients are only defective in the GG-NER pathway, while XP-A patients are hampered in both GG-NER and TC-NER sub-pathways [<sup>3</sup>].

In mice, similar characteristics to the human disorders can be mimicked by knocking out one of these XP genes. In a previous study we presented the spontaneous phenotypes of the *Xpa*- and *Xpc*-deficient knock-out mouse models in a congenic C57BL/6J background [<sup>17</sup>]. We established that *Xpa*<sup>-/-</sup> and *Xpc*<sup>-/-</sup> mice (hereafter referred to as *Xpa* and *Xpc*, respectively) are both cancer prone and, although being part of the same DNA repair pathway, show a divergent tumor phenotype. Compared to wild type C57BL/6J mice, both mouse models showed an increase in hepatocellular tumors (10% in *Xpa*, 13% in *Xpc*), but strikingly *Xpc* also exhibited an even higher incidence of lung tumors (16%). Mutant frequency analyses demonstrated that the tumor phenotype could be correlated to the mutational load, which accumulated over time in these mouse models. A significant increase in *LacZ* mutant levels in liver and lung was visible for *Xpc* mice, while *Xpa* only showed a significant increase in liver. These findings pointed towards an increased sensitivity of *Xpc* mice to oxygen exposure and a putative role of XPC in a process, besides NER, preventing or removing oxidative DNA damage.

In the present study, we examined the hypothesis whether *Xpc*-deficient cells and mice are more sensitive to exogenous oxidant exposure than *Xpa* and wild type cells and mice, plus set out to unravel part of the underlying differences by gene expression profiling.

## Material & Methods

### *Cell culture*

Primary mouse embryonic fibroblasts (MEFs) were isolated from E13.5 day embryos, all in C57BL/6J background, and genotyped and cultured as described previously [49;50]. MEFs were cultured for 3 days per passage at 3% or 20% O<sub>2</sub>. The first passage for all groups was performed at 3% O<sub>2</sub>, subsequently they were split to either 3% or 20% O<sub>2</sub> for two more passages. A minimum of three different embryos, all from different mothers, was used per genotype.

### *LacZ mutant frequency analyses*

From frozen liver, lung or mouse embryonic fibroblasts, DNA was extracted and analyzed for mutant frequency as described previously [17]. Briefly, between 10 and 20 µg of genomic DNA were digested with HindIII for 1 h in the presence of magnetic beads recoated with *LacI-LacZ* fusion protein. Plasmid DNA was subsequently eluted from the beads and circularized with T4 DNA ligase. Next, ethanol-precipitated plasmids were used to transform *E. coli* C (*DLacZ*, *galE*-) cells. Dilutions of the transformed cells were plated on the titer plate (with X-gal) and the remainder on the selective plate (with p-gal). The plates were incubated for 15 h at 37°C. Mutant frequencies were determined as the number of colonies on the selective plates versus the number of colonies on the titer plate (times the dilution factor). Two-way ANOVA analyses and post-hoc t-tests to compare mutant frequencies between all groups were performed, and were considered significant if  $p < 0.05$ .

### *Mice*

The generation and characterization of *Xpa* and *Xpc* mice has been described before [51;52]. The heterozygous mutant mouse strains, as well as C57BL/6J controls, were crossed with pUR288-*LacZ* C57BL/6J transgenic mice line 30, homozygous for *LacZ* integration on chromosome 11 [49]. Mice were genotyped by a standard PCR reaction using DNA isolated from tail tips. Primers to amplify the wild type and targeted *Xpa* and *Xpc* allele, as well as primer sequences for *LacZ* determination have been described previously [49;50]. The experimental setup of the studies was examined and agreed upon by the institute's Ethical Committee on Experimental Animals, according to national legislation. The health state of the mice was checked daily. During exposure, the animals were weighed weekly for the first eight weeks of exposure and biweekly for the remainder of the exposure study to monitor health conditions of the animals. Food uptake was measured for the first 5 weeks.

During the entire experiment, animals were kept in the same stringently controlled environment, fed *ad libitum* and kept under a normal day/night rhythm. Animals were removed from the study when found dead or moribund. Autopsy was performed on animals of all cohorts; tissues were stored for further histopathological analysis. In addition, a selective set of different tissues were snap frozen in liquid N<sub>2</sub> for *LacZ* mutant frequency analysis and gene expression profiling.

### ***In vivo experimental design***

Ten-week-old wild type (C57BL/6J), *Xpa* and *Xpc* mice were marked, genotyped and randomized in cohorts, in which the mice were sacrificed 39 weeks after start of the exposure. All genotypes were exposed to either control feed or the compounds di(2-ethylhexyl) phthalate (DEHP (CAS 117-81-7), 6,000 ppm, female mice) or methyl viologen (paraquat (CAS 1910-42-5), 100 ppm, male mice). All groups consisted of 20 animals.

The concentrations of DEHP (6,000 ppm) and paraquat (100 ppm) were used, and were chosen based on results of 2 year bioassay carcinogenicity testing in rodents [<sup>18;30</sup>].

### ***Histopathology***

Tissue samples (amongst others liver, kidney, lung and tissues having gross lesions) of each animal were preserved in a neutral aqueous phosphate-buffered 4% solution of formaldehyde. Tissues required for microscopic examination were processed, embedded in paraffin wax, sectioned at 4µm and stained with haematoxylin and eosin. Detailed microscopic examination was performed on liver, lung and kidney of all mice and on all gross lesions suspected of being tumors or representing major pathological conditions. Non-neoplastic findings were either scored using 1) an ordinal scale (1-5) and averaged per group for comparisons or 2) based on incidence.

Unstained slides were mounted with Cytoseal-XYL (Richard-Allan Scientific, Thermo Fisher Scientific, MI, USA) and viewed under UV light for semiquantitative assessment of lipofuscin deposition.

### ***Micro-array analysis***

Total RNA was isolated with the Minikit (Qiagen) using the QIAcube (Qiagen) according to manufacturer's protocol. RNA quality was tested using automated gel electrophoresis (Bioanalyzer 2100; Agilent Technologies, Amstelveen, the Netherlands). All RNA samples passed RNA integrity number QC (>7.0). RNA samples (wild-type, *Xpa* and *Xpc* : n=6 per genotype) were amplified, labeled and hybridized to Nimblegen 12x135k *Mus musculus* microarrays as described in detail in Pennings et al. 2011 [<sup>53</sup>].

### ***Data analysis***

Gene expression differences between experimental groups were compared with ANOVA. Obtained p-values were corrected for multiple testing by calculating the False Discovery Rate (FDR). Probes with a FDR<0.05 were considered significant. When multiple probes corresponding to the same gene were significant, their data were averaged to remove redundancy in further analysis.

Gene expression differences were visualized using GeneMaths XT (Applied Maths, St-Martens-Latem, Belgium). Regulated genes were analyzed for functional overrepresentation of GeneGo pathway maps and GO processes using MetaCore (www.GeneGO.com). Pathway map overrepresentation was considered significant if  $p < 0.05$ . Pathway- or gene set-level effects were specific for *Xpc* if it was either significant in *Xpc* and not in both WT and *Xpa*, or vice versa. Complete raw and normalized microarray

data and their MIAME compliant metadata have been deposited at GEO ([www.ncbi.nlm.nih.gov/geo](http://www.ncbi.nlm.nih.gov/geo)) under accession number GSE28296.

## Results

### *Increased mutational load in Xpc MEFs upon atmospheric oxygen exposure*

In our previous study we have shown that *Xpc*-deficient mice are more prone to lung cancer than *Xpa* and wild type mice. Additionally, mouse embryonic fibroblasts (MEFs) of *Xpc* mice are more sensitive in terms of survival to atmospheric oxygen levels than *Xpa* and wild type MEFs [17]. In the present study, we first verified if the decreased survival observed at atmospheric oxygen conditions in *Xpc* MEFs could be correlated to the amount of oxidative DNA damage that has been fixed as mutations. We therefore cultured wild type, *Xpa* and *Xpc* MEFs at either normoxic (3%) or atmospheric (20%) oxygen levels under the same conditions as in our previous study [17]. *LacZ* mutant frequency analyses revealed that in MEFs cultured at 3% oxygen pressure, the mutant frequency in both *Xpa* and *Xpc* cells was already slightly, but not significantly, increased compared to wild type cells (Figure 1). However at 20% oxygen pressure, *LacZ* mutant frequencies were only increased in *Xpc* MEFs compared to their normoxic treated controls ( $p < 0.01$ ). The increased oxidative DNA damage in these cells demonstrated an inverse correlation with the previously found decreased survival response in *Xpc* cells [17].

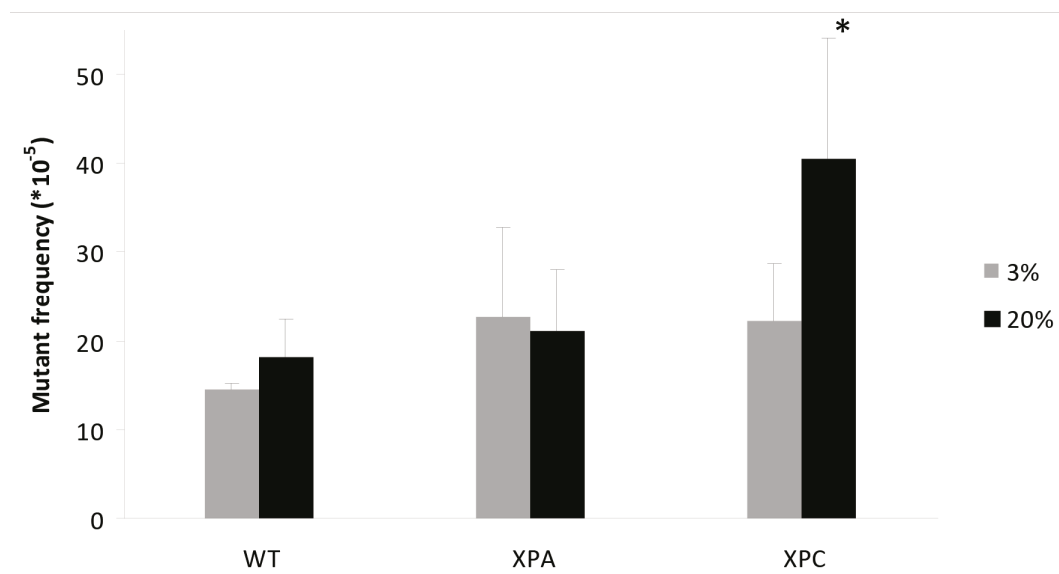


**Figure 1.** *LacZ* mutant frequencies in MEFs cultured at normoxic (3% O<sub>2</sub>) or atmospheric (20% O<sub>2</sub>) conditions. MEFs were cultured at 3% O<sub>2</sub> pressure the first passage and for two subsequent passages at either 3% or 20% oxygen pressure. Error bars indicated SD. \*  $p < 0.01$  20% O<sub>2</sub> versus 3% O<sub>2</sub> level

**Neoplastic and non-neoplastic lesions upon *in vivo* pro-oxidant exposures**

To verify whether XPC deficiency also results in an increased sensitivity towards oxidative damage *in vivo*, wild type, *Xpa* and *Xpc* mice (all harboring the *LacZ* gene for mutational analysis) were exposed to pro-oxidative compounds for either 12 weeks (for *LacZ* analyses) or 39 weeks (for histopathological and *LacZ* analyses). Female mice were exposed to DEHP (6,000 ppm, via feed), while male mice were exposed to paraquat (100 ppm, via feed).

Body weight measurements over the duration of exposures demonstrated a decrease in all genotypes for DEHP exposure, while paraquat exposure only had a minor effect on body weight (SI01). Dietary uptake in both exposure groups was comparable to the uptake of the control diet group (SI02).

**A**

Neoplastic		Control	DEHP
WT	Liver	0%	0%
	Lung	0%	5% (1 adenoma)
XPA	Liver	5% (1 adenoma)	5% (1 adenoma)
	Lung	0%	0%
XPC	Liver	0%	10% (2 carcinomas)
	Lung	5% (1 lymphoma)	0%

**B**

Non-neoplastic		WT	XPA	XPC
		DEHP	DEHP	DEHP
Liver	Karyomegaly severity	- -		-
	Lipofuscin autofluorescence severity	++	+++	+++
	Eosinophilic cytoplasm incidence	+++	+++	+++
	Cholestasis incidence	+++	+++	++
	Glycogenosis incidence		-	- - -
Kidney	Hydronephrosis incidence	+++	++	+++
	Tubule dilatation incidence	+++	+++	+++
	Scarring severity	+++	+++	+++
	Macrophages incidence	+++	+++	+
		Paraquat	Paraquat	Paraquat
Lung	Septum thickness severity	+++	+	+++
	Peribronchiolar fibrosis severity		+	++
	Lymphoid hyperplasia severity		+	+++
	Inflammatory cells diffuse infiltration severity		+	+++
	Peribronchiolar edema incidence			+

**Table 1.** Neoplastic and non-neoplastic observations after 39 week pro-oxidant exposure.

**A.** Neoplastic lesion incidents in percentage per group (n=20), bracketed numbers indicate the number of tumors. None of the tumor incidences are significant when compared to their untreated genotype control ( $p < 0.05$ ). Exposure to paraquat did not result into tumorigenesis.

**B.** Non-neoplastic changes per group (n=20). (- / + = 10-20%, -- / ++ = 20-30%, --- / +++ = >30% changes relative to the untreated concordant genotype group based on either incidences or averaged ordinal score of severity)

Long-term (39 weeks) exposed mice were analyzed macroscopically during autopsy and afterwards liver, kidney, and lung and eventual gross lesions were subjected to histopathological analyses. The results are summarized in Table 1. In total, few neoplastic lesions (Table 1A) were found after long-term exposure. In the livers of exposed wild type and *Xpa* mice 1 benign tumor (adenoma) for each genotype, but no malignant tumors, were observed. Also one benign tumor (adenoma) was identified in the group of untreated *Xpa* mice. The only malignant liver tumors (2 carcinomas) in the study were observed in the DEHP-treated *Xpc* animals. Also, one malignant tumor (lymphoma) in lung was found in the untreated *Xpc* group. None of the animals (male mice) exposed to paraquat, nor any of their concurrent controls, carried a tumor.

Paraquat exposure had little effect on pathology in liver and kidney. Overall, the response to DEHP was stronger compared to paraquat. Histopathological findings clearly confirmed DEHP exposure in liver and kidney, but no differences between the three genotypes were observed (Table 1B, non-neoplastic findings). Hepatocytes of all DEHP-treated mice diffusely showed eosinophilic cytoplasm consistent with peroxisome proliferation (the most distinct mode of action of DEHP). Furthermore, lipofuscin and cholestasis, indicative for increased oxidative stress, were also apparent. DEHP induced a strong increase in hydronephrosis, tubule dilatation, scarring, and vacuolized and pigmented macrophages in kidney, while paraquat showed no obvious pathology in these two tissues. Even though paraquat was administered through the diet, paraquat induced histopathological lesions in the lungs, especially in *Xpc* mice. For instance, severity of peribronchiolar fibrosis, lymphoid hyperplasia and diffuse infiltration of inflammatory cells were all increased in *Xpc* mice only (Table 1B).

### ***Higher mutational load in Xpc mice due to oxidant exposure***

To assess potential differences in sensitivity for oxidative DNA damage between the genotypes we also analyzed the mutational load, as an early tumor risk marker, in the tissues where pathological evidence for exposure and carcinogenesis was found (liver and lung). Mutant frequencies in the *LacZ* gene were measured in both tissues after 12 and 39 weeks of exposure to the pro-oxidants DEHP and paraquat to assess the amount and rate of possible mutation induction due to oxidative stress.

The 12 week exposures to DEHP or paraquat did not result in any significant changes in mutational load in liver or lung of all genotypes compared to the untreated corresponding genotype (Figure 2A). However, the long-term exposure of 39 weeks to both DEHP and paraquat resulted in a statistically significant and exposure-related two-fold increase in mutant frequency in livers of *Xpc* mice only ( $p < 0.01$ ) (Figure 2B). Long-term pro-oxidant exposure did not result in a significantly enhanced mutational load in lung compared to their untreated controls. Mutational loads in the lungs of *Xpc* mice, however, tended to increase faster over time when compared to WT and *Xpa* (Figure 2B). SI03 provides an overview of  $p$ -values between all groups.

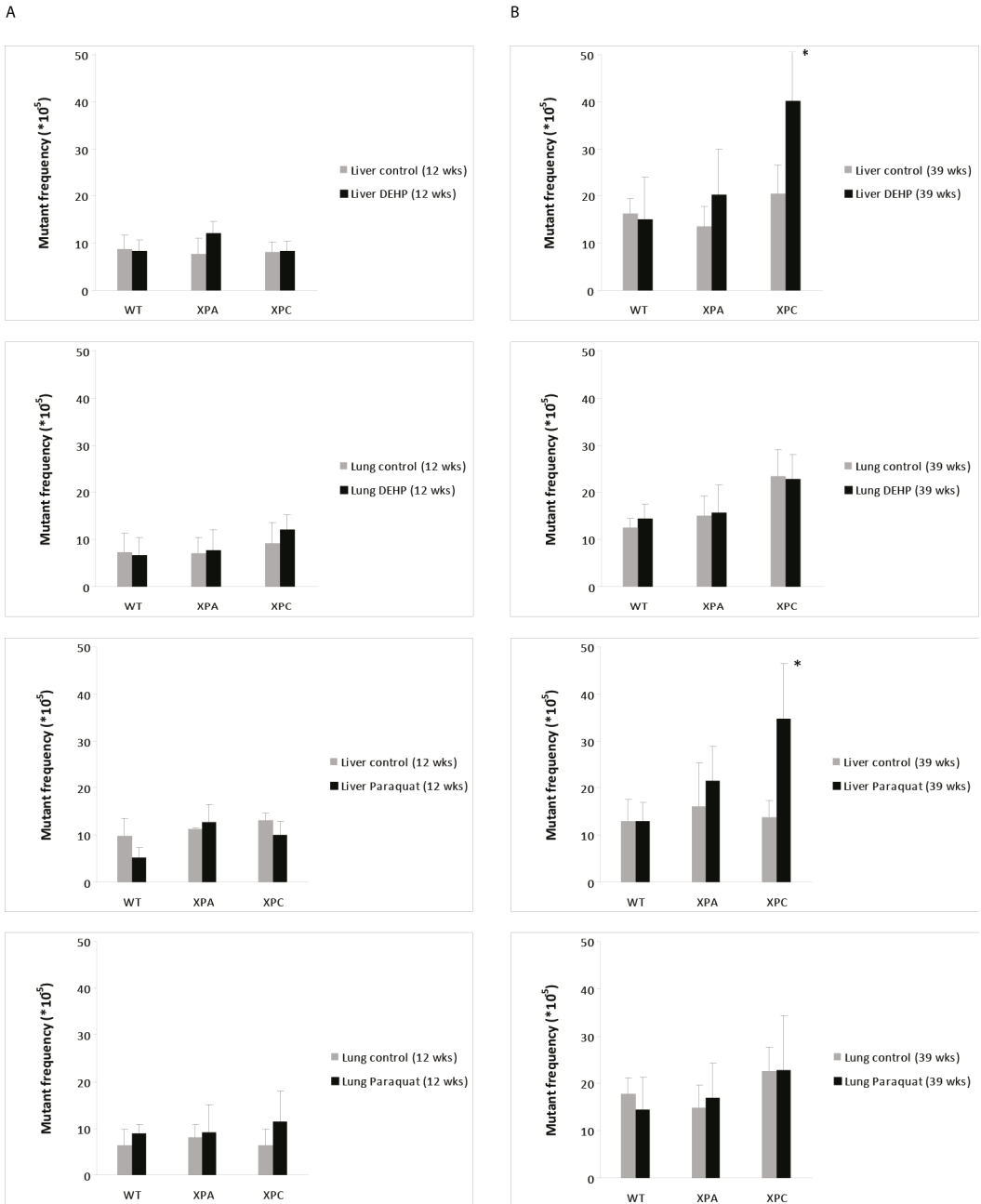


**Figure 2.** *LacZ* mutant frequencies in liver and lung after pro-oxidant exposure of 12 (**A**, left column) and 39 weeks (**B**, right column). Mice were exposed to either DEHP (female mice), paraquat (male mice) or control feed for 39 weeks. \* $p < 0.05$  treatment versus control.



***Divergent transcriptomic response for glutathione metabolism in *Xpc* mice***

We subsequently attempted to unravel part of the underlying mechanism(s) of the observed increased mutational sensitivity towards oxidative DNA damage in *Xpc* mice by performing genome-wide expression analyses on long-term (39 weeks) DEHP-treated and untreated liver tissue of all three genotypes (GEO database, accession number GSE28296).

The base-line (untreated) transcriptional profiles between the three genotypes were highly similar. One-way analysis of variance (ANOVA) with a False Discovery Rate (FDR) < 0.05 on all untreated samples revealed only 15 differentially expressed genes (DEGs) between the three genotypes, amongst which down regulation of the *Xpa* and *Xpc* gene in their concurrent knockout mouse model (data not shown). These results indicated the basal liver gene expression profiles of the genotypes are similar without exposure.

Subsequently, differences in gene expression in liver upon DEHP exposure were quantified (One-way ANOVA, FDR < 0.05). This analysis revealed 2,278 DEGs in wild type, 3,205 DEGs in *Xpa*, and only 1,449 DEGs in *Xpc* mice. Since these numerical differences could represent a generally higher or lower gene expression level of respectively *Xpa* and *Xpc* (compared to wild type), this could give rise to misleading results. We therefore implemented the following approach to analyze for functional differences between the genotypes. For functional analyses, we used either the DEGs or the top 2,278 genes (ranked on FDR) of each genotype as input. Metacore GeneGO pathway analyses ( $p < 0.01$ , SI04, data not shown in this thesis) and Gene Ontology (GO) analyses ( $p < 0.00001$ , SI05, data not shown in this thesis) were performed for both the DEG and the top 2,278 approach. In the latter approach, the wild type differential gene expression profile (2,278 DEGs) was used as a benchmark to ensure more robust results emphasizing the difference between the genotypes. In this approach, for all genotypes the top 2,278 genes (ranked on FDR) was used as input (GEO database, accession number GSE28296). For instance, for *Xpc* it could be the case that the lower number of DEGs is indicative for a lower overall gene expression level. Consequently, many genes did not make the cut-off of FDR < 0.05, resulting in a lack of overrepresented pathways for *Xpc*. So, only if an overrepresented pathway in wild type mice was absent in *Xpc* mice for both types of analyses (DEGs and top 2,278 genes), it was considered as a truly different response from wild type animals.

Using the DEGs and the top 2,278 genes as input for, we screened for functional responses upon pro-oxidant exposure that could explain the observed mutational responses described above. To ensure a more robust pathway analysis we only considered a pathway to be truly regulated if it was generated by both approaches (Overlap results are fully depicted in SI06). The overlap in pathways found with both approaches showed a strong DEHP signature: pathways involved in PPAR regulation of lipid metabolism and fatty acid omega oxidation were up-regulated in all genotypes (Table 2A, SI06) [18-20]. Results of the GO processes corroborated these DEHP exposure-related changes in lipid metabolism (SI05).

Since we were interested in the response and mechanisms behind the observed mutational sensitivity in *Xpc* upon long-term oxidative damage, we examined where *Xpc* mice responded in a significantly different manner from *Xpa* and wild type mice. For this, we used GeneGO pathway analyses. *Xpc* specific pathways (Table 2B & SI06) regulated in both approaches (DEGs and top 2,278 genes as input) were amongst others a down-regulation in nitrogen and glycine, serine, cysteine and threonine

metabolism and also an up-regulation of cell DNA replication in early S phase. Reciprocally, pathways regulated in both wild type and *Xpa*, but not in *Xpc* (Table 2B) included a significant up-regulation of glutathione metabolism, apoptosis-related BAD phosphorylation and spindle assembly and chromosome separation, plus down-regulated aldosterone-mediated regulation of epithelial sodium channel sodium transport.

#### A. Pathways differentially regulated in all genotypes

GeneGO p<0.01 in WT & XPA & XPC	Regulation
Regulation of lipid metabolism_PPAR regulation of lipid metabolism	up
Fatty Acid Omega Oxidation	up
Cell adhesion_Plasmin signaling	down
Blood coagulation_Blood coagulation	down
Immune response_Lectin induced complement pathway	down
Cytoskeleton remodeling_TGF, WNT and cytoskeletal remodeling	mix
Cytoskeleton remodeling_Cytoskeleton remodeling	mix
Atherosclerosis_Role of ZNF202 in regulation of expression of genes involved in Atherosclerosis	mix

#### B. Pathways differentially regulated between WT+XPA versus XPC

GeneGO p<0.01 only in WT & XPA	Regulation
Glutathione metabolism / Rodent version	up
Apoptosis and survival_BAD phosphorylation	up
Cell cycle_Spindle assembly and chromosome separation	up
Transport_Aldosterone-mediated regulation of ENaC sodium transport	down
GeneGO p<0.01 only in XPC	Regulation
Cell cycle_Start of DNA replication in early S phase	up
Nitrogen metabolism/ Rodent version	down
Glycine, serine, cysteine and threonine metabolism	down
Development_Mu-type opioid receptor signaling via Beta-arrestin	down

**Table 2.** GeneGO pathway overlap (DEGs and top2278 genes input,  $p < 0.01$ )

Other research groups have implicated XPC functionality in base excision repair (BER), redox homeostasis and cell cycle regulation (overview in [21]). Therefore, we also assessed these responses in more detail at single gene level. All genes that have previously been associated with XPC functionality in literature (listed in Table 3A) appeared not to be differentially regulated on transcriptional level in our current study, and if so, no clear difference between the three genotypes was observed. One gene that is involved in BER and redox homeostasis [22] was slightly differentially regulated in *Xpc* mice compared to *Xpa* and wild type mice: *Apex1* was up-regulated in *Xpa* and wild type (1.6 and 1.4 times respectively), and less in *Xpc* (1.2). Additionally, *Nrf1* (*NFE2L1*) was up-regulated in wild type (1.4) and only 1.2 times in *Xpa* and *Xpc*.

A.					
Reference	Gene	WT DEHP-Control	XPA DEHP-Control	XPC DEHP-Control	Process
D'Errico et al. 2006	Ogg1	1.02	-1.02	-1.02	BER
Shimizu et al. 2003, 2010	TDG	1.24	1.10	1.06	BER
Shimizu et al. 2010	SMUG1	1.01	-1.02	-1.03	BER
Meira et al. 2001	Apex	1.63	1.39	1.24	BER/Redox
Wang et al. 2003, 2004	p53	1.00	1.00	1.02	Cell cycle
Colton et al. 2006	ATM	1.00	-1.02	-1.01	Cell cycle
Auclair et al. 2003, 2004	ATR	1.29	1.41	1.27	Cell cycle
Ray et al. 2009	SNF5 (Smarcb1)	1.28	1.11	1.14	Cell cycle
Rezvani et al. 2011	DNAPK (Prkdc)	1.18	1.04	1.15	DNA damage/Redox
Rezvani et al. 2011	NOX1	1.05	-1.03	-1.01	Redox
Rezvani et al. 2011	AKT1	-1.07	1.01	-1.09	Redox
Han et al. 2012	Nrf1 (NFE2L1)	1.36	1.15	1.15	Glutathione metabolism
Liu et al. 2011, Langie et al. 2007	Overall process, no specific gene	-	-	-	Glutathione metabolism

B.					
Melis et al. 2012	SQSTM1	1.79	1.55	1.19	Antioxidant response/Glutathione
Genes involved in glutathione metabolism	GSTA1	3.72	2.40	1.86	Glutathione metabolism
	GSTA2	2.85	1.52	1.45	Glutathione metabolism
	GSTA4	1.37	1.32	1.03	Glutathione metabolism
	GSTK1	1.24	1.06	1.11	Glutathione metabolism
	GSTM1	1.96	1.87	1.35	Glutathione metabolism
	GSTM2	1.17	-1.02	1.03	Glutathione metabolism
	GSTM3	4.31	4.12	2.04	Glutathione metabolism
	GSTM4	2.54	1.83	1.88	Glutathione metabolism
	GSTM5	1.07	1.03	-1.02	Glutathione metabolism
	GSTM6	1.44	1.01	1.08	Glutathione metabolism
	GSTM7	1.08	-1.12	-1.16	Glutathione metabolism
	GSTO1	1.10	-1.02	1.06	Glutathione metabolism
	GSTO2	1.00	-1.08	-1.03	Glutathione metabolism
	GSTP1	2.68	2.85	2.11	Glutathione metabolism
	GSTP2	2.77	2.82	2.20	Glutathione metabolism
	GSTT1	-1.05	-1.13	-1.12	Glutathione metabolism
	GSTT2	1.68	2.08	1.81	Glutathione metabolism
	GSTT3	1.11	-1.20	-1.22	Glutathione metabolism
	GSTT4	-1.01	1.02	-1.04	Glutathione metabolism
	GSTCD	1.11	-1.03	1.02	Glutathione metabolism
	GSTZ1	-1.15	-1.19	-1.23	Glutathione metabolism
	GPX1	1.37	1.22	1.12	Glutathione metabolism
	GPX2	1.44	1.26	1.42	Glutathione metabolism
	GPX3	1.13	1.21	1.15	Glutathione metabolism
	GPX4	1.44	1.34	1.30	Glutathione metabolism
	GPX5	1.01	-1.03	-1.06	Glutathione metabolism
	GPX6	-1.49	-1.71	-1.24	Glutathione metabolism
	GPX7	1.54	1.70	1.47	Glutathione metabolism
	GPX8	1.01	-1.01	1.07	Glutathione metabolism
	Mgst1	1.28	1.01	1.14	Glutathione metabolism
	Mgst2	-1.14	-1.01	1.05	Glutathione metabolism
	Mgst3	1.61	1.62	1.37	Glutathione metabolism
	GSR	1.61	1.32	1.23	Glutathione metabolism
	GSS	1.26	1.29	1.06	Glutathione metabolism
	GCLC	2.33	1.31	1.50	Glutathione metabolism
	CTH (CGL)	-1.15	-1.45	-1.84	Glutathione metabolism
	CBS	-1.38	-1.41	-2.04	Glutathione metabolism
	Oplah	1.85	1.88	1.59	Glutathione metabolism
	Anpep	1.28	1.29	1.25	Glutathione metabolism

Xpc < WT and Xpa
 Xpc < WT or Xpa
 Xpc > WT and Xpa

**Table 3.** XPC-related functionality.**A.** Genes and process (fold changes (DEHP vs control)) implicated with additional XPC functionality**B.** Fold changes of genes involved in glutathione metabolism (DEHP vs control)

Previous *in vitro* studies also showed that XPC deficiency resulted in an affected glutathione metabolism [10;23;24]. In our 9 month *in vivo* study, the glutathione metabolism and related pathways (nitrogen metabolism and glycine, serine, cysteine and threonine metabolism) revealed a different transcriptional response in *Xpc* compared to both wild type and *Xpa*. Besides pathway analysis we also looked at the expression data of single genes known to be involved in glutathione metabolism (Table 3B). At the gene expression level, *Xpc* mice appeared to be less responsive in comparison to *Xpa* and wild type mice since the majority of these genes showed a lower fold change in *Xpc* mice. Another less responsive gene in *Xpc* is p62/SQSTM1 (Table 3B), which is part of the TFIIH complex, but is also involved in antioxidant response functioning. The XPC protein contains two binding domains for p62, one of them overlapping with the binding site of BER protein OGG1 [1]. In our study on transcriptional

level, p62/SQSTM1 was differentially up-regulated in both wild type (1.8) and *Xpa* (1.6), but less in *Xpc* (1.2) (Table 3B).

## Discussion

We, and others, hypothesized that XPC is involved in the prevention or removal of oxidative DNA damage by functionality outside of NER [6-10;17;21;23;25-28]. *Xpc* deficiency therefore could lead to more DNA damage as a consequence of their reduced capability to cope with oxidative stress. This could explain the observed increase in lung tumor incidence and corresponding increase in mutational load in *Xpc* mice compared to wild type and *Xpa* mice [17]. *Xpc* mice revealed an increase in lung and liver tumors, while in *Xpa* mice only liver tumor incidence was increased at final autopsy compared to wild type mice. Hollander et al. also showed an enhanced lung tumor incidence in *Xpc* mice [29]. Our previous study also demonstrated a decreased survival of *Xpc* MEFs upon normoxic versus atmospheric oxygen exposure in comparison to *Xpa* and wild type cells.

We assessed if the decreased survival response exhibited in *Xpc* MEFs was correlated to an increase in mutations using different oxygen exposure levels. Our results demonstrated that *Xpc* cells are specifically more sensitive towards oxidative DNA damage when compared to wild type and *Xpa* cells. Others have also previously implicated XPC in the prevention or removal of oxidative DNA damage *in vitro* using exposures to oxidative stressors [6-10;23;25-28]. It was however still unclear if, and at what rate, XPC deficiency contributes to the level of oxidative DNA damage *in vivo*. Therefore, we exposed *Xpa*, *Xpc* and wild type mice to the well-known pro-oxidants DEHP and paraquat through the diet and measured several parameters after a 12 week and a 39 week exposure to these compounds.

Histopathological analyses showed only a minor or no response in tumor formation after 39-week exposure to the low potent carcinogen DEHP or non-carcinogen paraquat, respectively. Paraquat does not induce tumors in rodents (EPA database, <http://www.epa.gov/iris/subst/0183.htm>, 2012) and exposure in the present study also did not lead to significant tumor formation in all three genotypes tested. The only malignant tumors observed in our current studies were found in *Xpc* mice. DEHP is carcinogenic to mice in a classical 2-year rodent bioassay at a dose of 6,000 ppm [18]. Apparently, shorter exposure times do not lead to a significant tumor response in mice, not even in the DNA repair-deficient models *Xpa* and *Xpc*. This finding is in line with our previous results in wild type and *Xpa* mice [30].

DEHP induced oxidative stress in liver since increased levels of lipofuscin and cholestasis [31-33] were found in exposed animals of all three genotypes. The effect of paraquat on histopathology in the liver was only marginal (data not shown), but did show a genotypical difference in *Xpc* lungs.

Since we expected that pro-oxidant exposure would enhance oxidative DNA-damaging events, we tested whether *Xpc* mice accumulated more mutations due to the exposure of DEHP and paraquat. *LacZ* mutant frequency analyses demonstrated a significant increase in mutational load after pro-oxidant exposure in livers of *Xpc* mice only. This increase however was only detected after 39 weeks of exposure. At 12 weeks of pro-oxidant exposure no significant increase the mutational load in any of the genotypes was observed. In lung, *LacZ* mutant frequency analyses did not show any DEHP or paraquat exposure-related effect. However, *LacZ* mutant frequencies were higher in lung of all female and male *Xpc* mice, most likely due to oxygen exposure. The mutational load of these 1 year old mice

(age of the mice after 39 weeks of exposure) is comparable to previous studies with C57BL/6J mice at that age [17].

Since XPC and XPA are both part of NER, the increases in mutational load after DEHP, paraquat and oxygen exposure implicates that the XPC protein has additional functionality outside NER, which appears to be involved in the prevention or the removal of oxidative DNA damage. The fact that mutant frequencies were only affected after 39 weeks of DEHP exposure and not after 12 weeks suggests a slow accumulation of mutations upon oxidative stress in *Xpc* mice. This could be due to either the relatively slow cell division in adult livers or to an additional function of XPC that involves a mechanism which prevents oxidative DNA damage accumulation in a time-related manner.

Using microarray analyses we set out to elucidate the underlying differences between *Xpa* and *Xpc* sensitivity *in vivo* towards mutation accumulation and consequential divergent tumor response. DEHP exposure-related effects [18;34;35] in liver of all three genotypes were apparent, in particular the disturbed regulation of lipid and fatty acid metabolism was distinct.

XPC functionality outside of NER has been implied in base excision repair [6;8;9;28]. In this study, no convincing transcriptional evidence was found implicating supplemental functionality of XPC in base excision repair. However, epigenetic factors, post-translational modifications and protein interactions could be responsible for these previously proposed interactions and effects. Concerning these protein interactions, our gene expression data indicated that Nrf2-target and antioxidant enhancer p62/SQSTM1 was up-regulated in both wild type and *Xpa* mice, but less in *Xpc* mice. The XPC protein holds two binding sites for p62/SQSTM1 interaction. A recent study pointed out that p62/SQSTM1 plays a critical role in an oxidative stress response pathway by its direct interaction with the ubiquitin ligase adaptor Kelch-like ECH-associated protein 1 (KEAP1), resulting in constitutive activation of the transcription factor NRF2 [36]. P62/SQSTM1 contributes to activation of NRF2 target genes in response to oxidative stress through creating a positive feedback loop [37]. Since the XPC protein contains binding sites for interaction with p62/SQSTM1, the loss of XPC could cause a disturbed oxidative DNA damage signaling resulting in a lower antioxidant (glutathione) response. Decreased p62/SQSTM1 transcript and protein levels by siRNA silencing have been correlated to a decrease in glutathione levels [38], which is in line with our current *in vivo* observations.

The divergent glutathione response and related pathways like nitrogen and cysteine metabolism were, despite the substantial DEHP-related gene expression signature and an overall comparable response between the three genotypes, one of the most interesting and distinct differences observed between on the one hand *Xpc* and on the other hand both *Xpa* and wild type. After exposure to DEHP, one expects a sufficient induction of antioxidant defense systems to cope with the increased oxidative stress levels [39-41]. One of the key players in such an antioxidant response is the glutathione metabolism [42-45]. Glutathione scavenges harmful molecules such as electrophiles and reactive oxygen species, thereby inhibiting or preventing DNA damage [46]. At the pathway level, glutathione metabolism and amino acid metabolism involved in this process were indeed significantly up-regulated in both wild type and *Xpa* mice upon long-term DEHP exposure, but these responses were not significantly affected in *Xpc* mice. Additionally, the p62/SQSTM1 gene and a multitude of genes involved in glutathione response were less responsive in *Xpc* [36]. Very recently, glutathione homeostasis was also directly linked to XPC functionality *in vitro*, since *Nrf1* regulates *Xpc* expression and subsequent DNA damage repair through maintaining GSH levels [23]. Moreover, reduced

glutathione levels and a subsequent imbalanced redox status were demonstrated in *Xpc* silenced cells [<sup>10</sup>]. *In vitro*, interplay between NER and glutathione antioxidant response was previously suggested [<sup>24</sup>]. We subsequently attempted to measure glutathione-related biological parameters in the long-term exposed liver samples, but were unfortunately not able to reliably establish a clear difference between the three genotypes using these tissues. This could be explained by either the multiple freeze-thaw cycles the samples underwent prior to these analyses or by the possibility that the differences are only subtle *in vivo* considering the fact that the mutational load also increased slowly over time.

Taken together, our current results and the growing number of data published by others suggest an affected redox status in XPC-deficient mice and cells, which may contribute to the observed increased levels of oxidative DNA damage in our study. Some bulky oxidative DNA lesions might remain unrepaired by a deficient NER in both *Xpc* and *Xpa* cells [<sup>47,48</sup>]. In *Xpc* mice, an insufficient antioxidant response in combination with a possibly affected BER (XPC also contains a binding site for BER protein OGG1) appears to result into an increased sensitivity towards oxidative DNA damage. Our results additionally indicate that this is a slowly accumulating process *in vivo* and has therefore probably not been observed *in vivo* before.

### Conflict of interest

Authors declare there is no conflict of interest.

### Acknowledgements

We thank the Animal Facilities of the Netherlands Vaccine Institute (NVI) and the MicroArray Department Amsterdam for their skillful support. We also thank Prof. Dr. Errol Friedberg for providing us with the *Xpc* mouse model. The work presented here was in part financially supported by NIH/NIEHS (Comparative Mouse Genomics Centers Consortium) Grant 1U01 ES11044 and by STW Grant STW-LGC.6935.

### Supplemental information

Supplementary information is available at the journal's website. Complete raw and normalized microarray data and their MIAME compliant metadata have been deposited at GEO ([www.ncbi.nlm.nih.gov/geo](http://www.ncbi.nlm.nih.gov/geo)) under accession number GSE28296.

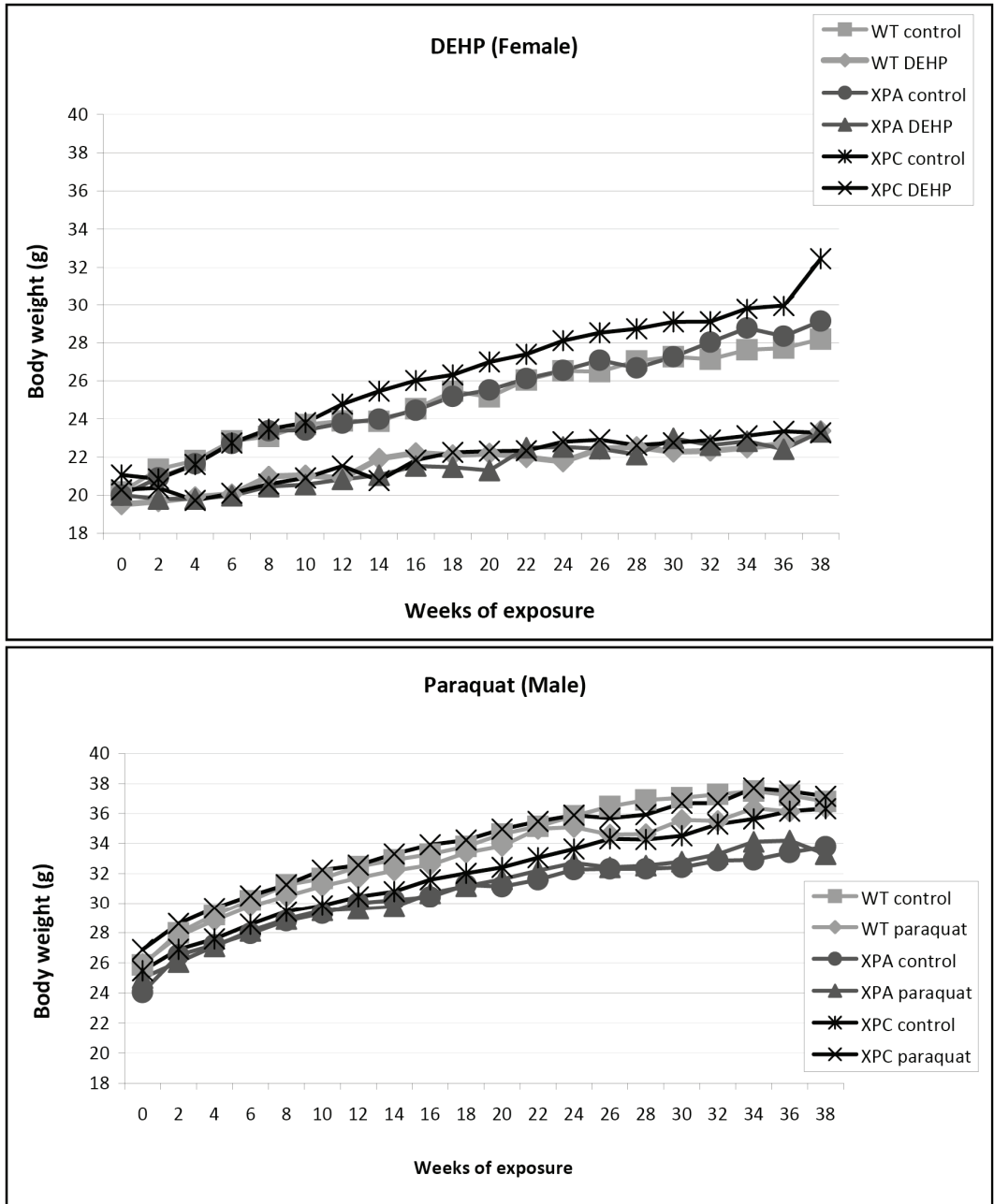
## Reference List

- [1] J.E.Cleaver, E.T.Lam, I.Revet. Disorders of nucleotide excision repair: the genetic and molecular basis of heterogeneity, *Nat.Rev.Genet.*, 10, (2009) 756-768.
- [2] A.Y.Maslov, J.Vijg. Genome instability, cancer and aging, *Biochim.Biophys.Acta*, 1790, (2009) 963-969.
- [3] E.C.Friedberg, G.C.Walker, W.Siede, R.D.Wood, R.A.Schultz, T.Ellenberger. *DNA Repair and Mutagenesis*, ASM Press, 2006.
- [4] M.Dizdaroglu. Base-excision repair of oxidative DNA damage by DNA glycosylases, *Mutat.Res.*, 591, (2005) 45-59.
- [5] B.van Loon, E.Markkanen, U.Hubscher. Oxygen as a friend and enemy: How to combat the mutational potential of 8-oxo-guanine, *DNA Repair (Amst)*, 9, (2010) 604-616.
- [6] S.N.Kassam, A.J.Rainbow. Deficient base excision repair of oxidative DNA damage induced by methylene blue plus visible light in xeroderma pigmentosum group C fibroblasts, *Biochem.Biophys.Res.Comm.*, 359, (2007) 1004-1009.
- [7] Y.Okamoto, P.H.Chou, S.Y.Kim, N.Suzuki, Y.R.Laxmi, K.Okamoto, X.Liu, T.Matsuda, S.Shibutani. Oxidative DNA damage in XPC-knockout and its wild mice treated with equine estrogen, *Chem.Res.Toxicol.*, 21, (2008) 1120-1124.
- [8] M.D'Errico, E.Parlanti, M.Teson, B.M.de Jesus, P.Degan, A.Calcagnile, P.Jaruga, M.Bjoras, M.Crescenzi, A.M.Pedrin, J.M.Egly, G.Zambruno, M.Stefanini, M.Dizdaroglu, E.Dogliotti. New functions of XPC in the protection of human skin cells from oxidative damage, *EMBO J.*, 25, (2006) 4305-4315.
- [9] Y.Shimizu, S.Iwai, F.Hanaoka, K.Sugasawa. Xeroderma pigmentosum group C protein interacts physically and functionally with thymine DNA glycosylase, *EMBO J.*, 22, (2003) 164-173.
- [10] S.Y.Liu, C.Y.Wen, Y.J.Lee, T.C.Lee. XPC silencing sensitizes glioma cells to arsenic trioxide via increased oxidative damage, *Toxicol.Sci.*, 116, (2010) 183-193.
- [11] P.J.Brooks, D.S.Wise, D.A.Berry, J.V.Kosmoski, M.J.Smerdon, R.L.Somers, H.Mackie, A.Y.Spoonde, E.J.Ackerman, K.Coleman, R.E.Tarone, J.H.Robbins. The oxidative DNA lesion 8,5'-(S)-cyclo-2'-deoxyadenosine is repaired by the nucleotide excision repair pathway and blocks gene expression in mammalian cells, *J.Biol.Chem.*, 275, (2000) 22355-22362.
- [12] K.H.Kraemer, M.M.Lee, J.Scotto. DNA repair protects against cutaneous and internal neoplasia: evidence from xeroderma pigmentosum, *Carcinogenesis*, 5, (1984) 511-514.
- [13] K.H.Kraemer, M.M.Lee, J.Scotto. Xeroderma pigmentosum. Cutaneous, ocular, and neurologic abnormalities in 830 published cases, *Arch.Dermatol.*, 123, (1987) 241-250.
- [14] K.H.Kraemer. Sunlight and skin cancer: another link revealed, *Proc.Natl.Acad.Sci.U.S.A*, 94, (1997) 11-14.
- [15] P.C.Hanawalt, J.M.Ford, D.R.Lloyd. Functional characterization of global genomic DNA repair and its implications for cancer, *Mutat.Res.*, 544, (2003) 107-114.
- [16] T.Yasuda, K.Sugasawa, Y.Shimizu, S.Iwai, T.Shioimi, F.Hanaoka. Nucleosomal structure of undamaged DNA regions suppresses the non-specific DNA binding of the XPC complex, *DNA Repair (Amst)*, 4, (2005) 389-395.
- [17] J.P.Melis, S.W.Wijnhoven, R.B.Beems, M.Roodbergen, B.J.van den, H.Moon, E.Friedberg, G.T.van der Horst, J.H.Hoeijmakers, J.Vijg, H.van Steeg. Mouse models for xeroderma pigmentosum group A and group C show divergent cancer phenotypes, *Cancer Res.*, 68, (2008) 1347-1353.
- [18] R.M.David, M.R.Moore, D.C.Finney, D.Guest. Chronic toxicity of di(2-ethylhexyl)phthalate in mice, *Toxicol.Sci.*, 58, (2000) 377-385.
- [19] H.Yamashita, A.Itsuki, M.Kimoto, M.Hiemori, H.Tsuji. Acetate generation in rat liver mitochondria; acetyl-CoA hydrolase activity is demonstrated by 3-ketoacyl-CoA thiolase, *Biochim.Biophys.Acta*, 1761, (2006) 17-23.
- [20] C.C.Willhite. Weight-of-evidence versus strength-of-evidence in toxicologic hazard identification: Di(2-ethylhexyl)phthalate (DEHP), *Toxicology*, 160, (2001) 219-226.

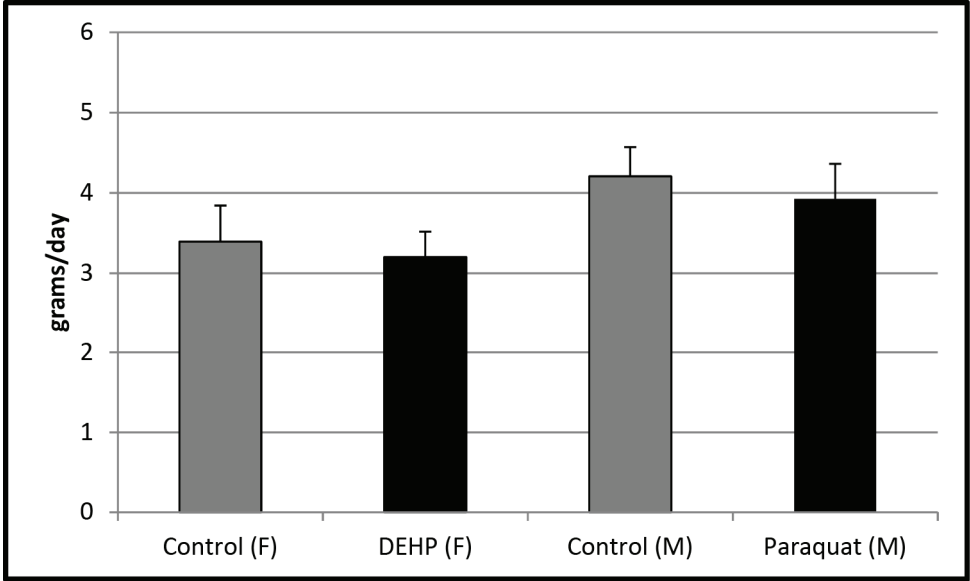
- [21] J.P.Melis, M.Luijten, L.H.Mullenders, H.van Steeg. The role of XPC: implications in cancer and oxidative DNA damage, *Mutat.Res.*, 728, (2011) 107-117.
- [22] L.B.Meira, A.M.Reis, D.L.Cheo, D.Nahari, D.K.Burns, E.C.Friedberg. Cancer predisposition in mutant mice defective in multiple genetic pathways: uncovering important genetic interactions, *Mutat.Res.*, 477, (2001) 51-58.
- [23] W.Han, M.Ming, R.Zhao, J.Pi, C.Wu, Y.Y.He. The Nrf1 CNC-bZIP protein promotes cell survival and nucleotide excision repair through maintaining glutathione homeostasis, *J.Biol.Chem.*, (2012).
- [24] S.A.Langie, A.M.Knaapen, J.M.Houben, F.C.van Kempen, J.P.de Hoon, R.W.Gottschalk, R.W.Godschalk, F.J.van Schooten. The role of glutathione in the regulation of nucleotide excision repair during oxidative stress, *Toxicol.Lett.*, 168, (2007) 302-309.
- [25] R.Abbasi, T.Efferth, C.Kuhmann, T.Opatz, X.Hao, O.Popanda, P.Schmezer. The endoperoxide ascaridol shows strong differential cytotoxicity in nucleotide excision repair-deficient cells, *Toxicol.Appl.Pharmacol.*, 259, (2012) 302-310.
- [26] H.R.Rezvani, R.Rossignol, N.Ali, G.Benard, X.Tang, H.S.Yang, T.Jouary, H.de Verneuil, A.Taieb, A.L.Kim, F.Mazurier. XPC silencing in normal human keratinocytes triggers metabolic alterations through NOX-1 activation-mediated reactive oxygen species, *Biochim.Biophys.Acta*, 1807, (2011) 609-619.
- [27] H.R.Rezvani, A.L.Kim, R.Rossignol, N.Ali, M.Daly, W.Mahfouf, N.Bellance, A.Taieb, H.de Verneuil, F.Mazurier, D.R.Bickers. XPC silencing in normal human keratinocytes triggers metabolic alterations that drive the formation of squamous cell carcinomas, *J.Clin.Invest*, 121, (2011) 195-211.
- [28] Y.Shimizu, Y.Uchimura, N.Dohmae, H.Saitoh, F.Hanaoka, K.Sugasawa. Stimulation of DNA Glycosylase Activities by XPC Protein Complex: Roles of Protein-Protein Interactions, *J.Nucleic Acids*, 2010, (2010).
- [29] M.C.Hollander, R.T.Philburn, A.D.Patterson, S.Velasco-Miguel, E.C.Friedberg, R.I.Linnoila, A.J.Fornace, Jr. Deletion of XPC leads to lung tumors in mice and is associated with early events in human lung carcinogenesis, *Proc.Natl.Acad.Sci.U.S.A.*, 102, (2005) 13200-13205.
- [30] A.Mortensen, M.Bertram, V.Aarup, I.K.Sorensen. Assessment of carcinogenicity of di(2-ethylhexyl)phthalate in a short-term assay using *Xpa*<sup>-/-</sup> and *Xpa*<sup>-/-</sup>*p53*<sup>+/+</sup> mice, *Toxicol.Pathol.*, 30, (2002) 188-199.
- [31] R.S.Sohal, U.T.Brunck. Lipofuscin as an indicator of oxidative stress and aging, *Adv.Exp.Med.Biol.*, 266, (1989) 17-26.
- [32] T.Jung, A.Hohn, T.Grune. Lipofuscin: detection and quantification by microscopic techniques, *Methods Mol.Biol.*, 594, (2010) 173-193.
- [33] M.M.Tiao, T.K.Lin, P.W.Wang, J.B.Chen, C.W.Liou. The role of mitochondria in cholestatic liver injury, *Chang Gung.Med.J.*, 32, (2009) 346-353.
- [34] H.Yamashita, A.Itsuki, M.Kimoto, M.Hiemori, H.Tsuji. Acetate generation in rat liver mitochondria; acetyl-CoA hydrolase activity is demonstrated by 3-ketoacyl-CoA thiolase, *Biochim.Biophys.Acta*, 1761, (2006) 17-23.
- [35] C.C.Willhite. Weight-of-evidence versus strength-of-evidence in toxicologic hazard identification: Di(2-ethylhexyl)phthalate (DEHP), *Toxicology*, 160, (2001) 219-226.
- [36] I.P.Nezis, H.Stenmark. p62 at the Interface of Autophagy, Oxidative Stress Signaling, and Cancer, *Antioxid.Redox.Signal.*, (2012).
- [37] A.Jain, T.Lamark, E.Sjottem, K.B.Larsen, J.A.Awuh, A.Overvatn, M.McMahon, J.D.Hayes, T.Johansen. p62/SQSTM1 is a target gene for transcription factor NRF2 and creates a positive feedback loop by inducing antioxidant response element-driven gene transcription, *J.Biol.Chem.*, 285, (2010) 22576-22591.
- [38] I.M.Copple, A.Lister, A.D.Obeng, N.R.Kitteringham, R.E.Jenkins, R.Layfield, B.J.Foster, C.E.Goldring, B.K.Park. Physical and functional interaction of sequestosome 1 with Keap1 regulates the Keap1-Nrf2 cell defense pathway, *J.Biol.Chem.*, 285, (2010) 16782-16788.
- [39] J.Limon-Pacheco, M.E.Gonsebatt. The role of antioxidants and antioxidant-related enzymes in protective responses to environmentally induced oxidative stress, *Mutat.Res.*, 674, (2009) 137-147.



- [40] W.O.Osburn, T.W.Kensler. Nrf2 signaling: an adaptive response pathway for protection against environmental toxic insults, *Mutat.Res.*, 659, (2008) 31-39.
- [41] J.D.Hayes, L.I.McLellan. Glutathione and glutathione-dependent enzymes represent a co-ordinately regulated defence against oxidative stress, *Free Radic.Res.*, 31, (1999) 273-300.
- [42] K.P.Economopoulos, T.N.Sergentanis. GSTM1, GSTT1, GSTP1, GSTA1 and colorectal cancer risk: a comprehensive meta-analysis, *Eur.J.Cancer*, 46, (2010) 1617-1631.
- [43] K.W.Kang, S.J.Lee, S.G.Kim. Molecular mechanism of nrf2 activation by oxidative stress, *Antioxid.Redox.Signal.*, 7, (2005) 1664-1673.
- [44] K.A.Jung, M.K.Kwak. The Nrf2 system as a potential target for the development of indirect antioxidants, *Molecules.*, 15, (2010) 7266-7291.
- [45] E.Laborde. Glutathione transferases as mediators of signaling pathways involved in cell proliferation and cell death, *Cell Death.Differ.*, 17, (2010) 1373-1380.
- [46] R.Franco, J.A.Cidowski. Apoptosis and glutathione: beyond an antioxidant, *Cell Death.Differ.*, 16, (2009) 1303-1314.
- [47] K.Randerath, E.Randerath, C.V.Smith, J.Chang. Structural origins of bulky oxidative DNA adducts (type II I-compounds) as deduced by oxidation of oligonucleotides of known sequence, *Chem.Res.Toxicol.*, 9, (1996) 247-254.
- [48] Y.Wang. Bulky DNA lesions induced by reactive oxygen species, *Chem.Res.Toxicol.*, 21, (2008) 276-281.
- [49] M.E.Dolle, H.Giese, C.L.Hopkins, H.J.Martus, J.M.Hausdorff, J.Vijg. Rapid accumulation of genome rearrangements in liver but not in brain of old mice, *Nat.Genet.*, 17, (1997) 431-434.
- [50] S.W.Wijnhoven, H.J.Kool, L.H.Mullenders, R.Slater, A.A.van Zeeland, H.Vrieling. DMBA-induced toxic and mutagenic responses vary dramatically between NER-deficient Xpa, Xpc and Csb mice, *Carcinogenesis*, 22, (2001) 1099-1106.
- [51] D.L.Cheo, H.J.Ruven, L.B.Meira, R.E.Hammer, D.K.Burns, N.J.Tappe, A.A.van Zeeland, L.H.Mullenders, E.C.Friedberg. Characterization of defective nucleotide excision repair in XPC mutant mice, *Mutat.Res.*, 374, (1997) 1-9.
- [52] A.de Vries, H.van Steeg. Xpa knockout mice, *Semin.Cancer Biol.*, 7, (1996) 229-240.
- [53] J.L.A.Pennings, Wendy Rodenburg, Sandra Imholz, Maria P.H.Koster, Conny T.M.van Oostrom, Timo M.Breit, Peter C.J.I.Schielen, Annemieke de Vries. Gene Expression Profiling in a Mouse Model Identifies Fetal Liver- and Placenta-Derived Potential Biomarkers for Down Syndrome Screening, *PLoS ONE*, 6, (2011) e18866.



**Supplemental information 1.** Body weight curves. Body weight curves of all three genotypes during either pro-oxidant exposure or control feed.

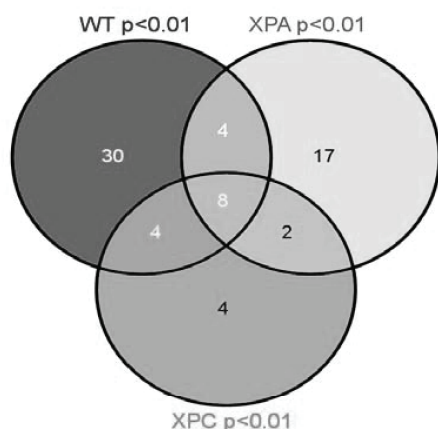


**Supplemental information 2.** Average daily food uptake per mouse per exposure group. Food uptake was monitored in 6 cages per per exposure (2 of each genotype) for 5 weeks. Uptake between the genotypes was comparable for all food types. (F) = female mice, (M) = male mice.

<b>Liver</b>			<b>Lung</b>		
<b>DEHP</b>	WT control vs XPA control	p = 0.2530	<b>DEHP</b>	WT control vs XPA control	p = 0.2663
	WT control vs XPC control	p = 0.1534		WT control vs XPC control	<b>p = 0.0043</b>
	XPA control vs XPC control	p = 0.0426		XPA control vs XPC control	p = 0.0321
	WT dehp vs XPA dehp	p = 0.3589		WT DEHP vs XPA DEHP	p = 0.6722
	WT dehp vs XPC dehp	<b>p = 0.0012</b>		WT DEHP vs XPC DEHP	p = 0.0142
	XPA dehp vs XPC dehp	<b>p = 0.0062</b>		XPA DEHP vs XPC DEHP	p = 0.0743
<b>Liver</b>			<b>Lung</b>		
<b>Paraquat</b>	WT control vs XPA control	p = 0.4666	<b>Paraquat</b>	WT control vs XPA control	p = 0.4944
	WT control vs XPC control	p = 0.7304		WT control vs XPC control	p = 0.2215
	XPA control vs XPC control	p = 0.5755		XPA control vs XPC control	p = 0.0219
	WT paraquat vs XPA paraquat	p = 0.0291		WT Paraquat vs XPA Paraquat	p = 0.2603
	WT Paraquat vs XPC Paraquat	<b>p = 0.0014</b>		WT Paraquat vs XPC Paraquat	p = 0.0479
	XPA Paraquat vs XPC Paraquat	p = 0.0406		XPA Paraquat vs XPC Paraquat	p = 0.1503

**Supplemental information 3.** Additional information to figure 2. All group t-test comparisons, *p*-values after 39 weeks of pro-oxidant exposure. *P*-values < 0.01 are indicated in bold

**Supplemental information 6.** Venn diagram of distribution of all GeneGO pathways generated by top 2278 significant genes and DEGs. Pathways that were considered to be truly regulated (yielded by both the DEGs and the top 2278 genes as Metacore input) were used in the overlap analysis (Venn diagram) shown here. Table 2 shows a selection of the fields of this Venn distribution.



**Common elements in "WTp0.01", "XPAp0.01" and "XPCp0.01" (8 pathways)**

Regulation of lipid metabolism\_PPAR regulation of lipid metabolism  
 Cytoskeleton remodeling\_TGF, WNT and cytoskeletal remodeling  
 Cytoskeleton remodeling\_Cytoskeleton remodeling  
 Fatty Acid Omega Oxidation  
 Cell adhesion\_Plasmin signaling  
 Atherosclerosis\_Role of ZNF202 in regulation of expression of genes involved in Atherosclerosis  
 Blood coagulation\_Blood coagulation  
 Immune response\_Lectin induced complement pathway

**Common elements in "WTp0.01" and "XPAp0.01" (4 pathways)**

Apoptosis and survival\_BAD phosphorylation  
 Glutathione metabolism / Rodent version  
 Cell cycle\_Spindle assembly and chromosome separation  
 Transport\_Aldosterone-mediated regulation of ENaC sodium transport

**Elements only in "XPCp0.01" (4 pathways)**

Cell cycle\_Start of DNA replication in early S phase  
 Development\_Mu-type opioid receptor signaling via Beta-arrestin  
 Nitrogen metabolism/ Rodent version  
 Glycine, serine, cysteine and threonine metabolism

**Common elements in "XPAp0.01" and "XPCp0.01" (2 pathways)**

Immune response\_Classical complement pathway  
 Immune response\_Alternative complement pathway

**Common elements in "WTp0.01" and "XPCp0.01" (4 pathways)**

Cell adhesion\_Chemokines and adhesion  
 Cell cycle\_ESR1 regulation of G1/S transition  
 Immune response\_IL-15 signaling  
 Cell adhesion\_ECM remodeling

**Elements only in "WTp0.01" (30 pathways)**

Development\_Glucocorticoid receptor signaling  
 Glutathione metabolism / Human version  
 Development\_EGFR signaling pathway  
 Development\_IGF-1 receptor signaling  
 Immune response\_HMGB1/RAGE signaling pathway  
 Development\_Gastrin in cell growth and proliferation  
 n-6 Polyunsaturated fatty acid biosynthesis  
 n-3 Polyunsaturated fatty acid biosynthesis  
 Mucin expression in CF via TLRs, EGFR signaling pathways  
 Transcription\_Ligand-dependent activation of the ESR1/SP pathway  
 Transport\_RAN regulation pathway  
 Signal transduction\_PKA signaling  
 Development\_WNT signaling pathway. Part 2  
 Immune response\_Fc epsilon RI pathway  
 PGE2 pathways in cancer  
 Transcription\_Role of Akt in hypoxia induced HIF1 activation  
 Mitochondrial ketone bodies biosynthesis and metabolism  
 Immune response\_HMGB1 release from the cell  
 Transcription\_ChREBP regulation pathway  
 Development\_A3 receptor signaling  
 Immune response\_CD40 signaling  
 Apoptosis and survival\_Lymphotoxin-beta receptor signaling  
 Transport\_Rab-9 regulation pathway  
 Development\_Angiopoietin - Tie2 signaling  
 Apoptosis and survival\_HTR1A signaling  
 Transcription\_Role of heterochromatin protein 1 (HP1) family in transcriptional silencing  
 Regulation of metabolism\_Role of Adiponectin in regulation of metabolism  
 Immune response\_IL-1 signaling pathway  
 Apoptosis and survival\_Beta-2 adrenergic receptor anti-apoptotic action  
 Role of prenatal nicotine exposure in apoptosis and proliferation of pancreatic beta cells

**Elements only in "XPAP0.01":**

Protein folding and maturation\_POMC processing  
 Apoptosis and survival\_TNFR1 signaling pathway  
 G-protein signaling\_RhoA regulation pathway  
 Apoptosis and survival\_Role of IAP-proteins in apoptosis  
 Development\_Inhibition of angiogenesis by PEDF  
 Chemotaxis\_Lipoxin inhibitory action on fMLP-induced neutrophil chemotaxis  
 Development\_MAG-dependent inhibition of neurite outgrowth  
 Regulation of lipid metabolism\_RXR-dependent regulation of lipid metabolism via PPAR, RAR and VDR  
 Oxidative stress\_Angiotensin II-induced production of ROS  
 Regulation of CFTR activity (norm and CF)  
 Apoptosis and survival\_Caspase cascade  
 Blood coagulation\_GPCRs in platelet aggregation  
 Apoptosis and survival\_Role of CDK5 in neuronal death and survival  
 Muscle contraction\_GPCRs in the regulation of smooth muscle tone  
 Cell cycle\_Chromosome condensation in prometaphase  
 Triacylglycerol metabolism p.1  
 Cell cycle\_Role of 14-3-3 proteins in cell cycle regulation



# Chapter 5

# Chapter 5

## Detection of genotoxic and non-genotoxic carcinogens in *Xpc<sup>-/-</sup>p53<sup>+/-</sup>* mice

**Melis JPM**, Speksnijder EN, Kuiper RV, Salvatori DCF, Schaap MM, Maas S, Robinson J, Verhoef A, van Benthem J, Luijten M, van Steeg H.

Detection of genotoxic and non-genotoxic carcinogens in *Xpc<sup>-/-</sup>p53<sup>+/-</sup>* mice

**Submitted, Toxicology and Applied Pharmacology, 2012**

*"In for a round of overexposure, the thing mother nature provides"*

Bottle Up And Explode! - Elliott Smith, 1998



## Abstract

An accurate assessment of the carcinogenic potential of chemicals and pharmaceutical drugs is essential to protect humans and the environment. Therefore, substances are extensively tested before they are marketed to the public. Currently, the rodent two-year bioassay is used to assess the carcinogenic potential of substances. However, over the years it has become clear that this assay yields false positive results and also has several economic and ethical drawbacks including the use of large numbers of animals, the long duration, and the high cost. The need for a suitable alternative assay is therefore high. Previously, we have proposed the *Xpa*\**p53* mouse model as a very suitable alternative to the two-year bioassay. We now show the *Xpc*\**p53* mouse model preserves all the beneficial traits of the *Xpa*\**p53* model for short-term carcinogen identification and can identify both genotoxic and non-genotoxic carcinogens. Moreover, *Xpc*\**p53* mice appear to be more responsive than *Xpa*\**p53* mice towards several genotoxic and non-genotoxic carcinogens. Furthermore, *Xpc*\**p53* mice are far less sensitive than *Xpa*\**p53* mice for the toxic activity of DNA-damaging agents and as such clearly respond in a similar way as wild type mice do. The advantageous traits of the *Xpc*\**p53* model make it a better alternative for *in vivo* carcinogen testing than *Xpa*\**p53*. We propose that *Xpc*\**p53* mice are suited for routine short-term testing of both genotoxic and non-genotoxic carcinogens and as such are a suitable alternative to possibly replace the murine life time cancer bioassay.

## Introduction

Cancer ranks as one of the most frequent causes of death worldwide. Reasons for this high frequency in Western countries can mostly be attributed to lifestyle and environmental factors. Cancer incidence with a prominent hereditary cause is only ~5-10% [1]. Lifestyle and environmental factors are thought to enhance abnormalities in the (epi)genetic material of cells, thereby facilitating the onset of the disease [2]. Carcinogenesis is considered as a multi-step process. Although genomic instability is represented in virtually all tumors, it is believed to be an enabling characteristic that allows evolving populations of premalignant cells to reach the biological hallmarks that eventually characterizes them as cancerous [3,4]. In the current study we show that genomic instability could provide a suitable and alternative tool for prediction and risk assessment of carcinogens *in vivo*.

Cancer risk assessment follows a standard strategy, consisting of a qualitative (hazard identification) and a sub-sequential quantitative (dose-response analysis) component [5]. Several *in vitro* and *in vivo* genotoxicity assays are generally used for hazard identification of large numbers of chemicals for possible carcinogenic properties. A substance is suspected to be carcinogenic based on the results of *in vitro* and *in vivo* genotoxicity tests and a two-year bioassay is performed to obtain hazard confirmation and information with regards to cancer potency (*i.e.* dose-response analysis).

The current test strategy is not without disadvantages, given that genotoxicity tests are not perfect in predicting the carcinogenic potential of chemicals and are not designed to detect non-genotoxic carcinogens and hence can provide false negative results. Misclassification of these non-genotoxic carcinogens can have harmful effects on society and the environment. In addition, the two-year bioassay has several disadvantages. Firstly, the number of animals needed is large, plus the assay is highly time consuming and expensive. Moreover, there is considerable scientific doubt about the reliability of the assay, since too many false positive results have been observed. The need for a good alternative for genotoxic as well as non-genotoxic carcinogenicity testing is therefore high.

In previous studies we have demonstrated that the *Xpa*<sup>-/-</sup>*Trp53*<sup>+/-</sup> mouse model (hereafter named *Xpa*\**p53*) is deficient in both global genome as well as transcription coupled nucleotide excision repair (GG-NER and TC-NER), and is heterozygous for p53 (*Trp53*<sup>+/-</sup>), resulting in an increased cancer susceptibility upon carcinogen exposure as compared to wild type mice [6,7]. The *Xpa*\**p53* mice have a relatively low spontaneous tumor background and, when exposed to carcinogens, exhibit tumor types that are similar to those found in wild type (WT) C57BL/6J mice [6,7]. This increased susceptibility can be beneficial in carcinogenicity testing since the number of animals as well as the time of exposure can be decreased to accurately identify carcinogens. A concomitant advantage of the *Xpa*\**p53* model is its responsiveness to several non-genotoxic carcinogens [6]. A disadvantage of the *Xpa*\**p53* model is, however, its enhanced sensitivity towards toxicity, especially when induced by genotoxic carcinogens, making more quantitative (potency) comparisons unrelated to what is observed in wild type animals. Concentrations used for carcinogenicity testing in wild type mice cannot always be used in *Xpa*\**p53* mice, since these doses might be toxic ([8], unpublished results).

We and others have shown that, although *Xpa* and *Xpc*-deficient mice have many similarities in terms of their general cancer proneness, they exhibit a few striking differences. *Xpc* mice are less sensitive, as compared to *Xpa* mice, to the toxic effects of (mostly) genotoxic compounds [9,10]. It was suggested [9-12] that this difference in sensitivity is caused by the defect that *Xpa* mice have in the TC-NER

pathway. In this aspect *Xpa* mice resemble the NER-deficient *Csb* mice, which are also hypersensitive to genotoxigants (e.g. UV radiation) and have a defective TC-NER but a proficient GG-NER (this in contrast to *Xpa* mice). Given the fact that *Xpc* mice have an active TC-NER, and are therefore supposed to be less sensitive to genotoxic agents, we set out to test the use of the *Xpc*<sup>-/-</sup>\**Trp53*<sup>-/-</sup> mouse model (hereafter named *Xpc*\**p53*) for carcinogenicity testing. Above that, we tested whether *Xpc*\**p53* mice display the same response to non-genotoxic carcinogens as the *Xpa*\**p53* mouse model does.

## Material & Methods

### Mice

The generation of the NER-deficient *Xpc* and *Xpa* mouse models has been described previously [13;14]. *Xpc* and *Xpa* mice were crossed with *Trp53*<sup>-/-</sup> mice [15] to generate both *Xpc*\**p53* (used in this study for carcinogenicity studies and generation of primary hepatocytes) and *Xpa*\**p53* mice (used in this study to generate primary hepatocytes). All mouse models were generated in a pure C57BL/6J genetic background. Genotyping of the different mice was performed via allele-specific PCR analysis for altered genes as been described previously [9;15;16].

### Chemicals

2-Acetylaminofluorene (2-AAF, CAS #53-96-3), Diethylstilbestrol (DES, CAS #56-53-1), Di(2-ethylhexyl)phthalate (DEHP, CAS #117-81-7), Wyeth-14.643 (WY, CAS #50892-23-4), Phenacetin (Phe, CAS #62-44-2), Aflatoxin B1 (AFB1, CAS #1162-65-8) and Mitomycin C (MMC, CAS #50-07-7) were purchased from Sigma (St. Louis, MO, USA). Cyclosporin A (CsA, CAS #59865-13-3) was kindly provided by Novartis Pharma AG (Basel, Switzerland).

### Experimental setup

Short-term carcinogenicity studies were performed as follows: wild type and *Xpc*\**p53* mice (8-10 weeks old) were exposed through feed (Altromin, Lage, Germany) for 39 weeks to either a genotoxic carcinogen (GTXC), a non-genotoxic carcinogen (NGTXC) or control diet. After 39 weeks of exposure all animals were fed control diet for another 2 weeks. Both female and male mice (*n*=20 per exposure group, *n*=40 per untreated control group) were used. Table 1 gives an overview of the experimental setup of the (exposure) studies. The doses used were based on previous dose-range finding studies obtained with wild type or *Xpa* and *Xpa*\**p53* mice [6;17-19]. *Xpa*\**p53* data to compare with the studies in this manuscript were derived from previous short-term carcinogenicity studies [6;7].

The health status of the mice was monitored daily from weaning. Animals were weighed biweekly (Average body weight curves are depicted in Figure 1). Average weekly food uptake per cage was measured for the duration of the experiment for all cages. Weekly uptake, averaged per mice, is depicted in Supplemental Figure 1. During the entire duration of the experiment, animals were kept in the same stringently controlled (specific pathogen-free, spf) environment, fed *ad libitum*, and kept under a normal day/night rhythm (12hr/12hr). The microbiological status of the cohorts was monitored every 3 months. Animals were removed from the study when found moribund or dead.

Autopsy was performed on animals of all groups; several tissues were isolated from each animal and stored for further histopathology analysis (see below). The experimental setup of the studies was examined and approved by the institute's Ethical Committee on Animal Experimentation, in accordance with national and European legislation.

### **Pathology**

Based on previous *Xpa\*<sup>p53</sup>* exposure studies, using the carcinogens as shown in Table 1, target tissues were selected based on the carcinogen in question and observed gross abnormalities during necropsy. Tissue samples (liver, kidney, spleen, urinary bladder, thymus, femur, pituitary, mesenteric lymph nodes, cervix and those tissues showing gross lesions) from each animal were preserved in a neutral aqueous phosphate-buffered 4% solution of formaldehyde solution. Tissues selected for detailed microscopic examination were processed, embedded in paraffin wax, sectioned at 4µm and stained with haematoxylin and eosin.

### **Isolation and culture of primary mouse hepatocytes**

Primary mouse hepatocytes were isolated from 8-10 weeks old male mice (C57/BL6, *Xpa\*<sup>p53</sup>* and *Xpc\*<sup>p53</sup>*) by a modified two-step collagenase perfusion technique (collagenase type IV, Sigma, St. Louis, MO, USA), as previously described [20]. Hepatocyte suspensions with at least 80% viability, determined by trypan blue exclusion, were seeded to 6-wells plates coated with 1 mg/ml neutralized collagen type I (BD Biosciences, Breda, The Netherlands) at  $1.3 \times 10^6$  cells per well. After two hours of incubation in a humidified atmosphere at 37°C and 5% CO<sub>2</sub>, unattached hepatocytes were removed by washing and a sandwich configuration was achieved by adding a second layer of neutralized collagen to the cells. After one hour, serum-free DMEM (Invitrogen, Bleiswijk, The Netherlands) was added, containing 2% penicillin/streptomycin (Invitrogen), 7 ng/ml glucagon (Sigma), 7.5 µg/ml hydrocortisone (Sigma) and 0.5 U/ml insulin (from bovine pancreas, Sigma). Cells were kept in serum-free medium and the culture medium was changed daily until exposures were performed.

### **Cytotoxicity analyses**

Cytotoxicity analyses were performed for Aflatoxin B1, Mitomycin C, Wyeth-14,643 and Cyclosporin A. Forty-six hours after isolation, hepatocytes were exposed for 24 hours to the substances dissolved in DMSO (AFB1, CsA and Wy) or PBS (MMC) at multiple doses (Figure 3). Final DMSO or PBS concentrations in medium were 0.5 % (v/v) in all exposure studies, including the vehicle controls. After 24 h cells were given fresh serum-free medium and after another 48 h (t = 72h) the cytotoxicity of all substances was tested, using the MTT reduction method [21], with some modifications. In short, cultures were incubated for one hour with 0.5 mg/ml MTT (3-(4,5-dimethylthiazol-2-yl)-2,5-diphenyltetrazolium bromide, Invitrogen). The medium was removed and the formazan crystals formed were solubilized in DMSO. Absorbance was measured in triplicate at 570 nm and a reference wavelength at 670 nm. Vehicle-treated cells were used as a solvent control and were taken as a 100% cell viability control. Dose-response calculations were done using PROAST software ([www.rivm.nl/proast](http://www.rivm.nl/proast)) [22].

## Statistical analyses

Statistical analyses on the (Kaplan-Meier plotted) survival curves were performed in PASW Statistics 17.0.2 (SPSS) using Log Rank (Mantel-Cox) analyses. Statistical analyses on the incidence of tumor bearing animals and preneoplastic lesions were performed using a one-sided Fisher's Exact test.

## Results

### *Divergent survival dynamics of wild type and *Xpc\*<sup>p53</sup>* mice after GTXC and NGTXC exposure*

Short-term (39 weeks) exposures studies with several human and rodent carcinogens (Table 1) were performed. We tested a range of different compounds, either with a genotoxic or non-genotoxic mode of action and with different carcinogenic potencies. In addition, untreated cohorts (male and female mice) were used as controls. Body weight dynamics of wild type and *Xpc\*<sup>p53</sup>* mice were generally comparable (Figure 1). Exposure to WY induced a clear effect on body weight in both genotypes. All Wyeth-exposed mice (only females were used in this study) exhibited a body weight reduction from the start of exposure and maintained a very low body weight throughout the study. The decrease in body weight coincides with the decreased food uptake that was measured during the Wyeth exposure (Supplemental Figure 1). Exposure to 2-AAF resulted in lower body weights of *Xpc\*<sup>p53</sup>* mice compared to wild type animals. This effect is accentuated near the end of the exposure due to intercurrent loss of mice (especially males). Food uptake of 2-AAF on average of the *Xpc\*<sup>p53</sup>* male mice was a little lower than the wild type males, which could have contributed to the slight divergence in body weight between the genotypes (Supplemental information 1).

Exposure	Dose	GTXC/NGTXC	Sex
Control	0	-	F + M
2-Acetylaminofluorene (2-AAF)	300 ppm	GTXC (human)	F + M
Phenacetin (Phe)	7500 ppm	GTXC (human)	M
Cyclosporin A (CsA)	500 ppm	NGTXC (human)	M
Diethylstilbestrol (DES)	1.5 ppm	NGTXC (human)	F
Wyeth-14,643 (WY)	250 ppm	NGTXC (rodent)	F
Di(2-ethylhexyl)phthalate (DEHP)	6000 ppm	NGTXC (rodent)	F

**Table 1.** Experimental setup. For all exposures both wild type and *Xpc\*<sup>p53</sup>* mice were used. GTXC = genotoxic carcinogen, NGTXC = non-genotoxic carcinogen

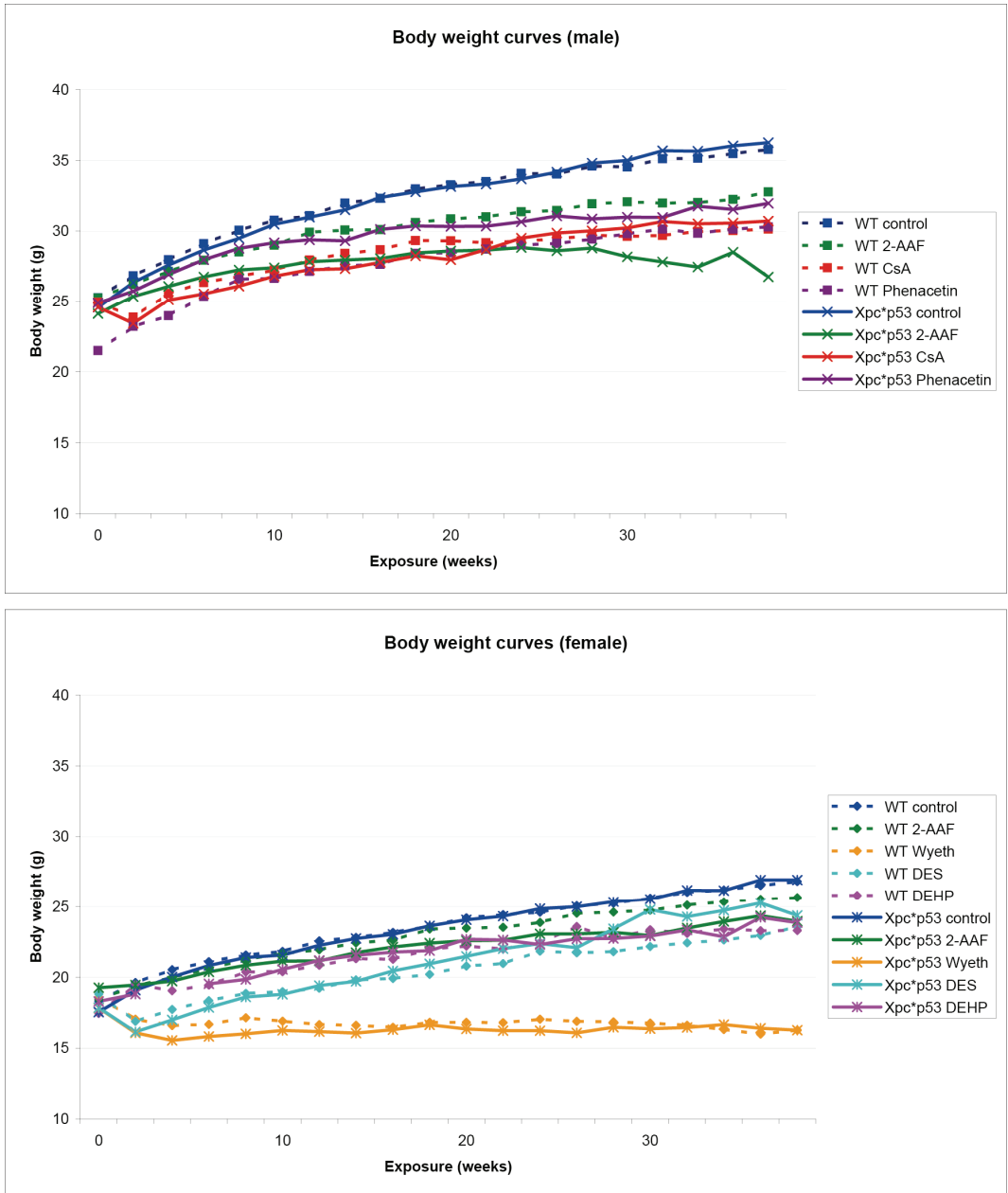


**Figure 1.** Body weight curves male (A) and female (B) mice. Body weight curves of wild type and *Xpc\**p53** (male and female) mice during 39 week exposure to genotoxic or non-genotoxic carcinogens mixed through feed. Curves depict average absolute body weights.

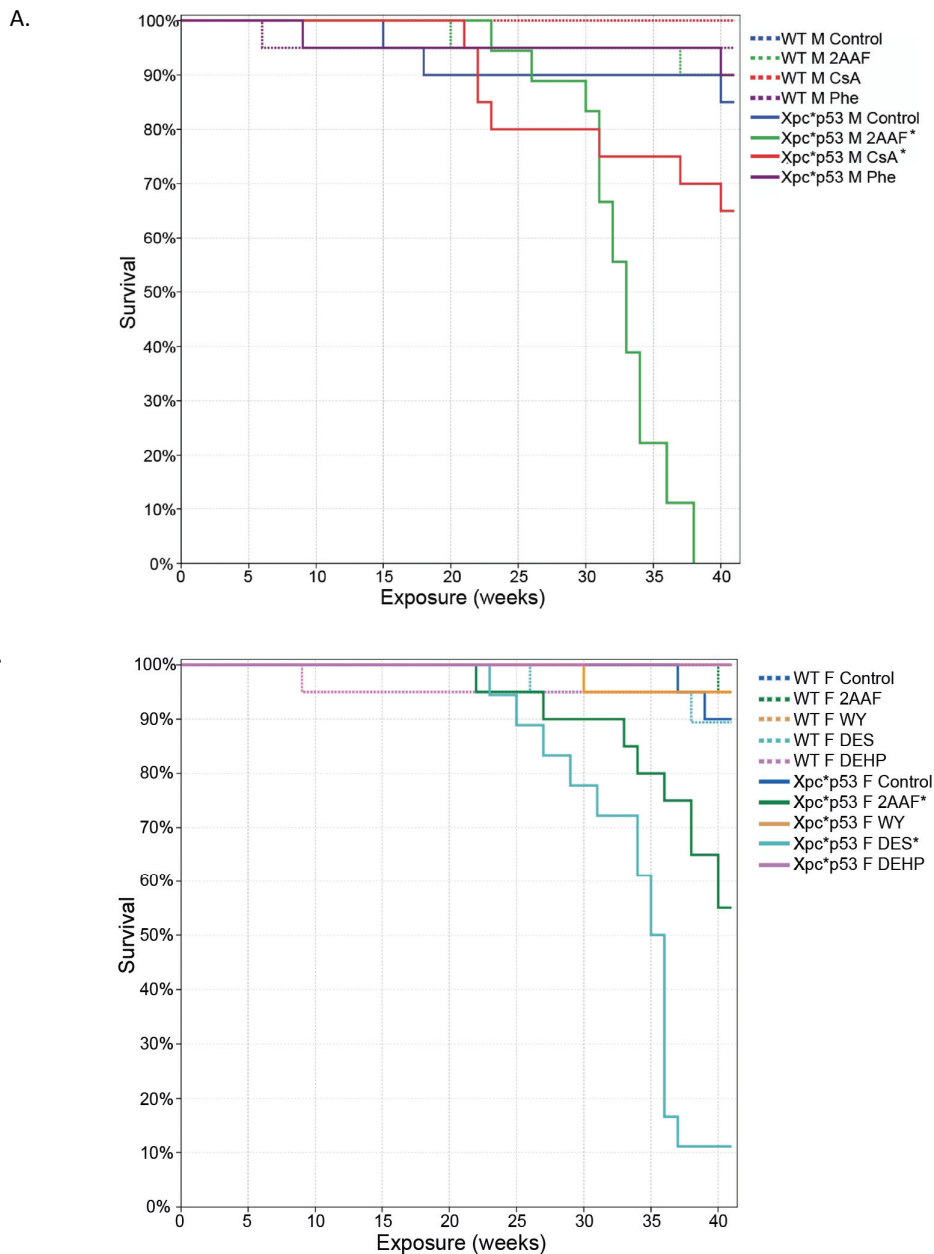


**Figure 2.** Survival curves of wild type and *Xpc*\**p53* male (A) and female (B) mice after short-term carcinogen exposure. Mice of 8-10 weeks old were exposed to genotoxic (2-AAF, Phe) and non-genotoxic (CsA, DES, WY, DEHP) carcinogens for 39 weeks, followed by a 2-week recovery period (see Table 1 for details).

\* =  $p < 0.05$  compared to untreated group of same genotype.

The survival curves are depicted in Figure 2. Only a minor, non-significant ( $p < 0.05$ ) reduction in survival was observed in untreated *Xpc\*<sup>p53</sup>* mice compared to the untreated wild type mice, indicating that wild type and *Xpc\*<sup>p53</sup>* mice show similar spontaneous survival up to this age. Results demonstrated a clear and significant effect of exposure on survival of the *Xpc\*<sup>p53</sup>* mice for the strong genotoxic agent 2-AAF ( $p < 0.05$ ); none of the male mice survived the 39 week duration of the exposure and had to be sacrificed intercurrently. Upon 2-AAF exposure, female *Xpc\*<sup>p53</sup>* mice showed a less dramatic decrease in survival, but still 45% (9/20) did not survive the full 39 weeks of exposure ( $p < 0.05$ ). In contrast, only 10% (2/20,  $p > 0.05$ ) of the wild type male mice and 5% (1/20,  $p > 0.05$ ) of the females did not survive the 39 weeks of 2-AAF exposure. The human non-genotoxic carcinogen CsA caused a decrease in survival of the male *Xpc\*<sup>p53</sup>* mice only (35%, 7/20,  $p < 0.05$ ); all wild type males survived the full exposure duration. Short-term exposure to the human non-genotoxic carcinogen DES induced a small reduction (10%, 2/20,  $p > 0.05$ ) in survival of wild type female mice, while the survival of the *Xpc\*<sup>p53</sup>* females was dramatically decreased (89%, 17/19,  $p < 0.05$ ). The low potent genotoxic carcinogen Phe and rodent non-genotoxic carcinogens DEHP and WY had no or only a slight (non-significant,  $p > 0.05$ ) effect on survival of both wild type and *Xpc\*<sup>p53</sup>* mice.

### ***Increased cancer response in *Xpc\*<sup>p53</sup>* mice after GTXC and NGTXC exposure***

Comprehensive pathological analyses were performed on all known target tissues and all gross lesions of all wild type and *Xpc\*<sup>p53</sup>* mice to assess possible tumor development due to exposures. Results of these analyses are shown in Table 2A (males) and 2B (females). *Xpc\*<sup>p53</sup>* mice developed neoplastic disease, identifying several of the genotoxic and non-genotoxic carcinogens tested here, after 39 weeks of exposure. Incidences of neoplastic lesions upon 2-AAF, CsA and DES exposure were highly increased ( $p < 0.001$ ) when compared to their untreated controls. The potent genotoxicant 2-AAF resulted in a 100% and 75% tumor incidence in *Xpc\*<sup>p53</sup>* male and female mice respectively ( $p < 0.001$ ). Not only genotoxic carcinogen exposure caused elevated tumor incidences, also the non-genotoxic carcinogens CsA and DES induced tumors in very high percentages of *Xpc\*<sup>p53</sup>* mice (60% and 72% respectively), this in contrast to wild type mice (10% and 15%, respectively). Wild type mice did not reach significant levels ( $p > 0.001$ ) of tumor incidence upon 2-AAF, CsA or DES exposure. The tumor incidence for WY was too low to reach significant levels in both genotypes. However, a significant ( $p < 0.001$ ) increase in preneoplastic lesions (e.g. hyperplastic or eosinophilic foci of cellular alteration) was found in livers of *Xpc\*<sup>p53</sup>* mice, while this was not the case in wild type mice. Finally, the duration and doses used for phenacetin and DEHP appeared to be insufficient to significantly induce a tumor response in both wild type and *Xpc\*<sup>p53</sup>*, which is also in line with our previous short-term carcinogenicity studies using wild type and *Xpc\*<sup>p53</sup>* mice.



## A.

Exposure	Wild type				Xpc*p53			
	Untreated	2-AAF	Phe	CsA	Untreated	2-AAF	Phe	CsA
Total no. mice	40	20	20	20	40	18	20	20
TBA (%)	1 (3%)	7 (35%)	0 (0%)	2 (10%)	5 (13%)	18 (100%*)	0 (0%)	12 (60%*)
<b>Liver</b>	<b>1 (3%)</b>	<b>4 (20%)</b>	<b>0</b>	<b>0</b>	<b>0</b>	<b>3 (15%)</b>	<b>0</b>	<b>0</b>
hep cell adenoma	1	3	-	-	-	-	-	-
hep cell carcinoma	-	1	-	-	-	-	-	-
cholangioma	-	-	-	-	-	3	-	-
preneoplastic FCA	-	1	-	-	-	-	-	-
<b>Urinary Bladder</b>	<b>0</b>	<b>1 (5%)</b>	<b>0</b>	<b>0</b>	<b>0</b>	<b>18 (100%)</b>	<b>0</b>	<b>0</b>
papilloma	-	-	-	-	-	1	-	-
carcinoma	-	1	-	-	-	16	-	-
fibrosarcoma	-	-	-	-	-	1	-	-
preneoplastic FCA	2	9*	-	-	2	-	-	-
<b>Hematopoietic</b>	<b>0</b>	<b>2 (10%)</b>	<b>0</b>	<b>1 (5%)</b>	<b>5 (13%)</b>	<b>4 (20%)</b>	<b>0</b>	<b>12 (60%)</b>
lymphoma	-	2	-	1	4	3	-	9
histiocytic sarcoma	-	-	-	-	1	1	-	3
leukemia	-	-	-	-	1	-	-	1
preneoplastic FCA	-	-	-	18*	2	-	-	17*
<b>Other</b>	<b>0</b>	<b>0</b>	<b>0</b>	<b>1 (5%)</b>	<b>0</b>	<b>0</b>	<b>0</b>	<b>0</b>
hemangioma	-	-	-	1	-	-	-	-

## B.

Exposure	Wild type					Xpc*p53				
	Untreated	2-AAF	WY	DES	DEHP	Untreated	2-AAF	WY	DES	DEHP
Total no. mice	40	20	20	20	20	40	20	20	18	19
TBA (%)	0 (0%)	1 (5%)	4 (20%)	3 (15%)	3 (15%)	5 (13%)	15 (75%*)	5 (25%)	13 (72%*)	0 (0%)
<b>Liver</b>	<b>0</b>	<b>0</b>	<b>4 (20%)</b>	<b>0</b>	<b>0</b>	<b>3 (8%)</b>	<b>13 (65%)</b>	<b>5 (25%)</b>	<b>1 (6%)</b>	<b>0</b>
hep cell adenoma	-	-	4	-	-	1	10	5	-	-
hep cell carcinoma	-	-	-	-	-	-	3	-	1	-
cholangioma	-	-	-	-	-	2	-	-	1	-
preneoplastic FCA	-	2	4	-	-	-	2	10*	-	-
<b>Urinary Bladder</b>	<b>0</b>	<b>0</b>	<b>0</b>	<b>0</b>	<b>0</b>	<b>0</b>	<b>0</b>	<b>0</b>	<b>0</b>	<b>0</b>
papilloma	-	-	-	-	-	-	-	-	-	-
carcinoma	-	-	-	-	-	-	-	-	-	-
fibrosarcoma	-	-	-	-	-	-	-	-	-	-
preneoplastic FCA	3	3	-	-	-	2	2	-	-	-
<b>Hematopoietic</b>	<b>0</b>	<b>1 (5%)</b>	<b>0</b>	<b>2 (10%)</b>	<b>3 (15%)</b>	<b>2 (5%)</b>	<b>4 (20%)</b>	<b>0</b>	<b>4 (22%)</b>	<b>0</b>
lymphoma	-	1	-	2	3	2	3	-	4	-
histiocytic sarcoma	-	-	-	-	-	-	-	-	-	-
leukemia	-	-	-	-	-	-	1	-	-	-
preneoplastic FCA	-	-	-	-	-	-	-	-	-	-
<b>Bone</b>	<b>0</b>	<b>0</b>	<b>0</b>	<b>1 (5%)</b>	<b>0</b>	<b>0</b>	<b>0</b>	<b>0</b>	<b>9 (50%)</b>	<b>0</b>
osteosarcoma	-	-	-	-	-	-	-	-	6	-
histiocytic sarcoma	-	-	-	-	-	-	-	-	2	-
bone marrow lymphoma	-	-	-	1	-	-	-	-	1	-
<b>Pituitary</b>	<b>0</b>	<b>0</b>	<b>0</b>	<b>0</b>	<b>0</b>	<b>0</b>	<b>0</b>	<b>0</b>	<b>2 (11%)</b>	<b>0</b>
adenoma	-	-	-	-	-	-	-	-	2	-
<b>Other</b>	<b>0</b>	<b>0</b>	<b>0</b>	<b>0</b>	<b>0</b>	<b>1 (3%)</b>	<b>2 (10%)</b>	<b>0</b>	<b>0</b>	<b>0</b>
osteosarcoma	-	-	-	-	-	1	2	-	-	-

**Table 2.** Neoplastic and preneoplastic lesions after carcinogen exposure in *Xpc\**p53** and wild type male (A) and female (B) mice. Summarized neoplastic and preneoplastic findings of short-term carcinogenicity studies in wild type and *Xpc\**p53** mice. The total number of animals per exposure group, plus the number and percentage of tumor bearing animals (TBA) are shown in the upper part (grey) of the table. Some tumor bearing animals had more than one tumor. Underneath, specific tumor incidences per organ are depicted (grey rows). Tumor types and total number of preneoplastic FCA (foci of cellular alteration) are specified per organ at the bottom of each segment (white rows). \* =  $p \leq 0.001$  treated group versus corresponding controls (Fisher Exact test, one sided).

***Divergent non-neoplastic responses after GTXC exposure between *Xpc\*<sup>p53</sup>* and wild type mice***

Besides divergence in (pre-)neoplastic lesions between wild type and *Xpc\*<sup>p53</sup>* mice, incidences of several non-neoplastic lesions differed between the two genotypes (Table 3). 2-AAF exposure, for example, induced a marked increase in hydronephrosis incidence in *Xpc\*<sup>p53</sup>* male and female mice and not in wild type male or female mice. Similarly, a striking difference was observed after phenacetin exposure, causing increased hypertrophy and eosinophilia in liver, as well as pronounced tubular anisokaryosis in the kidney, a known target tissue of phenacetin. Here, *Xpc\*<sup>p53</sup>* mice displayed a large increase for these types of lesions, while this response is absent in wild type mice. In general, the non-neoplastic lesions induced by exposure to genotoxic carcinogens were more severe in *Xpc\*<sup>p53</sup>* mice than in wild type mice, while most non-neoplastic lesions after NGTX carcinogen exposure were of a comparable degree in both genotypes.

Increased incidence of hydronephrosis, for instance, was also observed after DEHP and DES exposure, but at similar incidences in both genotypes. Although in a progressed stage this is a harmful lesion, in the present study no clinical effects were observed. Several non-neoplastic lesions confirmed the compound exposures, like for example the increase in periarteriolar lymphocyte sheath (PALS) depletion in spleen and Kupffer cell activation in liver upon CsA exposure. CsA is known to interfere with normal immune surveillance [19]. Hyperostosis and fibrous osseous lesions are classical findings related to DES exposure [17] and are considered predictive of the bone tumor induction exhibited in this and other studies. The increase of lipofuscin accumulation upon DEHP exposure is also a classical response [23], which can be explained by the enhanced levels of oxidative stress caused by DEHP exposure and subsequent biotransformation.

Carcinogen	Tissue	Sexe	Observation	WT	XpcP53
2-AAF	Liver	M	Hypertrophy and eosinophilia	=	+++++
		M	Kupffer cell activation	=	++++
	Kidney	F	Hydronephrosis	=	+
		M	Hydronephrosis	=	+++
		F	Tubular anisokaryosis	-	++
Phe	Liver	M	Lipofuscin	+++	+++
		M	Hypertrophy and eosinophilia	+	+++++
	Kidney	M	Tubular anisokaryosis	=	++++
CsA	Liver	M	Kupffer cell activation	++	+++
		M	Oval cell proliferation	+	+
	Spleen	M	Pals depletion/expansion	+++++	++++
		M	Lympholysis	+++	=
	Mesenterial lymph nodes	M	Lympholysis	-	---
	Thymus	M	Cortical apoptosis	+	=
DES	Liver	F	Anisokaryosis	-	-
		F	Oval cell proliferation	+	+++
		F	Lymphohistiocytic aggregates	--	---
	Kidney	F	Hydronephrosis	++	+++
	Femur	F	Fibrous osseous lesions	+++	+++++
		F	Hyperostosis	++++	+++++
	Uterus	F	Stromal collagen deposistion	+++++	=
		F	Stromal hyperplasia	+++++	+
		F	Atrophic uterus	+++	+++++
	Pituitary	F	Pars distalis degeneration	++	+
		F	Angiectasis	+++	++
WY	Liver	F	Anisokaryosis	-	-
		F	Pigmented macrophages	+++++	+++++
		F	Oval cell proliferation	++++	+++++
DEHP	Liver	F	Lipofuscin	+++	+++
	Kidney	F	Hydronephrosis	+++++	+++++

**Table 3.** Overview of most notable changes in non-neoplastic lesion incidence or severity upon carcinogen exposure in wild type and *Xpc\*<sup>p53</sup>* mice, compared to the untreated mice within its own genotype. An increase or decrease in lesion incidence or severity is scored ranging from minor (+ or -) to severe (+++++ or - - - -) respectively. No change observed (=).

### ***Divergent genotoxic response between primary hepatocytes of *Xpa\*<sup>p53</sup>* and *Xpc\*<sup>p53</sup>* mice***

Previous studies showed that genotoxic substances are more toxic to *Xpa*-deficient mice than *Xpc* mice [9]. Since the doses used in the present study were based on previous dose range finding studies with *Xpa* or *Xpa\*<sup>p53</sup>* mice, some of the substances tested in our current study with *Xpc\*<sup>p53</sup>* mice could possibly have been dosed higher. For the assessment of carcinogenic risk it would be beneficial if

the higher (but tolerated) dosages used for wild type mice can also be used in the alternative testing model, without inducing a cytotoxic response. As a first step to compare toxicity between the genotypes, we tested cytotoxicity dynamics upon exposure to several carcinogens in primary mouse hepatocytes of all three genotypes. For this purpose we used the colorimetric MTT assay (Figure 3) and tested cell survival upon exposure to several carcinogens. We tested two non-genotoxic carcinogens that were also used in our *in vivo* studies; CsA and WY. Mitomycin C and Aflatoxin B1 were selected as GTX carcinogens, since the solubility of 2-AAF is very poor and phenacetin is a very weak genotoxic compound. Results (see Fig 3, E-H) indicated that *Xpc\*<sup>p53</sup>* primary hepatocytes follow the cytotoxicity dynamics of wild type cells. Hepatocytes isolated from these two genotypes are equally tolerant to high doses of the genotoxic carcinogens tested, whereas on average, *Xpa\*<sup>p53</sup>* hepatocytes are approximately threefold more sensitive (compare Fig 3A, B with Fig 3E, F). All three genotypes tested showed a comparable response to the non-genotoxic carcinogens WY and CsA is comparable between all three genotypes tested (see Fig 3C, D, G, H).

## Discussion

Society would benefit from a more accurate, speedier, less expensive alternative model for carcinogenicity testing that also addresses the three R's of Russell and Burch. Ideally, such a test system would combine broad applicability with high prediction accuracy for the human situation. To achieve this full cell, organ and systemic functioning (*e.g.* functional biotransformation, immune response and signal transduction) is preferred, if not required. Secondly, the model should be suited to test all substances in a relevant dosage, preferably mimicking human exposure routes (*e.g.* solid, solved or volatile substances that are administrated orally, by inhalation or contact).

We previously demonstrated that the *Xpa\*<sup>p53</sup>* mouse model can predict carcinogens with both genotoxic and non-genotoxic modes of action after only a 39 weeks of exposure. *Xpa\*<sup>p53</sup>* mice, however, suffer from enhanced toxicity when exposed to, in particular, genotoxic carcinogens, making them less attractive to use in quantitative cancer risk assessment. Therefore, we tested whether the *Xpc\*<sup>p53</sup>* mouse model is a more suitable model.

Whilst covering the abovementioned preferable traits of an alternative carcinogenicity test system, our studies showed promising results. The *Xpc\*<sup>p53</sup>* mouse model not only responded to genotoxic, but also to non-genotoxic carcinogens. In contrast to wild type mice, a very strong and significant tumor response was observed for the genotoxicant 2-AAF and the non-genotoxic human carcinogens CsA and DES in *Xpc\*<sup>p53</sup>* mice. Unexposed *Xpc\*<sup>p53</sup>* mice had a low spontaneous tumor incidence (13%), which is comparable to the low incidence of 11% previously found in the *Xpa\*<sup>p53</sup>* mouse model in a 39-week exposure setting [6]. Exposure to 2-AAF resulted in a strong increase in tumor bearing animals compared to the *Xpa\*<sup>p53</sup>* model (100% versus 53% respectively in male mice, 75% versus 60% in female mice) [6]. A large portion of the *Xpc\*<sup>p53</sup>* mice (100% of the male mice, 45% of the female mice) did not survive the 39 weeks of 2-AAF exposure. These animals died from life-threatening tumors, which occur apparently at lower frequencies in 2-AAF-treated *Xpa\*<sup>p53</sup>* mice [24].

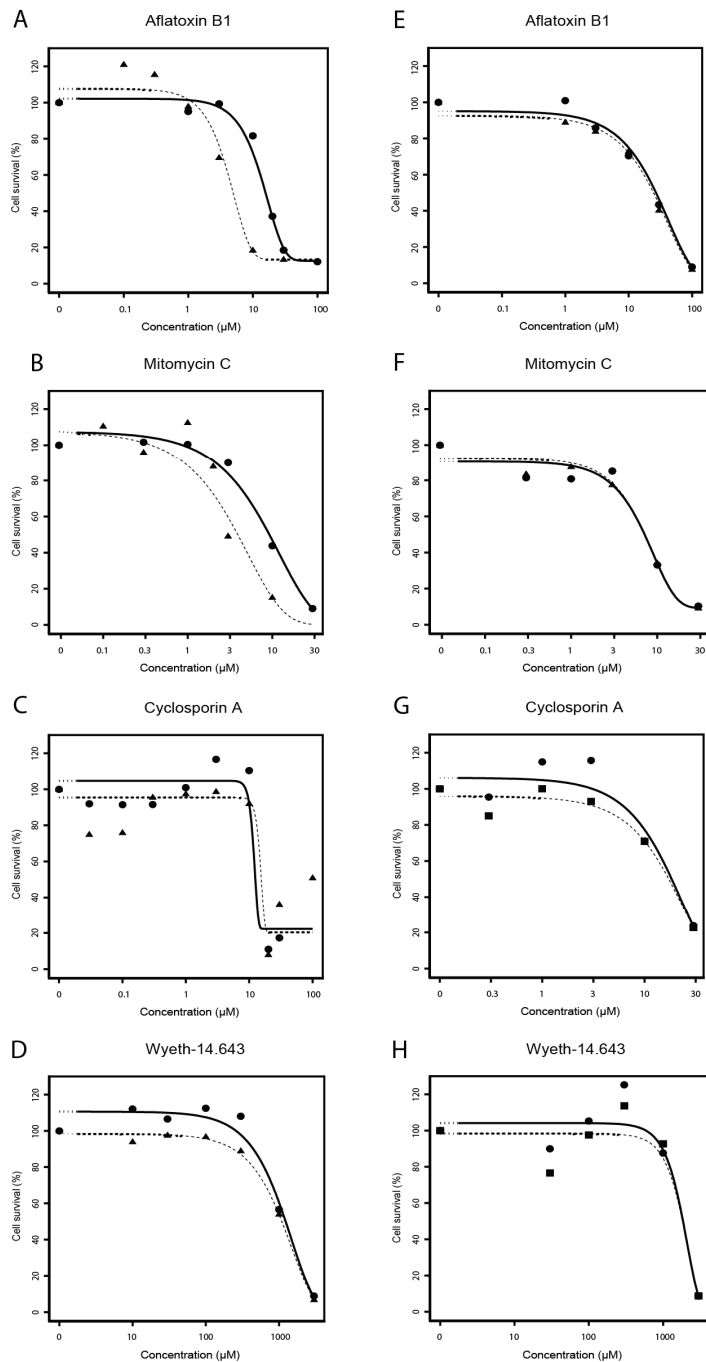


**Figure 3.** Cytotoxicity (MTT) dynamics of primary hepatocytes upon exposure to a dose-range of genotoxic (AFB1 and MMC) and non-genotoxic (CsA and WY) carcinogens. Panel A-D show the response of exposed wild type ( $\bullet$ ) versus *Xpa\*<sup>p53</sup>* ( $\blacktriangle$ ) cells. Panel E-H show the response of exposed wild type ( $\bullet$ ) versus *Xpc\*<sup>p53</sup>* ( $\blacksquare$ ) cells.

Exposure to DES in *Xpc*\**p53* mice also resulted in an increase in tumor induction compared to *Xpa*\**p53* and wild type mice (72% versus 47% versus 15% respectively) [6]. Other alternative *in vivo* models, like the Tg.AC and the neonatal models for carcinogenicity testing, did not identify this substance as a carcinogen [25;26]. The *p53*<sup>+/-</sup> mouse model did also identify CsA and DES as a carcinogen, which indicates the heterozygous state of *p53* could be a key factor in the carcinogenic response. CsA and DES are regarded as non-genotoxic carcinogens and are believed to facilitate tumor promotion, instead of tumor initiation. It is our hypothesis that the higher spontaneous mutational load in both XP models, detected in our previous studies [27], will trigger tumor initiation. Accumulation of initiated cells could be the underlying principle in *Xpa*\**p53* and *Xpc*\**p53* mice of the observed tumor proneness in response to exposure to non-genotoxic carcinogens like CsA and DES.

WY exposure showed a relatively weak carcinogenic response in both wild type and *Xpc*\**p53* mice, although a significant increase in preneoplastic lesions was found for the latter genotype. The 39 weeks of WY exposure was not long enough to undoubtedly demonstrate the carcinogenic potential of this compound, but also demonstrates WY is a relatively weak non-genotoxic rodent carcinogen, possibly harmless to humans. DEHP shares part of its mode of action with WY, namely peroxisome proliferation [23;28]. Even though the applied dose of DEHP in this study was much higher than that of WY, it did not significantly induce cancer in wild type or *Xpc*\**p53* mice, which is consistent with previous studies [6].

Exposure to the low potent genotoxic carcinogen phenacetin, did not result in identification of the compound as a carcinogen in wild type, *Xpa*\**p53* or *Xpc*\**p53* model in our studies. Previously, 75-80 week exposures to phenacetin in female and male wild type (C57BL/6) mice did not result into any tumor induction [29;30]. Additionally, previous 39-week exposures to phenacetin using *Xpa* and *Xpa*\**p53* mice did not result in an increased tumor response [6;18]. Other alternative *in vivo* models (*p53*<sup>+/-</sup>, Tg.AC and neonatal carcinogenicity model) plus several *in vitro* tests (e.g. SHE cell transformation assay, DNA-repair test) were also not able to identify this carcinogen [25;31;32]. Interestingly, although phenacetin is a (very weak) substrate to NER [33], it does not give rise to an enhanced tumor response even in a NER-deficient genetic setting. It is possible that phenacetin is only harmful at extremely high doses. In our present study the phenacetin dose used was equal to the highest dose of phenacetin used in the dose range finding study performed with *Xpa* and *Xpa*\**p53* mice [18]. Possibly, wild type and *Xpc*\**p53* mice can be dosed higher without interference of a (geno)toxic response, as observed *Xpa* or *Xpa*\**p53* mice.

In the past, Wijnhoven et al. have demonstrated an increased sensitivity of *Xpa*, as compared to *Xpc* mice, towards toxic effects induced by DNA-damaging agents [9]. Additional *in vivo* data from our lab (unpublished results) supported that *Xpa* mice are more sensitive towards genotoxicant-induced cytotoxicity than *Xpc* mice, due to a defective TC-NER (in addition to GG-NER defect). The *Xpa* mice exhibited a strong apoptotic response, resulting in cell death [8;34-36]. Our current study shows that primary mouse hepatocytes derived from *Xpc*\**p53* mice can be exposed to higher doses of genotoxicants than *Xpa*\**p53* cells, before cytotoxicity occurs. It appears the divergence in toxicity response between *Xpa* and *Xpc*-deficient systems is not altered when additional *p53* heterozygosity is introduced. The same doses as wild type cells were tolerated by the *Xpc*\**p53*-derived hepatocytes. This was in contrast to the situation in *Xpa*\**p53*-derived cells, which appeared to be approximately threefold more sensitive to genotoxic carcinogens than wild type cells. As *Xpc*\**p53* cells responded similarly to genotoxicant-induced cellular toxicity as wild type cells, we hypothesize that *Xpc*\**p53* and

wild type mice will exhibit similar dose-responses in (short-term) carcinogenicity testing although this assumption needs further validation.

As noted, the *Xpc*\**p53* mice have an additional advantage over *Xpa*\**p53* mice since they are supposed to be not only sensitive to NER-inducing compounds, but also to other DNA-damaging agents. We showed previously [27] that *Xpa* and *Xpc* mice have divergent tumor phenotypes in this respect. Therefore, we conclude that the *Xpc*\**p53* mouse model is a promising potential alternative tool for carcinogenicity testing. The deficiency of XPC (like XPA) also facilitates the most common enabling characteristic of carcinogenesis, namely genomic instability and is, therefore, suitable to predict both true genotoxic as well as non-genotoxic carcinogens, which several other alternative *in vivo* carcinogenicity models are incapable of. Using this beneficial feature, more carcinogenic compounds should be tested *in vivo* to ensure that the *Xpc*\**p53* is a reliable and accurate alternative candidate in short-term carcinogenicity testing.

### Acknowledgements

We thank the Animal Facilities of the Leiden University Medical Center and the National Institute for Public Health and the Environment for their skillful (bio)technical support. We would like to acknowledge Dr. Erroll Friedberg for providing us with the *Xpc*-deficient mice.

### Conflict of Interest Statement

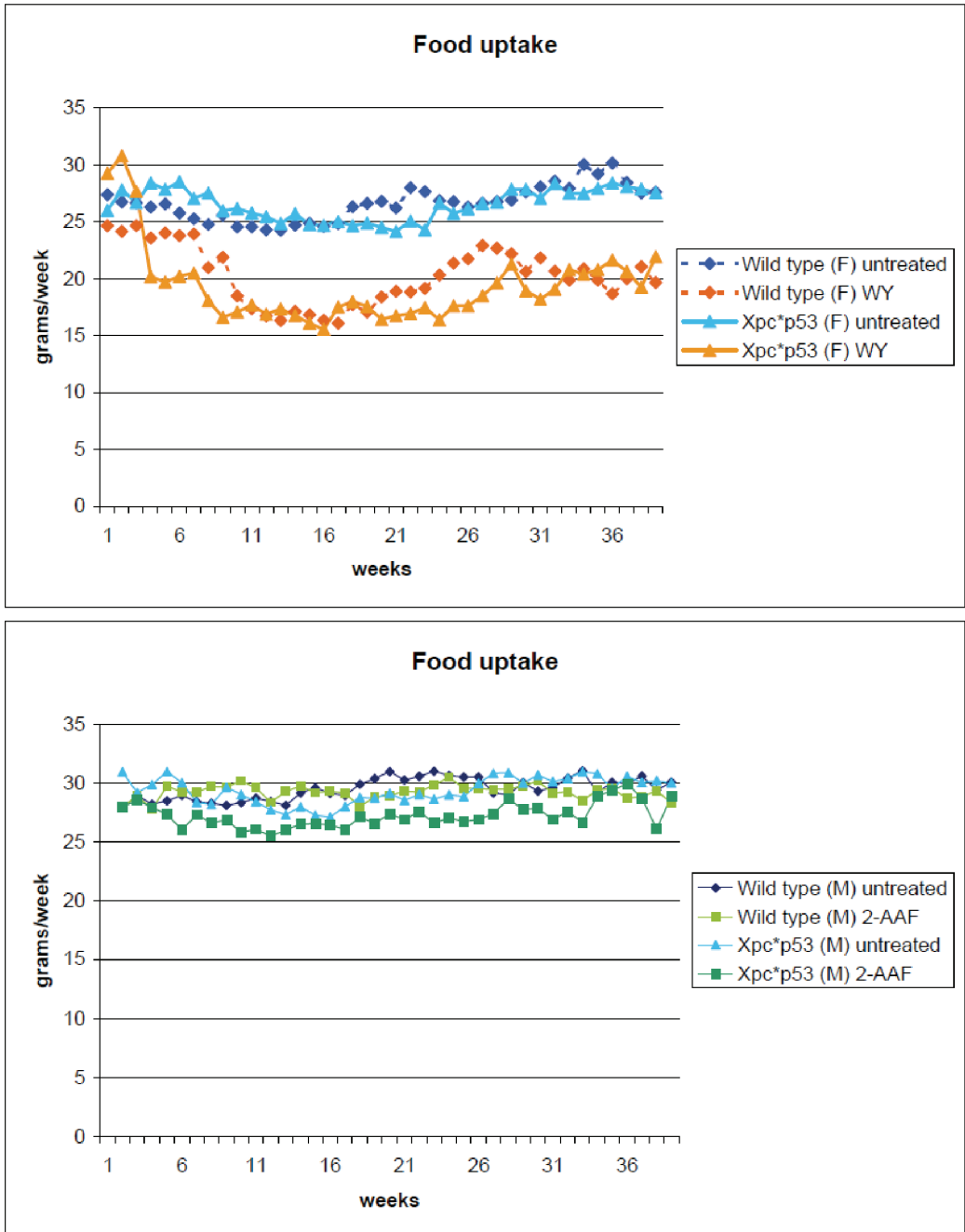
None declared.

## Reference List

- [1] R.Nagy, K.Sweet, C.Eng. Highly penetrant hereditary cancer syndromes. *Oncogene* 23(38), 6445-6470. 8-23-2004.
- [2] Kinzler KW, Vogelstein B. The genetic basis of human cancer, McGraw-Hill, New York, 2002.
- [3] D.Hanahan, R.A.Weinberg. Hallmarks of cancer: the next generation. *Cell* 144(5), 646-674. 3-4-2011.
- [4] D.Hanahan, R.A.Weinberg. The hallmarks of cancer. *Cell* 100(1), 57-70. 1-7-2000.
- [5] L.G.Hernandez, H.van Steeg, M.Luijten, J.van Benthem. Mechanisms of non-genotoxic carcinogens and importance of a weight of evidence approach. *Mutat.Res.* 682(2-3), 94-109. 2009.
- [6] C.F.van Kreijl, P.A.McAnulty, R.B.Beems, A.Vynckier, H.van Steeg, R.Fransson-Steen, C.L.Alden, R.Forster, J.W.van der Laan, J.Vandenberghe. Xpa and Xpa/p53<sup>+/+</sup> knockout mice: overview of available data. *Toxicol.Pathol.* 29 Suppl, 117-127. 2001.
- [7] H.van Steeg, A.de Vries, C.T.van Oostrom, J.van Benthem, R.B.Beems, C.F.van Kreijl. DNA repair-deficient Xpa and Xpa/p53<sup>+/+</sup> knock-out mice: nature of the models. *Toxicol.Pathol.* 29 Suppl, 109-116. 2001.
- [8] J.C.Klein, R.B.Beems, P.E.Zwart, M.Hamzink, G.Zomer, H.van Steeg, C.F.van Kreijl. Intestinal toxicity and carcinogenic potential of the food mutagen 2-amino-1-methyl-6-phenylimidazo[4,5-b]pyridine (PhIP) in DNA repair deficient XPA<sup>-/-</sup> mice. *Carcinogenesis* 22(4), 619-626. 2001.
- [9] S.W.Wijnhoven, H.J.Kool, L.H.Mullenders, R.Slater, A.A.van Zeeland, H.Vrieling. DMBA-induced toxic and mutagenic responses vary dramatically between NER-deficient Xpa, Xpc and Csb mice. *Carcinogenesis* 22(7), 1099-1106. 2001.
- [10] M.van Oosten, H.Rebel, E.C.Friedberg, H.van Steeg, G.T.van der Horst, H.J.van Kranen, A.Westerman, A.A.van Zeeland, L.H.Mullenders, F.R.de Gruijl. Differential role of transcription-coupled repair in UVB-induced G2 arrest and apoptosis in mouse epidermis. *Proc.Natl.Acad.Sci.U.S.A* 97(21), 11268-11273. 10-10-2000.
- [11] S.W.Wijnhoven, H.J.Kool, L.H.Mullenders, A.A.van Zeeland, E.C.Friedberg, G.T.van der Horst, H.van Steeg, H.Vrieling. Age-dependent spontaneous mutagenesis in Xpc mice defective in nucleotide excision repair. *Oncogene* 19(43), 5034-5037. 10-12-2000.
- [12] A.van Hoffen, A.S.Balajee, A.A.van Zeeland, L.H.Mullenders. Nucleotide excision repair and its interplay with transcription. *Toxicology* 193(1-2), 79-90. 11-15-2003.
- [13] D.L.Cheo, H.J.Ruven, L.B.Meira, R.E.Hammer, D.K.Burns, N.J.Tappe, A.A.van Zeeland, L.H.Mullenders, E.C.Friedberg. Characterization of defective nucleotide excision repair in XPC mutant mice. *Mutat.Res.* 374(1), 1-9. 3-4-1997.
- [14] A.de Vries, C.T.van Oostrom, F.M.Hofhuis, P.M.Dortant, R.J.Berg, F.R.de Gruijl, P.W.Wester, C.F.van Kreijl, P.J.Capel, H.van Steeg, . Increased susceptibility to ultraviolet-B and carcinogens of mice lacking the DNA excision repair gene XPA. *Nature* 377(6545), 169-173. 9-14-1995.
- [15] T.Jacks, L.Remington, B.O.Williams, E.M.Schmitt, S.Halachmi, R.T.Bronson, R.A.Weinberg. Tumor spectrum analysis in p53-mutant mice. *Curr.Biol.* 4(1), 1-7. 1-1-1994.
- [16] M.E.Dolle, H.Giese, C.L.Hopkins, H.J.Martus, J.M.Hausdorff, J.Vijg. Rapid accumulation of genome rearrangements in liver but not in brain of old mice. *Nat.Genet.* 17(4), 431-434. 1997.
- [17] P.A.McAnulty, M.Skydsgaard. Diethylstilbestrol (DES): carcinogenic potential in Xpa<sup>-/-</sup>, Xpa<sup>-/-</sup> / p53<sup>+/+</sup>, and wild-type mice during 9 months' dietary exposure. *Toxicol.Pathol.* 33(5), 609-620. 2005.
- [18] B.A.Lina, R.A.Woutersen, J.P.Bruijntjes, J.van Benthem, J.A.van den Berg, J.Monbaliu, B.J.Thoolen, R.B.Beems, C.F.van Kreijl. Evaluation of the Xpa-deficient transgenic mouse model for short-term carcinogenicity testing: 9-month studies with haloperidol, reserpine, phenacetin, and D-mannitol. *Toxicol.Pathol.* 32(2), 192-201. 2004.
- [19] P.C.van Kesteren, R.B.Beems, M.Luijten, J.Robinson, A.de Vries, H.van Steeg. DNA repair-deficient Xpa/p53 knockout mice are sensitive to the non-genotoxic carcinogen cyclosporine A: escape of initiated cells from immunosurveillance? *Carcinogenesis* 30(3), 538-543. 2009.



- [20] P.C.van Kesteren, P.E.Zwart, J.L.Pennings, W.H.Gottschalk, J.C.Kleinjans, J.H.van Delft, H.van Steeg, M.Luijten. Deregulation of cancer-related pathways in primary hepatocytes derived from DNA repair-deficient *Xpa*⁻/*p53*⁺/- mice upon exposure to benzo[a]pyrene. *Toxicol.Sci.* 123(1), 123-132. 6-29-2011.
- [21] T.Mosmann. Rapid colorimetric assay for cellular growth and survival: application to proliferation and cytotoxicity assays. *J.Immunol.Methods* 65(1-2), 55-63. 12-16-1983.
- [22] W.Slob. Dose-response modeling of continuous endpoints. *Toxicol.Sci.* 66(2), 298-312. 2002.
- [23] IARC Monograph DEHP. IARC (2000) Monograph Summary, Volume 77, Di(2-ethylhexyl)phthalate. 2000. IARC.
- [24] H.van Steeg. The role of nucleotide excision repair and loss of p53 in mutagenesis and carcinogenesis. *Toxicol.Lett.* 120(1-3), 209-219. 3-31-2001.
- [25] S.M.Cohen, D.Robinson, J.MacDonald. Alternative models for carcinogenicity testing. *Toxicol.Sci.* 64(1), 14-19. 2001.
- [26] S.M.Cohen. Alternative models for carcinogenicity testing: weight of evidence evaluations across models. *Toxicol.Pathol.* 29 Suppl, 183-190. 2001.
- [27] J.P.Melis, S.W.Wijnhoven, R.B.Beems, M.Roodbergen, B.J.van den, H.Moon, E.Friedberg, G.T.van der Horst, J.H.Hoeijmakers, J.Vijg, H.van Steeg. Mouse models for xeroderma pigmentosum group A and group C show divergent cancer phenotypes. *Cancer Res.* 68(5), 1347-1353. 3-1-2008.
- [28] D.S.Marsman, R.C.Cattley, J.G.Conway, J.A.Popp. Relationship of hepatic peroxisome proliferation and replicative DNA synthesis to the hepatocarcinogenicity of the peroxisome proliferators di(2-ethylhexyl)phthalate and [4-chloro-6-(2,3-xylydino)-2-pyrimidinylthio]acetic acid (Wy-14,643) in rats. *Cancer Res.* 48(23), 6739-6744. 12-1-1988.
- [29] A.W.Macklin, R.J.Szot. Eighteen month oral study of aspirin, phenacetin and caffeine, in C57Bl/6 mice. *Drug Chem.Toxicol.* 3(2), 135-163. 1980.
- [30] IARC Monograph Phenacetin. IARC Monographs 100A-25: Phenacetin. 2009. IARC.
- [31] S.De Flora, P.Russo, M.Pala, G.Fassina, A.Zunino, C.Bennicelli, P.Zanacchi, A.Camoirano, S.Parodi. Assay of phenacetin genotoxicity using in vitro and in vivo test systems. *J.Toxicol.Environ.Health* 16(3-4), 355-377. 1985.
- [32] R.D.Storer, F.D.Sistare, M.V.Reddy, J.J.DeGeorge. An industry perspective on the utility of short-term carcinogenicity testing in transgenic mice in pharmaceutical development, *Toxicol.Pathol.*, 38, (2010) 51-61.
- [33] M.Luijten, E.N.Speksnijder, N.van Alphen, A.Westerman, S.H.Heisterkamp, J.van Benthem, C.F.van Kreijl, R.B.Beems, H.van Steeg. Phenacetin acts as a weak genotoxic compound preferentially in the kidney of DNA repair deficient *Xpa* mice. *Mutat.Res.* 596(1-2), 143-150. 4-11-2006.
- [34] Y.Arima, M.Nitta, S.Kuninaka, D.Zhang, T.Fujiwara, Y.Taya, M.Nakao, H.Saya. Transcriptional blockade induces p53-dependent apoptosis associated with translocation of p53 to mitochondria. *J.Biol.Chem.* 280(19), 19166-19176. 5-13-2005.
- [35] S.Queille, C.Drougard, A.Sarasin, L.Daya-Grosjean. Effects of XPD mutations on ultraviolet-induced apoptosis in relation to skin cancer-proneness in repair-deficient syndromes. *J.Invest Dermatol.* 117(5), 1162-1170. 2001.
- [36] V.Chigancas, L.F.Batista, G.Brumatti, G.P.Amarante-Mendes, A.Yasui, C.F.Menck. Photorepair of RNA polymerase arrest and apoptosis after ultraviolet irradiation in normal and XPB deficient rodent cells. *Cell Death.Differ.* 9(10), 1099-1107. 2002.



**Supplemental information 1.** Food uptake (weekly average uptake per mouse) of wild type and *Xpc\*<sup>p53</sup>* mice exposed to control feed and WY (females, **A**) or 2-AAF (males, **B**).



# Chapter 6

# Chapter 6

## Genotoxic exposure: novel cause of selection for a functional $\Delta$ N-p53 isoform

**Melis JPM**, Hoogervorst EM, van Oostrom CTM, Zwart E, Breit TM, Pennings JLA, de Vries A, van Steeg H.

Genotoxic exposure: novel cause of selection for a functional  $\Delta$ N-p53 isoform

**Oncogene**. 2011 Apr 14;30 (15):1764-72.

*"But there's a warnin' sign, on the road ahead"*

Rockin' In The Free World – Neil Young, 1989

## Abstract

The *p53* gene is frequently mutated in cancers and it is vital for cell cycle control, homeostasis and carcinogenesis. We describe a novel *p53* mutational spectrum, different to those generally observed in human and murine tumors. Our study shows a high prevalence of nonsense mutations in the p53 N-terminus of 2-AAF induced urinary bladder tumors. These nonsense mutations forced downstream translation initiation at codon 41 of *Trp53*, resulting in the aberrant expression of the p53 isoform  $\Delta$ N-p53 (or p44). We propose a novel mechanism for the origination and the selection for this isoform. We show that chemical exposure can act as a novel cause of selection for this truncated protein. Additionally, our data suggest that the occurrence of  $\Delta$ N-p53 accounts, at least in mice, for a cancer phenotype. We also show that gene-expression profiles of ES cells carrying the  $\Delta$ N-p53 isoform in a p53 null background are divergent from p53 knock-out ES cells, and therefore postulate that  $\Delta$ N-p53 itself has functional transcriptional properties.

## Introduction

The tumor suppressor p53 regulates significant cellular functions to prevent the initiation and prolongation of cancer and is intensively studied. Several isoforms of p53 have been identified [1-4] and point mutations influencing the functionality of p53 were elucidated and mimicked *in vivo* [5-9]. The p53 gene is the most frequently mutated gene in cancer and analysis of many different human tumor types have shown a high prevalence of missense mutations located primarily in the central DNA binding domain [10]. Frequently, these mutations result in the expression of mutant p53 proteins, which are often more stable than wild type p53 [11]. A small variety of isoforms, which lack an N-terminal and/or C-terminal part of the protein have been discovered [1,3] and can result in a dominant-negative inhibition of the wild type p53 protein [8]. Although, a gain-of-function phenotype of mutant p53 which enhances the oncogenic properties of p53 has also been proposed [12,13].

To gain more functional insight into p53 and the effect of alterations in its gene, several transgenic mouse models have been generated [14]. For example, the *Trp53*<sup>+/-</sup> model appears to be more susceptible than wild type mice to carcinogenesis, both spontaneous and chemically-induced [15,16]. We have previously investigated the effect of p53 heterozygosity to the exposure of the carcinogen 2-acetylaminofluorene (2-AAF), a strong inducer of urinary bladder tumors [16]. Since stress signals like DNA damage can affect p53 function, we also investigated *Trp53*<sup>+/-</sup> in combination with a deficiency in the DNA repair gene *Xpa*. Carcinogenesis in both models is putatively caused by *Trp53* mutations in the remaining wild type allele, demonstrated by the presence of mutated p53 protein in early atypical preneoplastic lesions and tumors [16]. Here, we reveal a mutational spectrum in tumors divergent from that generally observed after carcinogen exposure (<http://p53.free.fr/index.html>). A high frequency of predominantly N-terminal nonsense mutations was found in the *Trp53* gene resulting in the selective expression of an N-terminally truncated P53-isoform ( $\Delta$ N-p53). We further investigated the impact of this isoform by creating and analyzing embryonic stem cells harboring a nonsense mutation at codon 5, expressing the  $\Delta$ N-p53 isoform. We showed this isoform has functional transcriptional properties that differ from both wild type and p53 knock out cells.

## Material and Methods

### Induction of urinary bladder tumors

2-AAF induced urinary bladder tumors in *Trp53*<sup>+/-</sup> and *Xpa*<sup>-/-</sup>/*Trp53*<sup>+/-</sup> mice were obtained from our previously reported study [16]. Briefly, mice were treated for 39 weeks with 300 ppm 2-AAF in the diet. Liver, spleen and urinary bladder were collected at autopsy and fixed in 3.8% formaldehyde. The formaldehyde fixed samples were embedded in paraffin wax, cut into 5  $\mu$ m sections, and stained with haematoxylin and eosin (H&E).

### Immunohistochemical detection of p53 protein

P53 protein accumulation was detected in paraffin embedded, formalin-fixed sections from urinary bladder tumors. Polyclonal CM5 antibody, which recognizes several epitopes of both wild type and mutant mouse p53 protein (Novacastra), the Pab240 antibody specific for mutant p53 protein (Labvision), and the 1C12 antibody (Cell Signaling) recognizing the N-terminal part of the p53 protein,

were used (previously described by Hoogervorst *et al.*, 2004). The level of CM5, Pab240 and 1C12 staining was scored by dividing the area of p53 positive fields by the total area of the tumor \* 100% and the final result was scored either negative (-;  $\leq 5\%$ ) or positive (+;  $\geq 5\%$ ).

### ***Trp53 mutation analyses by DNA and cDNA sequencing***

Formalin fixed, paraffin embedded urinary bladder tumors were analyzed for *Trp53* mutations by direct sequencing of genomic DNA. P53 positive and negative fields were marked on the p53 stained slides. Tumor regions were isolated on an adjacent 14  $\mu\text{m}$  section slides. Genomic DNA was isolated with the QIAamp DNA minikit (QIAGEN) according to the manufacturer's protocol. The coding region of the *Trp53* gene, spanning from exon 2 to 8 was amplified using the HotStarTaq Master Mix Kit (QIAGEN) and a dedicated set of primers (Supplemental figure 2, primer set 1). Subsequently, exon 2, exon 3 and 4, exon 5 and 6 plus exon 7 and 8 were reamplified by using primer set 2 (Supplemental figure 2).

Frozen bladder tumor sections were analyzed for *Trp53* mutations by RT-PCR. RNA was isolated with TRIzol reagent (Invitrogen) as described by the manufacturer's protocol. For RT-PCR, performed with the Titan One Tube RT-PCR System (Roche), the primers used are depicted in supplemental figure 2, primer set 3. Subsequently, exon 2 to 5, exon 5 and 6, exon 7 and 8 and exon 9 to 11 were reamplified by using the primers of primer set 4 (Supplemental figure 2).

Purified PCR products (QIAquick PCR Purification Kit, QIAGEN) were directly sequenced using the Big Dye Terminator Sequence kit version 3.1 (Applied Biosystems) and an ABI 3700 DNA sequencer, with identical primers as used for reamplification PCR.

### ***Generation of mutant embryonic stem (ES) cells***

#### ***p53.E5stop and p53.E5stop.M41I mutant targeting vectors***

The p53.E5stop and p53.E5stop.M41I targeting vectors were constructed by introducing single base pair mutations in exon 2 and/or exon 4 in a genomic p53 fragment (Figure 3 + supplemental figure 1). The mutations lead to a glutamic acid-to-stop and a methionine-to-isoleucine substitution at codon 5 and 41, respectively. Primer set 5 was used to introduce the mutations into the *Trp53* sequence (supplemental figure 2).

The targeting vectors (Figure 3 + supplemental figure 1) were constructed by cloning the mutated fragment into flanking genomic p53 fragments comprising intron 4 to 3' end of the gene [<sup>6</sup>] together with the transcriptional stop-cassette described by Olive *et al* [<sup>35</sup>]. This stop-cassette contains a puromycin selection marker flanked by LoxP-sites. Targeting vectors contained a pGK-DTA selection marker (kindly provided by F. Gertler, Massachusetts Institute of Technology) at the 3' end of the vector for negative selection.

*Homologous-recombination experiments in ES cells*

The targeting vectors (Figure 3 + supplemental figure 1) were linearized and electroporated into p53<sup>-/-</sup> D3 ES cells (kindly provided by prof. T. Jacks, MIT, Cambridge) using standard procedures [36]. Puromycin resistant ES cell clones were analyzed for correct homologous integration of the targeting vector by Southern blot analysis (Supplemental figure 1). Recombination was examined by using an exon 1 probe (previously described in Jacks et al., 1994) (EcoR1-Stu1 digestion) and a 1.3 kb probe spanning exons 7 to 9 (BamH1 digestion). Correctly targeted ES cell clones were expanded and electroporated with circular pMC-CreN plasmid (kindly provided by F. Alt, Harvard Medical School, Boston). Clones that had lost the selectable marker cassette were selected for, by adding puromycin to the culture medium. Correctly targeted clones that were used for blastocyst injection procedures or cellular assays were analyzed for additional (undesired) mutations.

**Western blot analyses**

Protein analyses were executed as previously described [37]. Western blotting was performed with CM5 anti-p53 rabbit polyclonal antibody (Novacastra). Primary antibodies were detected by incubating with HRP-linked donkey anti-rabbit IgG (Amersham Pharmacia Biotech) and staining was done using ECL-plus reagent (Amersham Pharmacia Biotech). Actin protein levels, detected by a peroxidase (HRP) linked anti-actin affinity purified goat polyclonal antibody (I-19; Santa Cruz), were determined a loading control.

**Microarray analysis**

Wild type, *Trp53*<sup>stop5/-</sup> and *Trp53*<sup>-/-</sup> ES cells were cultured as a monoculture for 26 hours (using a 0.1% gelatin coating, no feeder layers were used to prevent mixed cell type sampling). Proliferation rates of all the four genotypes (including the *p53.E5stop.M41I* variant) were in the same range and were examined by XTT test (Roche) (results not shown). Total RNA was isolated using the RNeasy Mini Kit (Qiagen, Valencia, CA, USA). RNA quality was tested using automated gel electrophoresis (Bioanalyzer 2100; Agilent technologies, Amstelveen, the Netherlands). All RNA samples used had an RNA integrity number (RIN) > 9.9.

RNA samples (Wild type *Trp53*<sup>+/+</sup>, *Trp53*<sup>stop5/-</sup>, *Trp53*<sup>-/-</sup>; n = 5 per genotype) were labeled and hybridized to Mouse GeneChip 430 2.0 (Affymetrix, Santa Clara, CA, USA) according to manufacturer's protocol. Due to technical quality control one *Trp53*<sup>-/-</sup> sample was discarded as a technical outlier.

The microarray data were normalized by RMA [38] using a custom CDF as described by de Leeuw et al [39]. Of the hybrid probe set definitions included in the annotation, 16.331 probe sets (<http://brainarray.mbni.med.umich.edu/Brainarray/Database/CustomCDF>) and the 4.648 Affymetrix probe sets corresponding to an Entrez Gene ID were used in further analysis. Subsequent data analyses were performed using R [40], Microsoft Excel and GeneMaths (Sint-Martens-Latem, Belgium). Log transformed gene expression values were compared between a pair of two groups using a Welch's T-test, and genes with a p-value < 0.001 and a fold ratio (defined as maximum/minimum average group value) > 1.5 were considered differentially expressed. Functional annotation and Gene Ontology term enrichment was performed using the DAVID/EASE [41,42] web application. The normalized enrichment



score (NES) reflects the degree of overrepresentation of a gene set at the top or bottom of a ranked list of genes, which is then normalized to account for the size of the set and underlying correlations. Q-PCR analysis on *Trp53* (Mm01731290\_g1, Applied Biosystems) was performed to check and verify *Trp53* gene expression in the different genotypes.

## Results

### *P53 mutational analysis in urinary bladder tumors*

In our previous study [16], wild type, *Trp53*<sup>+/-</sup> and *Xpa*<sup>-/-</sup>/*Trp53*<sup>+/-</sup> mice were exposed to either 2-AAF or control feed. Of the 49 2-AAF exposed wild type mice there was only 1 mouse with a urinary bladder tumor, in contrast to the other two genotypes. Of the *Trp53*<sup>+/-</sup> and *Xpa*<sup>-/-</sup>/*Trp53*<sup>+/-</sup> mice 29% (12 out of 45) and 63% (22 out of 40) carried urinary bladder tumors. To analyze the integrity of the p53 protein in urinary bladder tumors induced by 2-AAF-exposure, we stained tumor samples of the *Trp53*<sup>+/-</sup> and *Xpa*<sup>-/-</sup>/*Trp53*<sup>+/-</sup> mice with the CM5 antibody and the Pab240 antibody (data not shown) to identify positive mutant p53 tumor fields. Sequence analysis of exon 2 to 8 was carried out on DNA isolated from both mutant p53 positive and negative tumor fields. The DNA sequence results are summarized in Table 1 and mutational hotspots are depicted in Figure 1.

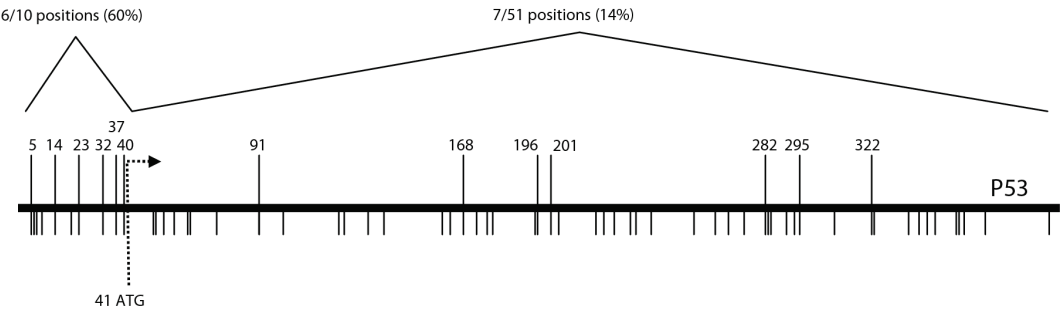


**Figure 1.** Mutational target sites for nonsense mutations in p53 in 2-AAF exposed urinary bladder tumors. Possible mutational transversion G:C → T:A targets in the p53 protein that can transverse into a stop codon due to a 2-AAF driven G:C → T:A transversion are indicated by bars below the schematic p53 protein. Numbered targets depicted above the schematic p53 protein were discovered in urinary bladder tumors after exposure to 2-AAF. Location 41 indicates an alternative start site in p53, upstream of codon 41.

In total, 78% of the examined urinary bladder tumors (21 out of 27) harbored a mutation in the *Trp53* gene. A wide variety of *Trp53* mutations was observed (Table 1). The majority of mutations identified were single base changes found in *Trp53* DNA. Mutations were confirmed at the mRNA level, indicating that p53 transcripts were stable even though many of them carried a translational stop codon at the 5' region of the transcript. The mutations comprised predominantly G:C → T:A transversions (28 out of 36 single base mutations = 78%), consistent with the mutations frequently found after 2-AAF exposure [17,18]. In compliance with previous exposure studies, 61% of the mutations were found in the DNA binding domain (exon 4 to 8) were missense mutations (14 from 23).

Codon	Exon	Base change*	Amino acid change**	Frequency affected** *	Genotype
5	2	<u>G</u> AG→ <u>I</u> AG	Glu→Stop	1	<i>Trp53</i> <sup>+/-</sup>
14	2	<u>G</u> AG→ <u>I</u> AG	Glu→Stop	4	<i>Trp53</i> <sup>+/-</sup> + <i>Xpa</i> <sup>-/-</sup> / <i>Trp53</i> <sup>+/-</sup>
23	2	<u>T</u> CA→ <u>T</u> AA	Ser→Stop	3	<i>Trp53</i> <sup>+/-</sup> + <i>Xpa</i> <sup>-/-</sup> / <i>Trp53</i> <sup>+/-</sup>
32	3	<u>G</u> AA→ <u>I</u> AA	Glu→Stop	1	<i>Trp53</i> <sup>+/-</sup>
	3-4	del	del 36-122	2	<i>Xpa</i> <sup>-/-</sup> / <i>Trp53</i> <sup>+/-</sup>
37	4	<u>T</u> CA→ <u>T</u> AA	Ser→Stop	1	<i>Trp53</i> <sup>+/-</sup>
40	4	<u>T</u> GC→ <u>T</u> GA	Cys→Stop	1	<i>Xpa</i> <sup>-/-</sup> / <i>Trp53</i> <sup>+/-</sup>
91	4	<u>T</u> CA→ <u>T</u> AA	Ser→Stop	1	<i>Trp53</i> <sup>+/-</sup>
114	4	<u>G</u> GG→ <u>G</u> AG	Gly→Glu	1	<i>Xpa</i> <sup>-/-</sup> / <i>Trp53</i> <sup>+/-</sup>
122	4	<u>A</u> CG→ <u>A</u> AG	Thr→Lys	1	<i>Xpa</i> <sup>-/-</sup> / <i>Trp53</i> <sup>+/-</sup>
124	5	<u>T</u> CT→ <u>T</u> TT	Ser→Phe	1	<i>Xpa</i> <sup>-/-</sup> / <i>Trp53</i> <sup>+/-</sup>
131	5	<u>T</u> TC→ <u>T</u> TA	Phe→Leu	1	<i>Trp53</i> <sup>+/-</sup>
168	5	<u>G</u> AG→ <u>I</u> AG	Glu→Stop	1	<i>Xpa</i> <sup>-/-</sup> / <i>Trp53</i> <sup>+/-</sup>
176	5	<u>C</u> AT→ <u>A</u> AT	His→Asn	1	<i>Trp53</i> <sup>+/-</sup>
176	5	<u>C</u> AT→ <u>I</u> AT	His→Tyr	1	<i>Xpa</i> <sup>-/-</sup> / <i>Trp53</i> <sup>+/-</sup>
	Intron 5/exon 6	agGC→a <u>I</u> GC		1	<i>Xpa</i> <sup>-/-</sup> / <i>Trp53</i> <sup>+/-</sup>
196	6	<u>G</u> GA→ <u>I</u> GA	Gly→Stop	1	<i>Trp53</i> <sup>+/-</sup>
201	6	<u>G</u> AG→ <u>I</u> AG	Glu→Stop	1	<i>Trp53</i> <sup>+/-</sup>
202	6	<u>T</u> AT→ <u>T</u> TT	Tyr→Phe	2	<i>Trp53</i> <sup>+/-</sup>
	Intron 7/exon 8	agTG→a <u>I</u> TG		1	<i>Xpa</i> <sup>-/-</sup> / <i>Trp53</i> <sup>+/-</sup>
	Intron 7/exon 8	agTG→aa <u>T</u> G		1	<i>Xpa</i> <sup>-/-</sup> / <i>Trp53</i> <sup>+/-</sup>
238	7	<u>T</u> CC→ <u>T</u> AC	Ser→Tyr	1	<i>Xpa</i> <sup>-/-</sup> / <i>Trp53</i> <sup>+/-</sup>
253	7	<u>A</u> CA→ <u>A</u> AA	Thr→Lys	1	<i>Trp53</i> <sup>+/-</sup>
270	8	<u>C</u> GT→ <u>C</u> TT	Arg→Leu	1	<i>Xpa</i> <sup>-/-</sup> / <i>Trp53</i> <sup>+/-</sup>
276	8	<u>G</u> GG→ <u>A</u> GG	Gly→Arg	1	<i>Xpa</i> <sup>-/-</sup> / <i>Trp53</i> <sup>+/-</sup>
278	8	<u>G</u> AC→ <u>I</u> AC	Asp→Tyr	1	<i>Xpa</i> <sup>-/-</sup> / <i>Trp53</i> <sup>+/-</sup>
282	8	<u>G</u> AA→ <u>I</u> AA	Glu→Stop	1	<i>Xpa</i> <sup>-/-</sup> / <i>Trp53</i> <sup>+/-</sup>
291	8	<u>G</u> TC→ <u>G</u> CC	Val→Ala	1	<i>Xpa</i> <sup>-/-</sup> / <i>Trp53</i> <sup>+/-</sup>
295	8	<u>G</u> AA→ <u>I</u> AA	Glu→Stop	2	<i>Trp53</i> <sup>+/-</sup> + <i>Xpa</i> <sup>-/-</sup> / <i>Trp53</i> <sup>+/-</sup>
322	9	<u>G</u> GA→ <u>I</u> GA	Gly→Stop	1	<i>Trp53</i> <sup>+/-</sup>

**Table 1.** Analysis of *Trp53* mutations in 2-AAF induced urinary bladder tumors of *Trp53*<sup>+/-</sup> and *Xpa*<sup>-/-</sup>/*Trp53*<sup>+/-</sup> mice by direct sequencing. \* The affected nucleotide is underlined. \*\* Nonsense mutations are indicated in bold. \*\*\* Indicates in how many different tumors from different animals the mutation has been found.

Of the single base mutations, 53% (19 out of 36) were nonsense mutations. Of these, a relatively high percentage (11 out of 19 = 63%) was found between codon 1 and 41 of the N-terminal part of the p53 protein. To illustrate this bias: 6 of the 10 (60%) possible G:C → T:A transversion target sites (amino acids that can be changed into a nonsense codon by a G:C→T:A transversion) upstream of codon 41, which may lead to a nonsense codon, were found mutated in the tumor set analyzed in this study. In

contrast, only 7 out of 51 (14%) in the remaining part of the p53 protein (Table 1 and Figure 1), which is a significant difference ( $p = 0.0011$  Chi-square test). Additionally, some of these nonsense mutations were present more frequently for a few codons (Table 1). These nonsense mutations at the 5' end of the *Trp53* gene accounted for 31% (11 out of 36) of the total number of single base p53 mutations found. Clearly, a selection of nonsense mutations at the extreme 5' end of the *p53* gene seems to occur after 2-AAF exposure.

No p53 protein was detectable by immunohistochemistry in tumors carrying a nonsense mutation present downstream of codon 41 (data not shown). However, when staining was performed on a selection of tumors containing nonsense codons upstream of codon 41 (codons 5, 14 and 23 were investigated) the presence of p53 protein was still observed, as was shown by immunohistochemistry analyses using both CM5 (Figure 2C) and Pab240 antibody (staining not shown). These tumor fields did not however show staining with the 1C12 antibody (Figure 2D), only recognizing the N-terminal part of the p53 protein. Therefore, an altered version of the p53 protein appears to be present lacking some amino acid residues at the N-terminus (Figure 2).

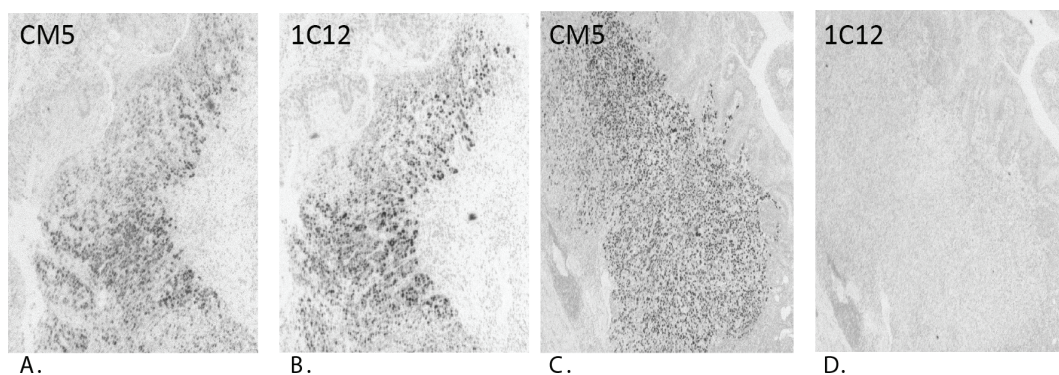


**Figure 2.** Immunohistochemistry staining of a 2-AAF-induced urinary bladder tumor. **A, C.** CM5 antibody staining in two different urinary bladder tumors. **B, D.** 1C12 antibody staining in two different urinary bladder tumors. The tumor shown in 2A and B carries a mutant p53 protein including the N-terminal part. The tumor shown in 2C and D carries a mutant p53 protein, missing the N-terminal part (1C12 negative).

### **Functional analysis of nonsense mutations at the 5' end of *Trp53* in ES cells**

A downstream ATG site in the *Trp53* sequence is present at codon 41, surrounded by sequences that match the Kozak consensus criteria [19]. This codon may, therefore, act as an alternative translational start site, which may explain the exhibited absence of 1C12 antibody staining of mutant P53 protein in tumors carrying specific N-terminal stop codons.

To provide evidence for this hypothesis, we generated 2 different knock-in mutant ES cell lines. The targeting constructs were introduced into a p53 null cell line. In one cell line, we introduced a TAG translational stop at codon 5 (stop5), mimicking the p53 mutation found in the 2-AAF induced bladder tumors (Figure 3A + supplemental figure 1A). In a second cell line, this TAG stop codon was complemented with a mutation at codon 41, where this presumptive alternative translational start codon ATG was replaced by an ATA (Ile encoding) codon (stop5 + ATA41, Figure 3A + supplemental

figure 1B). Expression of p53 protein was analyzed by Western blotting (Figure 3B). The cell line carrying the TAG stop at codon 5 led to the expression of a truncated version of the p53 protein;  $\Delta$ N-p53 (Figure 3B, lane 4). Possible protein products originating from splice variants of both the wild type and the  $\Delta$ N-p53 isoform are not visible on the Western Blot, but could theoretically still be present in very low amounts. Additional replacement of the alternative start codon 41 eliminated the translation of  $\Delta$ N-p53 completely (Figure 3B, lane 5), leading to the conclusion that this variant indeed protein originates from translational initiation at codon ATG41. Western blotting (Figure 3B) and Q-PCR analysis of *Trp53* (data not shown) on these two knock-in mutant genotypes showed that the  $\Delta$ N-p53 variant isoform originates from a stable transcript. Transcripts from the double mutant (stop5 + ATA41) however appeared to be unstable, only 4% steady state levels, as compared to wild type, were observed. This again supports our view that the ATG41 is used as a start signal for translation, which leads to stabilization of the transcript.

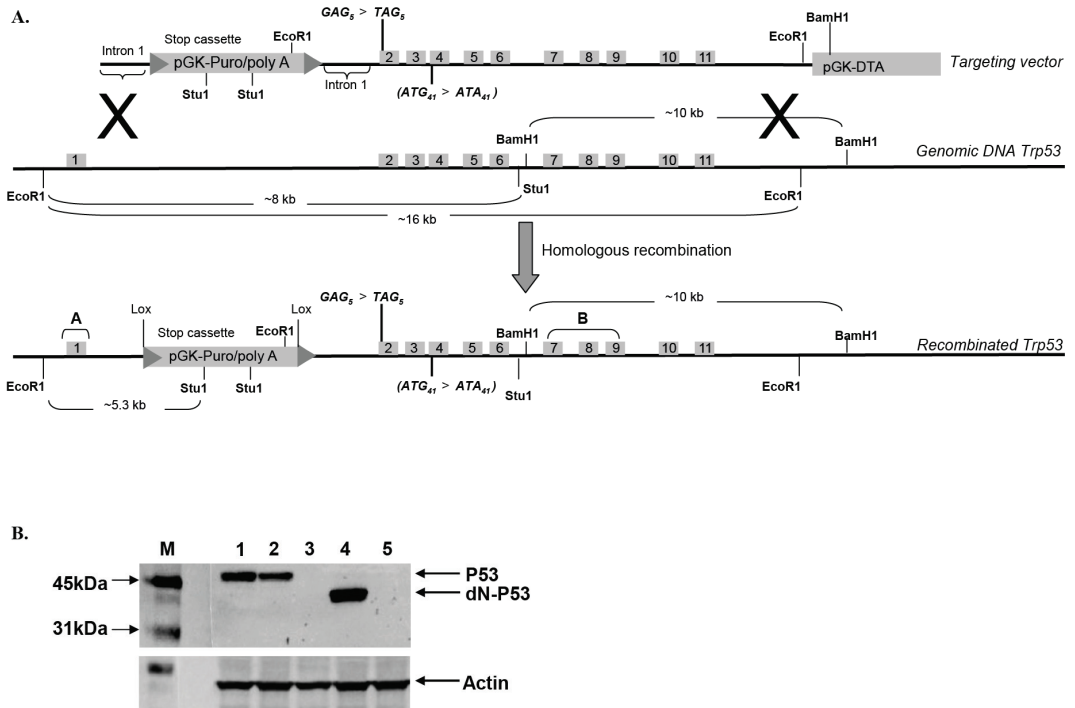


**Figure 3. A.** Schematic representation of the targeting construct (stop5) and (stop5 + ATA41) used for introducing a stop codon at codon 5 (and an isoleucine at the alternative startcodon at codon 41) in the p53 gene. The stop cassette contains a selective puromycin marker flanked by LoxP sites and a pGK-DTA selection marker is introduced at the 3' end of the construct. **B.** Western blot analysis of p53 and  $\Delta$ N-p53 in control and knocked in ES cells. Lane 1. *Trp53*<sup>+/+</sup> Lane 2. *Trp53*<sup>+/-</sup> Lane 3. *Trp53*<sup>-/-</sup> Lane 4. *Trp53*<sup>stop5/-</sup> Lane 5. *Trp53*<sup>stop5 + ATA41/-</sup>.

### Transcriptomics in ES cells carrying the $\Delta N$ -p53 protein

Subsequently, gene expression profiles of ES cells with various genotypes were analyzed to examine the functional impact of the p53 isoform and to investigate whether it showed differences with a p53 knock-out genotype. The genotypes studied included wild type ( $Trp53^{+/+}$ ), knock-out p53 ( $Trp53^{-/-}$ ) and cells that harbored a stop mutation at codon 5 in one allele combined with a deletion of the other p53 allele ( $Trp53^{stop5/-}$ ).

When  $Trp53^{-/-}$  and  $Trp53^{stop5/-}$  ES cells are compared to wild type cells these genotypes both show a divergent regulated expression from the wild type cells (Figure 4A). Although  $Trp53^{stop5/-}$  ES cells show quite some overlap in gene expression with the p53 knock out ES cells (Cat.2, 348 genes), there were differences apparent between the two genotypes. In general, more genes appear transcriptionally regulated ( $p < 0.001$  and Fold Ratio (FR)  $> 1.5$ ) in  $Trp53^{stop5/-}$  (838 genes) compared to  $Trp53^{-/-}$  (567 genes). Additionally, 490 genes (Cat.3) are significantly regulated in  $Trp53^{stop5/-}$  ES cells only, which is more than double the amount of significantly regulated genes in the knock-out ES cells only (Cat.1, 219 genes).

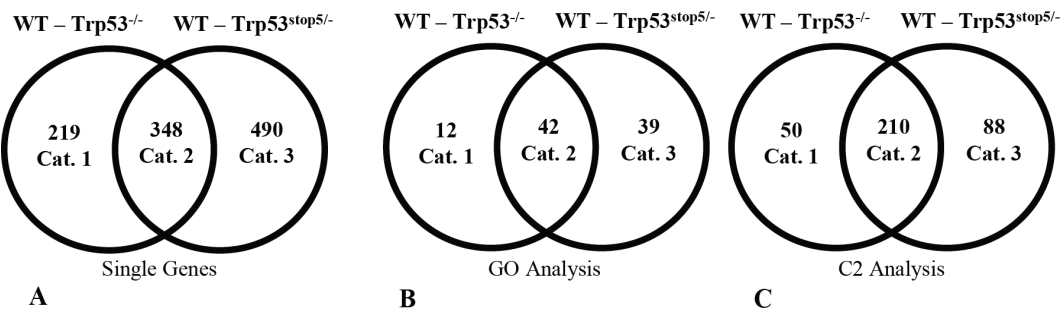


**Figure 4.** Venn diagram ( $p < 0.001$  and  $FR > 1.5$ ) of differential gene-expression (A) and gene ontology (GO) (B) and gene set enrichment (C2) (C) analysis between wild type versus  $Trp53^{-/-}$  and wild type versus  $Trp53^{stop5/-}$  genotypes. Category 1 indicates the number of parameters (single genes, GO or C2) solely significantly regulated between wild type and  $Trp53^{-/-}$  cells. Category 3 indicates the number of parameters (single genes, GO or C2) solely significantly regulated between wild type and  $Trp53^{stop5/-}$  cells. Category 2 shows the overlapping parameters between both the genotype comparisons. Categories 1 + 2 together indicate the total number of significantly regulated parameters (single genes, GO or C2) between wild type and  $Trp53^{-/-}$  cells. Categories 2 + 3 together indicate the total number of significantly regulated parameters between wild type versus  $Trp53^{stop5/-}$  genotypes.

Whole genome analyses on gene ontology (GO) and gene set enrichment (C2) ( $p < 0.005$  and  $FDR = 0.1$ ) on wild type versus  $Trp53^{-/-}$  and wild type versus  $Trp53^{stop5/-}$  genotypes was performed (Figure 4B + 4C). Again,  $Trp53^{stop5/-}$  appears to be more differentially (de)regulated compared to wild type than  $Trp53^{-/-}$ , but both show a larger overlap (42 GO terms and 210 gene sets overlap, Cat. 2 in Figure 4B + 4C) when compared to the transcriptionally significant regulated single genes in Figure 4A. These results together indicate that the present  $\Delta N$ -p53 isoform does in some way reacts similar to the knock-out genotype, but also shows aberrant regulation in several pathways and gene sets. 39 GO terms (Cat.3, Figure 4B) seem to be divergently regulated only in  $Trp53^{stop5/-}$  when compared to wild type, and not when the knock-out is compared to wild type. Amongst these are several developmental processes, plus the GO terms extracellular space, angiogenesis and actin filament binding. C2 analysis resulted in 88 gene sets (Cat.3, Figure 4C) which are only significantly regulated in the  $Trp53^{stop5/-}$

compared to wild type cells. A full overview of the GO and C2 analyses is shown in the Supplementary Info Table 1 (data not shown in this thesis).

A

GO pathway	NES
Extracellular Matrix*	2,08
Collagen*	2,07
Proteinaceous Extracellular Matrix*	2,06
Structural Constituent of Muscle	2,03
Extracellular Matrix Part*	1,98
Regulation of Heart Contraction	1,92
Muscle Development	1,88
Actin Cytoskeleton*	1,87
Developmental Maturation*	1,86
Structural Molecule Activity*	1,83

B

C2 gene set	Description gene set	NES
VEGF_MMMEC_6HRS_UP*	Up-regulated at 6hrs following VEGF treatment of human myometrial microvascular endothelial cells	2,17
CROONQUIST_IL6_STROMA_UP*	Genes upregulated in multiple myeloma cells exposed to the pro-proliferative cytokine IL-6 versus those co-cultured with bone marrow stromal cells	2,14
IRITANI_ADPROX_VASC*	Blood_vascular EC	2,13
GILDEA_BLADDER_UP*	Top 30 genes differentially expressed in metastatic (T24T) and nonmetastatic (T24) human bladder cancer cell lines	2,03
VEGF_MMMEC_12HRS_UP	Up-regulated at 12hrs following VEGF treatment of human myometrial microvascular endothelial cells	2,03
HSA04510_FOCAL_ADHESION*	Focal adhesion	2,02
TSA_HEPATOMA_CANCER_UP*	Cancer-related genes up-regulated in any of four human hepatoma cell lines following 24-hour treatment with 200ng/mL of trichostatin A	2,02
HSA01430_CELL_COMMUNICATION*	Genes involved in cell communication	1,99
CORDERO_KRAS_KD_VS_CONTROL_UP*	Genes up-regulated in kras knockdown vs control in a human cell line	1,98
BRENTANI_CELL_ADHESION	Cancer related genes involved in cell adhesion and metalloproteinases	1,95
JECHLINGER_EMT_UP	Genes up-regulated for epithelial plasticity in tumor progression	1,93
IGLESIAS_E2FMINUS_UP*	Genes that increase in the absence of E2F1 and E2F2	1,93
HSA04512_ECM_RECEPTOR_INTERACTION*	Genes involved in ECM-receptor interaction	1,92
EMT_UP*	Up-regulated during the TGFbeta-induced epithelial-to-mesenchymal transition (EMT) of Ras-transformed mouse mammary epithelial (EpH4) cells (EMT is representative of late-stage tumor progression and metastasis)	1,89
LEE_MYC_E2F1_UP*	Genes up-regulated in hepatoma tissue of Myc+E2f1 transgenic mice	1,88
TGFBETA_ALL_UP*	Up-regulated by TGF-beta treatment of skin fibroblasts, at any time point	1,87
TGFBETA_EARLY_UP*	Up-regulated by TGF-beta treatment of skin fibroblasts at 30 min (clusters 1-3)	1,85
TGFBETA_C2_UP	Up-regulated by TGF-beta treatment of skin fibroblasts, cluster 2	1,83
LEE_E2F1_UP*	Genes up-regulated in hepatoma tissue of E2f1 transgenic mice	1,81
RUTELLA_HEPATGFSNDCS_UP	Genes up-regulated by HGF treatments, growth factor treatment	1,79
BRCA_BRCA1_NEG*	Genes whose expression is consistently negatively correlated with brca1 germline status in breast cancer - higher expression is associated with BRCA1 tumors	1,75
BAF57_BT549_UP*	Up-regulated following stable re-expression of BAF57 in Bt549 breast cancer cells that lack functional BAF57	1,75
BRCA1_OVEREXP_PROSTATE_UP*	Up-regulated with stable, ectopic overexpression of BRCA1 in DU-145 human prostate cancer cell lines, compared to neo-only controls	1,69
HDACI_COLON_BUT12HRS_UP*	Up-regulated by butyrate at 12 hrs in SW260 colon carcinoma cells	1,67

**Table 2.** Significant differential Gene Ontology pathways (A) and GSEA C2 gene sets (B) between *Trp53*<sup>stop5/-</sup> and *Trp53*<sup>-/-</sup> genotypes.  $p < 0.005$  and FDR = 0.1, NES = normalized enrichment score. \* Already significantly differential from wild type in *Trp53*<sup>-/-</sup> and *Trp53*<sup>stop5/-</sup>.

We subsequently conducted whole genome GO and C2 analyses ( $p < 0.005$  and FDR = 0.1) between the *Trp53*<sup>-/-</sup> and the *Trp53*<sup>stop5/-</sup> genotypes to further elucidate the differences between the two (Supplementary Info Table 2, data not shown in this thesis). The GO analysis shows 10 pathways differentially and significantly regulated between the two genotypes (Table 2A), while 82 gene sets are aberrantly regulated. Seven out of the 10 GO terms overlap with those shown in Figure 4B, and are, therefore, even stronger significantly upregulated in *Trp53*<sup>stop5/-</sup>. Again, collagen and extracellular matrix pathways are more regulated in *Trp53*<sup>stop5/-</sup> when compared to the knock out ES cells.

The 82 differential C2 gene sets contain several gene sets which are linked to cancer, growth, invasiveness and TGF-beta signaling pathways. Of these gene sets, 48 were present in the overlapping 210 gene sets in Figure 4C, which means they were already significantly differential from wild type in both p53 impaired ES cells. A selection of gene sets is shown in Table 2B. In addition, Supplemental Info Table 3 (data not shown in this thesis) shows a selection of single genes, most of which are involved in the pathways and gene sets mentioned in Table 2.

## Discussion

P53 is the most commonly mutated gene in mammalian tumors [<sup>20</sup>]. Its role as a tumor suppressor in the prevention of cancer is multifaceted, since the p53 protein interacts with and transactivates a wide variety of key proteins. P53-deficient organisms show a strong increase in the rate of tumor onset and subsequently in the development of multiple tumor types [<sup>21-23</sup>].

In our present study, 2-AAF induced urinary bladder tumors in *Trp53*<sup>+/-</sup> and *Xpa*<sup>-/-</sup>/*Trp53*<sup>+/-</sup> mice harboring *Trp53* mutations. Single base mutations, predominantly in specific G:C → T:A transversions, were found. In agreement with other studies [<sup>24;25</sup>], we found several missense mutations in the DNA binding domain. Interestingly however, a high percentage of nonsense mutations was present predominantly at the 5' end of the *Trp53* gene. There is a significant selection ( $p = 0.0011$  Chi-square test) for these N-terminal nonsense mutations found in the bladder tumors induced after 2-AAF exposure.

Immunohistochemical staining confirmed that p53 protein was present in the tumor cells, but the protein lacked the N-terminal domain. Using homologous recombination experiments in ES cells we demonstrated that codon 41 is used as a novel start site when a nonsense mutation is present at codon 5. This is most likely also the case for the other nonsense mutation variants we found located upstream of codon 41 (Table 1). The manner in which this 'forced' isoform translation takes place due to the 5' nonsense mutations is unknown and needs further investigation. Previous reports have shown that internal ribosomal entry sites (IRES) can play a role and can be phase-dependent on the cell cycle [<sup>4;26</sup>]. Another option might be that translational leakage occurs and 'false' initiation takes place at codon 41, which is surrounded by a Kozak consensus sequence [<sup>19</sup>].

The existence of ΔN-p53 has already been reported [<sup>1;27</sup>], but up to now it was not known that selectively induced N-terminal stop mutations could be the origin of this p53-isoform. Unlike many other studies which have only focused on sequencing the DNA binding domain (exon 4 to 8) our studies characterized exon 2 to 8 of the *Trp53* gene. This could be one of the reasons why these

specific 5' end stop mutations went undetected until now. Additionally, bladder tumors are not amongst the most commonly found tumor types.

Previously, it was shown that  $\Delta$ N-p53 originates from alternative splicing events [28;29] or occurs as a natural isoform [1;30]. Courtois et al. proposed that alternative translation initiation at codon 41 was not inducible in response to stress [1]. However, our results show that genotoxic stress can be a cause of selection for the  $\Delta$ N-p53 isoform due to the 2-AAF induced 5' end nonsense mutations.

It has been reported that  $\Delta$ N-p53 does not carry autonomous transcriptional activity, most likely due to the lack of the N-terminal transactivation domain [1;3;29]. However, Powell et al. performed vector transfection induced expression in H1299 human lung cells, conducted macroarray profiling investigating 84 p53-related genes and showed stress-dependent changes in gene expression [31]. Ohki et al. showed deletion of the complete p53 first activation domain (including the alternative start codon 41) in *Saos2*-cells induced apoptotic genes that were not induced by the full length p53 [32]. We are the first to investigate if the  $\Delta$ N-p53 isoform has different functional transcriptional properties in a stable knock-in mutant cell line, comparing untreated cells to wild type and p53 knock out cell lines derived from the same genetic background on a full genome scale.

Results showed a clear difference at the transcriptional level between the wild type and both the *Trp53<sup>stop5/-</sup>* and *Trp53<sup>-/-</sup>* ES cells, but additional evident disparities between the *Trp53<sup>stop5/-</sup>* and *Trp53<sup>-/-</sup>* genotypes were also discovered. Several developmental and regulatory processes, together with pathways involved in extracellular space, angiogenesis and actin filament binding are expressed at higher levels in *Trp53<sup>stop5/-</sup>* cells than in p53 knock out cells. The same holds when GO term analysis was applied, processes involved in the formation of the extracellular matrix and the production of collagen are expressed at higher levels in *Trp53<sup>stop5/-</sup>* cells than *Trp53<sup>-/-</sup>* cells (Table 2A). These pathways are also found upregulated in invasive tumors and are known to be involved in metastasis [33;34]. Additionally, gene sets (Table 2B) and single genes (Supplemental Info Table 3) which are correlated with cancer, growth, invasiveness, metastasis and TGF-beta signaling are significantly regulated in an increased manner in *Trp53<sup>stop5/-</sup>* ES cells when compared to knock-out cells.

The effects on gene expression were all examined in ES cells and suggest that *Trp53<sup>stop5/-</sup>* cells have a distinct phenotype compared to *Trp53<sup>-/-</sup>* cells. However, the selective outcome of exposure to 2-AAF was seen in epithelial bladder tissue. For a fair characterization of the functional effect of  $\Delta$ N-p53 an *in vivo* analysis is more suitable. We, therefore, are currently creating mouse models which transcribe the isoform of p53 in different genotypical backgrounds (*Trp53<sup>stop5/+</sup>* and *Trp53<sup>stop5/-</sup>*). Exposure of these models to 2-AAF and/or other stressors should shed more light on the origin, selection and function of the p53 isoform. Additionally, it can not be excluded that the gene expression profiles of wild type and *Trp53<sup>stop5/-</sup>* cells are also influenced by splice variants of *Trp53*. Some splice variants of *Trp53* which are present in normal cells might also occur for the  $\Delta$ N-p53 isoform, therefore the expression profiles could be the result of a combined expression, eventhough Western blotting shows no additional other sized proteins.

In conclusion, our data suggest that the N-terminal truncated p53 isoform can originate upon genotoxic stress due to the introduction of selective nonsense mutations in the p53 gene. Additionally, this study provides evidence that the transcriptional activity in cells expressing the  $\Delta$ N-p53 isoform is



functionally divergent from p53 knock-out cells and may lead to an even more malignant phenotype and possibly has some gain-of-function properties.

### **Conflict of interest**

The authors declare no conflict of interest.

### **Acknowledgements**

We would like to thank the Animal Facilities of the Netherlands Vaccine Institute (NVI) for their skillful (bio)technical support. The work presented here was in part supported by NIH/NIEHS (Comparative Mouse Genomics Centers Consortium) grant 1U01 ES11044.

**Supplementary information** is available at [www.nature.com/onc/index.html](http://www.nature.com/onc/index.html)

## Reference List

- [1] S.Courtois, G.Verhaegh, S.North, M.G.Luciani, P.Lassus, U.Hibner, M.Oren, P.Hainaut. DeltaN-p53, a natural isoform of p53 lacking the first transactivation domain, counteracts growth suppression by wild-type p53, *Oncogene*, 21, (2002) 6722-6728.
- [2] M.M.Candeias, D.J.Powell, E.Roubalova, S.Apcher, K.Bourougaa, B.Vojtesek, H.Bruzzoni-Giovanelli, R.Fahraeus. Expression of p53 and p53/47 are controlled by alternative mechanisms of messenger RNA translation initiation, *Oncogene*, 25, (2006) 6936-6947.
- [3] V.Marcel, P.Hainaut. p53 isoforms - a conspiracy to kidnap p53 tumor suppressor activity?, *Cell Mol.Life Sci.*, 66, (2009) 391-406.
- [4] R.Grover, M.M.Candeias, R.Fahraeus, S.Das. p53 and little brother p53/47: linking IRES activities with protein functions, *Oncogene*, (2009).
- [5] C.Heinlein, F.Krepulat, J.Lohler, D.Speidel, W.Deppert, G.V.Tolstonog. Mutant p53(R270H) gain of function phenotype in a mouse model for oncogene-induced mammary carcinogenesis, *Int.J.Cancer*, 122, (2008) 1701-1709.
- [6] S.W.Wijnhoven, E.Zwart, E.N.Speksnijder, R.B.Beems, K.P.Olive, D.A.Tuveson, J.Jonkers, M.M.Schaap, B.J.van den, T.Jacks, H.van Steeg, A.de Vries. Mice expressing a mammary gland-specific R270H mutation in the p53 tumor suppressor gene mimic human breast cancer development, *Cancer Res.*, 65, (2005) 8166-8173.
- [7] E.M.Hoogervorst, W.Bruins, E.Zwart, C.T.van Oostrom, G.J.van den Aardweg, R.B.Beems, B.J.van den, T.Jacks, H.van Steeg, A.de Vries. Lack of p53 Ser389 phosphorylation predisposes mice to develop 2-acetylaminofluorene-induced bladder tumors but not ionizing radiation-induced lymphomas, *Cancer Res.*, 65, (2005) 3610-3616.
- [8] A.de Vries, E.R.Flores, B.Miranda, H.M.Hsieh, C.T.van Oostrom, J.Sage, T.Jacks. Targeted point mutations of p53 lead to dominant-negative inhibition of wild-type p53 function, *Proc.Natl.Acad.Sci.U.S.A*, 99, (2002) 2948-2953.
- [9] T.Iwakuma, G.Lozano. Crippling p53 activities via knock-in mutations in mouse models, *Oncogene*, 26, (2007) 2177-2184.
- [10] A.J.Levine. p53, the cellular gatekeeper for growth and division, *Cell*, 88, (1997) 323-331.
- [11] S.Hailfinger, M.Jaworski, P.Marx-Stoelting, I.Wanke, M.Schwarz. Regulation of P53 stability in p53 mutated human and mouse hepatoma cells, *Int.J.Cancer*, 120, (2007) 1459-1464.
- [12] S.Strano, S.Dell'Orso, S.Di Agostino, G.Fontemaggi, A.Sacchi, G.Blandino. Mutant p53: an oncogenic transcription factor, *Oncogene*, 26, (2007) 2212-2219.
- [13] Y.Xu. Induction of genetic instability by gain-of-function p53 cancer mutants, *Oncogene*, 27, (2008) 3501-3507.
- [14] G.Lozano. The oncogenic roles of p53 mutants in mouse models, *Curr.Opin.Genet.Dev.*, 17, (2007) 66-70.
- [15] E.M.Hoogervorst, H.van Steeg, A.de Vries. Nucleotide excision repair- and p53-deficient mouse models in cancer research, *Mutat.Res.*, 574, (2005) 3-21.
- [16] E.M.Hoogervorst, C.T.van Oostrom, R.B.Beems, J.van Benthem, S.Gielis, J.P.Vermeulen, P.W.Wester, J.G.Vos, A.de Vries, H.van Steeg. p53 heterozygosity results in an increased 2-acetylaminofluorene-induced urinary bladder but not liver tumor response in DNA repair-deficient Xpa mice, *Cancer Res.*, 64, (2004) 5118-5126.
- [17] J.A.Ross, S.A.Leavitt. Induction of mutations by 2-acetylaminofluorene in lacI transgenic B6C3F1 mouse liver, *Mutagenesis*, 13, (1998) 173-179.
- [18] K.H.Vousden, J.L.Bos, C.J.Marshall, D.H.Phillips. Mutations activating human c-Ha-ras1 protooncogene (HRAS1) induced by chemical carcinogens and depurination, *Proc.Natl.Acad.Sci.U.S.A*, 83, (1986) 1222-1226.
- [19] M.Kozak. Compilation and analysis of sequences upstream from the translational start site in eukaryotic mRNAs, *Nucleic Acids Res.*, 12, (1984) 857-872.

- [20] L.Y.Lim, N.Vidnovic, L.W.Ellisen, C.O.Leong. Mutant p53 mediates survival of breast cancer cells, *Br.J.Cancer*, 101, (2009) 1606-1612.
- [21] A.Matheu, A.Maraver, M.Serrano. The Arf/p53 pathway in cancer and aging, *Cancer Res.*, 68, (2008) 6031-6034.
- [22] A.J.Levine, J.Momand, C.A.Finlay. The p53 tumour suppressor gene, *Nature*, 351, (1991) 453-456.
- [23] M.Hollstein, D.Sidransky, B.Vogelstein, C.C.Harris. p53 mutations in human cancers, *Science*, 253, (1991) 49-53.
- [24] A.Sigal, V.Rotter. Oncogenic mutations of the p53 tumor suppressor: the demons of the guardian of the genome, *Cancer Res.*, 60, (2000) 6788-6793.
- [25] T.Soussi. p53 alterations in human cancer: more questions than answers, *Oncogene*, 26, (2007) 2145-2156.
- [26] P.S.Ray, R.Grover, S.Das. Two internal ribosome entry sites mediate the translation of p53 isoforms, *EMBO Rep.*, 7, (2006) 404-410.
- [27] B.Maier, W.Gluba, B.Bernier, T.Turner, K.Mohammad, T.Guise, A.Sutherland, M.Thorner, H.Scrable. Modulation of mammalian life span by the short isoform of p53, *Genes Dev.*, 18, (2004) 306-319.
- [28] Y.Yin, C.W.Stephen, M.G.Luciani, R.Fahraeus. p53 Stability and activity is regulated by Mdm2-mediated induction of alternative p53 translation products, *Nat.Cell Biol.*, 4, (2002) 462-467.
- [29] A.Ghosh, D.Stewart, G.Matlashewski. Regulation of human p53 activity and cell localization by alternative splicing, *Mol.Cell Biol.*, 24, (2004) 7987-7997.
- [30] P.S.Ray, R.Grover, S.Das. Two internal ribosome entry sites mediate the translation of p53 isoforms, *EMBO Rep.*, 7, (2006) 404-410.
- [31] D.J.Powell, R.Hrstka, M.Candeias, K.Bourougaa, B.Vojtesek, R.Fahraeus. Stress-dependent changes in the properties of p53 complexes by the alternative translation product p53/47, *Cell Cycle*, 7, (2008) 950-959.
- [32] R.Ohki, T.Kawase, T.Ohta, H.Ichikawa, Y.Taya. Dissecting functional roles of p53 N-terminal transactivation domains by microarray expression analysis, *Cancer Sci.*, 98, (2007) 189-200.
- [33] H.Denys, G.Braems, K.Lambein, P.Pauwels, A.Hendrix, A.De Boeck, V.Mathieu, M.Bracke, O.De Wever. The extracellular matrix regulates cancer progression and therapy response: implications for prognosis and treatment, *Curr.Pharm.Des*, 15, (2009) 1373-1384.
- [34] S.M.Pupa, S.Menard, S.Forti, E.Tagliabue. New insights into the role of extracellular matrix during tumor onset and progression, *J.Cell Physiol*, 192, (2002) 259-267.
- [35] K.P.Olive, D.A.Tuveson, Z.C.Ruhe, B.Yin, N.A.Willis, R.T.Bronson, D.Crowley, T.Jacks. Mutant p53 gain of function in two mouse models of Li-Fraumeni syndrome, *Cell*, 119, (2004) 847-860.
- [36] T.Jacks, L.Remington, B.O.Williams, E.M.Schmitt, S.Halachmi, R.T.Bronson, R.A.Weinberg. Tumor spectrum analysis in p53-mutant mice, *Curr.Biol.*, 4, (1994) 1-7.
- [37] W.Bruins, E.Zwart, L.D.Attardi, T.Iwakuma, E.M.Hoogervorst, R.B.Beems, B.Miranda, C.T.van Oostrom, B.J.van den, G.J.van den Aardweg, G.Lozano, H.van Steeg, T.Jacks, A.de Vries. Increased sensitivity to UV radiation in mice with a p53 point mutation at Ser389, *Mol.Cell Biol.*, 24, (2004) 8884-8894.
- [38] R.A.Irizarry, B.M.Bolstad, F.Collin, L.M.Cope, B.Hobbs, T.P.Speed. Summaries of Affymetrix GeneChip probe level data, *Nucleic Acids Res.*, 31, (2003) e15.
- [39] W.C.de Leeuw, H.Rauwerda, M.J.Jonker, T.M.Breit. Salvaging Affymetrix probes after probe-level re-annotation, *BMC.Res.Notes*, 1, (2008) 66.
- [40] R Development Core Team. A language and environment for statistical computing. 2008.
- [41] G.Dennis, Jr., B.T.Sherman, D.A.Hosack, J.Yang, W.Gao, H.C.Lane, R.A.Lempicki. DAVID: Database for Annotation, Visualization, and Integrated Discovery, *Genome Biol.*, 4, (2003) 3.
- [42] D.A.Hosack, G.Dennis, Jr., B.T.Sherman, H.C.Lane, R.A.Lempicki. Identifying biological themes within lists of genes with EASE, *Genome Biol.*, 4, (2003) R70.





# Chapter 7

# Chapter 7

## Discussion

*"Keep your head up, we are nearly there"*

Strange Colour Blue – Madrugada, 1999

## Discussion and Future Prospects

DNA damage, mutations and genomic instability are established driving forces of cancer and other age-related diseases. Mutations in tumor suppressor genes and oncogenes are very frequently found in tumors and genomic instability is the most common enabling characteristic of cancer. Aging can be characterized by progressive functional decline, gradual deterioration of physiological function, decrease in fertility and viability and increase in vulnerability. Also aging is believed to be enabled, amongst others, by genomic instability. DNA repair pathways and cell cycle control processes are therefore vital to organisms, since these processes counteract or prevent genomic instability, and are thought to underlie, when affected, aging and age-related diseases like cancer.

To unravel the functions, mechanisms and pathways involved in the onset of aging and age-related diseases we have investigated several mouse models deficient in either DNA repair capacity (**Chapter 3, 4**), cell cycle control (**Chapter 6**) or both (**Chapter 5**), and compared this to a wild type situation (**Chapter 2**).

The use of mouse models enabled us to investigate cancer and aging in a controlled environment, minimizing possible confounding factors. Additionally, the mouse models can be useful to identify carcinogens that can be harmful to the society and the environment (**Chapter 4**).

This thesis emphasizes the importance of functional DNA repair by investigating the consequences of deficient DNA repair. To assess the 'abnormal', one should first try to investigate or establish the 'normal' situation. We therefore investigated wild type C57BL/6J mice together with two knockout mouse models (also in C57BL/6J genetic background) that are deficient for the Nucleotide Excision Repair (NER) pathway. NER is a very important, versatile and highly conserved DNA repair pathway in mammals, eukaryotes and prokaryotes. **Chapter 2** describes the processes that are apparent over time during the entire aging process using cross sectional time points during the lifespan of the C57BL/6J wild type mice. Here, we show chronological and biological (individual) aging is hard to capture by just a few parameters and both the chronological as well as the biological aspect are of importance. However integrating the two enabled us to verify certain aging markers and propose novel biomarkers related to chronological and biological aging. This study also pointed out that aging is an inevitable but stochastic process that results in many different outcomes and that even in the same animal tissues age differently. Overall in spleen and kidney for example, immune responses appear to be regulated mostly during aging. In liver, energy homeostasis demonstrated to be one of the most regulated processes.

Processes that are believed to facilitate cancer and other age-related characteristics were hard to capture in this setting. However, if specific genes in DNA repair pathways are knocked out, the effect of DNA damage on aging and cancer can be investigated. First, we have characterized the *Xpa* and *Xpc*-deficient mouse models in a comprehensive survival study in **Chapter 3** and demonstrated that deficiencies in NER resulted in an increased mutational load and cancer incidence, together with a significant decrease in survival for *Xpc* mice only. The XPA and XPC proteins belong to the same repair pathway and both have a cancer prone phenotype, but still though we found a divergent outcome. *Xpc* mice showed a broader tumor spectrum than *Xpa* mice. Besides the overlapping increase in liver

tumor incidence, lung tumors were significantly elevated in *Xpc* only. A strong elevated lung tumor incidence was also found in *Xpc* mice with a mixed genetic background (C57BL/6-129) [1].

XPA is functional in both routes of NER, Transcription Coupled Repair (TC-NER) and Global Genome Repair (GG-NER) while XPC only functions in GG-NER. The divergent tumor phenotype of the two mouse models directed us to the possibility that XPC could be functional outside NER as well. Since the incidence of lung tumors was elevated and the mice were only exposed to control feed, water and air, oxidative DNA damage could be the reason for the increased sensitivity exhibited by *Xpc* mice. In **Chapter 3** and **Chapter 4** we directly demonstrated, for the first time *in vivo*, that this is indeed the case. XPC is involved in the prevention and/or removal of oxidative DNA damage. When functional XPC is absent, mutations accumulate significantly upon oxidative stress, which is not the case when XPA is not functional or in wild type mice and cells. Also the anti-oxidant response is decreased and the cell cycle progression appears increased in the *Xpc* mouse model, compared to wild type and *Xpa* mice. These processes would facilitate fixation of oxidative DNA damage into mutations. Recent (mostly *in vitro*) data from other studies support the hypothesis that XPC is functional outside NER and is possibly involved in base excision repair, redox homeostasis or cell cycle control. It has previously been suggested that mutations in internal tumors of XP-C patients could be the result of unrepaired lesions caused by oxidative damage. This is now supported by our *in vivo* data. XP-C patients and carriers of SNPs in this gene could benefit from this knowledge, since they might be more sensitive to other sources of DNA damage besides UV and other bulky adduct inducing agents. These novel findings lead to new understandings of the function of XPC.

The broader tumor spectrum and possible additional functions of XPC could be a useful asset in the search of suitable alternatives for carcinogenicity testing. Currently, the 2-year bioassay in mice and rats is considered as the golden standard to predict carcinogenic features of chemicals. This assay is however extremely time-consuming, expensive and requires many animals for testing.

Our previous studies showed that the *Xpa*\**p53* model is able to predict carcinogenic potential of chemical compounds with high accuracy and is even able to identify non-genotoxic carcinogens [2,3]. These predictions were accomplished upon 39 weeks (short-term) of exposure and more importantly with a strong decrease in the number of animals needed. As a next step we tested the *Xpc*\**p53* mouse model in *in vivo* carcinogenicity exposure studies. In **Chapter 5** we showed that the *Xpc*\**p53* mouse model is an attractive candidate to use in short-term carcinogenicity testing. The model conserves all the beneficial aspects of the *Xpa*\**p53* mouse model (prediction of both genotoxic and non-genotoxic carcinogens after short-term exposure), but additionally the response to toxicity is similar to the wild type situation. *Xpa*\**p53* mice are more sensitive towards genotoxicity compared to wild type mice. Consequently the use of lower dosages in *Xpa*\**p53* mice, compared to wild type, for carcinogenicity testing is required, which is a complicating factor in risk assessment.

The outcome of the short-term carcinogenic exposure to 2-AAF in both *Xpa*\**p53* as well as *Xpc*\**p53* mice resulted in a severe increase in bladder cancer incidence. In **Chapter 6** we further characterized the 2-AAF induced bladder tumors from *Xpa*\**p53* mice. We found an unusual mutation spectrum in the wild type *p53* allele, which appeared to be the cause for the increased incidence of the bladder cancers, as described in **Chapter 5**. Besides confirming the very high percentage of *Trp53* mutations in the set of urinary bladder tumors of these mice, we made the surprising discovery that a selection for a functional N-terminal truncated isoform of *p53* occurred after 2-AAF exposure. Hereby, we showed



dN-p53 isoform formation does not only occur by alternative splicing events [<sup>4</sup>], but can also be driven by genotoxic exposure. In the presence of full length p53 the isoform could either have a dominant negative effect, inhibiting both p53 transcriptional activity and p53-mediated apoptosis [<sup>5,6</sup>]. However, the induction of this p53 isoform could on the other hand possibly have a protective effect in a normal cell where both functional alleles of *Trp53* are present: if one *Trp53* allele is damaged by genotoxic exposure, translocation for degradation of p53 by MDM2 could possibly be slowed down, since MDM2 cannot bind to an N-terminal region anymore. The formation of a dN-p53 isoform could therefore putatively result in a prolonged cell cycle arrest or apoptotic response. Previous studies showed an enhanced p53 transcriptional activation [<sup>7</sup>]. Also, a recent finding in human ovarian tumors indicated that high levels of dN-p53 indicated a favorable role of dN-p53 in patients with mucinous ovarian cancer [<sup>8</sup>].

### **Future Prospects**

The work of this thesis presents novel insights in DNA repair and cell cycle control mechanisms. But, as is usually the case with research, besides solving a few questions, even more are raised by the obtained results. It is clear that NER is an important asset to counteract aging and age-related diseases like cancer, but deficiencies of different proteins in the NER pathway can result into a divergent pathological outcome (also indicated in Table 2 of **Chapter 1**). These findings also broaden the scope of DNA repair and show that pathways do not solely act on their own, but interact and complement each other even more than previously was assumed. These results urge scientists to look further and explore these mechanisms even more closely. New technologies and research areas of e.g. microRNA and post-translational regulation are an interesting addition to the presented research in this thesis. Methylation, acetylation, ubiquitination, sumoylation and phosphorylation together with regulation by microRNAs are most likely important factors in the regulation of DNA repair and cell cycle control. The available data on these processes is only the tip of the iceberg and should be investigated more thoroughly.

Besides a fundamental approach, these results provide a good starting point for more applied science. The discovery of possible novel XPC functions could be beneficial to XP-C patients and carriers of certain XPC variant alleles, which might be more sensitive towards oxidative stress. Intervention treatments using antioxidants or compounds stimulating antioxidant response are putative beneficial applications. Furthermore, the functions of the several p53 isoforms (and also their closely related family members, isoforms of p63 and p73) are yet to be fully revealed and could possibly be used in cancer therapy if clinical relevance and effects on prognosis is further confirmed.

Additionally, the double transgenic mouse models *Xpa*\**p53* and *Xpc*\**p53* proved to be promising alternatives in carcinogenicity testing and can already be directly applied. The *Xpa*\**p53* mouse model has been adopted by the International Conference on Harmonization Expert Working Group on Safety in combination with the traditional 2-year cancer bioassay in rats for the evaluation of the carcinogenic potential of pharmaceuticals. Under the European REACH policy this model is recommended as a good alternative to the 2-year bioassay. Further research could do the same for the *Xpc*\**p53* mouse model. Moreover, implementation of these alternatives should be recognized by industries and where necessary encouraged by legislative and governmental bodies. Implementation could mean a strong decrease in the use of animals for carcinogenicity testing, would speed up the

process of identifying harmful carcinogens and be economically beneficial. This would especially hold true when transgenic rat models could also be used as an alternative for the 2-year rat bioassay. With the current available technologies it should be possible to replace the current testing strategy with a more suitable strategy in the near future.

## Reference List

- [1] M.C.Hollander, R.T.Philburn, A.D.Patterson, S.Velasco-Miguel, E.C.Friedberg, R.I.Linnoila, A.J.Fornace, Jr. Deletion of XPC leads to lung tumors in mice and is associated with early events in human lung carcinogenesis, *Proc.Natl.Acad.Sci.U.S.A*, 102, (2005) 13200-13205.
- [2] C.F.van Kreijl, P.A.McAnulty, R.B.Beems, A.Vynckier, H.van Steeg, R.Fransson-Steen, C.L.Alden, R.Forster, J.W.van der Laan, J.Vandenbergh. Xpa and Xpa/p53+/- knockout mice: overview of available data, *Toxicol.Pathol.*, 29 Suppl, (2001) 117-127.
- [3] H.van Steeg, H.Klein, R.B.Beems, C.F.van Kreijl. Use of DNA repair-deficient XPA transgenic mice in short-term carcinogenicity testing, *Toxicol.Pathol.*, 26, (1998) 742-749.
- [4] J.C.Bourdon, K.Fernandes, F.Murray-Zmijewski, G.Liu, A.Diot, D.P.Xirodimas, M.K.Saville, D.P.Lane. p53 isoforms can regulate p53 transcriptional activity, *Genes Dev.*, 19, (2005) 2122-2137.
- [5] S.Courtois, G.Verhaegh, S.North, M.G.Luciani, P.Lassus, U.Hibner, M.Oren, P.Hainaut. DeltaN-p53, a natural isoform of p53 lacking the first transactivation domain, counteracts growth suppression by wild-type p53, *Oncogene*, 21, (2002) 6722-6728.
- [6] A.Ghosh, D.Stewart, G.Matlashewski. Regulation of human p53 activity and cell localization by alternative splicing, *Mol.Cell Biol.*, 24, (2004) 7987-7997.
- [7] R.U.Janicke, V.Graupner, W.Budach, F.Essmann. The do's and don'ts of p53 isoforms, *Biol.Chem.*, 390, (2009) 951-963.
- [8] G.Hofstetter, A.Berger, R.Berger, A.Zoric, E.I.Braicu, D.Reimer, H.Fiegl, C.Marth, A.G.Zeimet, H.Ulmer, U.Moll, R.Zeillinger, N.Concin. The N-terminally truncated p53 isoform Delta40p53 influences prognosis in mucinous ovarian cancer, *Int.J.Gynecol.Cancer*, 22, (2012) 372-379.



# Samenvatting

## Nederlandse samenvatting

Alle cellen in ons lichaam bevatten DNA. DNA is de blauwdruk van het leven en bevat alle genetische informatie die het mogelijk maakt om te functioneren en je te ontwikkelen. Het DNA bevat duizenden specifieke stukken informatie (genen). Deze genen zijn verantwoordelijk voor de productie van functionele en structurele bouwstenen in onze cellen (eiwitten).

Het is van belang om de genetische informatie zo min mogelijk beschadigd te laten raken zodat cellen normaal kunnen blijven functioneren. DNA wordt echter constant blootgesteld aan schadelijke factoren van buitenaf (exogeen), zoals UV-straling van het zonlicht, tabaksrook, stoffen in voedsel en dranken. Maar ook factoren die het lichaam zelf genereert (endogeen) kunnen schadelijk zijn. Een voorbeeld hiervan is je metabolisme, waarbij onder andere reactieve zuurstofradicalen kunnen ontstaan.

Schadelijke moleculen kunnen reageren met het DNA en daar beschadigingen veroorzaken. Dit gebeurt in groten getale. In iedere cel vinden naar schatting door endogene factoren alleen al ongeveer 50.000 DNA beschadigingen per dag plaats! Een uurtje zonnebaden op een zonnige dag levert ongeveer 80.000 DNA beschadigingen op per blootgestelde cel. In het totale lichaam loopt het aantal dagelijkse DNA beschadigingen dus op tot in de biljoenen.

DNA schade en de daaruit voortkomende mutaties en genomische instabiliteit in cellen zijn de drijvende kracht achter het ontstaan van kanker en andere verouderingsgerelateerde ziekten bij mens en dier. Zo zorgt teveel UV-straling door onbeschermd zonnen of veel roken bijvoorbeeld voor veel extra DNA schade en de kans dat hierdoor kanker ontstaat wordt daardoor groter. Tijdens het leven en veroudering groeit het aantal beschadigingen in het DNA waardoor cellen en processen in het lichaam minder goed of efficiënt functioneren. **Hoofdstuk 2** beschrijft het proces van veroudering over 6 verschillende levensfasen (onderzocht in muizen). We volgden hier de pathologische veranderingen tijdens het leven en koppelden dit waar mogelijk aan de veranderingen in activiteit van alle genen om zo meer inzicht te krijgen over processen die tijdens veroudering een rol kunnen spelen.

Het lichaam heeft een aantal erg goede afweersystemen om DNA schade te voorkomen of te repareren. Zo neutraliseren antioxidanten in de cellen zoveel mogelijk reactieve zuurstofradicalen waardoor ze niet meer met het DNA kunnen reageren. Ook probeert ons lichaam zo snel mogelijk schadelijke stoffen af te breken, zodat ze niet meer met het DNA kunnen reageren en geen schade kunnen veroorzaken. Dit mechanisme is echter niet genoeg om het DNA schadevrij te houden en daarom zijn DNA herstelmechanismen van groot belang in ons lichaam. Deze mechanismen repareren en beperken de DNA schade zodat cellen (zolang mogelijk) normaal kunnen blijven functioneren.

Er zijn verschillende reparatiesystemen in het lichaam actief die allemaal op een specifieke manier werken en verschillende soorten DNA schade repareren. Eén van deze DNA herstelmechanismen in het Nucleotide Excisie Reparatie (NER) mechanisme, die beschadigingen repareert die de helixstructuur van het DNA verstoren (bijvoorbeeld door UV-straling en sommige stoffen in tabaksrook of voedselwaren). NER kan worden onderverdeeld in twee sub-routes: transcriptie-gekoppeld (TC-NER) herstel en globaal genoomherstel (GG-NER). TC-NER repareert de schade in actieve genen, terwijl GG-NER schade in het hele genoom verwijdert. De twee NER-routes verschillen in de manier van het

herkennen van de DNA schade, maar repareren vervolgens op eenzelfde manier de schade. NER bestaat uit meer dan 30 eiwitten die samenwerken om de schade te repareren.

Wanneer één van de meest essentiële NER-factoren defect is kan dit leiden tot zeldzame ziektes zoals Xeroderma pigmentosum (XP), Trichothiodystrophy (TTD) of Cockayne syndroom (CS). XP patiënten hebben een extreem hoog risico (>1000x zo hoog als gezonde mensen) op huidkanker wanneer ze bloot worden gesteld aan zonnestraling. CS en TDD patiënten hebben een defect TC-NER, wat zich voornamelijk manifesteert in groei- en neurologische afwijkingen. In **hoofdstuk 3** is het belang van twee essentiële NER-factoren (XPA en XPC) onderzocht. Muizen die een defect *Xpa* of *Xpc* gen hebben blijken gevoeliger te zijn voor spontane ontwikkeling van kanker dan normale muizen gedurende veroudering. In een *Xpa* muis is TC-NER en GG-NER defect, in een *Xpc* muis alleen GG-NER. We ontdekten dat de kankergevoeligheid van *Xpa* en *Xpc* muizen ook van elkaar verschilde en *Xpc* gevoeliger was, ondanks het feit dat alleen GG-NER niet functioneert. Beide muismodellen lieten een vergelijkbare toename in levertumoren zien, maar in *Xpc* muizen ontstonden daarnaast nog meer longtumoren. Dit laatste was niet het geval in *Xpa* en normale (wild type) muizen. Aangezien de longen worden blootgesteld aan zuurstof hebben we in **hoofdstuk 4** onderzocht of *Xpc* muizen gevoeliger zijn dan normale en *Xpa* muizen voor schade die door zuurstofradicalen wordt veroorzaakt. DNA schade door zuurstofradicalen wordt voor het grootste gedeelte niet gerepareerd door NER, maar door een ander DNA herstelmechanisme: Base Excisie Reparatie (BER). Onze resultaten duiden erop dat *Xpc* muizen inderdaad meer blijvende DNA schade (in de vorm van mutaties) ophopen na blootstelling aan stoffen die zorgen voor meer zuurstofradicalen in de cellen, in tegenstelling tot wild type en *Xpa* muizen. De XPC-factor lijkt daarom ook betrokken te zijn bij processen buiten NER, die DNA schade door zuurstofradicalen voorkomen of achteraf repareren.

Muizen met een defect DNA herstelmechanisme zoals de *Xpa* en *Xpc* muizen, kunnen niet alleen gebruikt worden voor het bestuderen van kankerontwikkeling en verouderingsgerelateerde ziektes, maar kunnen ook ingezet worden om nauwkeuriger, efficiënter en goedkoper kankerverwekkende stoffen te identificeren. Mens en milieu dienen zo min mogelijk in aanraking te komen met kankerverwekkende stoffen. Daarom worden stoffen uitvoerig getest alvorens ze op de markt mogen worden gebracht en verwerkt mogen worden in consumentengoederen. Om deze stoffen te identificeren worden momenteel testen gebruikt die niet heel erg nauwkeurig zijn en grote aantallen proefdieren vereisen. Daarnaast duren deze onderzoekstudies erg lang (tot >3 jaar) en kosten veel geld. **Hoofdstuk 5** beschrijft de mogelijke toepassing van de *Xpa* en *Xpc* muismodellen in het identificeren van kankerverwekkende (carcinogene) stoffen. Deze twee muismodellen zijn al kankergevoelig doordat ze sneller en meer mutaties in het DNA ophopen in vergelijking met normale muizen (die momenteel nog het meest gebruikt worden als proefdieren). Deze muismodellen hebben we ingekruist met een muismodel dat een defect p53 gen heeft. P53 is een belangrijk eiwit in het tegengaan van kankerverwekkende processen (p53 is een tumor suppressor). De aanmaak van het p53 eiwit wordt na een bepaalde mate van DNA schade geactiveerd en zorgt ervoor dat cellen waarvan het DNA beschadigd is niet verder kunnen delen voordat de schade gerepareerd is. Als de schade te ernstig is en niet meer gerepareerd kan worden zorgt signalering via onder andere p53 ervoor dat deze cel zal afsterven en geen schade meer kan veroorzaken. De door ons ontwikkelde *Xpa*\*p53 en *Xpc*\*p53 muismodellen hebben dus een defect dat ervoor zorgt dat er sneller en meer mutaties ontstaan door schadelijke stoffen voor het DNA (genotoxische stoffen) en een minder goed functionerend veiligheidssysteem hebben waardoor cellen met schade in leven blijven en zich kunnen

gaan vermenigvuldigen (tumorvorming). Als we deze muismodellen blootstellen aan kankerverwekkende stoffen ontwikkelen ze veel sneller en vaker tumoren dan normale muizen. Door deze gevoeligheid zijn er veel minder muizen nodig om een kankerverwekkende stof te identificeren en kan het veel tijd en geld besparen. *Xpc*\**p53* muizen blijken qua identificatie van carinogene stoffen nog gevoeliger te zijn dan *Xpa*\**p53* muizen. Daarnaast laten we zien dat deze muismodellen geschikt zijn om tot voorheen moeilijk op te sporen carcinogene stoffen te identificeren, de zogenaamde niet-genotoxische carcinogenen (stoffen die niet direct schade veroorzaken aan het DNA, maar tumorvorming op een andere manier bevorderen).

Mannelijke *Xpa*\**p53* en *Xpc*\**p53* muizen die blootgesteld werden aan de genotoxische carcinogeen 2-AAF in de hierboven beschreven carcinogeniteitstesten lieten een zeer verhoogde incidentie van blaastumoren zien na 9 maanden blootstelling. In **hoofdstuk 6** onderzochten we of deze verhoging in tumorincidentie te herleiden was naar een volledige deficiëntie van het p53 gen, veroorzaakt door mutaties geïnduceerd door de genotoxische 2-AAF blootstelling. Deze resultaten leidden tot de ontdekking van een mechanisme waarbij mutaties in het eerste (N-terminale) deel van het p53 gen zorgen voor de productie van een alternatief en ingekort p53 eiwit (de dN-p53 isovorm). Ons onderzoek toont aan dat deze isovorm dN-p53 een functioneel eiwit is, maar verschilt in functie van het normale p53 eiwit.



# CV & Publications

## Curriculum Vitae

Joost Petrus Maria Melis werd geboren op 13 februari 1978 in Eindhoven. Na het behalen van het VWO-diploma aan de Scholengemeenschap Philips van Horne te Weert in 1996, begon hij datzelfde jaar met de opleiding Bioprocestechnologie aan de Wageningen Universiteit met als specialisatie Moleculaire en Cellulaire Biologie. Tijdens deze opleiding heeft hij onderzoekservaring opgedaan middels twee afstudeeropdrachten aan de Wageningen Universiteit (afdeling Moleculaire Biologie en afdeling Moleculaire Genetica van Industriële Micro-organismen). Vervolgens heeft hij een afstudeeropdracht uitgevoerd aan de afdeling Molecular and Cellular Biology aan de University of New England in Australië. Tot slot voerde hij nog een extra afstudeeropdracht uit bij DSM te Delft. Na het succesvol afronden van zijn universitaire studie in 2002 ging hij als projectleider bij de afdeling Voorlichting aan de Wageningen Universiteit aan de slag om vervolgens een jaar de wereld rond te reizen. Bij terugkomst in Nederland begon hij als onderzoeksmedewerker aan verouderings- en kankeronderzoek bij de afdeling Toxicologie, Pathologie en Genetica van het Rijksinstituut voor Volksgezondheid en Milieu (RIVM). In februari 2007 startte hij zijn promotieonderzoek bij de groep van Prof. Dr. Harry van Steeg op het Laboratorium voor Gezondheidsbeschermingsonderzoek (RIVM) in samenwerking met de afdeling Toxicogenetica van Prof. Dr. Leon Mullenders van het Leiden Universitair Medisch Centrum (LUMC). Tijdens dit promotieonderzoek onderzocht hij de rol van DNA schade herstelmechanismen en het tumor suppressor eiwit p53 in relatie tot veroudering en kanker. Dit onderzoek is beschreven in het huidige proefschrift. Vanaf februari 2011 is Joost Melis werkzaam als post-doctoraal wetenschapper in het veld van kanker-, verouderings- en toxicologieonderzoek aan de afdeling Toxicogenetica van het LUMC.



## Publications

**Melis JPM**, Wijnhoven SW, Beems RB, Roodbergen M, van den Berg J, Moon H, Friedberg E, van der Horst GTJ, Hoeijmakers JHJ, Vijg J, van Steeg H. Mouse models for xeroderma pigmentosum group A and group C show divergent cancer phenotypes. **Cancer Res.** 2008 Mar 1;68(5):1347-53. Impact factor 2011: 8.2

**Melis JPM**, Hoogervorst EM, van Oostrom CTM, Zwart E, Breit TM, Pennings JLA, de Vries A, van Steeg H. Genotoxic exposure: novel cause of selection for a functional  $\Delta$ N-p53 isoform. **Oncogene.** 2010 Dec 13 [Epub]. 2011 Apr 14;30(15):1764-72. Impact factor 2011: 6.9

**Melis JPM**, Luijten M, Mullenders LHF, van Steeg H. The role of XPC: Implications in cancer and oxidative DNA damage. **Mutation Research - Reviews in Mutation Research.** 2011 Jul 7 [Epub]. 2011 Nov; 728(3):107-17. Impact factor 2011: 7.9

**Melis JPM**, Luijten M, Mullenders LHF, van Steeg H. Nucleotide Excision Repair and Cancer, **DNA Repair and Human Health.** 2011 Sonya Vengrova (Ed.), ISBN: 978-953-307-612-6, InTech, <http://www.intechopen.com/books/dna-repair-and-human-health/nucleotide-excision-repair-and-cancer>

**Melis JPM**, van Steeg H, Luijten M. Oxidative DNA damage and Nucleotide Excision Repair, **Antioxid Redox Sign. [accepted].** Impact factor 2011: 8.5

**Melis JPM**, Jonker MJ, Kuiper RV, van der Hoeven T, Robinson J, van der Horst GTJ, Breit TM, Vijg J, Dollé ME, Hoeijmakers JHJ, van Steeg H. Lifelong murine gene expression profiles in relation to chronological and biological aging in multiple organs. **Aging Cell [revisions].** Impact factor 2011: 7.1

**Melis JPM**, Schaap MM, Speksnijder EN, Kuiper RV, Salvatore DCF, Robinson J, Verhoef A, van Benthem J, Luijten M, van Steeg H. Detection of genotoxic and non-genotoxic carcinogens in *Xpc<sup>-/-</sup> p53<sup>+/-</sup>* mice. **Toxicology and Applied Pharmacology [submitted].** Impact factor 2011 4.4

**Melis JPM**, Kuiper RV, Pennings JLA, Zwart E, Robinson J, van Oostrom CTM, Mullenders LHF, Luijten M, van Steeg H. Divergent mutational and transcriptional response in *Xpc<sup>-/-</sup>* mice upon oxidative stress exposure. **Antioxid Redox Sign. [revisions].** Impact factor 2011: 8.5

Pothof J, Kloet DEA, **Melis JPM**, Tresini M, van Ijcken W, Wiemer EA, van Steeg H, Burgering BMT, Hoeijmakers JHJ. A microRNA signature in aging associated with DNA damage regulates cell survival via PTEN and NRF2. **Nature [revisions].** Impact factor 2011: 36,2

**Melis JPM**, Derks K, Wackers P, Schaap MM, Zwart E, Jonker MJ, Pothof J, van Steeg H, Luijten M. MicroRNA and mRNA biomarkers for *in vivo* carcinogen identification. **In preparation**

**Melis JPM**, Wackers P, Schaap MM, Zwart E, Jonker MJ, van Steeg H, Luijten M. mRNA biomarkers for *in vivo* carcinogen identification. **In preparation**

Visser WE, Bombardieri C, Ottaviani A, van der Pluijm I, van Nimwegen M, Kaptein E, van Heerebeek R, van Toor H, Brandt R, Garinis GA, Peeters RP, van Ham W, de Waard MC, de Krijger RR, Kopchick JJ, List EO, **Melis JPM**, Darras VM, Dollé ME, van der Horst GTJ, Hoeijmakers JHJ, Visser TJ. Suppressed thyroid hormone signaling and induction of the thyroid hormone-inactivating type 3 deiodinase in accelerated and normal aging mice. **In preparation**

### Abstracts published in journals

**Melis JPM**, Wijnhoven SW, van der Horst GTJ, Hoeijmakers JHJ, Vijg J, Beems RB, van Steeg H. Mutagenic and carcinogenic responses in NER-deficient mice. **Mutagenesis**. 2009 Nov; 24(6): 525. Abstract: 7 Impact factor 2011: 3.7

**Melis JPM**, Kuiper RV, Pennings JLA, Zwart E, Robinson J, van Oostrom CTM, Luijten M, van Steeg H. Oxidative DNA damage accumulation in *Xpc<sup>-/-</sup>* mice increases mutagenicity and cancer susceptibility. **Mutagenesis**. 2011 26(5): 719 Abstract: 93 Impact factor 2011: 3.7

**Melis JPM**, Derks K, Wackers P, Schaap MM, Zwart E, Jonker MJ, Breit T, Pothof J, van Steeg H, Luijten M. *In vivo* biomarkers for genotoxic and non-genotoxic carcinogen identification. **Environmental and Molecular Mutagenesis** 2012 Aug; 53(7): 493-577 Abstract: 26 Impact factor 2011: 3.7

**Melis JPM**, Schaap MM, Speksnijder EN, Kuiper RV, Salvatore DCF, Robinson J, Verhoef A, van Benthem J, Luijten M, van Steeg H. Detection of genotoxic and non-genotoxic carcinogens in *Xpc<sup>-/-</sup> p53<sup>+/-</sup>* mice. **Environmental and Molecular Mutagenesis** 2012 Aug; 53(7): 493-577 Abstract: P115 Impact factor 2011: 3.7

### Patent

*In vitro* method for determining genotoxic and non-genotoxic carcinogenicity of a compound

### Conferences

MGC Symposium - Leiden 2007 (selected speaker)

2<sup>nd</sup> German-French DNA Repair Meeting - Toulouse 2007 (poster)

NVT Conference - Veldhoven 2009 (invited speaker, Best Discussion Award)

UKEMS Conference – Leeds 2009 (invited speaker)

The 15<sup>th</sup> International p53 workshop - Philadelphia 2010 (poster)

Workshop on Biomarkers of Exposure and Oxidative DNA Damage – Münster 2011 (poster)

Responses to DNA Damage – Egmond aan Zee 2011

43<sup>rd</sup> Annual EMS Meeting 2012 – Bellevue 2012 (2x poster, 2x selected speaker)

